Polymer Therapeutics to Modify Cellular Responses in Impaired Human Wound Healing

Joseph Thomas Hardwicke
MBChB, MRCS

A Thesis submitted to Cardiff University in partial fulfilment of the requirements for the degree of Doctor of Philosophy

Wound Biology Group
Tissue Engineering and Reparative Dentistry
School of Dentistry
Cardiff University
United Kingdom

February, 2009

ProQuest LLC
789 East Eisenhower Parkway
P.O. Box 1346
Ann Arbor, MI 48106-1346

DECLARATION

This work has not previously been accepted in substance for any Degree and is not concurrently submitted in candidature for any Degree.

Signed 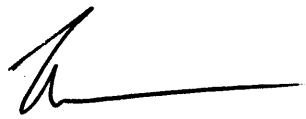 Date 17/7/09

STATEMENT 1

This Thesis is being submitted in partial fulfilment of the requirements for the Degree of PhD.

Signed 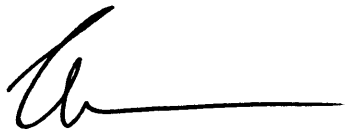 Date 17/7/09

STATEMENT 2

This Thesis is the result of my own independent work / investigation, except where otherwise stated. Other sources are acknowledged by explicit references.

Signed  Date 17/7/09

STATEMENT 3

I hereby give consent for my Thesis, if accepted, to be available for photocopying and for inter-library loan, and for the title and summary to be made available to outside organisations.

Signed  Date 17/7/09

ACKNOWLEDGEMENTS

Firstly, I would like to express my sincere gratitude to my supervisors, Professors David Thomas and Ruth Duncan, and Dr. Ryan Moseley. Their support and enthusiasm has been invaluable, as well as their combined insight and motivation. I must give a special thank you to Professor Thomas for his encouragement and allowing me to combine my academic interest with my clinical practice. I greatly appreciate having the opportunity to contribute to such an exciting field of research and would also like to recognise The Healing Foundation and the Welsh Office for Research and Development (WORD), for their joint funding of my PhD Fellowship. With the support of the charitable donations to The Healing Foundation, and Mr. Brendan Eley, I hope that I have fulfilled their objectives to champion the cause of people living with disfigurement and visible loss of function.

I would also like to thank Dr. Jeff Hart and Dr. Andrea Bell, of Cica Biomedical, for their assistance with the *in vivo* Study; and Dr. Bing Song, of the University of Aberdeen, for his advise and help in developing the *ex vivo* model of wound healing. I am also grateful to Dr. Alastair Sloan for experimental samples utilised in the present Study.

Dr. Elaine Ferguson has been a fountain of knowledge throughout my studies, and she knows that I would not have been able to complete my research without her help and guidance. I would also like to acknowledge all my friends and colleagues in the School of Dentistry: Professor Phil Stephens for his valuable support; Dr. Matt Caley for having all the answers; Dr. Lindsay Davies, Dr. Matthew Peake, Dr. Dan Evans, Dr. Charlotte Emmanuel and Mr. James Roberts for offering me their friendship, support and assistance. Special thanks to Ms. Nicole Kane-Maguire and Dr. Sarah Bamford, for sharing the tiniest office with me, in the deepest darkest depths of the School of Dentistry. I must also thank Dr. Kerry Wallom and Mr. Sam Deacon, at the Centre for Polymer Therapeutics, Welsh School of Pharmacy, for never hesitating in joining me for a cup of coffee.

Finally, the completion of this PhD would also not have been possible without the love, support (emotional and financial!), and belief of my darling wife, Rachael. She has unfaltering faith and belief in me, and although I don't always show it, these feelings are reciprocated! I love you!

ABSTRACT

Chronic ulceration of the lower limb represents a significant clinical challenge in today's aging society. Depletion of growth factors at the chronic wound site by proteinases and reactive oxygen species, can lead to a protracted non-healing wound. Growth factors are known to act in concert to promote wound repair, but their topical application rarely leads to a significant clinical improvement in chronic wounds, due to premature inactivation in the wound environment. The aim of this Study was to synthesise and characterise a polymer-growth factor conjugate and to investigate whether the novel concept, called **P**olymer-masking-**U**n**M**asking-**P**rotein **T**herapy (PUMPT), may be used to generate bioresponsive, polymer therapeutics, promoting tissue repair. Dextrin and recombinant human epidermal growth factor (rhEGF) were chosen as a first model combination.

Dextrin was first modified by succinoylation and conjugated to rhEGF. The synthesised dextrin-rhEGF conjugate exhibited increased stability towards proteolytic degradation by the clinically relevant enzyme, neutrophil elastase. The dextrin component was degraded on exposure to physiological levels of α-amylase, leading to sustained release of free rhEGF. Biological activity was assessed in proliferation assays *in vitro*, using cells involved in the normal healing response. Polymer conjugation reduced rhEGF bioactivity, however, after exposure to physiological concentrations of α-amylase, dextrin degradation led to restoration of bioactivity of rhEGF, to the level observed with unmodified rhEGF. Dextrin-rhEGF was demonstrated to induce phosphorylation of the epidermal growth factor receptor (EGFR), and confirmed a mechanism of action by stimulation of classical signal transduction pathways.

Analysis of *ex vivo* acute and chronic wound fluids, confirmed the presence of α-amylase, at levels similar to those used *in vitro*. Chronic wound fluid also contained active neutrophil elastase. In an *ex vivo* organotypic model of acute corneal wound healing, α-amylase-exposed dextrin-rhEGF was demonstrated to enhance wound healing, above that of free rhEGF. In an *in vivo* model of impaired wound healing in the genetically diabetic (db/db) mouse, dextrin-rhEGF was observed to significantly enhance dermal wound healing, on topical application, at delayed intervals. This is the first application of the PUMPT hypothesis *in vivo*, and supports the further development of polymer-protein conjugates as bioresponsive nanomedicines for tissue repair.

CONTENTS

LIST OF FIGURES

LIST OF TABLES

ABBREVIATIONS

3-D	3-dimensional
AGE	Advanced glycation end (products)
ALL	Acute lymphoblastic leukaemia
ANOVA	Analysis of variance
ATCC	American type culture collection
AU	Arbitrary units
BCA	Bicinchoninic acid
BM	Basement membrane
BSA	Bovine serum albumin
Da	Dalton (g/mol)
DAG	Diacylglycerol
DAPI	4',6-diamidino-2-phenylindole
db/db	Genetically diabetic (homozygous)
ddH_2O	Double distilled water
DED	Dermo-epidermal junction
DMAP	4-Dimethylaminopyridine
DMEM	Dulbecco's modified Eagle's medium
DMF	N,N-dimethylformamide
DMSO	Dimethyl sulphoxide
DNA	Deoxyribonucleic acid
DTT	Dithiothreitol
DVD	Digital versatile disc
DVT	Deep venous thrombosis
ECL	Electrochemiluminescence
ECM	Extracellular matrix
EDTA	Ethylenediaminetetraacetic acid
EDC	1-Ethyl-3(3-dimethylaminopropyl) carbodiimide
EGF	Epidermal growth factor
EGFR	Epidermal growth factor receptor
ELISA	Enzyme-linked immunosorbant assay
EMEM	Eagle's minimum essential medium
EPR	Enhanced permeability and retention (effect)
ESF	European Science Foundation
ET	Endothelin
FACS	Fluorescence-activated cell sorting
FCS	Foetal calf serum
FDA	US Food and Drug Administration
FGF	Fibroblast growth factor
FITC	Fluorescein isothiocyanate
FPLC	Fast protein liquid chromatography
F-SCM 10%	Fibroblast-serum containing media (10 % serum v/v)
F-SCM 1%	Fibroblast-serum containing media (1 % serum v/v)
F-SFM	Fibroblast-serum free media
FTIR	Fourier transform infrared spectroscopy
GAG	Glycosaminoglycan
GCSF	Granulocyte colony stimulating factor
GPC	Gel permeation chromatography
GRAS	Generally recognised as safe

HbA_{1C}	Glycosylated haemoglobin
HB-EGF	Heparin-binding epidermal growth factor
H&E	Haematoxylin and eosin
HEp2	Human epidermoid carcinoma
HGF	Hepatocyte growth factor
HOCl	Hypochlorous acid
HPMA	*N*-(2-hydroxypropyl) methacrylamide
H-SCM 10%	HEp2-serum containing media (10 % serum v/v)
H-SCM 1%	HEp2-serum containing media (1 % serum v/v)
HSE	Human skin equivalent
H-SFM	HEp2-serum free media
hTERT	Human telomerase, reverse transcriptase
IR	Infra-red
IGF	Insulin-like growth factor
IgG	Immunoglobulin G
IL	Interleukin
IP_3	Inositol 1,4,5-triphosphate
i.u.	International units
IV	Intravenous
JAK	Janus kinase
KGF	Keratinocyte growth factor
K-SCM 10%	Keratinocyte-serum containing media (10 % v/v)
K-SCM 1%	Keratinocyte-serum containing media (1 % v/v)
K-SFM	Keratinocyte-serum free media
LDL	Low density lipoprotein
LREC	Local research ethics committee
MALP	Macrophage-activating lipopeptide
MAPK	Mitogen-activated protein kinase
mol%	Mole percent
MMP	Matrix metalloproteinase
MSH	Melanocyte stimulating hormone
MTT	3-(4,5-dimethylthiazol-2-yl)-2,5-diphenyl-2H-tetrazoliumbromide
MWCO	Molecular weight cut-off
NaCMC	Sodium carboxymethylcellulose
NCS	Neocarzinostatin
$NO^{\cdot}$	Nitric oxide radical
NRG	Neuregulin
$O_2^{\cdot -}$	Superoxide radical
ob/ob	Genetically obese (homozygous)
OG	Oregon green
$^{\cdot}OH$	Hydroxyl radical
$ONOO^{\cdot}$	Peroxynitrite radical
p	Probability
PBS	Phosphate buffered saline
PDGF	Platelet-derived growth factor
PDI	Polydispersity index
PEG	Polyethylene glycol
PGA	Polyglutamic acid
PIP_2	Phosphatidylinositol 4,5-bisphosphate

PKC	Protein kinase C
PLCγ	Phospholipase C γ
PUMPT	Polymer masking unmasking protein therapy
PVDF	Polyvinyl difluoride
PVP	Polyvinyl pyrolidone
®	Registered trademark
R^2	Coefficient of determination of linear regression
RFU	Relative fluorescence units
rhEGF	Recombinant human epidermal growth factor
RI	Refractive index
RNS	Reactive nitrogen species
ROS	Reactive oxygen species
RP-HPLC	Reverse-phase-high performance liquid chromatography
RT	Room temperature
RTK	Receptor tyrosine kinase
SCID	Severe combined immunodeficiency disease
S.D.	Standard deviation
SDS	Sodium dodecyl sulphate
SDS-PAGE	Sodium dodecyl sulphate-polyacrylamide gel electrophoresis
S.E.M.	Standard error of the mean
SFM	Serum-free media
SMA	Styrene maleic anhydride
SMANCS	Styrene-co-maleic anhydride-neocarzinostatin
SPARC	Secreted protein, acidic and rich in cysteine
STAT	Signal transducers and activators of transcription
Sulfo-NHS	N-hydroxysulfosuccinimide
TGF-ß	Transforming growth factor-ß
TIMP	Tissue inhibitor of metalloproteinase
™	Trademark
TNF-α	Tumour necrosis factor-α
tPA	Tissue-type plasminogen activator activator
uPA	Urokinase-type plasminogen
USA	United States of America
UV	Ultraviolet
v/v	Volume/volume
V_0	Void volume
V_t	Total volume
Val	Valine
VEGF	Vascular endothelial growth factor
VLDL	Very low density lipoprotein
vWF	von Willebrand's factor
wt%	Weight percent
w/v	Weight/volume

PUBLICATIONS ARISING FROM THIS THESIS

PAPERS

1. **Hardwicke J**, Schmaljohann D, Boyce D, Thomas D (2008) Epidermal growth factor therapy and wound healing – Past, present and future perspectives. *The Surgeon* **6:** 172-177

2. **Hardwicke J**, Ferguson EL, Moseley R, Stephens P, Thomas DW, Duncan R (2008) Dextrin-rhEGF conjugates as bioresponsive nanomedicines for wound repair. *Journal of Controlled Release* **130:** 275-283

3. **Hardwicke J**, Stephens P, Harding KG, Moseley R, Thomas DW (2009) Promotion of acute and chronic wound healing by bioresponsive dextrin-rhEGF polymer conjugates. *Submitted to Journal of Investigative Dermatology*

4. **Hardwicke J,** Moseley R, Song B, Thomas DW (2009) Corneal wound healing is enhanced by a bioresponsive polymer conjugate in an ex vivo whole eye organ culture model. *Submitted to Wound Repair and Regeneration*

ABSTRACTS

5. **Hardwicke J,** Ferguson E, Moseley R, Stephens P, Duncan R, Thomas DW (2008) Designing polymer therapeutics to promote tissue repair. *Molecular Pharmaceutics* **5:** 473-679

6. **Hardwicke J** (2007) Tissue regeneration aspects of nanomedicine. *International Journal of Lower Extremity Wounds* **6:** 168

7. **Hardwicke J,** Moseley R, Schmaljohann D, Stephens P, Duncan R, Thomas DW (2007) Bioresponsive polymer conjugates to promote tissue regeneration in impaired dermal wound healing. *International Journal of Lower Extremity Wounds* **6:** 188

8. **Hardwicke J,** Moseley R, Schmaljohann D, Stephens P, Duncan R, Thomas DW (2007) Bioresponsive dextrin-rhEGF conjugates designed to promote tissue regeneration in impaired human wound healing. *Proceedings of the International Symposium on Polymer Therapeutics* 44

9. **Hardwicke J,** Moseley R, Schmaljohann D, Stephens P, Duncan R, Thomas DW (2007) Bioresponsive polymer-conjugates to promote tissue regeneration in impaired wound healing. *Proceedings of the British Society for Dental Research* 163

Chapter One

General Introduction

Chapter One: General Introduction

Contents

1.1 Introduction

Chronic ulceration of the skin presents a major clinical challenge. In Western countries, the incidence of ulceration is rising as a result of the aging population and the increase in risk factors, such as smoking, obesity and diabetes (Mekkes *et al*, 2003). The prevalence in the UK population aged > 60 years is 3% (Davies *et al*, 2007), while recent US figures predict the current figure at 15% of the elderly, rising to 25% by 2050 (Harlin *et al*, 2008). The lack of adequate treatments can result in an extremely poor quality of life (Price and Harding, 2004).

Growth factors are known to act in concert to promote wound repair, but their topical application rarely leads to a significant clinical improvement in chronic wounds, due to premature growth factor inactivation in the wound environment. The aims of this Study were to synthesise a polymer-growth factor conjugate and investigate whether the novel concept, Polymer-masking-UnMasking-Protein Therapy (PUMPT), may be used to generate bioresponsive, polymer therapeutics as nanomedicines, capable of promoting tissue repair.

1.2 Structure of the skin

The skin is the largest organ system in the human body. It provides a tough protective barrier between the individual and the environment. It consists of three distinct layers (Figure 1.1).

1.2.1 The epidermis

The outer, keratinised layer of the skin (epidermis) is composed of a series of distinct layers. The multilayer stratified squamous epidermis consists of *stratum germinativum* (basal cell layer), *stratum spinosum, stratum granulosum, stratum lucidem and stratum corneum*, the outermost keratinized layer (Underwood, 1994). The different layers represent progressive cellular differentiation and proliferation. The cells migrate from the basal layer in an immature form, to the *stratum corneum* where they become flattened, differentiated, keratin-filled cells, prior to their shedding. The epidermis contains no blood vessels and the cells rely on the underlying dermis for nutritional support. Other cell types present, include Langerhans cells (immune-derived), melanocytes (pigment producing) and Merkel cells (sensory nerve endings) (Fuchs, 2007; Boulais and Misery, 2008).

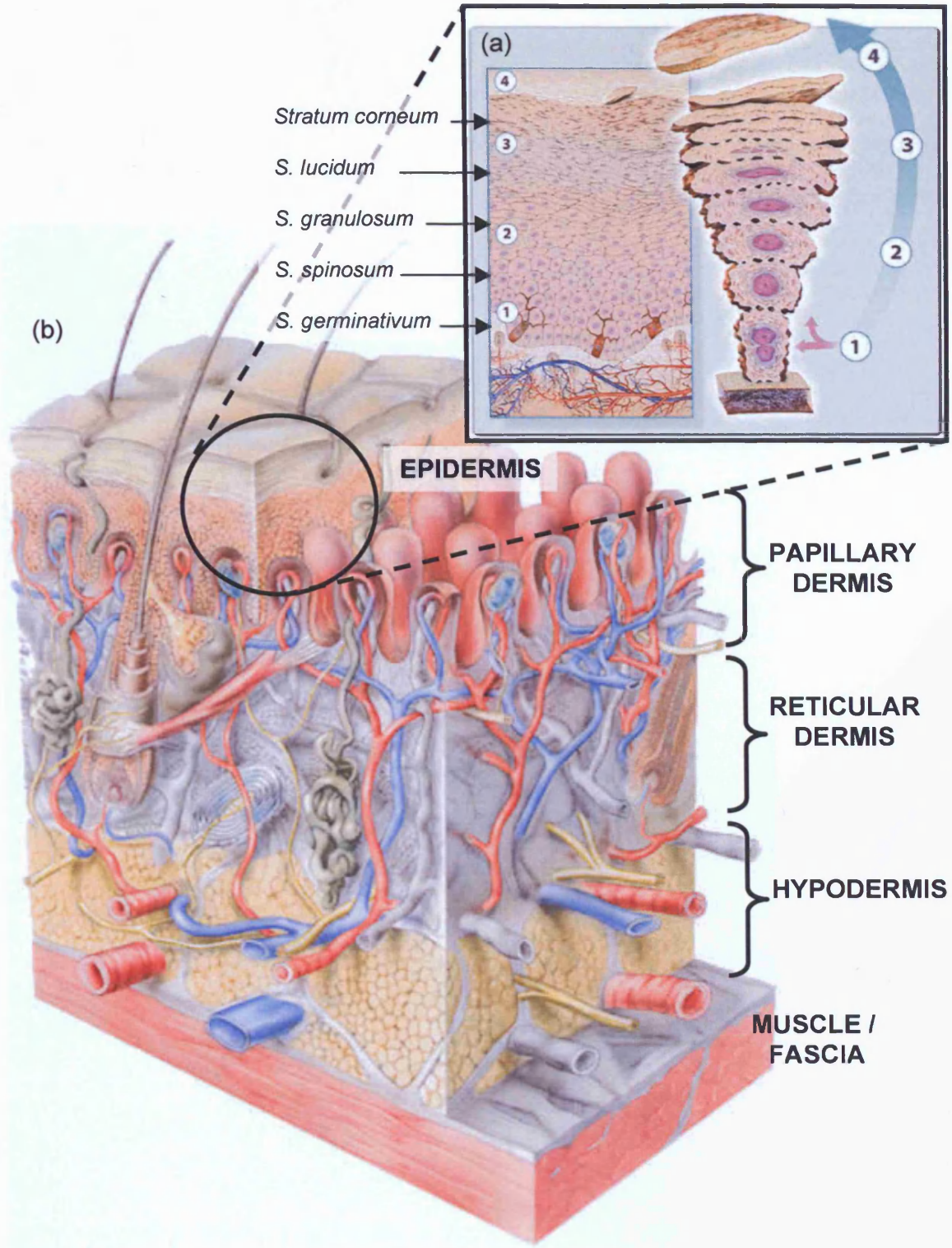

Figure 1.1 **The structure of human skin.** (a) The outer epidermis (magnified), consists of distinct layers of keratinocytes. As the cells mature, there is outward progression through the stratified epithelium (① - ④). (b) The epidermis is supported on the dermis, in which the dermal neuro-vascular plexus is located, in addition to dermal and epidermal derivatives, such as hair follicles and sweat glands (Skin Care Forum, 2001a and 2001b).

The proliferation and differentiation of basal keratinocytes is regulated by a number of factors, including the extracellular matrix (ECM) (Even-Ram and Yamada, 2005), hormones, cytokines and growth factors (Werner *et al*, 1994; auf dem Keller *et al*, 2004; Sivamani *et al*, 2007).

1.2.2 The basement membrane

The basement membrane (BM), is a specialized basal lamellar structure that separates the basal layer of keratinocytes from the dermis. It is attached to the basal keratinocytes by hemidesmosomes, and to the dermis by anchoring fibrils of type VII collagen. It consists of two layers, the upper *lamina lucida*, containing laminin and entactin, and the lower *lamina densa*, rich in type IV collagen (Borradori and Sonnenberg, 1996; Chan, 1997; Shimizu, 1998; Ghohestani *et al*, 2001; Masanuga, 2006). The BM acts as a barrier to large molecules, between the dermis and epidermis.

1.2.3 The dermis

The dermis is the inner layer of the skin, consisting of the upper papillary zone and lower reticular zone. The papillary dermis consists of mainly type I collagen, with some type II collagen and elastin. These connective tissue fibres are embedded in an ECM rich in proteoglycans and glycoproteins (Carrino *et al*, 2003). The reticular dermis consists of a more dense arrangement of collagen and elastin and contains blood vessels, nerves and skin appendages (hair follicles, sweat glands). The cells of the dermis are mainly fibroblasts, located in the papillary zone (Sorrell *et al*, 2007).

The papillary dermis is the interface between the dermis and the epidermis (the dermo-epidermal junction, DED). It consists of irregular papillae, which project into the epidermis, providing a large surface area for the transfer of nutrients. Nerves also traverse the DED, via these papillae. The amorphous ECM, which comprises the bulk of the dermal tissue, binds water, allowing nutrients, hormones and waste products to pass through the dermis (Burgeson and Christiano, 1997).

1.2.4 The hypodermis

The hypodermis, or *subcutis*, is not strictly part of the skin, but it does provide support for the overlying structures and attachment for deeper tissues. It contains adipose tissue, fibrous tissue, blood vessels, lymphatics and nerves, to and from the skin (Kanitakis, 2002).

1.3 Wound healing

Wound healing is a dynamic pathway that optimally leads to restoration of tissue integrity and function. Under normal conditions, it is a complex process involving a highly regulated cascade of biochemical and cellular events, designed to achieve a healed wound over a predictable time-frame. Healing can occur by regeneration of the damaged tissues, such as in hepatic injury (Fausto, 2000); or more commonly by repair, in which damaged tissues are replaced by collagenous scar tissue, which acts to restore tissue continuity and function (Gurtner *et al*, 2008). Over time, this scar can mature to be almost clinically indistinguishable from the surrounding undamaged tissue.

1.3.1 Normal wound healing

Normal wound healing occurs in three phases, an inflammatory phase, a proliferative phase and a maturational phase. The inflammatory phase is characterised by haemostasis and inflammation. It is clinically characterised by the cardinal signs of redness (*rubor*), heat (*calor*), swelling (*tumour*), pain (*dolor*) and loss of function (Underwood, 1994).

1.3.2 Inflammatory phase

The inflammatory phase begins at the time of wounding and lasts 24-48 hours. Collagen exposed during wounding activates the clotting cascade (both intrinsic and extrinsic pathways), via clotting factors, kinins, tissue factor and platelets. This in turn initiates the inflammatory phase. Injured cells release thromboxane A_2, causing local vasoconstriction to stem the flow of blood, followed by the release of histamine, which produces a vasodilatory action, increasing the concentration of inflammatory and wound repair mediators (Andrews *et al*, 1997; Martin, 1997). The complement cascade of plasma proteins is also activated to aid

coagulation and combat infection. These immediate vascular responses allow the next step of cellular responses to occur in the vicinity of the wound.

The coagulation cascade produces a cross-linked fibrin plug at the wound site. This provides the provisional matrix for cellular migration (Martin, 1997; Broughton *et al*, 2006a; Broughton *et al*, 2006b; Werner *et al*, 2007). The initial platelet response involves degranulation and the release of multiple chemokines, including epidermal growth factor (EGF) and platelet-derived growth factor (PDGF); fibronectin; fibrinogen; histamine; serotonin and von Willebrand's factor (vWF) (Martin, 1997; Goldman, 2004; Li *et al*, 2007). These factors help to stabilize the wound through clot formation and act to control bleeding and limit the extent of injury. Platelet degranulation also activates the complement cascade, specifically via C5a, which is a potent chemoattractant for neutrophils, the second cellular type to enter the wound. The neutrophil is responsible for debris scavenging, the complement-mediated opsonisation of bacteria and bacterial phagocytosis, via reactive oxygen species (ROS) production in the form of superoxide radical species ($O_2^{\cdot -}$) and hydrogen peroxide (H_2O_2) (Wlaschek and Scharfetter-Kochanek, 2005). The neutrophils decontaminate the wound, removing bacteria and foreign debris (Moseley *et al*, 2004). Local disruption of blood flow, due to the vasoactive mediators, produces margination of the neutrophils, allowing them to attach to the vascular endothelium. This is aided by interleukin-1 (IL-1); tumour necrosis factor-α (TNF-α); histamine; bradykinin; and the complement and coagulation cascade proteins (Gillitzer and Goebeler, 2001; Oberyszyn, 2007). Neutrophils can directly kill bacteria, but also release potent chemokines and immunoglobulins (Hubner *et al*, 1996; Wetzler *et al*, 2000).

The next cellular types to enter the wound are monocytes/macrophages. The macrophage plays a critical role in removing debris and bacteria, but most importantly, orchestrates the subsequent events in wound healing (DiPietro, 1995; Martin and Leibovich, 2005). These are a primary source of cytokines and growth factors, such as TNF-α, PDGF, and transforming growth factor-β (TGF-ß), that in addition to the stimulation of ECM production by fibroblasts, promote angiogenesis and the stimulation of keratinocytes (Sunderkotter *et al*, 1994; Tredget *et al*, 2005; Bandyopadhyay *et al*, 2006; Werner *et al*, 2007). These growth factors also act in an autocrine fashion to dramatically amplify their expression tremendously (Holman

and Kalaaji, 2006). This step marks the transition between inflammation and cellular proliferation.

1.3.3 Proliferative phase

The second stage of normal wound healing is the proliferative phase that typically begins at day three, following wounding. Re-epithelialisation, angiogenesis, granulation tissue formation and collagen deposition, are the principle steps in this anabolic phase of wound healing. The previously dominant neutrophils and macrophages are also replaced by fibroblasts (Clark, 1993).

The fibroblasts from the adjoining, undamaged tissues, migrate into the wound matrix, under the influence of cytokines. The movement of cells is possible, due to their ability to bind and release fibronectin, fibrin and vitronectin (constituents of the thrombus) (Greilling and Clark, 1997; Clark *et al*, 2004; Briggs, 2005; Lygoe *et al*, 2007) and the action of proteolytic enzymes (matrix metalloproteinases, MMP - 1, -2, and -3) (Sasaki *et al*, 2000; Brown *et al*, 2007). The MMPs permit cell migration through the matrix. There is also proliferation of native, as well as newly arrived mesenchymal cells. These fibroblasts synthesise and secrete collagen and proteoglycans (Hardingham and Fosang, 1992; Yanagishita, 1993; McGrath and Eady, 1997; Lee *et al*, 2004; Meshel *et al*, 2005; Larsen *et al*, 2006) of the connective tissue ECM that unites wound edges together, by assuming the polymeric form (Sottile and Hocking, 2002; Gildner *et al*, 2004). Normal layers of epidermis are restored in 2-3 days. If the basement membrane has been destroyed, similar to deep-dermal and full-thickness burns, then the wound is re-epithelialised from the normal cells in the periphery and from skin appendages, if intact (e.g. sweat glands, hair follicles) (Martin, 1997; Fuchs, 2007; Sivamani *et al*, 2007; Woo *et al*, 2007).

Angiogenesis can be initiated by multiple stimuli, including raised lactate levels, a decreased pH, and growth factors, such as vascular endothelial growth factor (VEGF) (Madri *et al*, 1996; Carmeliet and Jain, 2000). These capillary sprouts grow by proliferation of their endothelial cells. During wound healing, the new vessels soon adjoin with their counterparts and recanalisation occurs, thus restoring blood flow. In wounds healing by secondary closure, or secondary intention (i.e. wound edges not directly apposed by surgical sutures), the new capillaries fuse with their neighbours migrating in a similar direction, so forming granulation tissue. The granulation phase and tissue deposition require nutrients supplied by the capillaries,

although failure for this to occur may result in a chronically unhealed wound. In this granulation sub-phase, fibroblasts differentiate to synthesise the ECM (Martin, 1997; Desmouliere *et al*, 2005). The ECM is deposited into the wound bed, whilst collagen is then deposited as the wound goes under the final stages of repair. Cytokines and growth factors, such as insulin-like growth factor (IGF), EGF and PDGF, are involved in this process (Gillitzer and Goebeler, 2001; Edmondson *et al*, 2003; Grazul-Bilska *et al*, 2003).

Re-epithelialisation can be divided into separate cellular events, including cell differentiation, mitosis, migration and proliferation, which begin within hours of injury and results in the resurfacing of the denuded area (Martin, 1997). The earliest aspect of this process is the thickening of the basal layer at the wound edge. The marginal basal layer then elongates and detaches from the basement membrane, with subsequent migration into the wound. These keratinocytes migrate in a single layer in a "sliding sheet" fashion (Zhao *et al*, 2003), exhibiting contact guidance, usually along the orientation of the collagen fibres, until they meet similar cell types and the process reverts to a resting phase, due to contact inhibition (Sivamani, 2007). Cells from this monolayer subsequently differentiate into the multilayer, stratified squamous epidermis. Subsequently, new surface cells begin to keratinise. This process occurs under the influence of hepatocyte growth factor (HGF), keratinocyte growth factor (KGF), EGF, TGF-α, IGF and members of the fibroblast growth factor (FGF) family (Werner *et al*, 1994; Toyoda *et al*, 2001).

1.3.4 Maturational phase

The final phase of normal wound healing is the maturational phase. This commences at about 8 days, post-injury, and continues over the following months or years (Broughton *et al*, 2006b). Once the fibroblast has migrated into the wound, it switches its main function to that of protein synthesis. Collagen is the major component of the skin, granulation tissue and mature scar and is synthesised primarily by fibroblasts (Van der Rest and Garrone, 1991; Prockop and Kivirikkö, 1995). The rate of production increases rapidly over the initial 2-4 weeks, until collagen production and collagen degradation, due to MMPs and other mediators of ECM turnover become equal (Tyrone and Mustoe, 1999). This balance occurs between the action of MMPs and tissue inhibitors of MMPs (TIMPs), which

regulates the dynamic remodelling of the dermal ECM (Bode *et al*,1999; Lauer-Fields *et al*, 2002; Bode and Maskos, 2003; Visse and Nagase, 2003; Nagase *et al*, 2006). After 4 weeks, the production of collagen begins to decline. Collagen is deposited randomly in the acute wound granulation tissue. Initially, type III collagen is deposited, but becomes replaced by type I collagen fibrils, which are laid down in a more well-aligned formation, to increase the tensile strength of the wound. This progresses until the ratio of type I: type III collagen is restored to that of normal skin. With remodelling, there is a dynamic turnover of collagen, in response to tensile forces, where collagen synthesis equals collagenolysis (Chiquet *et al*, 2003; Silver *et al*, 2003).

Replacement of the dermal ECM is complex, as it contains components other than collagen. These include proteoglycans, fibronectin and elastin. Proteoglycans are synthesised primarily by fibroblasts and consist of a protein core, covalently linked to glycosaminoglycans (GAG), including chondroitin sulphate or dermatan sulphate (Sugahara *et al*, 2003; Raman *et al*, 2005; Taylor and Gallo, 2006). Hyaluronan is also an important structural and functional component of the ECM wherever there is rapid tissue proliferation, regeneration and repair (Chen and Abatangelo, 1999). Hyaluronan stabilises the clot matrix, activates inflammatory cells, and modulates all stages of wound repair (Laurant and Fraser, 1992; Almond, 2007; Meran *et al*, 2007; Price *et al*, 2007). Fibronectins are primarily attachment proteins and important in the phases or wound healing, including fibroblast migration (Briggs, 2005). The formation of a new ECM results in a tensile strength plateau, achieved after approximately 2 years, to about 80% of the normal strength of the surrounding undamaged tissues, past which the strength will not increase. 50% of this strength is gained in the first 6 weeks, post-injury (Tyrone and Mustoe, 1999).

The wound is eventually closed by the migration of epithelial cells from the wound edge, filling the defect until they reach other epithelial cells and halt their advance, by the process of contact inhibition. Although this adds nothing to wound strength, and remodelling continues under the epithelial cover (Martin *et al*, 1992). When wound fibroblasts reach a concentration with which their density causes contact inhibition, they differentiate into myofibroblasts, containing α-smooth muscle actin fibrils (Gabianni, 1992; Desmouliere *et al*, 2005; Darby and Hewitson, 2007; Hinz, 2007; Hinz *et al*, 2007). This begins 4-5 days, post-injury, and is

represented by the centripetal movement of the wound edges towards the centre of the wound. Myofibroblasts in the injured area are believed to be responsible for wound contraction. Over time, the volume of injured tissue is replaced by uninjured tissue. The scar becomes reduced in cell content and blood supply, represented clinically by the change in colour, texture and size of the scar, as the body tries to remodel the immature scar tissue (Bond *et al*, 2008).

1.3.5 Chronic impaired wound healing

A chronic wound can be clinically described as a wound that has not healed after 3 months (Tyrone and Mustoe, 1999). It can be more accurately diagnosed by the presence of high levels of chronic inflammatory cells, including neutrophils, macrophages and lymphocytes, a defective wound ECM, and a failure of epithelialisation (Herrick *et al*, 1992). Impaired wound healing can result from local or systemic causes. Local causes include trauma, infection, ischaemia, foreign bodies and elevated tissue pressure, whilst systemic causes, such as diabetes, advanced age, drug therapy and endocrine disturbance, can compound the effects of the build up of chronic wound metabolites (Broughton *et al*, 2006a).

Dermal fibroblasts play a pivotal role in controlling wound healing responses and variations in fibroblast phenotype have been observed, relating to the wound healing phenotype (i.e. the acute or chronic wound) (Sempowski *et al*, 1995; Stephens *et al*, 1996; Al-Khateeb *et al*, 1997; Stephens *et al*, 2001; Wall *et al*, 2008). Numerous alterations have been described in association with aging and the onset of cellular senescence, including increases in MMP-1 and -2 production, increased ROS generation, increased IL-1 and IL-15 expression, and decreased IL-6 expression (West *et al*, 1989; Mendez *et al*, 1998; Shelton *et al*, 1999) The accumulation of senescent fibroblasts within the chronic wound tissues, play an important role in mediating inflammation and impaired ECM remodelling, which is a key feature of the disease (Stephens *et al*, 2003).

A number of growth factors (e.g. EGF, PDGF, VEGF, TGF-β), act in concert to promote normal wound repair (Goldman, 2004; Blakytny and Jude, 2006; Li *et al*, 2007), but have been shown to be at reduced levels in chronic wound exudates (Yager *et al*, 1997; Trengove *et al*, 1999). This is likely due to rapid protein degradation by chronic wound proteinases, especially neutrophil elastase, and/or

denaturation by ROS (Yager *et al*, 1997; Wlashek *et al*, 1997; James *et al*, 2003; Moseley *et al*, 2004; Wlashek and Scharfetterr-Kochanek, 2005).

ROS is a term encompassing oxygen free-radicals, including the $O_2^{\cdot -}$ and hydroxyl ($^{\cdot}OH$) radical species, as well as non-radical oxygen derivatives, such as H_2O_2 and hypochlorous acid (HOCl) (Moseley *et al*, 2004). Reactive nitrogen species (RNS) are similar, and include the nitric oxide ($NO^{\cdot}$) radical species and peroxynitrite ($ONOO^{\cdot}$) (Waddington *et al*, 2000). RNS and ROS are derived from both inflammatory cells and endothelial cells and possess beneficial roles in wound healing, enhancing bactericidal activity and modulating many functions including: vasodilatation, granulation tissue formation, re-epithelialisation and ECM turnover (Stallmeyer *et al*, 1999; Waddington *et al*, 2000; Pollock *et al*, 2001; Sen *et al*, 2002; Rizk *et al*, 2004). The overproduction of ROS and RNS in chronic wounds can lead to an imbalance in the oxidant / antioxidant status and cause indiscriminate damage to cellular constituents, including deoxyribonucleic acid (DNA), lipids and proteins. In addition, ROS and RNS can directly and indirectly modify and degrade the ECM components of the skin, including collagen, proteoglycans and hyaluronan (Moseley *et al*, 2004). Direct cellular effects of ROS and RNS include impaired migratory, proliferative and ECM synthetic properties of dermal fibroblasts and keratinocytes (Ågren *et al*, 1997; Pfeilschifter *et al*, 2001; Moseley *et al*, 2002; Wlascheck and Scharffetter-Kochanek, 2005). The various roles of these biochemical markers of chronic wound healing are summarised in Figure 1.2.

The normal healing process is "stalled" in a chronic inflammatory process, high in pro-inflammatory cytokines and wound proteinases, and low in growth factors, which are essential for the normal progression to the proliferative phase of wound healing. Without such progression, the clinical entity of the non-healing wound, is apparent.

1.3.6 Pathophysiology of chronic wounds

The aetiology of leg ulcers, includes venous insufficiency, diabetes, arterial insufficiency or a combination of these factors (Mekkes *et al*, 2003). In these wounds, the structured normal healing process is frequently disrupted by an underlying abnormality; prolonging the inflammatory phase and limiting progression to the proliferative phase of wound healing. Thus, a cascade of responses are generated that perpetuate the non-healing state.

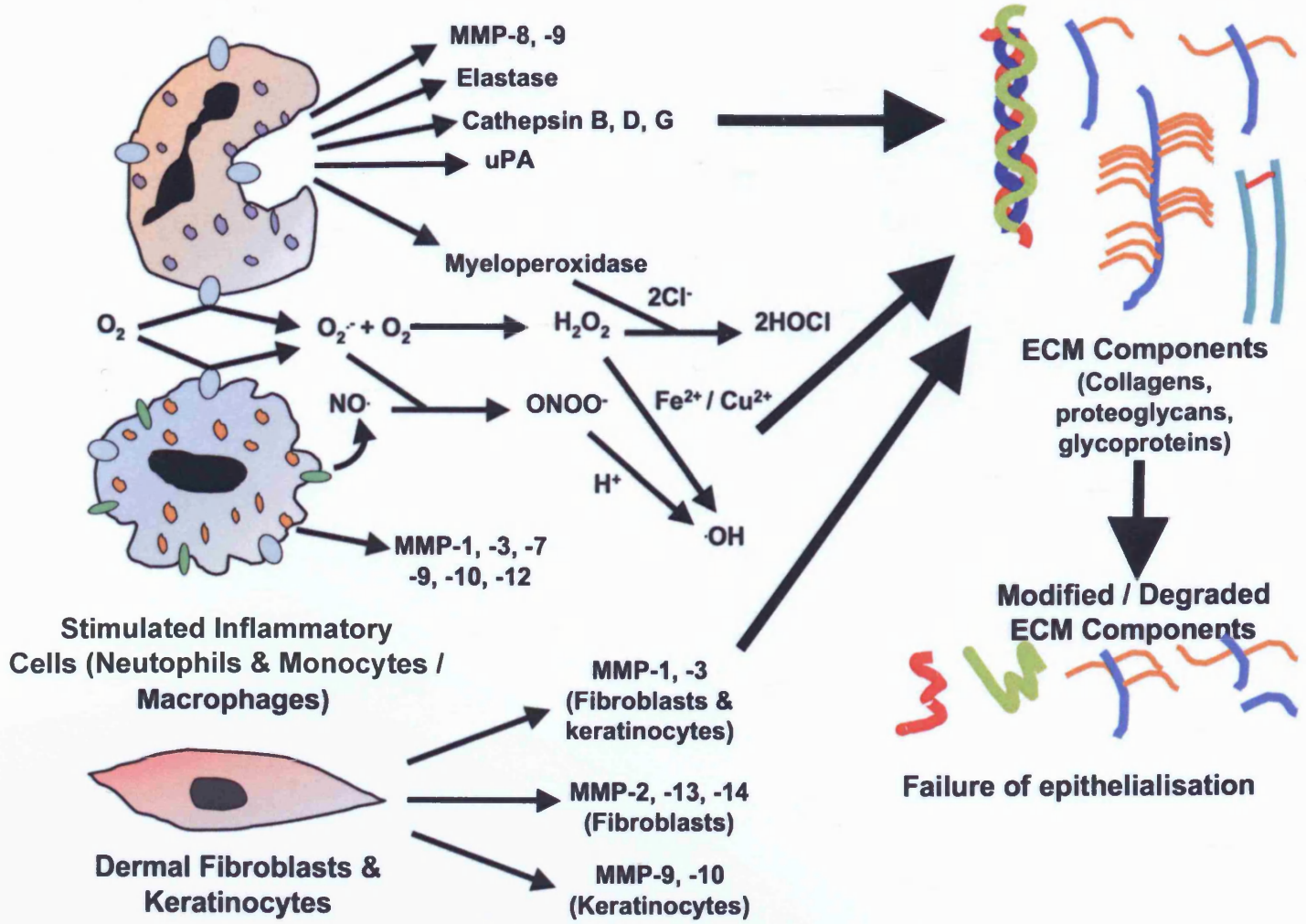

Figure 1.2 **Degradation of the extracellular matrix (ECM) by proteolysis and reactive oxygen species (ROS).** In the chronic wound, the ECM is degraded, leading to a failure of re-epithelialisation (adapted from Moseley *et al*, 2004).

1.3.7 Venous leg ulceration

Venous ulcers are the most common form of leg ulcer, accounting for about 70% of all cases in the UK (Sarkar and Ballantyne, 2000). Overall, these ulcers affect approximately 1% of the population (Fowkes *et al*, 2001). The concept of venous stasis suggests that stagnant blood lying in tortuous and dilated, superficial veins close to the skin, can cause tissue anoxia and cell death. There is usually an underlying causative factor, leading to the rise in venous pressure, which affects the capillary network, preventing the normal arterio-venous flow of blood. Nearly half of patients affected have a previous history of deep vein thrombosis (DVT), while the remainder have evidence of incompetent perforating veins that connect the deep and superficial venous systems of the leg (Valencia *et al*, 2001; Rajendran *et al*, 2007).

There is usually a preceding stage to ulceration, called lipodermatosclerosis (Herouy *et al*, 1999). Excessive proteolytic activity by proteinases, especially MMP-1, -2, -8 and -9, and fibrinolytic factors of the plasminogen activation system, lead to an abnormal ECM. There is also reduced expression of TIMPs and TGF-ß, leading to an imbalance in normal wound healing (Moseley *et al*, 2004). After the initial trigger and disruption of the epidermis, wound healing has already taken a pathological path.

Venous stagnation can cause ulceration, via tissue anoxia, resulting in cell damage/death. Other propagating factors can include, the leakage of macromolecules into the ECM, that leads to an accumulation of fibrin that can create a barrier for oxygen and nutrient transfer (Dormandy, 1997; Stacey *et al*, 2000; Brown, 2005). Trapped neutrophils can also block superficial lymphatics, further impeding the flow of toxins from the skin and surrounding area (Scott, *et al*, 1991; Falanga and Eaglestein, 1993). Other systemic diseases, that can compound a venous ulcer, include peripheral oedema from heart and renal failure, arthritis that limits mobilisation, and diabetes, which, via various mechanisms, markedly limits successful wound healing.

1.3.8 Diabetic foot ulceration

Diabetic foot ulcers occur as a result of a variety of factors. These include mechanical changes in the conformation of the bony architecture of the foot, peripheral neuropathy, atherosclerotic arterial disease and a reduction in the propensity to heal (Leung, 2007). Diabetic foot ulcers are responsible for more

hospitalisations than any other complication of diabetes. In the USA, there are 16 million diabetics, 15% of which will develop a foot ulcer (Reiber *et al*, 1998).

Atherosclerosis can affect the non-diabetic population, as well as the diabetic population. In diabetics, the disease is more common in the infra-popliteal region, affecting smaller vessels and the microvasculature. This is believed to result from a number of metabolic abnormalities, including high low-density lipoprotein (LDL) and very low-density lipoprotein (VLDL) levels, elevated plasma vWF, inhibition of prostacyclin synthesis, increased plasma fibrinogen levels and increased platelet adhesion (Stillman, 2008).

Diabetics have a higher incidence of atherosclerosis, thickening of capillary basement membranes, arteriolar hyalinosis and endothelial proliferation (Mauer *et al*, 1992). Peripheral neuropathy occurs due to a multifactorial process. It clinically produces decreased sensation in a "glove and stocking" distribution, usually affecting the feet. Initially vibration sense, proprioception and light touch are lost, but over time, this can progress to an insensate foot that will be prone to trauma (Sugimoto *et al*, 2000). It is believed to results from reduced blood supply to the nerve via the *vasa nervosum*, due to the microcirculatory pathology. Other possibilities involve a deficiency in myoinositol, altering myelin synthesis, diminishing sodium-potassium adenine triphosphatase activity, chronic hyperosmolarity, leading to oedema of nerve trunks, and increased fructose and sorbitol (Quan, 2008).

Any of these factors can initiate a wound that can become chronic, due to repeated trauma. There is also an interruption of the inflammatory and proliferative phases of wound healing (Blakytny and Jude, 2006), as neutrophils and macrophages cannot adequately control the bacterial load of the wound, as glycosylation is inhibitory to phagocytic function, due to advanced glycation end products (AGE) (Schmidt *et al*, 1993). Glycosylated haemoglobin (HbA_{1C}) also causes red cells to become less pliable, resulting in reduced oxygen delivery and microvascular sludging (Candiloros *et al*, 1995).

1.3.9 Pressure ulceration

Pressure ulcers have been described as *decubitus* ulcers and pressure sores. Both terms have been interchangeable in the medical literature. Pressure sores have mulitfactorial causation. Many factors contribute to the development of a pressure

sore, but pressure leading to ischaemia and cell death is the final common pathway (Baranoski, 2006).

In the USA, the prevalence in nursing homes is 17-28%, amongst the neurologically impaired is 5-8% annually, and in acutely hospitalised patients, is 3-11% (Revis and Caffee, 2006). Anatomically, the hip and buttock region account for two-thirds of all pressure sores, with the ischial tuberosity, greater trochanter and sacral areas, most commonly affected. The lower extremity accounts for one quarter of pressure sores, with the malleolus, heel, knee and pre-tibial areas, usually affected. The remaining sores can occur at any place on the body, but with greater likelihood over a bony prominence (Barczak *et al*, 1997; Wilhelmi and Neumeister, 2008).

Pressure is exerted upon the skin, soft tissue, muscle and bone, by the weight of the individual onto the surface beneath. These pressures are often in excess of capillary filling pressure, approximately 32 mm Hg (Revis and Caffee, 2006). Tissues are capable of withstanding much higher pressures in short duration, with no lasting damage. However, sustained pressure, just above the capillary filling pressure, is enough to cause an ulcer. Shear forces and friction can aggravate the pressure effect, as can tissue maceration. Microcirculatory occlusion leads to tissue anoxia, cell death and ulceration. Irreversible changes can happen within 2 hours of uninterrupted pressure (Ryan, 2000).

In patients with normal mobility, sensation and mental faculty, pressure sores do not occur. Conscious and unconscious feedback allows individuals to adjust their weight to shift the pressure from one area to another and prevent damage. Individuals unable to avoid long periods of uninterrupted pressure, include the elderly, the neurologically impaired and patients hospitalised with acute illness. These are the groups most at risk of pressure sore development (Baranoski, 2006), who cannot protect themselves from the pressure exerted upon their bodies, unless they consciously change position or have assistance in doing so.

Although prolonged, uninterrupted pressure is the cause of a pressure sore, impaired mobility is probably the most common reason patients are exposed to it. Pressure effects can be augmented by bacterial contamination or macerated skin, due to urine and faecal incontinence, which may be high in these groups. Contractures and spasticity often contribute by rigidly holding a joint in flexion against a surface, and increasing the exposure to friction and shear forces (Klenck and Gebke, 2007).

1.4 Current treatment strategies

Due to the prolonged and excessive inflammation that perpetuates chronic wounds, current treatment strategies are aimed at reducing inflammation. Surgical debridement and wound care are aimed at decreasing the necrotic tissue and proteinase burden, thus providing a virtual resetting of the wound, to an acute healing phase (Menke *et al*, 2007). Other methods of debridement can include the use of larval therapy and wound dressings that can promote autolysis (Mumcuoglu, 2001). After suppression of the inflammatory response, current strategies include methods to replace the lost or abnormal dermis, with a synthetic or donor equivalent. Recent advances in wound dressings include acellular matrices, composed of GAG and collagen (Biobrane™, Smith & Nephew, UK), to provide a scaffold for native fibroblast growth (Balasubramani *et al*, 2001; Jones *et al*, 2002). Matrices containing cultured skin fibroblasts and keratinocytes (TransCyte™, Smith & Nephew, USA; MySkin™, CellTran Ltd., UK) have also been recently introduced (Moustafa *et al*, 2007; Tenenhaus *et al*, 2007).

To promote cellular proliferation and migration into the wound space, growth factors have also been studied in models of acute and chronic wound healing, both *in vitro* and *in vivo*. With the action of chronic wound proteinases, such as neutrophil elastase, and ROS, aforementioned, the levels of native growth factors are known to be reduced in the chronic wound environment (Yager *et al*, 1997; Wlashek *et al*, 1997; James *et al*, 2003; Moseley *et al*, 2004; Wlashek and Scharfetterr-Kochanek, 2005). Initial studies involving exogenous growth factors in impaired wound healing were initially disappointing, but as Falanga (1993) postulated "*If one looks at the development of most drugs, it becomes evident that an extended period of time is necessary before the proper use and full range of activities of the drug in treating human disease become apparent. In many cases, initial treatment failures are due to faulty expectations, as well as inadequate dosing and delivery systems. It is my opinion that growth factor therapy will follow a similar course but that it ultimately will have a role in the modulation of wound repair*".

1.4.1 Growth factors

In 1992, Pittelkow proposed seven growth factors - EGF, basic and acidic FGF, TGF-α and TGF-β, PDGF isoforms AA, -AB and -BB, and IGF, as being the

most promising as potential wound-healing agents (Pittelkow, 1992). To date, the only growth factor currently licensed for the treatment of chronic wounds in the UK and USA, is PDGF-BB (bacaplermin), in the form of a topical gel (Regranex™ 0.01% PDGF-BB; Johnson & Johnson, UK). In the UK, it is licensed as an adjunct treatment for full-thickness, neuropathic, diabetic ulcers (British National Formulary, 2008)

The pre-clinical development of Regranex™ involved multiple *in vitro* and *in vivo* studies (LeGrand, 1998). Regranex™ was shown to be a potent chemotactic, mitogenic, and activation agent for cell types (fibroblasts) thought to be essential in normal soft-tissue repair (Grotendorst *et al*, 1981; Deuel and Huang, 1982; Seppa *et al*, 1982). In animal models (rat, rabbit, pig, guinea pig, diabetic mouse), Regranex™ greatly accelerated normal tissue repair and reversed deficient repair in experimentally inflicted wounds, via the deposition of an enhanced provisional matrix and collagen (Pierce *et al*, 1988; 1989; Mustoe *et al*, 1989, 1991; Lynch *et al*, 1989; Senter *et al*, 1995; LeGrand, 1998).

Phase I/II clinical trials showed promising, but not significant, effects on wound healing in pressure ulcers, and no toxic effects were observed (Robson *et al*, 1992a; 1992b). Phase III studies of topical becaplermin in diabetic ulcers, in conjunction with good wound care, showed a significant decrease in the time for complete wound closure, with a safety profile similar to the placebo (Wieman *et al*, 1998). A meta-analysis of four phase III trials, involving 922 patients with diabetic ulcers, identified significant outcomes in small ulcers (< 1.5 cm^2), with enhanced wound closure, in conjunction with good wound care (Smiell *et al*, 1999). A phase IV clinical trial concluded that topical becaplermin should be used in diabetic ulcers that have not healed by more than 50 % after 4 weeks, using an appropriate wound treatment (Steed, 2006).

More recently, in March 2008, the Federal Drug Administration (FDA) reported an ongoing safety review of Regranex™, concluding that people who have used three or more tubes of becaplermin gel, and who have or develop cancer, are more likely to die from the cancer than people who have cancer, and who have not used becaplermin gel (Federal Drug Administration, 2008). However, despite these concerns, the product still remains licensed for use, at present.

The first clinical trials involving recombinant growth factors examined treatment with recombinant human EGF (rhEGF) of donor sites in patients who required skin grafting for either burns or reconstructive surgery (Brown *et al*, 1989). The topical effect of rhEGF, on wound healing, has been studied extensively in the literature (Figure 1.3). The topical application to acute wounds (Franklin and Lynch, 1979; Brown *et al*, 1989; Hong *et al*, 2006), has been shown to enhance healing. RhEGF has been available since 1984 (Brake *et al*, 1984), which led to a rapid upsurge in the wound healing research, relating to EGF. In the early 1990's, no significant effects of rhEGF in the treatment of chronic wounds was shown (Falanga *et al*, 1992), potentially due to growth factor degradation by chronic wound proteinases and ROS, thereby limiting rhEGF efficacy and bioactivity (Tarnuzzer *et al*, 1997; Wlascheck *et al*, 1997; Yager *et al*, 1997; Moseley *et al*, 2004; Wlaschek and Scharffetter-Kochanek, 2005).

rhEGF-containing topical gels for the treatment of diabetic foot ulcers are currently being marketed in India (ReGen-D™ 150; Bharat Biotech International, India), Cuba (Hebermin; Cuban Biotechnology, Cuba) and South Korea (E.G.F. Plus; Medikims Ltd., South Korea) (Mola *et al*, 2003; Frew *et al*, 2007). Although these products are gel matrices containing rhEGF, there is no chemical modification of the growth factor, or conjugation to the carrier matrix. In essence, these gels are a topical formulation of rhEGF that may be susceptible to the action of chronic wound proteinases. A phase IV clinical study (Krishna Mohan, 2007), has shown increased efficacy of one of the products (ReGen-D™ 150), in selected diabetic foot ulcers (< 200 cm^3, remaining unhealed after 2 weeks from diagnosis). A significant rate for wound size reduction was recorded, although time for total wound closure was similar to controls. This effect may be due to the short duration of rhEGF action, prior to possible proteolytic/ oxidative degradation. Stimulation of granulation tissue formation was noted to occur, but the rate of wound closure slowed as the study progressed (by the time 100% of the treated group had healed, over 90% of the control group had also healed without treatment). The study was also performed by the company that produced ReGen-D™, so a conflict of interest may exist, but such results are encouraging. Another rhEGF-related product (ReGen-D™ 60; Bharat Biotech International, India), is recommended for use in burn injury, but clinical trials are still in progress.

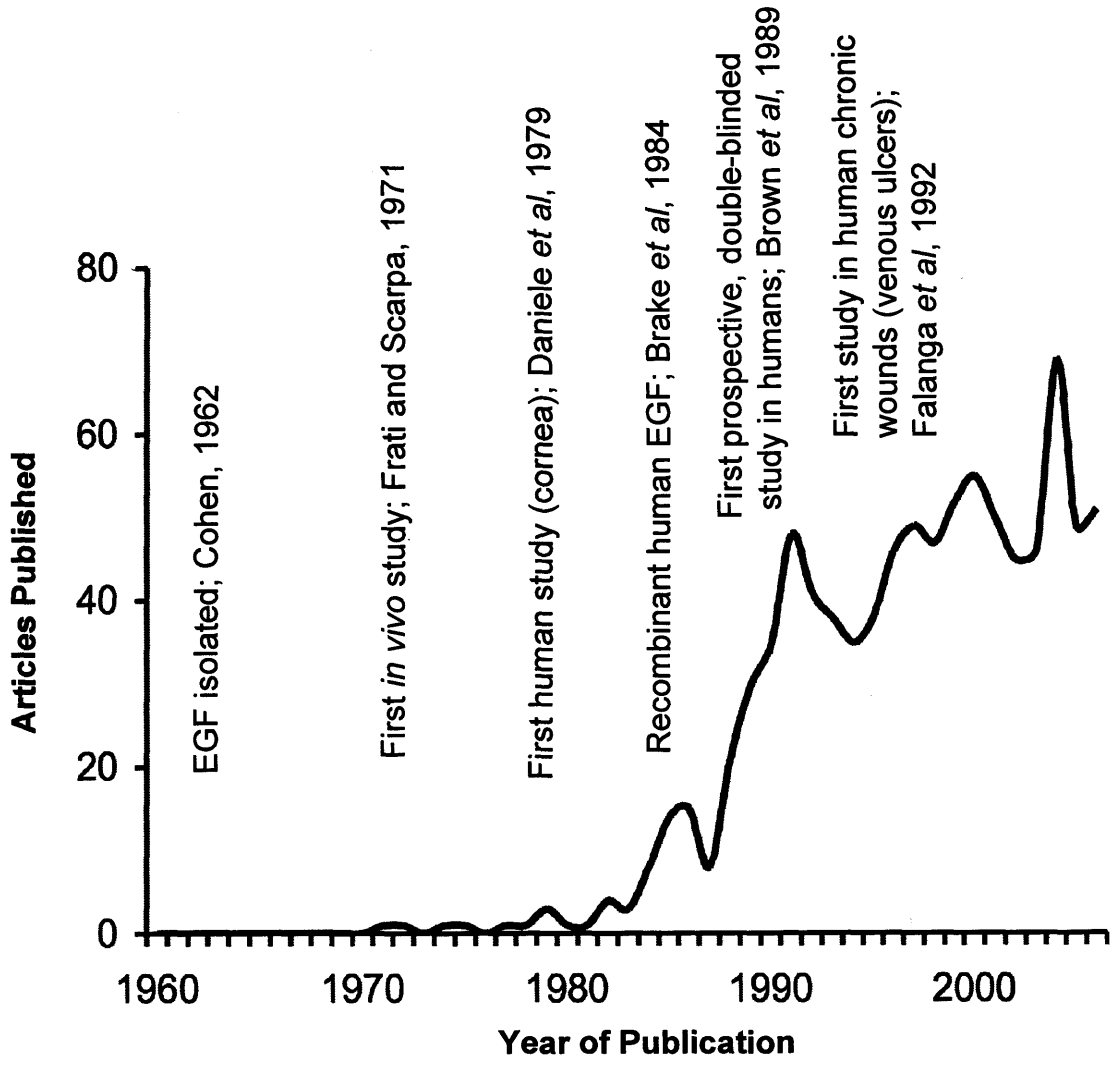

Figure 1.3 **The development of epidermal growth factor (EGF) in wound healing research.** A PubMed search was performed using the keywords [epidermal growth factor] + [EGF] + [wound] + [healing] and the number of articles per year published recorded. Seminal papers during this progression are noted.

1.4.2 Hypothesis of a polymer-rhEGF conjugate, as a novel therapy for chronic wounds

In this present Study, it is proposed that, by conjugating rhEGF to a polymer via reactive amine groups, the production of a polymer therapeutic agent could be a novel therapy for chronic wounds. Conjugation to a polymer may protect the rhEGF from proteolytic/oxidative degradation and allow the site-specific, controlled release of the growth factor. With the possibly enhanced stability of the protein, a reduced dose may be utilised to reduce unwanted side effects while, via the Enhanced Permeability and Retention (EPR) effect (Matsumura and Maeda, 1986) (*vide infra*), both systemic and topical delivery of the polymer therapeutic may be employed. The development of the conjugate will follow a similar stepwise plan as Regranex™, with initial *in vitro* studies leading to *ex vivo* and *in vivo* models of normal and impaired wound repair.

1.5 Polymer therapeutics as novel wound healing agents

The proposed polymer-rhEGF conjugate is a polymer therapeutic. This term encompasses many structures, including polymeric drugs, polymer–drug conjugates, polyplexes, polymer–protein conjugates and polymeric micelles. Figure 1.4 shows schematics for each of these polymer therapeutics.

Polymeric drugs are entities, which are biologically active in their own right. In this context, polymeric micelles are micelles in which a drug is covalently bound to the core of the micelle. Polymer-drug conjugates consist of a bioactive drug, covalently attached to a water-soluble polymer, through a spacer group. In order to target specific locations in the body, it is also possible to attach a targeting residue, which enhances receptor-mediated pinocytosis of the conjugate. Polymer-protein conjugates consist of a protein, conjugated to a water-soluble polymer (Duncan, 2003). These polymeric macromolecules are in the size range of one to hundreds of nanometres and are hence, referred to as nanomedicines (European Science Foundation, 2005).

1.5.1 Nanomedicines and wound healing

In recent years, there has been little published in relation to nanomedicines and wound healing. The majority of articles focus on non-dermal wound healing, for

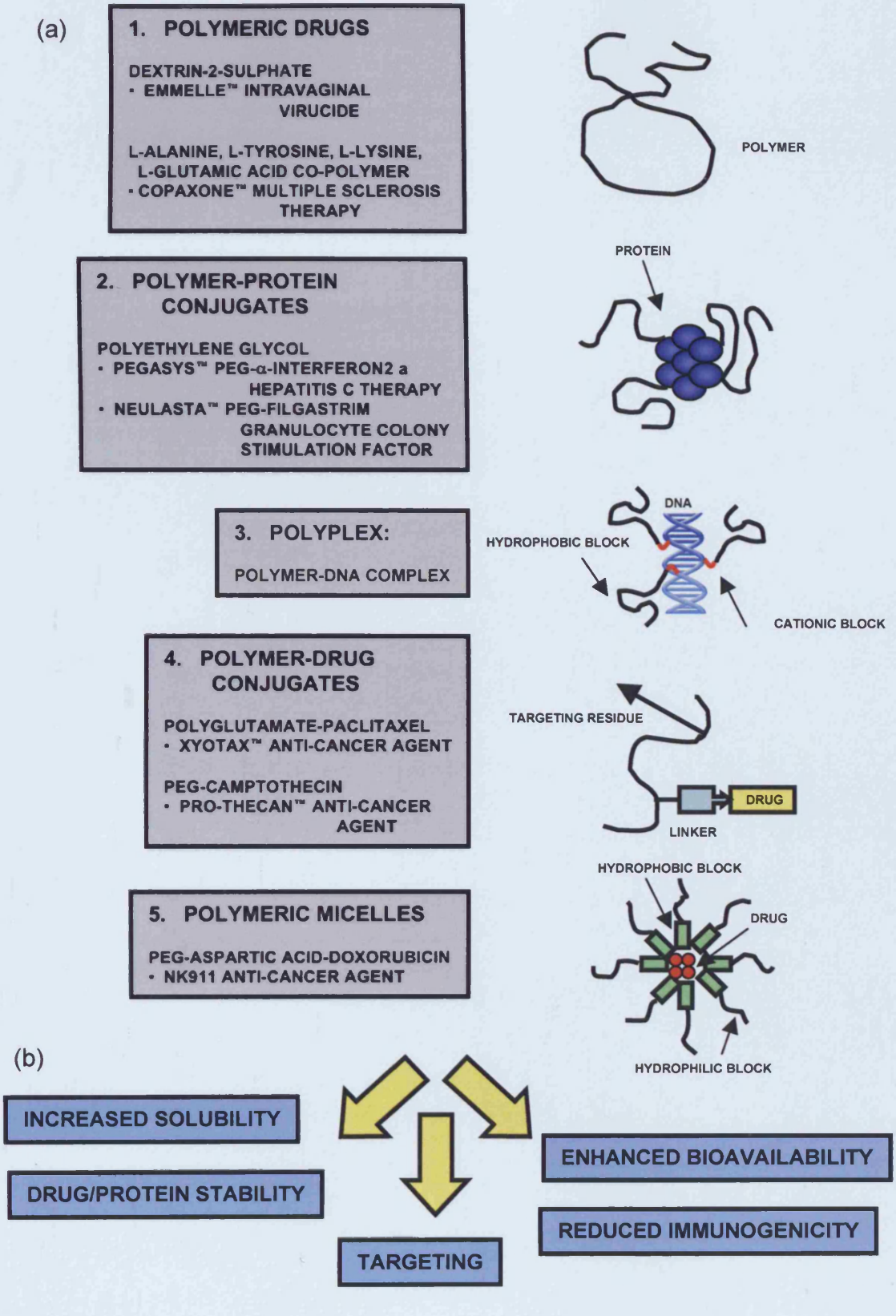

Figure 1.4 **Polymer therapeutics.** (a) The different classes of polymer therapeutics, with examples of entities that are either in clinical trials, or are licensed for use in the UK (adapted from Duncan, 2003). (b) Examples of the benefits of polymer therapeutics over traditional pharmaceutics.

example, spinal injury repair (Ellis-Behnke *et al*, 2006; Guo *et al*, 2007; Hampton, 2007). Nano-sized particles containing antibiotics or antimicrobials (Tian *et al*, 2005; Kim *et al*, 2007) can be applied to wound healing. Indeed, the use of silver nanoparticles, *in vivo*, has been shown to promote wound repair (Fong and Wood, 2006; Wong *et al*, 2006; Sibbald *et al*, 2007; Vlachou *et al*, 2007; Bhattacharyya and Bradley, 2008). A composite ECM (Han and Gouma, 2006), synthesised from cellulose acetate, has been electrospun to produce a urinary bladder matrix. Similar principles could be applied to the dermal ECM, as has been shown with electrospinning of various macromolecules (collagen, gelatins, chitosan) (Rho *et al*, 2006; Chong *et al*, 2007; Zhou *et al*, 2008). Accelerated wound healing has also been demonstrated using a self-assembling peptide nanoscaffold, in conjunction with rhEGF (Schneider *et al*, 2008). The reduction of scar tissue formation has also been noted with a variety of nanoscale materials (Shaunak *et al*, 2004; Webster, 2006).

1.5.2 Rationale for designing nanomedicines: The EPR effect

The underlying principle for attaching a protein to a polymer is that conjugation can extend the plasma half-life, reduce immunogenicity, mask protein charge, reduce toxicity, and can also allow passive targeting by the EPR effect (Matsumara and Maeda, 1986). Although originally described in the context of tumours, which tend to have an extensive and disorganised vasculature, compared to normal tissues, the process of neovascularisation that occurs in some wound healing states may mimic this (Nagy *et al*, 2008). The pathophysiology responsible for increased permeability can be attributed to an increase in fenestrae, a discontinuous basement membrane, enlarged inter-endothelial junctions and an increased number of vesicles (Hashizume *et al*, 2000; McDonald and Foss, 2000). Thus, the EPR effect can be exploited in the delivery of polymer therapeutics. While conventional, low molecular weight drugs, can pass readily through the bloodstream, into the tissue or be excreted, polymer therapeutics can accumulate in target tissues, due to the EPR effect (Seymour *et al*, 2002; Reddy, 2005). Although, initial studies will focus upon the topical application of polymer conjugates to the wound bed, the possible benefits of the EPR effect must also be considered in the drug design process.

1.5.3 Polymer-protein conjugates

Ever since dextran-streptokinase (Streptodekase®) was first used clinically (Torchilin *et al*, 1982), polymer therapeutics have become increasingly popular for delivering proteins, peptides and antibody-based therapeutics, with polymer-protein conjugates being the first polymer therapeutics to be used in practice. An ideal polymer-protein conjugate should be water-soluble, stable and bioactive. In addition, the polymer needs to be excreted safely following delivery of the protein payload (Veronese and Morpurgo, 1999).

1.5.4 Clinical development of polymer-protein conjugates

PEGylation was first proposed by Davis and Abuchowski in the 1970s (Abuchowski *et al*, 1977), and has since been used to deliver an extensive range of therapeutic proteins, enzymes, cytokines and monoclonal antibody (mAb) fragments. PEG is a pharmaceutical excipient that has been extensively studied as a protein conjugate. It is a flexible, water-soluble chain, which can extend to give a hydrodynamic radius many times greater than a globular protein of equal molecular weight. As such, PEG can conceal the protein to which it is bound (Veronese and Pasut, 2005).

In 1990, PEG-adenosine deaminase (Adagen™; Enzon Pharmaceuticals, USA) became the first polymer-protein conjugate to receive FDA approval. It is used for the treatment of severe combined immunodeficiency disease (SCID). Studies have demonstrated improved efficacy and reduced immunogenicity of Adagen®, than previous therapies, involving blood transfusion or administration of native enzyme (Hershfield *et al*, 1987; Chaffee *et al*, 1992). In Japan, in the 1980s, Maeda and colleagues synthesised styrene maleic anhydride neocarzinostatin (SMANCS), as an anticancer agent for localised administration via the hepatic artery, by covalently linking two styrene maleic anhydride chains (SMA) to neocarzinostatin (NCS), an anti-tumour protein (Maeda and Matsumara, 1989). Previously, NCS had proved to be too toxic for clinical use. However, following conjugation to SMA and subsequent dispersion in Lipiodol®, a phase contrast agent, it was possible to administer it specifically to liver tumour tissue, using visualisation by x-ray. It was licensed for use in Japan in 1993 (Duncan, 2003). Shortly after, a PEG-L-asparaginase conjugate (Oncaspar™; Enzon Pharmaceuticals, USA), received

approval by the FDA for the treatment of acute lymphoblastic leukaemia (ALL). Asparaginase is also available in a non-conjugated formulation, but Oncaspar™ demonstrates longer retention time in plasma, reduced immunogenicity and requires only a weekly administration, while unconjugated L-asparaginase requires daily administration and can induce anaphylaxis and other hypersensitivity reactions (Duncan, 2006; Pasut *et al*, 2008).

PEG has also been used to deliver cytokines, such as recombinant granulocyte colony-stimulating factor (GCSF) (Pegfilgrastim: Neulasta™, Amgen, UK; Kinstler *et al*, 2002), for the treatment of chemotherapy-induced neutropaenia. The PEGylated form of GCSF need only be administered as a single subcutaneous injection, while native GCSF requires daily dosing by injection for two weeks, to obtain equivalent prevention of neutropenia. Other polymer-protein conjugates that have come to the market are PEG-α-interferon 2a (Peginterferon alfa: Pegasys™, Roche Products Ltd., UK; Reddy *et al*, 2002) and PEG-α-interferon 2b (Peginterferon alfa: ViraferonPeg™, Shering-Plough, USA), for the treatment of both hepatitis B and hepatitis C, and PEG-human growth hormone antagonist, for the treatment of acromegaly (Pegvisomant: Somavert™, Pfizer, UK). Currently, all of the polymer-protein conjugates licensed for use in the UK (Neulasta™, Pegasys™, ViraferonPeg™ and Somavert™), are based on PEG conjugation.

Initially, polymer-protein conjugates were developed for the treatment of cancer and life-threatening, immunological and haematological disorders. More recently, their development has moved to the treatment of chronic diseases. However, there are presently no products in the wound management sector that are designed around a polymer therapeutic.

1.6 Rationale for design of polymer-rhEGF conjugates

From the viewpoint of the present Study, it was important to select the most appropriate polymer for conjugation to rhEGF, in order to fully achieve the therapeutic aim. Polymers are high molecular weight substances made from one or more small repeating units (monomers). There are many structures of polymers; and size, 3-D shape (including crosslinking) and asymmetry determine the properties of them. Homopolymers are chains of polymers containing one type of repeating monomer. Copolymers contain more than one monomer, and may be an alternating

copolymer chain, a block copolymer or a graft copolymer. The structure of the polymer also varies. It may be linear, star, branched or dendrimer (Duncan, 2005).

1.6.1 Biodegradable polymers for the masking/unmasking of rhEGF activity

Over recent years, the concept of using biodegradable polymers for the delivery of therapeutic proteins, has become increasingly attractive. The use of non- or slowly biodegradable polymers in macromolecular therapeutics, for an extended length of time, have the potential to cause the development of lysosomal storage disease (Chi *et al*, 2006), and, at high concentrations, may lead to other pathological metabolic changes (Miyasaki, 1975). In response to these issues, a number of polymers have been investigated as biodegradable carriers, including naturally occurring polysaccharides, such as dextran and dextrin (Schacht *et al*, 1987), and synthetic polymers, including polyglutamic acid (PGA) (Singer *et al*, 2003).

The aim of coupling a biodegradable polymer to rhEGF, via reactive amine groups, was to create a conjugate, which would not only benefit from the advantages of PEGylation, but also render rhEGF inactive, and thus, protect the active binding site from degradation by chronic wound proteinases and ROS, yet enable bioactivity to be reinstated at an appropriate rate, by triggered polymer degradation. Furthermore, since historical polymers for protein delivery were usually required to have a molecular weight of < 40,000 g/mol, to permit renal excretion, biodegradable polymers allow the selection of much larger polymers (Duncan, 2003).

1.6.2 Polymer masking UnMasking Protein Therapy (PUMPT)

The concept of PUMPT has recently been coined, using dextrin as a model polymer (Duncan *et al*, 2008). The hypothesis is that the conjugation of a biodegradable polymer to a biologically active protein can mask activity and enhance stability in the bloodstream, while subsequent regeneration of bioactivity can be achieved, by the triggered degradation of the polymer, at the target site. The main advantages, supporting the use of dextrin, are its multifunctionality and biodegradability. Multifunctionality allows the polymer to surround the protein, to "mask" protein activity and reduce immunogenicity, prior to "unmasking" of the protein, via degradation of the dextrin polymer at the site of action (Figure 1.5).

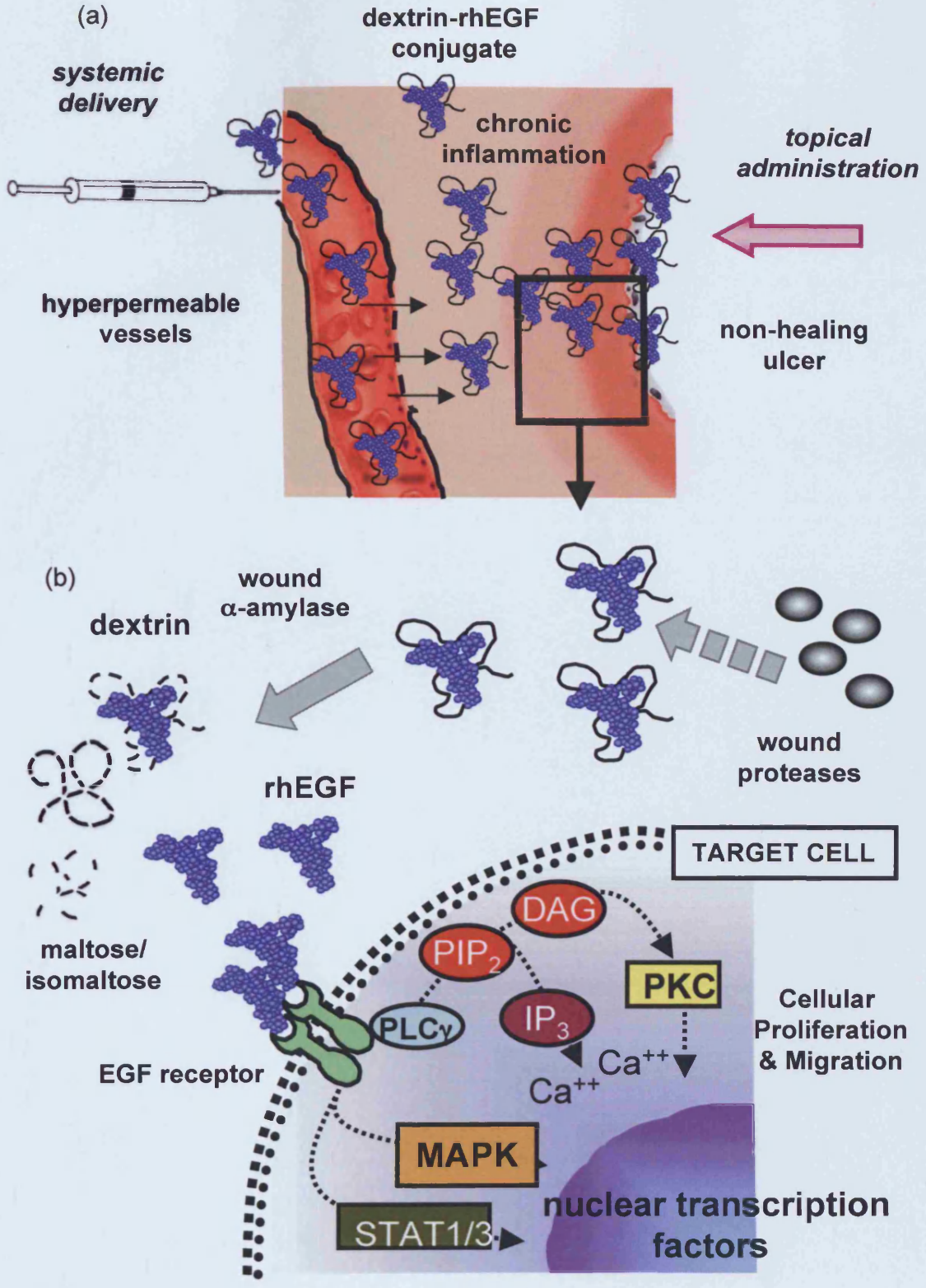

Figure 1.5 **The Polymer masking-UnMasking Protein Therapy (PUMPT) hypothesis.** Panel (a) shows conjugate delivery to the chronic wound by either topical, or systemic application, with passive accumulation by the EPR effect. Panel (b) shows the protection of rhEGF from proteolysis by the polymer, the release of rhEGF following exposure to wound fluid α-amylase, and the binding to the EGF receptor, with subsequent activation of intracellular pathways, leading to cellular proliferation and migration.

1.6.3 Dextrin

The polymer chosen as a model in the present Study was dextrin, a biodegradable polysaccharide produced from the enzymatic hydrolysis of cornstarch. Dextrin is a α-1,4 polymer of D-glucose, with less than 5 % α-1,6 links, resulting in minimal branching of the polymer. It is rapidly degraded by α-amylase, to yield the disaccharides maltose and iso-maltose, in just a few minutes (Hreczuk-Hirst *et al*, 2001a; 2001b). The amylases are a group of enzymes found in all living organisms, that breakdown starches into disaccharides, by acting upon α-1,4-glycosidic bonds. α-amylase is found in humans, although not exclusively, whereas β- and glucoamylase are found exclusively in plants and microorganisms (Janacek, 1997; Pandey *et al*, 2000). Studies on the α-amylase-mediated degradation of dextrin, have revealed that altering the degree of modification to the backbone by succinoylation can control the rate of enzymatic degradation (Hreczuk-Hirst *et al*, 2001a).

Dextrin was chosen as a model for these studies, as it has been used clinically for many years, is FDA approved and is Generally Recognised As Safe (GRAS), proving it to be non-toxic and non-immunogenic. Caloreen™ is composed of maltodextrin, and has been used as a dietary supplement in patients with renal and hepatic failure (Woolfson *et al*, 1976). Following successful clinical safety trials, icodextrin (Extraneal®, Baxter International, USA), a dextrin with a MW of ~ 20,000 g/mol, was approved for routine use as an intraperitoneal dialysis solution for chronic renal failure (Davies, 2006). Moreover, dextrin has also been used as a carrier for the delivery of 5-fluorouracil to the intraperitoneal cavity (Kerr *et al*, 1996; Hosie *et al*, 2003), and recent reports also describe dextrin's conjugation to various drugs, including doxorubicin, tyrosinamide and biotin (Hreczuk-Hirst *et al*, 2001b), and proteins, including trypsin and melanocyte-stimulating hormone (Duncan *et al*, 2008).

1.7 Aims of the study

The aim of this Study is to determine the potential of a novel polymer therapeutic strategy (PUMPT) for further development as a new treatment for chronic wounds. Dextrin has been selected as the most suitable polymer, and rhEGF selected as an appropriate growth factor, as it is known to promote wound repair, both *in vitro* and *in vivo*. A PUMPT agent will be synthesised and evaluated as

Chapter Two: General Materials And Methods

Contents

2.1 Chemicals

2.1.1 General chemicals, polymers and reagents

Recombinant human epidermal growth factor (rhEGF) was obtained from Prospec-Tany Technogene Ltd, (Rehovot, Israel) and type 1 dextrin from corn, was supplied by ML Laboratories (Liverpool, UK). Alexa Fluor® 488 dye-labeled EGF (EGF-Alexa488) was purchased from Molecular Probes (Invitrogen). 4-dimethylaminopyridine (DMAP), ethanol, methanol, acetic acid (glacial), anhydrous N,N-dimethylformamide (DMF), sodium chloride, diethyl ether, succinic anhydride, sodium dodecyl sulphate (SDS), anhydrous dimethylsulfoxide (DMSO), Tris hydrochloride (Tris-HCl), 1-ethyl-3- [3-dimethylaminopropyl] carbodiimide hydrochloride (EDC), Triton X100, tween 20, glycerol, dithiothreitol (DTT), ethylenediaminetetraacetic acid (EDTA), copper (II) sulphate pentahydrate (4% w/v solution), human neutrophil elastase, human salivary α-amylase, ninhydrin, hydrindantin, paraformaldehyde, lithium acetate dihydrate, 98% sodium hydroxide (NaOH), bicinchoninic acid solution (BCA), carboxymethylcellulose sodium salt, leupeptin, aprotinin (from bovine lung), cytochrome C (from bovine heart), carbonic anhydrase (from bovine erythrocytes), bovine serum albumin (BSA), and alcohol dehydrogenase (from *Saccharomyces cerevisiae*), were all purchased from Sigma-Aldrich (Poole, UK). Bromothymol blue was purchased from BDH Chemicals Ltd. (Poole, UK). *N*-hydroxysulfosuccinimide (sulfo-NHS) was obtained from Fluka (Gillingham, UK). DL-amino-2-propanol was purchased from Acros (Loughborough, UK). Marvel® dried skimmed milk powder was purchased from Cadbury (Birmingham, UK). Vectashield® mounting medium ± DAPI, was purchased from Vector Laboratories Ltd. (Peterborough, UK). Methoxy-alanine-alanine-proline-valine-7-amino-4-methylcoumarin was purchased from Bachem UK Ltd. (Liverpool, UK). 10% buffered formalin was obtained from Bios Europe, Skelmersdale, UK. Nitrogen gas was purchased from BOC (Guildford, UK). Unless otherwise stated, all chemicals were of analytical grade.

2.1.2 Chemicals for cell culture

Tissue culture grade DMSO, 3-[4,5-dimethylthiazol-2-yl]-2,5 diphenyltetrazolium bromide (MTT) and 0.02% trypan blue solution, were purchased from Sigma-Aldrich.

2.2 Cells and tissue culture media

Human epidermoid carcinoma (HEp2) (ATCC No: CCL-23) and Eagle's minimum essential media (EMEM), with L-glutamine and Earle's balanced salt solution, adjusted to contain 1.5 g/L sodium bicarbonate, non-essential amino acids, and sodium pyruvate, were purchased from LGC Promochem (Teddington, UK). Human HaCaT keratinocytes (Boukamp *et al*, 1988) and hTERT-immortalised, chronic wound fibroblast cell lines and patient-matched, normal dermal fibroblasts were donated by Dr. Ivan Wall and Dr. Mathew Caley (Wound Biology Group, Tissue Engineering and Reparative Dentistry, School of Dentistry, Cardiff University). Epilife® medium and HKGS kit (bovine pituitary extract, bovine insulin, hydrocortisone, bovine transferrin), were obtained from Cascade Biologics (Mansfield, UK). Dulbecco's minimum essential media (DMEM), Ham's F12 nutrient media, Trypsin-EDTA, penicillin G, streptomycin sulphate, amphotericin B, hydrocortisone, adenine, cholera toxin, insulin and foetal calf serum (FCS) were purchased from Invitrogen (Paisley, UK). Balanced salt solution (BSS Plus®) was purchased from Alcon Laboratories (Hemel Hemstead, UK).

2.3 Antibodies and enzyme-linked immunosorbant assay (ELISA)

The antibodies, anti-EGFR (phosphoY1173; anti-human, polyclonal IgG antibody, raised in rabbit), anti-STAT3 (phospho Y705; anti-human, polyclonal IgG antibody, raised in rabbit) and anti-CD31 (anti-mouse, polyclonal IgG antibody, raised in rabbit), were purchased from Abcam (Cambridge, UK). The antibodies, anti-actin (C-2; anti-human, monoclonal IgG antibody, raised in mouse), and anti-EGFR (F4; anti-human, monoclonal IgG, raised in mouse) and K562 and A431 whole cell lysates, were purchased from Santa Cruz Biotechnology (Santa Cruz, USA). Horseradish peroxidase-conjugated secondary antibodies (anti-rabbit, polyclonal IgG antibody, raised in goat; and anti-mouse, polyclonal IgG antibody, raised in goat) were obtained from Dako UK Ltd. (Ely, UK). A human EGF-ELISA kit was purchased from R&D Systems (Abingdon, UK).

2.4 Animals

Two-month old male Wistar Han rats were purchased from Charles River Laboratories (Margate, UK) and male diabetic mice (C57BLKs/Bom db/db; 12-13 weeks old) were purchased from The Jackson Laboratory (Bar Harbor, USA).

2.5 Equipment

2.5.1 Equipment for cell culture

With the exception of centrifugation steps, all cell culture was performed under sterile conditions, in a Class II, laminar flow Astec Microflow 2 cabinet (Bioquell UK, Andover, UK). All flasks and plates were maintained in a NuAire air-jacketed DH autoflow automatic CO_2 incubator, at 37°C/5% CO_2 (NuAire, Plymouth, USA). For general cell culture, an Olympus CK2 inverted bright field microscope was used (Olympus UK Ltd., Watford, UK). For routine cell counting, a Marienfield silver stained Neubauer haemocytometer (Lauda-Königshofen, Germany) was used. Tissue culture flasks (25, 75 and 175 cm^3), tissue culture sterile plates (12-well and 96-well), sterile pipettes (5, 10 and 25 mL), 100 mm Petri dishes, cryovials, sterile cell scrapers, kwills, universal containers, sterile centrifuge tubes (15 and 60 mL) and 7mL bijoux, were all purchased from Greiner Bio-One (Stonehouse, UK).

2.5.2 Analytical Equipment

2.5.2.1 Spectrophotometry: Ultraviolet-visible.

A UV-visible plate reader (Sunrise Touchscreen) was purchased from Tecan (Reading, UK). A UV-visible spectrophotometer (Cary 1G) was purchased from Varian Inc. (Walton-on-Thames, UK), with software version 2.0. A Dynex MRX Spectrophotometer (Dynex Technologies, Billinghurst, UK), equipped with a 540 nm filter, and a Fluostar Optima Microplate Reader (BMG Labtech, Aylesbury, UK), equipped with 520 nm and 620 nm filters, were also used.

2.5.2.2 Infrared (IR) spectroscopy

The FT-IR spectrophotometer (Avatar 360) was obtained from Thermo-Nicolet (Hemel Hemstead, UK), fitted with a Nicolet Smart Arc diffuse reflectance accessory. Nicolet E-Z Omnic ESP 5.2 software was used for data collection.

2.5.2.3 Fluorescence

A Fluostar Optima Microplate Reader (BMG Labtech), equipped with an excitation and emission filters, at 485 nm and 520 nm, respectively, was used for fluorescence analysis.

2.5.2.4 Sodium dodecyl sulphate-polyacrylamide gel electrophoresis (SDS-PAGE)

All electrophoresis equipment, including a Power Pac 300, Protean II electrophoresis tank and GelAir Drying Frame, were purchased from Bio-Rad Laboratories Ltd. (Hemel Hemstead, UK).

2.5.2.4 Gel permeation chromatography (GPC)

The aqueous GPC was equipped with a JASCO HPLC pump and two TSK-gel columns in series (4000 PW, followed by 3000 PW) and a guard column (progel PWXL), were purchased from Polymer Laboratories (Church Stretton, UK). The eluate was monitored using a differential refractometer (Gilson 153, Gilson, Inc., Middleton, USA) and a UV-vis spectrophotometer at 279 nm (UV Severn Analytical SA6504, Severn Analytical, Gloucester, UK), in series. PL Caliber Instrument software, version 7.0.4, obtained from Polymer laboratories (Church Stretton, UK), was used for data analysis.

2.5.2.6 Fast protein liquid chromatography (FPLC)

An ÄKTA FPLC system, purchased from GE Healthcare (Amersham, UK), was used. The unit was connected to a pre-packed Superdex 75 10/300 GL column and a Frac-950 fraction collector (GE Healthcare). The UV detector data was collected using Unicorn 3.20 software and analysed using FPLC director®, version 1.10 software.

2.5.2.7 Flow cytometry

Receptor-binding and uptake studies were performed using a Becton Dickinson FACSCalibur cytometer (Oxford, UK) equipped with an argon laser (488 nm) and emission filter (550 nm). Data were acquired in 1024 channels, with band pass filters (FL-1 530 nm ± 30 nm; FL-2 585 ± 42 nm; FL-3 670 nm long pass filter). Data were processed using CELLQuest®, version 3.3 software.

2.5.2.8 Centrifugation

A Precision Durafuge 200 (Thermo Fisher Scientific, Waltham, USA) was used for centrifugation at 1500 *g*; a Varifuge 3.0 (Heraeus Sepatech GmbH,

Osterode, Germany) at 4000 *g;* and an Eppendorf 5415-R (Eppendorf, Hamburg, Germany), at 15,000 *g* / 4°C.

2.5.2.9 Microscopy

Confocal microscopy was performed with a Leica TCS SP5 work-station, equipped with Leica DMI4000B Microscope, a 400-700 nm laser, a 350-700 nm laser and a 350-1050 nm laser, and run with Leica Application Suite Advanced Fluorescence (LAS AF) software (Leica Microsystems (UK) Ltd., Milton Keynes, UK). A microtome was also purchased from Leica Microsystems (UK). Time-lapse microscopy was performed using automated time-lapse microscope (Zeiss Axiovert 200M Inverted Microscope with XL-3 Incubator Housing, Carl Zeiss Ltd., Welwyn Garden City, UK; using Openlab 5 software, Improvision Ltd., Coventry, UK). An operating microscope (Stemi 2000-C) was also obtained from Carl Zeiss Ltd., and images recorded with a Nikon Coolpix 4500 digital camera (Nikon UK, Kingston-upon-Thames, UK). Fluorescein staining of specimens was performed with a Fluorets® Sterile Ophthalmic Strip (Chauvin Pharmaceutics, Kingston-upon-Thames, UK), and images recorded, under an ultraviolet light source, at 365nm (UVP Ltd., Cambridge, UK). BD Falcon CultureSlides® were obtained from BD Biosciences (London, UK).

2.5.2.10 Miscellaneous equipment

The pH meter (3150 pH meter) was purchased from Jenway (Leeds, UK). The Flexi Dry FD-1.540 freezer-dryer was obtained from FTS Systems (Stone Ridge, NY, USA), connected to a high vacuum pump (DD75 double stage), purchased from Javac (Middlesbrough, UK). Dialysis membranes Spectra/POR® CE (Cellulose Ester, molecular weight cut-off; MWCO = 10,000 g/mol) and Universal Closures were purchased from Pierce & Warriner (Chester, UK). Polyvinyl difluoride (PVDF) dialysis membrane (MWCO = 250,000 g/mol) was purchased from Fisher Scientific (Loughborough, UK). Black 96-well analytical plates were from Greiner Bio-One. Vivaspin 6 centrifugal concentrators were obtained from Sigma-Aldrich. Filters (0.2 μm) were purchased from Millipore (Watford, UK). Ready Gel® 4-15% Tris-HCl electrophoresis gels, Kaleidoscope Pre-stained Standards, a Trans-Blot Semi-Dry Electrophoretic Transfer Cell System

and the Bio-Rad DC Protein Assay were obtained from Bio-Rad Laboratories Ltd. A W-220F sonicator was obtained from Misonix, Farmingdale, USA. Amersham Hybond-P PVDF membrane, ECL Plus Western Blotting Detection Reagents and Hyperfilm ECL were purchased from G.E. Healthcare. A Curix 60 autodeveloper was obtained from Agfa-Gevaert (Mortsel, Belgium). Release® non-adherent and Bioclusive® film dressings were purchased from Johnson & Johnson Wound Management (Gargrave, UK). The Phadebas® Amylase Assay Kit was purchased from Magle Life Sciences (Lund, Sweden) and the EnzChek® Elastase Assay Kit was obtained from Molecular Probes (Invitrogen). An ultra-fine micro-knife (15° cutting angle, 5mm blade) was obtained from Fine Science Tools (Heidelberg, Germany). Cyanoacrylate adhesive gel was purchased from Henkel Loctite Adhesives Ltd. (Hemel Hemstead, UK). Surgical scalpels (15-blade) were purchased from Swann-Morton (Sheffield, UK). Cotton swabs were purchased from Medical Wire and Equipment Co. Ltd. (Corsham UK). Needles and syringes were purchased from Tyco Healthcare (Gosport, UK). Jackson-Pratt® surgical drains were purchased from Cardinal Health (Basingstoke, UK).

2.5.2.11 Image analysis software

Images (movies and stills) were processed and analysed using QuickTime® (version 7.1.5, Apple Computer, Inc, Cupertino, USA), Adobe Photoshop® (CS3; Adobe Systems Incorporated, San Jose, USA), and ImageJ® (1.37v; http://rsb.info.nih.gov/ij/), including MTrackJ plugin software (Erik Meijering; http://www.imagescience.org/meijering/ software/mtrackj/). Image Pro® image analysis software (version 4.1.0.0, Media Cybernetics, Bethesda, USA) was used for *in vivo* wound closure analysis.

2.6 Methods

This Section provides a detailed description of the general methods used in these Studies. Specific methods are described, as they are utilised in each Chapter. Methods used for conjugate synthesis and purification are described in detail in Chapter 3 (Section 3.2). However, the methods used for conjugate characterisation are described here, as these techniques apply for all the methods explored for polymer-protein conjugation.

2.6.1 Purification of the dextrin-rhEGF conjugate

Several methods were used to purify the dextrin-rhEGF conjugate to remove salts, unreacted protein and linking agents (Chapter 3). FPLC, in conjunction with ultra-filtration, was later chosen as the method of choice.

2.6.1.1 Purification of the dextrin-rhEGF conjugate, by FPLC

An ÄKTA FPLC system was used to separate free rhEGF and conjugated dextrin-rhEGF, according to their respective molecular weights. A pre-packed Superdex 75 10/300 GL column was washed with 2 column volumes (~ 48 mL) of filtered (0.2 μm) and degassed double-distilled water (ddH_2O). Next, the column was equilibrated with 3 column volumes (~ 72 mL) of filtered and degassed mobile phase, phosphate buffered saline (PBS, pH 7.4), prior to use. First, the column was calibrated (0.5 mL/min flow rate), using standardised proteins of various molecular weight: rhEGF, 6,200 g/mol; cytochrome C (from bovine heart), 12,400 g/mol; carbonic anhydrase (from bovine erythrocytes), 29,000 g/mol; albumin (from bovine serum), 66,000 g/mol; and alcohol dehydrogenase (from *Saccharomyces cerevisiae*), 150,000 g/mol (Figure 2.1a). A typical calibration curve is shown in Figure 2.1b. Dextrin-rhEGF samples (1 mL) were subsequently injected into a 2 mL loop ("partial fill" method) and allowed to run at a flow rate of 0.5 mL/min. When the conjugates were being purified, fractions (1 mL) were collected, corresponding to the dextrin-rhEGF fractions (6-9 mL), which were further purified by ultra-filtration, using Vivaspin 6 centrifugal concentrators. Other reactant fractions: free rhEGF (14-16 mL), DMAP (19-21 mL), sulfo-NHS (15-17 mL), were discarded.

The dextrin-rhEGF conjugate fractions were transferred to the Vivaspin 6 centrifugal concentrator, using a pipette and centrifuged at 4000 *g* for 10 min. The resulting sample was resuspended in 5 mL ddH_2O and the process repeated 5 times. Finally, the ultra-filtered sample was lyophilised over night, and stored at 4 °C, until required for further characterisation.

The limit of detection of rhEGF was determined using serial dilutions of rhEGF (40, 8, 1.6 and 0.32 μg/mL, in PBS). Peak heights were recorded and the limit of detection determined when no visible peak was detected, corresponding to free

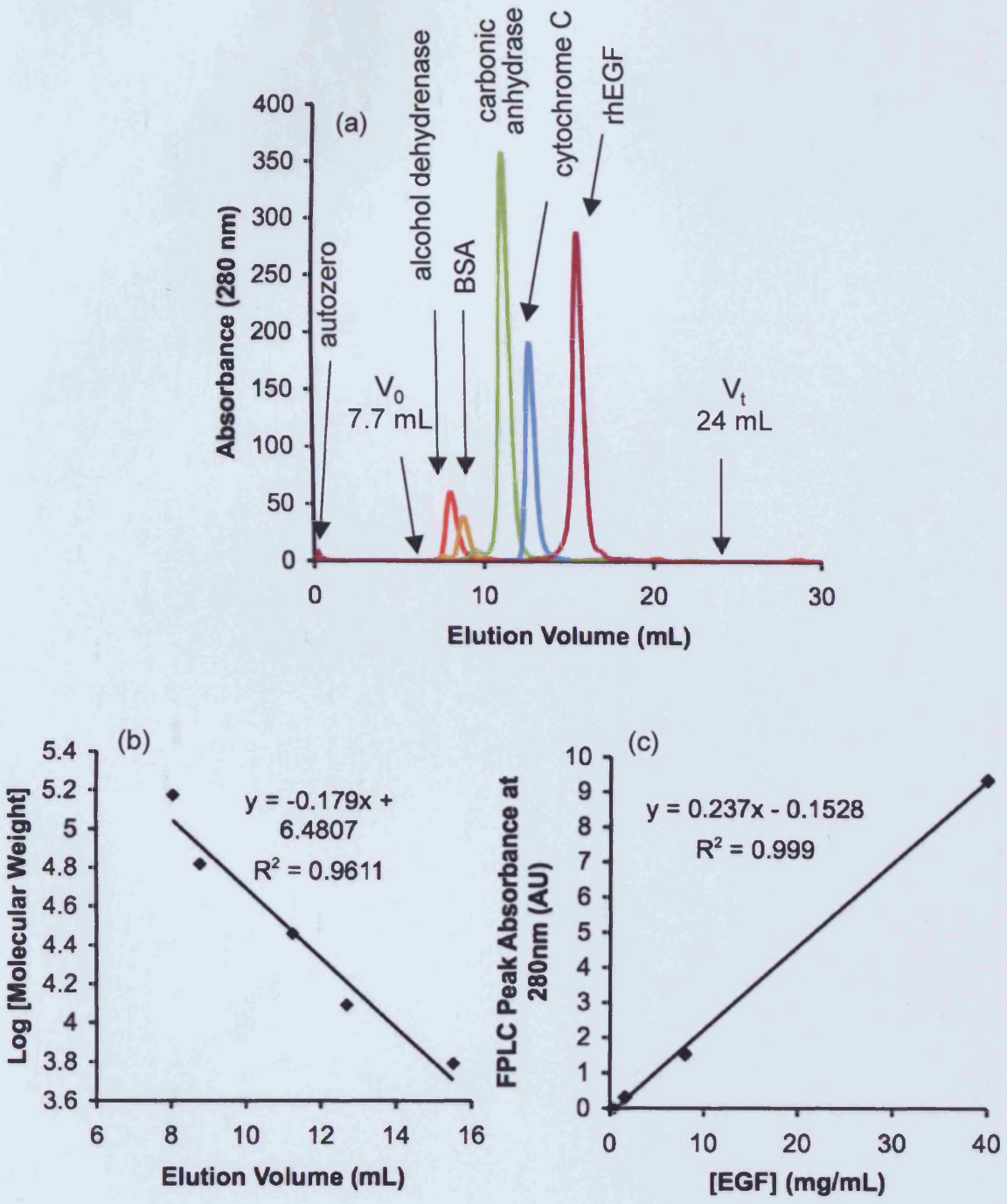

Figure 2.1 **Fast protein liquid chromatography (FPLC).** Panel (a) shows the calibration chromatogram, using protein standards: alcohol dehydrogenase, 150,000 g/mol; bovine serum albumin (BSA), 66,000 g/mol; carbonic anhydrase, 29,000 g/mol; cytochrome C, 12,400 g/mol; recombinant human epidermal growth factor (rhEGF), 6,200 g/mol. V_0 denotes the void volume and V_b, the bed volume. Panel (b) shows a typical calibration curve using the protein standards. Panel (c) shows the limit of detection for rhEGF, by FPLC, calculated to be approximately 0.7 μg/mL.

rhEGF (Figure 2.1c). The rhEGF limit of detection was 0.7 μg/mL. After use, the column was thoroughly washed with eluant, followed by ddH_2O, and finally stored in 20 % v/v ethanol.

2.6.2 Characterisation of the dextrin-rhEGF conjugate

Once synthesised, it was necessary to characterise the dextrin-rhEGF conjugates, in respect of their conjugate protein content, free protein content, molecular weight and polydispersity.

2.6.2.1 GPC and FPLC characterisation of the conjugate molecular weight

Polymer-protein conjugates are notoriously difficult to characterise, as they are neither protein nor polymer. Therefore, while it was not possible to accurately assign the molecular weight of the synthesised conjugates, GPC and FPLC were used in combination with SDS-PAGE, to quantitatively define the molecular weight of the conjugates and their purity, in respect of free rhEGF. The BCA assay was used to quantify the total protein content of the conjugates.

2.6.2.1.1 Characterisation by GPC

GPC, with a refractive index (RI) detector, is commonly used to separate polymers, according to their size and shape (hydrodynamic radius). Polysaccharide (pullulan) standards (molecular weights ranging from 11,800 to 210,000 g/mol), were used to produce a calibration curve (Figure 2.2). All samples were prepared in PBS (3 mg/mL). Of these solutions, approximately 60 μL was injected into the sample loop. PBS (filtered and degassed) was used as the mobile phase (flow rate 1.0 mL/min). Both RI and UV detection (at 279 nm) were used and the data analysed using PL Caliber Instrument software.

2.6.2.1.2 Characterisation by FPLC

FPLC, with a UV detector, was also used to estimate the dextrin-rhEGF conjugate molecular weight, in comparison to protein standards of various molecular weights (detailed in Section 2.6.1.1) and to measure the ratio of free and bound protein. The same FPLC system, used for purification, was used for characterisation.

rhEGF (Figure 2.1c). The rhEGF limit of detection was 0.7 μg/mL. After use, the column was thoroughly washed with eluant, followed by ddH_2O, and finally stored in 20 % v/v ethanol.

2.6.2 Characterisation of the dextrin-rhEGF conjugate

Once synthesised, it was necessary to characterise the dextrin-rhEGF conjugates, in respect of their conjugate protein content, free protein content, molecular weight and polydispersity.

2.6.2.1 GPC and FPLC characterisation of the conjugate molecular weight

Polymer-protein conjugates are notoriously difficult to characterise, as they are neither protein nor polymer. Therefore, while it was not possible to accurately assign the molecular weight of the synthesised conjugates, GPC and FPLC were used in combination with SDS-PAGE, to quantitatively define the molecular weight of the conjugates and their purity, in respect of free rhEGF. The BCA assay was used to quantify the total protein content of the conjugates.

2.6.2.1.1 Characterisation by GPC

GPC, with a refractive index (RI) detector, is commonly used to separate polymers, according to their size and shape (hydrodynamic radius). Polysaccharide (pullulan) standards (molecular weights ranging from 11,800 to 210,000 g/mol), were used to produce a calibration curve (Figure 2.2). All samples were prepared in PBS (3 mg/mL). Of these solutions, approximately 60 μL was injected into the sample loop. PBS (filtered and degassed) was used as the mobile phase (flow rate 1.0 mL/min). Both RI and UV detection (at 279 nm) were used and the data analysed using PL Caliber Instrument software.

2.6.2.1.2 Characterisation by FPLC

FPLC, with a UV detector, was also used to estimate the dextrin-rhEGF conjugate molecular weight, in comparison to protein standards of various molecular weights (detailed in Section 2.6.1.1) and to measure the ratio of free and bound protein. The same FPLC system, used for purification, was used for characterisation.

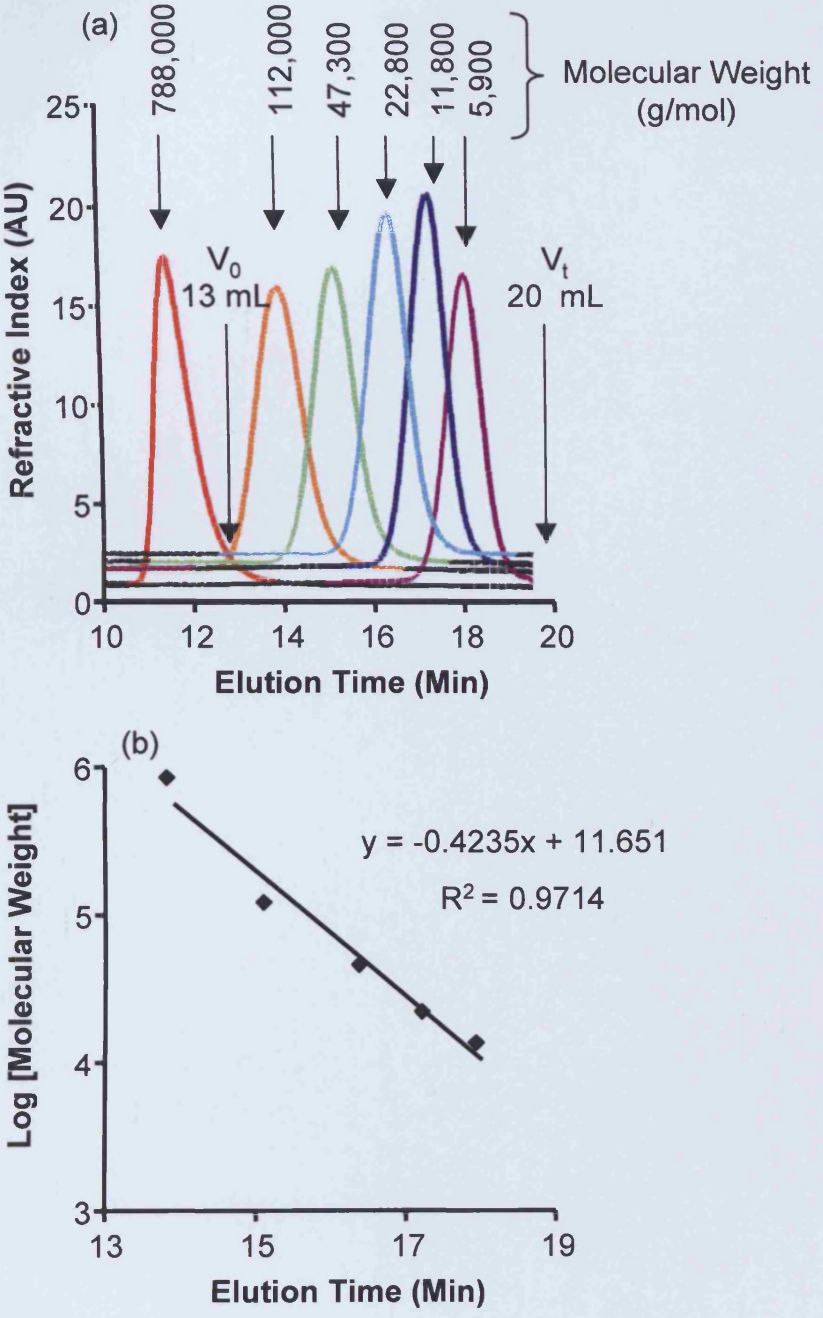

Figure 2.2 **GPC analysis of pullulan molecular weight standards,** using TSK gel columns G4000 PWXL and G3000 PWXL in series. Panel (a) shows the chromatogram of the pullulan standards (5,900 - 788,000 g/mol). Panel (b) represents a typical calibration curve for the estimation of sample molecular weight.

After appropriate equilibration and calibration, samples of purified conjugate (200 μL) were injected into the sample loop and allowed to run at a flow rate of 0.5 mL/min.

2.6.2.2 SDS-PAGE

The method was adapted from one described by Laemmli (1970). This method was used for both characterisation of the dextrin-rhEGF conjugate and for electrophoresis of cell lysates, prior to Western blot analysis (Chapter 5). Pre-cast, 4-15% Tris-HCl electrophoresis gels were used, in conjuction with Kaleidoscope Pre-stained standards (myosin, 197,211 g/mol; β-galactosidase, 125,275 g/mol; BSA, 83,426 g/mol; carbonic anhydrase, 37,095 g/mol; soybean trypsin inhibitor, 31,168 g/mol; lysozyme, 17,154 g/mol; and aprotinin, 6,990 g/mol).

Gels were prepared, as per the manufacturer's instructions, transferred to the electrophoresis tank and the tank filled with running buffer (0.25 M Tris-HCl, 1.92 M glycine in ddH_2O, 1 % SDS, pH 8.3). rhEGF (1 mg/ml) and dextrin-rhEGF conjugate (1 mg/mL rhEGF equivalent) were snap frozen, lyophilised, reconstituted in 20 μL of denaturing buffer (4 % SDS, 20 % glycine, 10 % 2-mercaptoethanol, 0.004 % bromophenol blue, 0.125 M Tris-HCl, in ddH_2O, pH 6.8), heated (100 °C, 5 min) and microcentrifuged (10 s). The prepared samples and molecular weight standards (10 μL) were added to the sample wells, using a microsyringe and separated by electrophoresis, at 200 V for 1 h. The gels were removed from the glass templates, rinsed with ddH_2O and stained (1 h) with 200mL of 1 % Coomassie Blue solution (in 50 % methanol, 10 % acetic acid). After destaining in 35 % methanol/5 % acetic acid solution and rehydration in 5 % methanol/7 % acetic acid solution, the gels were rinsed in ddH_2O and air-dried (2 days) between cellophane sheets, clamped in a GelAir Drying Frame. The limit of detection of rhEGF by SDS-PAGE was further determined with lyophilised samples of rhEGF (10, 5, 2.5, 1.25, 0.63, 0.31, 0.16, 0.08 μg), reconstituted in 20 μL of denaturing buffer, described above. The limit of detection was determined when no visible band, corresponding to rhEGF, was detected. This was estimated to occur at 200 ng rhEGF.

2.6.2.3 BCA protein assay

The BCA assay was used to determine the total protein content of the polymer-protein conjugates (Smith *et al*, 1985). The assay consists of two steps. First, the protein reduces the Cu^{2+} to Cu^{+} by the biuret reaction. The resulting Cu^{+} forms a coloured coordination complex with four to six nearby peptide bonds. Next, the BCA forms complexes with the remaining Cu^{2+}, which produces a purple coloured solution, detectable at 562 nm. The intensity of the colour is directly proportional to the number of peptide bonds participating in the reaction (Figure 2.3).

In a 96-well microtitre plate, calibration curves, using BSA and rhEGF as standards, were constructed over a range of concentrations (0.05–1 % w/v) (Figure 2.4a). Conversion of [BSA] to [rhEGF] was performed using a standard conversion factor, to allow calibration curves to be utilised with BSA, rather than rhEGF, typically using the equation below:

$$[\text{rhEGF}] = ([\text{BSA}] \times 0.6477) + 0.004$$

Reference wells of 20 μL volume were established in triplicate, using a range of BSA concentrations, diluted in PBS (0–1 mg/mL BSA). Samples of the dextrin-rhEGF conjugate (20 μL, 1 mg/mL) and rhEGF (20 μL, 1 mg/mL) were used for analysis. BCA reagent (200 μL; ratio 1 mL BCA: 20 μL $CuSO_4$) was added to each well. Each plate was lightly agitated and incubated in the dark, for 20 min at 37°C. The absorbance of each well was quantified using a Tecan Spectrophotometer, equipped with a 550 nm filter. The limit of detection of rhEGF by the BCA assay was determined by serial dilution of a rhEGF sample (50 μg/mL). At the point where there was no significant difference between a blank well and a sample well, the detection limit was said to have been reached (1.56 μg/mL; Fig. 2.4b).

2.6.2.4 Bio-Rad DC protein assay

The Bio-Rad DC protein assay was used as an alternative to the BCA assay, for protein quantification of cell lysate samples (Chapter 5), where a high concentration of DTT (1 mM), in the protein extraction buffer, would give false positive readings. This is a colourimetric assay based upon the reaction of protein with an alkaline copper tartrate solution and folin reagent. Colour development (pale

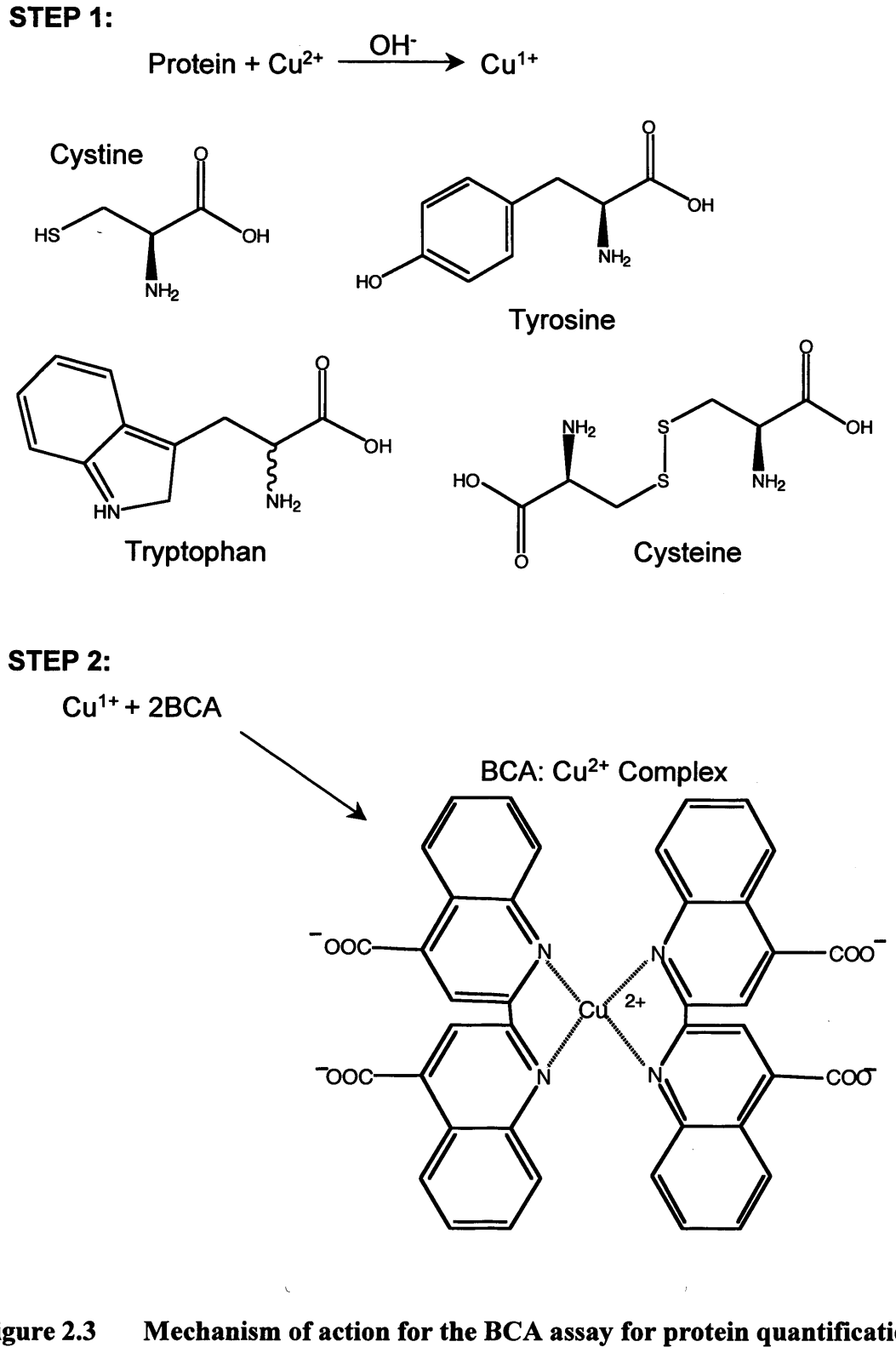

Figure 2.3 **Mechanism of action for the BCA assay for protein quantification** (adapted from the Pierce Chemical Protein Assay Technical Handbook, 2005).

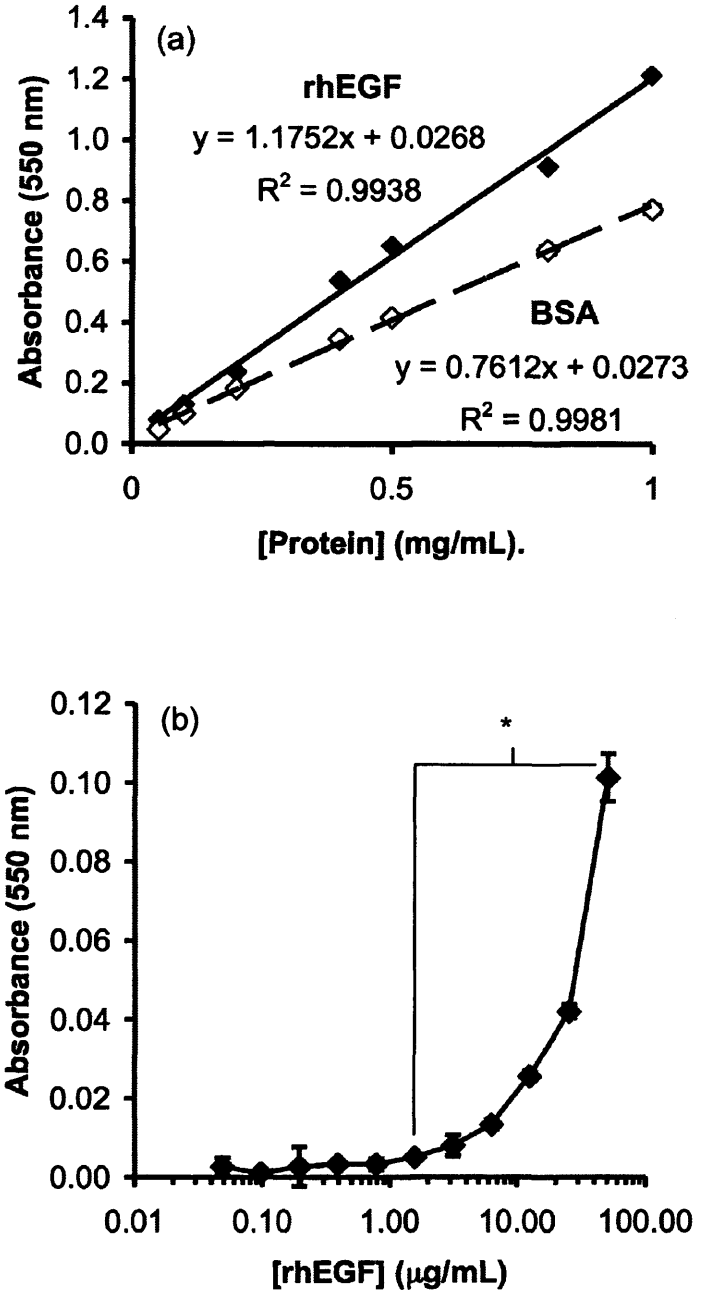

Figure 2.4 **Bicinchoninic acid (BCA) protein assay.** Panel (a) shows typical BCA protein assay standard calibration curves for recombinant human epidermal growth factor (rhEGF) and bovine serum albumin (BSA) (mean ± S.D., n = 3). Panel (b) shows the limit of detection of rhEGF via the BCA assay (mean ± S.D., n=3; * $p < 0.018$, Student's t-test comparison with blank).

yellow to blue) is primarily due to the amino acids, tyrosine and tryptophan, and to a lesser extent, cystine, cysteine and histidine (Lowry *et al*, 1951).

The protein content of the cell lysates was determined, using BSA as a standard. Stock solutions of extraction buffer, containing BSA (2 mg/mL), were prepared and diluted to a range of concentrations (0.2 - 2 mg/mL BSA). Standards and samples (5 μL) were added in triplicate to a 96-well microtitre plate. A stock solution consisting of 98 % DC protein assay reagent A, and 2 % DC protein assay reagent S, was prepared, as per the manufacturer's instructions. This solution (25 μL), and DC protein assay reagent B (200 μL), was added to the sample and calibration wells. Plates were incubated at room temperature, for 15 min. Absorbance was measured at 620 nm and a calibration curve constructed (Figure 2.5).

2.6.2.5 ELISA

For quantification of rhEGF, both liberated from the dextrin-rhEGF conjugate, and present in mouse plasma, a human EGF-ELISA kit was employed. A 96-well plate was supplied, pre-coated with a monoclonal antibody to human EGF. Samples (200 μL) were added and assayed against standards of rhEGF of known concentration (0 - 250 pg/mL) for 2 h. The supernatant was aspirated and the wells washed (x 3) with wash buffer (400 μL x 3; R&D Systems). A polyclonal antibody to human EGF, which has been conjugated to horseradish peroxidase, was added to the wells (200 μL; R&D Systems) for 1 h. The samples were washed (x 3), as described above. Substrate solution (200 μL; R&D Systems), was added for 20 min. A colour change from clear to blue occurred, with the reaction being terminated by the addition of stop solution (50 μL; R&D Systems). A blue to yellow colour change occurred, in proportion to the concentration of EGF. The absorbance of each well was measured using a Tecan plate-reader, at 450 nm, with correction at 540 nm (absorbance at 450 nm – absorbance at 540 nm). A typical calibration curve is shown in Figure 2.6.

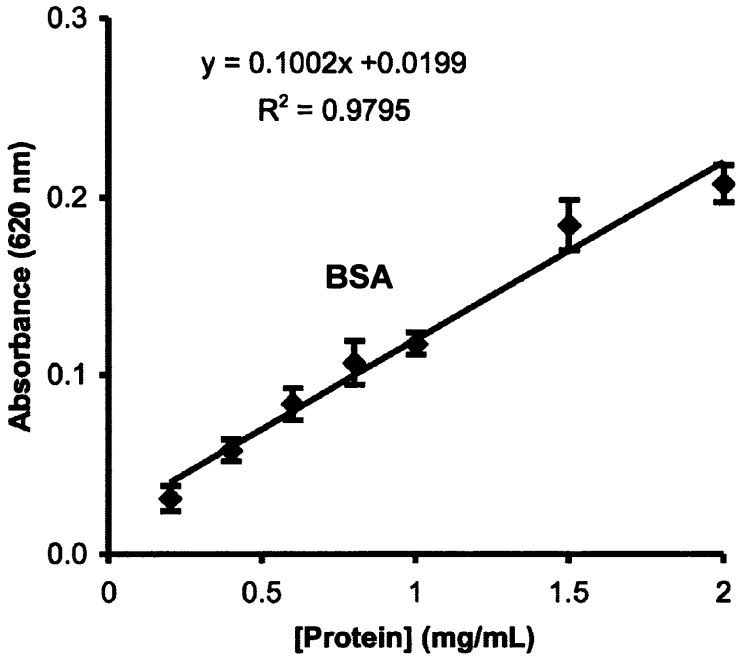

Figure 2.5 **Bio-Rad DC protein assay.** A typical Bio Rad DC protein assay standard calibration curve for BSA (mean ± S.D., n = 3).

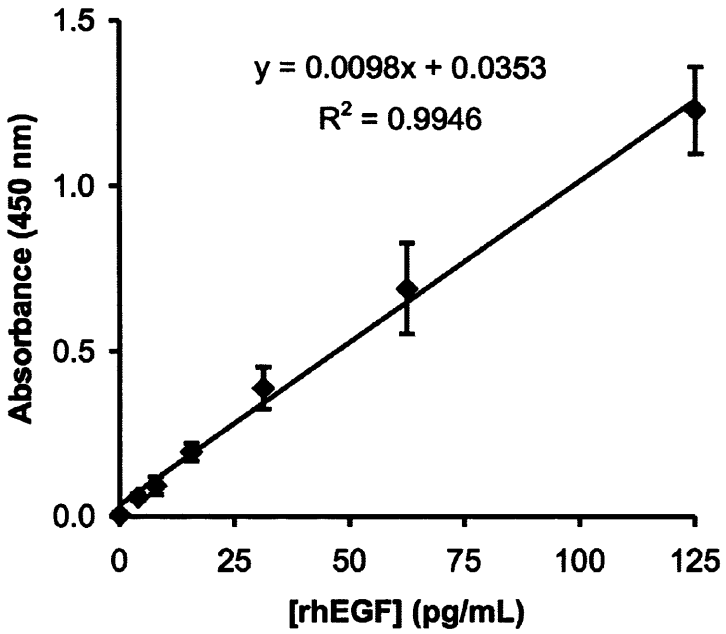

Figure 2.6 **Enzyme-linked immunosorbant assay (ELISA) analysis of rhEGF.** A typical calibration obtained curve against rhEGF standards (mean ± S.D., n = 3).

2.6.2.6 EnzChek® elastase assay

For quantification of neutrophil elastase activity in wound fluid samples, and exogenous elastase to which the dextrin-rhEGF conjugate was exposed, the EnzChek® elastase assay was utilised (Abdel-Latif *et al*, 2004). The assay was performed in accordance with the manufacturer's instructions: Reaction buffer (50 μL; Molecular Probes) and substrate (50 μL; DQ elastin, 100 μg/mL; Molecular Probes) were added to a black, 96-well analytical plate. A porcine pancreatic elastase standard (50 U/mL; Molecular Probes) was diluted to 0.250, 0.063, 0.016, 0.004 U/mL, in ddH_2O, and added (100 μL) to the reaction mixture. Analytical samples (100 μL) were also added, as necessary. Fluorescence was measured with a Fluostar Optima Microplate Reader (excitation 485 nm, emission 520 nm), at timed intervals, over a 1 h period. A typical calibration curve is shown in Figure 2.7.

2.6.3 Biological characterisation of the dextrin-rhEGF conjugate

Detailed methods for these bioactivity assays are fully described in Chapters 4 and 5.

2.6.3.1 Cell culture

In order to ensure sterility of the incubator, the safety cabinets and equipment were sprayed with 70 % v/v ethanol, in water. Those items not supplied pre-sterilised were sterilised by (a) autoclaving (120 °C, 15 lb/m^2, 15 min) for glassware, certain plastics, PBS and ddH_2O; (b) microfiltration (0.2 μm) for solutions; or (c) UV irradiation (30 min). Cells were maintained at 37 °C/5% CO_2, unless required.

2.6.3.2 HEp2 culture

HEp2 cells were seeded at $1.5x10^5$ cells/75 cm^2 tissue culture flask and incubated in 10 mL HEp2-serum containing medium (H-SCM 10 %: EMEM with penicillin G (100 U/mL), streptomycin sulphate (100 μg/mL), amphotericin B (0.25 μg/mL) and 10 % v/v FCS). Upon reaching 80-90 % confluence, the cells were sub-cultured, as follows. The cells were washed (x 2) with PBS and detached from the plastic by incubation with 1 mL of trypsin/EDTA (0.05 % trypsin, 0.53 mM EDTA), for approximately 5 min at 37 °C. Each flask was washed with H-SCM (9 mL), to

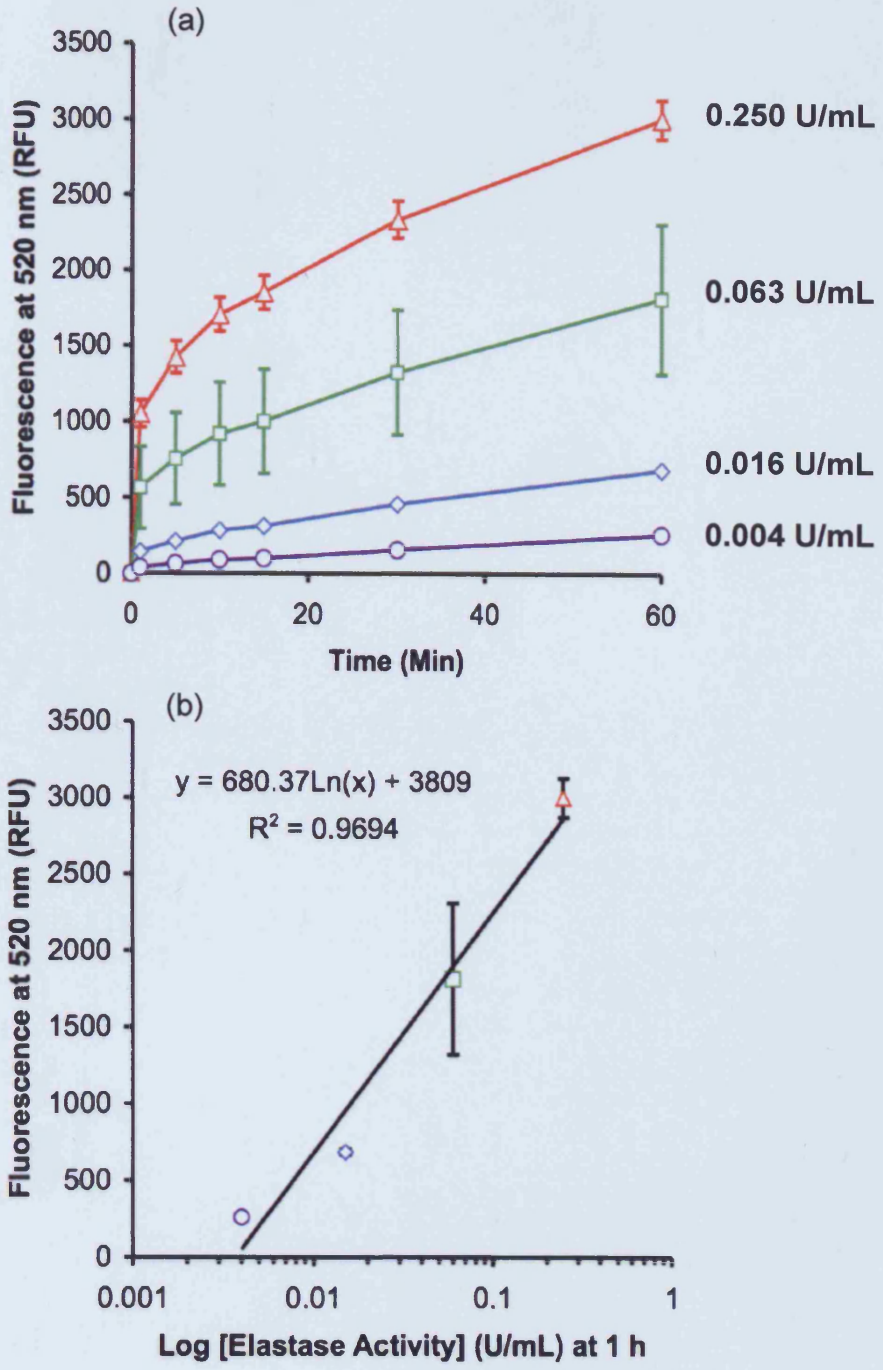

Figure 2.7 **EnzChek® elastase assay.** Panel (a) shows the typical fluorescence obtained, from a flurogenic substrate, in response to porcine pancreatic elastase standards, over a 1 h period (mean ± S.D., n = 3). Panel (b) shows a typical calibration curve of these standards at 60 min. The fluorescence was measured at 485 nm excitation and 520 nm emission, and background fluorescence subtracted (relative fluorescence units; RFU).

collect trypsinised cells. The cell suspension was then transferred to a 15 mL centrifuge tube and centrifuged at 1500 *g* for 5 min. The supernatant was aspirated and the resulting pellet was re-suspended in 1mL H-SCM 10 %. Viable cells were assessed with trypan blue staining (Section 2.6.3.6) and cells counted prior to sub-culture. The cell culture medium was changed twice weekly.

2.6.3.3 Keratinocyte culture

HaCaT keratinocytes were seeded at $1.5x10^5$ cells/75 cm^2 tissue culture flask and incubated in 10 mL keratinocyte-serum containing medium (K-SCM 10 %: consisting of 67.5 % DMEM / 22.5 % Ham's F12 nutrient media, supplemented with penicillin G (100 U/mL), streptomycin sulphate (100 μg/mL), amphotericin B (0.25 μg/mL), hydrocortisone (400 ng/mL), adenine (0.089 mM), cholera toxin (0.08 μg/mL), insulin (5 μg/mL), and 10 % v/v FCS). Upon reaching 80-90 % confluence, keratinocytes were sub-cultured, as described above (Section 2.6.3.2), resuspended in K-SCM 10 % and counted (Section 2.6.3.6). The cell culture medium was changed every 48 hours.

2.6.3.4 Fibroblast culture

Human normal dermal and chronic wound fibroblasts were seeded at $1.5x10^5/75cm^2$ tissue culture flask and incubated in 10mL fibroblast-serum containing medium (F-SCM 10 %: DMEM with penicillin G (100 U/mL), streptomycin sulphate (100 μg/mL), amphotericin B (0.25 μg/mL), L-glutamine (2 mM), puromycin (1 μg/mL) and 10 % v/v FCS). Upon reaching 80-90 % confluence, the fibroblasts were sub-cultured, as described above (Section 2.6.3.2), resuspended in F-SCM 10 % and counted (Section 2.6.3.6). Cell culture medium was changed twice weekly.

2.6.3.5 Cryopreservation and cell retrieval

For cryopreservation, all cell-types were resuspended in a mixture of 10 % (v/v) DMSO and 90 % (v/v) FCS and placed in cryogenic vials. These vials were then stored in liquid nitrogen, at -196 °C, for long-term cell storage.

Cryopreserved cells were retrieved from the storage in liquid nitrogen by rapid thawing at 37 °C. The cells were washed with serum-containing media (SCM10 %; cell-type specific) and following centrifugation (1500 *g*) for 5 min, the

pellets obtained were resuspended in 1mL of SCM and re-seeded at a density of 1.5 x 10^5 cells/75 cm^2 tissue culture flask.

2.6.3.6 Assessment of cell viability

At sub-culture, the viability of the cells was assayed using the Trypan Blue dye exclusion test (Tennant, 1964). An aliquot of the resuspended cells (25 μL) was mixed with an equal volume of 0.02 % (w/v) Trypan Blue solution, with 8 μL of the resulting solution being transferred to a Neubauer haemocytometer and the number of stained and non-stained cells was determined. Cells from two 0.1 mm^3 squares (one taken from the top chamber, and one taken from the bottom chamber of the haemocytometer) were counted. Non-viable cells (stained with trypan blue) were not included in the viable cell count. The following formula was used to determine cell concentrations:

$$\text{cells/mL} = \text{mean cell count} \times 2 \times 10^4$$

Where: mean is the arithmetic mean of the 2 values
2 takes into account the trypan blue dilution
10^4 accounts for the conversion from 0.1 mm^3 to mL

Typically, 80-90 % of cells (from each cell line) were viable, after cryo-retrieval.

2.6.3.7 MTT assay as a means to assess cell viability and proliferation

Cellular viability and proliferation were assessed using the MTT dye-reduction assay (Mosmann, 1983). MTT assay involves a redox reaction of the yellow substrate solution (MTT), with mitochondrial respiration products, NADH and NADPH, resulting in the formation of insoluble blue, formazan crystals. This reduction takes place only when mitochondrial reductase enzymes are active, and therefore, this conversion can be directly related to the number of viable cells. When the amount of purple formazan produced by cells treated with an agent is compared with the amount of formazan produced by untreated control cells, the effectiveness of the agent in causing cell proliferation can be quantified.

Cells were seeded into 96-well plates at densities of 10, 5, 2.5 and 1 x 10^3 cells/well and cell-specific, SCM added (250 μL). In the case of the HEp2 cells,

culture was performed in parallel with both SCM and serum-free media (SFM). Cells were cultured, as described above, and daily MTT assays performed over a 7 day period. MTT (5 mg/mL in PBS; 25 μL) was added to the cell media and incubated at 37 °C, for 5 h. The media was then removed and lysis buffer added (DMF (50 %) in ddH_2O, containing SDS (20 %), glacial acetic acid (2.5 %) and HCl (1M, 2.5 %), pH 4.7; 50 μL) and further incubated for 3 h at 37 °C. The absorbance of each sample were determined at 540 nm. Growth curves were constructed and presented as absorbance at 540 nm and as percentage increase in absorbance compared to day 0, as shown in Figures 2.8 – 2.10.

The results from the growth curve analysis would be used for optimisation of future cell proliferation assays:

- MTT assays were performed after 72 h, whilst all of the cell types were in the logarithmic growth phase.
- HEp2 cells were cultured in serum-free media, as a cell proliferation model, to exclude the influence of endogenous EGF within FCS.
- HEp2 cell culture was extended to 8 days, in SFM, to investigate the sustained release effects of rhEGF, from the dextrin-rhEGF conjugate.
- Cells were universally seeded at 2.5 x 10^3 cells/well, as this was either the optimum density, or showed no significant difference to other cell densities.

2.6.3.8 Determination of relative epidermal growth factor receptor (EGFR) density, by flow cytometry

Flow cytometry was used to study the receptor binding and uptake of EGF-Alexa488. EGF-Alexa488 was added to cells (Section 4.2.2) and at the end of the experiment, cells were suspended in cold PBS (200 μL) and analysed using a Becton Dickinson FACSCalibur Cytometer. Data were collected, with 10,000 total cell counts per sample, and processed using CELLQuest® version 3.3 software. Control cells (incubated with medium only), were used in all cases to account for background fluorescence output (M1). Data were acquired in 1024 channels with band pass filter FL-1 (530 nm ± 15 nm). Results were expressed as geometric mean x % positive cells / 100.

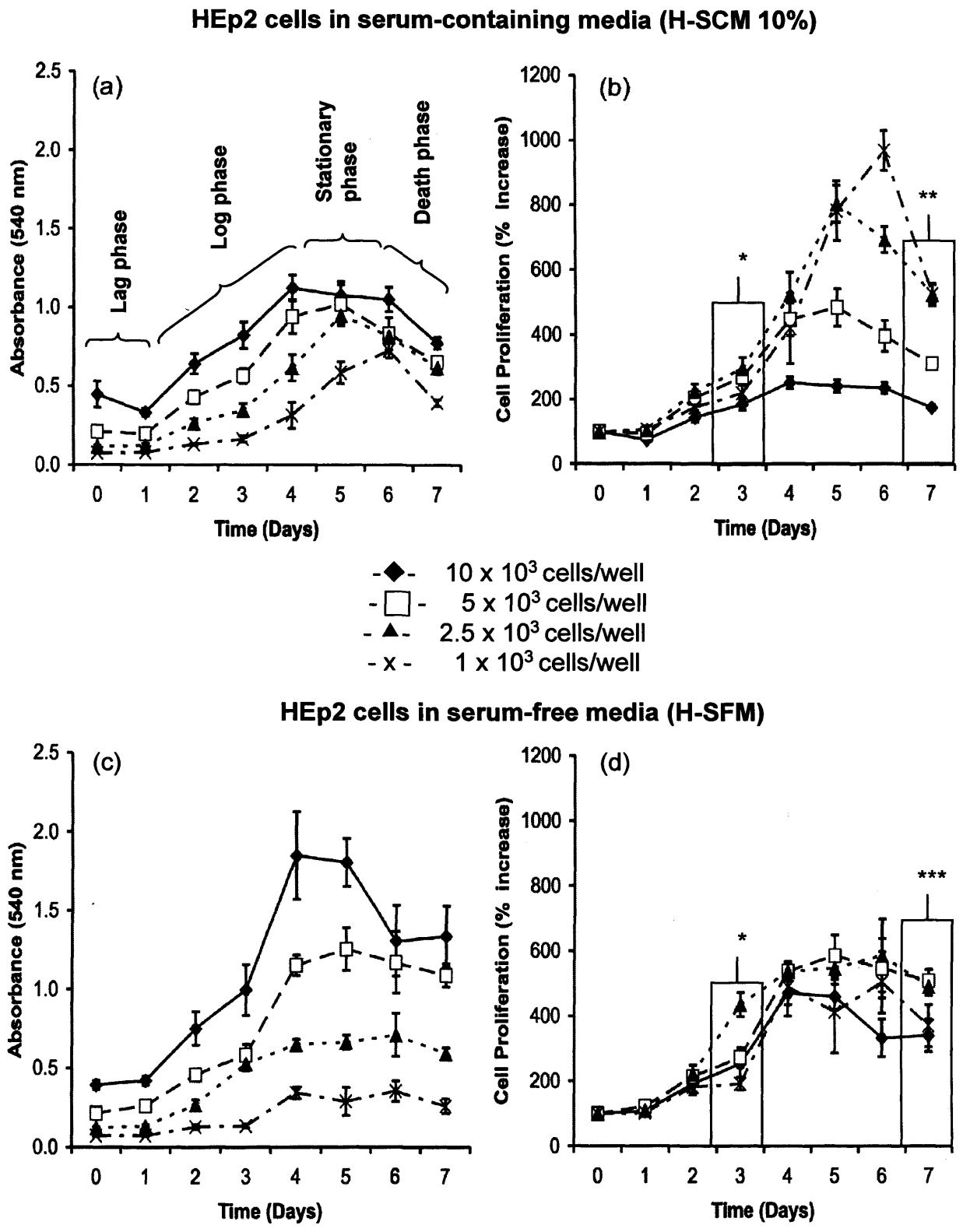

Figure 2.8 **Human epidermoid carcinoma (HEp2) cellular growth curves.** Panel (a) shows absorbance values from the MTT assay, performed over an 8 day period, and panel (b) shows absorbance as a percentage of the value at day 0, in response to 10% foetal calf serum-containing media (H-SCM 10 %). Panel (c) shows absorbance values from the MTT assay, again over 8 days, and panel (d) shows absorbance as a percentage of the value on day 0, in serum-free conditions (H-SFM) (mean ± S.D., n = 6, * 2.5 x 10^3 cells/well > all other cell densities, $p < 0.05$; ** 2.5 x 10^3 cells/well > 5 or 10 x 10^3 cells/well, $p < 0.001$; *** 2.5 x 10^3 cells/well > 1 or 10 x 10^3 cells/well, $p < 0.01$; ANOVA and Bonferroni *post-hoc* test).

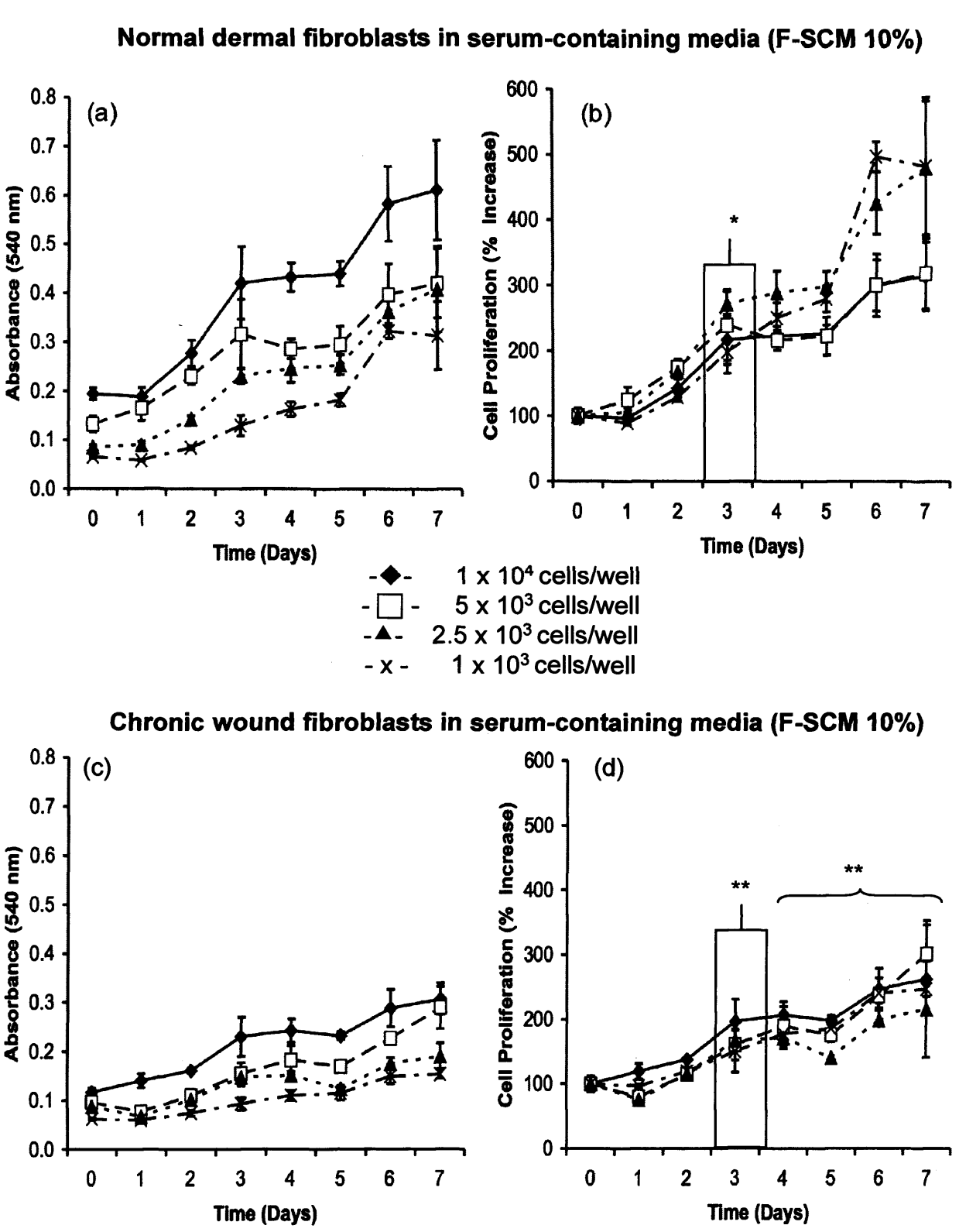

Figure 2.9 **Patient- and passage-matched normal dermal and chronic wound fibroblast cellular growth curves.** Panel (a) shows absorbance values from the MTT assay performed over an 8 day period, and panel (b) shows absorbance as a percentage of the value at day 0, of normal dermal fibroblasts, in response to 10% foetal calf serum-containing media (F-SCM 10 %). Panel (c) shows absorbance values from the MTT assay, over an 8 day period, for chronic wound fibroblasts, and panel (d) shows absorbance as a percentage of the value at day 0, in F-SCM 10% (mean ± S.D., n = 6 * 2.5 x 10^3 cells/well > 1 x 10^3 cells/well, $p < 0.05$; ** 2.5 x 10^3 cells/well not significantly different from other cell densities; ANOVA and Bonferroni *post-hoc* test).

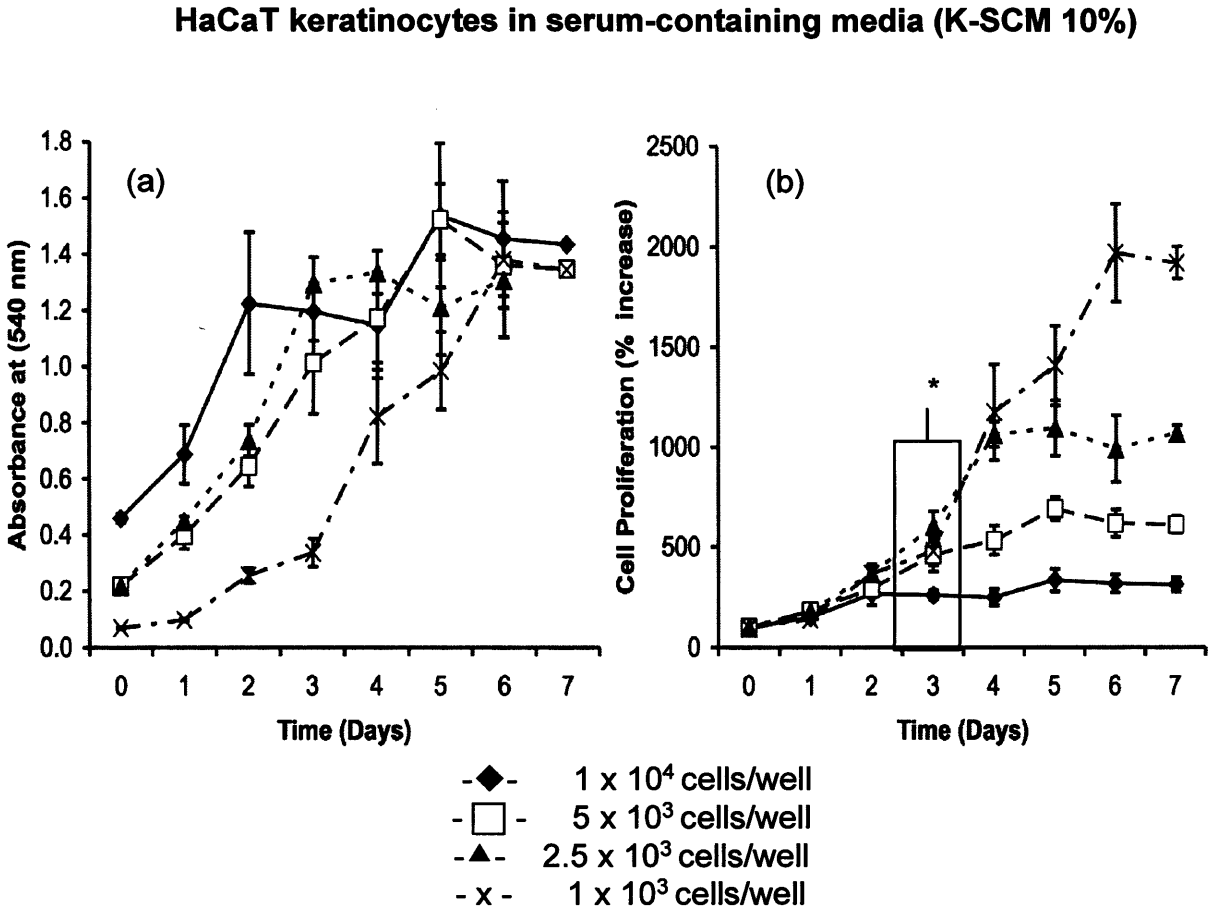

Figure 2.10 **Spontaneously immortalised keratinocyte (HaCaT) cellular growth curves.** Panel (a) shows absorbance values from the MTT assay performed over an 8 day period, and panel (b) shows absorbance as a percentage of the value at day 0, in response to 10% foetal calf serum-containing media (K-SCM 10 %) (mean ± S.D., n = 6, * 2.5 x 10^3 cells/well > other cell densities, $p < 0.05$, ANOVA and Bonferroni *post-hoc* test).

Several methods were used to interpret the flow cytometry data. An increase in fluorescence of the cell population can be estimated using two methods. Firstly, by measuring the increase in average fluorescence of the population using the mean, geometric mean or median. The second method involves analysis of the number of cells that have taken up the fluorescently-labelled compound. In this instance, control cells were compared to cells exposed to EGF-Alexa488, to account for background fluorescence. From this data, two regions were arbitrarily set (Figure 2.11). Region M1 corresponds to a region covering 98 % of the control population events, while M2 relates to any area with higher fluorescence than M1. As cell-associated fluorescence increased, so did the number of events in the M2 region.

2.7 Statistical analysis

Statistical analyses were undertaken using GraphPad Prism®, version 4.00 (GraphPad Software, San Diego, USA). Data were compared using a Student's t-test, a one-way ANOVA, with a Bonferroni post-test (parametric methods), and Kruskal-Wallace multivariate analysis, followed by *ad hoc* two sample Mann Whitney U-test (non-parametric methods). Results were expressed as a mean and standard deviation (S.D.), or standard error of the mean (S.E.M.). Statistical significance was considered at a probability of $p < 0.05$.

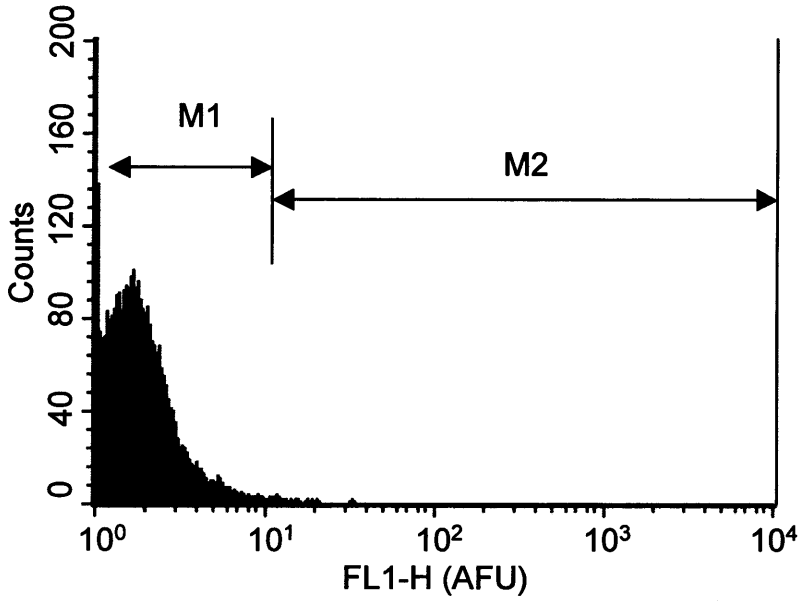

Figure 2.11 **Typical flow cytometry distribution.** Region M1 corresponds to a region covering 98 % of the control population events, while M2 relates to any area with higher fluorescence than M1.

Chapter Three

Synthesis And Characterisation of Dextrin-rhEGF Conjugates

Chapter Three: Synthesis And Characterisation of Dextrin-rhEGF Conjugates

Contents

3.1 Introduction

To explore the hypothesis that a polymer-protein conjugate would be a viable therapy for chronic wounds, as part of the Polymer-masking UnMasking Protein Therapy (PUMPT) concept, it was first necessary to select an appropriate polymer, to be used in conjunction with the bioactive protein or peptide of interest (Ferguson *et al*, 2006; Duncan *et al*, 2008). The choice of polymer was important to ensure biocompatibility, to allow conjugation to the protein of choice, and to be degradable by an endogenous human enzyme, that would be present in the wound environment, without the presence of toxic breakdown products. It was also important to generate a stable conjugate, which would mask the protein activity, when conjugated, but still allow the release of a bioactive agent, following polymer degradation.

The bioactive, recombinant protein, that would be the other component of the conjugate, should have been an established mediator of the normal wound healing response, and furthermore, should be commercially available, well-characterised and ideally, be found to be depleted in the chronic wound environment, by the action of proteinases. Vitally, this protein should also possess the chemistry to allow conjugation to the chosen polymer. It is well known that conjugation of a polymer to a protein can significantly improve biological efficacy *in vivo,* by reducing proteolytic degradation, extending plasma circulation time and reducing protein immunogenicity (Roberts *et al*, 2002; Sato, 2002; Harris and Chess, 2003; Werle and Bernkop-Schnurch, 2006).

3.1.1 Choice of polymer

Synthetic and natural polymers have been explored as drug carriers, but almost all polymers used clinically are non-biodegradable synthetic polymers, e.g. poly(ethyleneglycol) (PEG) (Veronese and Harris, 2002; Veronese and Pasut, 2005) and *N*-(2-hydroxypropyl) methacrylamide (HPMA) co-polymers (Vasey *et al*, 1999). Although well tolerated in man, such polymers are not biodegradable, and may lead to progressive accumulation after repeated doses (Dunn *et al*, 1998). Systemic administration of high molecular weight, non-degradable polymers (e.g. polyvinylpyrolidone; PVP), has been shown to cause bone marrow suppression and myelofibrosis, leading to the withdrawal from clinical use of PVP-based plasma expanders (Moffitt, 1975; Dunn *et al,* 1998). In order to ensure renal excretion, polymers of a molecular weight below the renal threshold (~40,000 g/mol), must be

utilised (Duncan, 2003). Although natural polymers, such as dextran and poly(amino acids), are frequently of high molecular weight and biodegradable, even low levels of modification to facilitate drug conjugation, can lead to a non-degradable adduct (Vercauteren *et al*, 1990). Dextrin, an α-1,4 polyglucose, derived from the enzymatic hydrolysis of corn or potato starch, has been selected for use in the present Study. It contains few (< 5%) α-1,6 links, so displays minimal branching, and is degraded by α-amylase (at α-1,4 glucosidic linkages), to produce the disaccharides maltose (α-1,4-linked) and iso-maltose (α-1,6-linked) (Roberts and Whelan, 1960; Davies, 1994; Burkart, 2004; Hreczuk-Hirst *et al*, 2001b). A number of other naturally occurring polymers, such as dextran are inherently biodegradable, but low levels of chemical modification can results in the generation of non-degradable adducts (Vercauteren *et al*, 1990; 1992). In addition, some natural polymers are not suitable for repeated administration, due to their immunogenicity (Bircher, 2006; Bisaccia *et al*, 2007).

3.1.1.1 Dextrin

Dextrin was chosen as a suitable polymer for protein conjugation, as it has proven biocompatibility and clinical tolerability. Dextrin has been used clinically for several years, initially as a dietary supplement (Caloreen™), for renal and hepatic failure (Woolfson *et al*, 1976; Alsop, 1994), and later as a component of peritoneal dialysis solution (icodextrin, Extraneal®) (Peers and Gokal, 1998; Frampton and Plosker, 2003; Davies *et al*, 2006). It has also been utilised as a carrier for 5-flurouracil, in the treatment of intra-peritoneal carcinoma (Kerr *et al*, 1996; Hosie *et al*, 2003). The safety and pharmacokinetic data for dextrin is well-established and it possesses both Federal Drug Administration (FDA) approval and is Generally Recognised as Safe (GRAS) listed (Day, 2003).

For the preparation of polymer-protein conjugates, conversion of the polysaccharide into a suitable reactive derivative, is usually required (Bruneel and Schacht, 1994). A large number of methods have been described to activate polysaccharides (Schacht *et al*, 1987), including periodate oxidation (Bruneel and Schacht, 1993a), chloroformate activation (Bruneel and Schacht, 1993b) and cyanogen bromide (Costa and Reis, 2004) (summarised in Table 3.1). Activation by these methods can lead to disruption and instability of the polymer backbone and in

Table 3.1 Methods of polysaccharide activation

Activation method	Method overview	Disadvantages	Example polysaccharides
Chloroformate activation	Introduces hydroxyl groups into the polymer	Possibility of formation of intra- or inter-chain carbonate esters. Formation of five-member rings can interfere with polymer backbone.	*Cellulose* (Rupprich *et al*, 1990) *Dextran* (Chiu *et al*, 1999)
Cyanogen bromide activation	Primary amine groups are introduced directly into the reactive intermediate	Reactive intermediate produced during activation of the hydroxyl group can disrupt the polymer backbone. Hydrogen cyanide is toxic and must be carefully removed. Linkage is unstable, resulting in slow release of pendant groups.	*Hyaluronate* (Mlcochova *et al*, 2006) *Starch* (Costa and Reis, 2004)
Periodate oxidation	Formation of an aldehyde groups by oxidation of 1,2- diol groups	Aldehyde groups can lead to toxicity if not completely neutralised.	*Dextran* (Devakumar and Mookambeswaran, 2007) *Mannan* (Ramirez *et al*, 2006)
Succinoylation	Uses succinic anhydride to introduce a carboxyl pendant group, without disturbing the polymer backbone		*Starch* (Lawal, 2004) *Chitosan* (Kato *et al*, 2004) *Dextrin* (Hreczuck-Hirst *et al*, 2001a)

some cases, release toxic by-products, including hydrogen cyanide and polyaldehydes (Hreczuk-Hirst *et al*, 2001a). Succinoylation has been used by others to modify pullulan (Bruneel and Schacht, 1994), which can react with succinic anhydride in dimethylsulfoxide (DMSO), using 4-dimethylaminopyridine (DMAP) as a catalyst. Hreczuk-Hirst *et al* (2001a) optimised dextrin succinoylation, with respect to temperature and reaction time. This Study concluded that 50 °C, with a minimum of 8 h reaction time, was optimal for dextrin succinoylation. Using these conditions, it was possible to reproducibly succinoylate dextrin, with a yield of ~ 50 %. Furthermore, it was demonstrated that different degrees of dextrin succinoylation could be achieved by variation of the reactant ratios, and that the rate of α-amylase degradation of the succinoylated dextrins could be prolonged, by increasing the degree of polymer modification (Hreczuk-Hirst *et al*, 2001a).

Dextrin is normally degraded very quickly in the body, by both salivary and pancreatic isoforms of α-amylase. This approach made dextrin a suitable polymer for use in targeted drug delivery and also, for use in protein modification, in the context of PUMPT. Several peptides have been conjugated to succinoylated dextrin, including phospholipase A_2 and trypsin (Ferguson *et al*, 2006; Duncan *et al*, 2008). These studies utilised the crosslinking agents, 1-ethyl-3- [3-dimethylaminopropyl] carbodiimide hydrochloride (EDC) and *N*-hydroxysulfosuccinimide (sulfo-NHS). EDC reacts with the carboxyl groups of an succinoylated dextrin intermediate, forming an amine-reactive O-acylisourea intermediate. This can further react with the amine groups of lysine residues in a protein, to give a conjugate joined by a stable amide bond. However, EDC alone is not particularly efficient. A failure of rapid amine reaction results in hydrolysis and regeneration of the carboxyl group, making it unstable and short-lived in aqueous solution. The addition of sulfo-NHS stabilises the amine-reactive intermediate, by converting it to an amine-reactive, sulfo-NHS ester, thus increasing the efficiency of EDC-mediated, coupling reactions. The amine-reactive sulfo-NHS ester intermediate has sufficient stability, to permit two-step crosslinking procedures, which allows the carboxyl groups on the protein to remain unaltered (*vide infra*). For this Study, a dextrin-fraction of average molecular weight ~ 51,000 g/mol was used, to provide adequate masking of the protein, and thus, reduce the bioactivity of the conjugated recombinant protein.

3.1.2 Choice of protein

The recombinant protein selected for this Study had to fulfil multiple criteria. It had to be an established mediator of the normal wound healing response. It should have a well-established and characteristic action on the cells involved in wound repair (i.e. the keratinocytes and fibroblasts), be commercially- and readily-available (at the mg quantity as required) and well-characterised structurally. The recombinant protein also needed to allow polymer conjugation, via accessible amino acid residues, be detectable by immunological and protein assays, and ideally, be of a low molecular weight, in comparison to the selected dextrin polymer (~51,000 g/mol). A recombinant growth factor was selected as the choice of protein, as their regulatory action is integral to the normal wound healing process and as they act upon specific cell surface receptors, thereby activating secondary intracellular signalling pathways (Martin, 1997). A selection of the recombinant growth factor candidates considered, is shown in Table 3.2.

3.1.2.1 Epidermal Growth Factor

Epidermal Growth Factor (EGF) is a polypeptide of 53 amino acids, containing three internal disulfide bridges, which was first isolated from the mouse submaxillary gland (Cohen, 1962). At physiological pH, EGF can exist as a dimer (Lu *et al*, 2001). EGF facilitates epidermal cell regeneration and plays an essential role in the process of wound healing, through stimulation of keratinocyte proliferation and migration (Werner and Grose, 2003). The initial doses of EGF, as well as other cytokines and growth factors, are delivered at the wound environment, via platelet degranulation, within the provisional fibrin clot (Nanney and King, 1996). EGF also promotes the formation of granulation tissue and stimulates fibroblast motility (Rheinwald and Green, 1977; Barrondon and Green, 1987). As a mitogen, EGF first binds with high affinity to specific cell-surface receptors (Carpenter and Cohen, 1990).

The EGF-receptor (EGFR; erbB-1) belongs to the family of ErbB receptor tyrosine kinases (Bazley and Gullick, 2005), which also includes c-erbB-2/HER2, c-erbB3-/HER3 and c-erbB4/HER4. All of these receptors are similar in structure, with a ligand-binding domain located extracellularly, a transmembrane domain and a cytoplasmic catalytic domain (Marques *et al*, 1999). The 11 ligands currently

Table 3.2 Potential growth factors for polymer conjugation

Growth factor	Molecular weight	Number of amino acids (number of lysine groups)	Action	Price (cheapest commercial source)	Reference
Epidermal growth factor (EGF)	6,200 g/mol	53 (2)	Motogenic and mitogenic influence on keratinocytes	$225 / mg*	Nanney and King (1996)
Platelet-derived growth factor-BB (PDGF-BB)	48,600 g/mol	218 (14)	Mitogenic and chemotactic influence on fibroblasts, extracellular matrix production Macrophage activation and chemotaxis	$3510 / mg*	Siegbahn *et al* (1990)
Transforming growth factor-β_1 and β_2 (TGF-β_1 and β_2)	β_1 = 25,000 g/mol β_2 = 25,000 g/mol	β_1 = 112 (8) β_2 = 112 (7)	Mitogenic and chemotactic influence on fibroblasts Keratinocyte migration Fibroblast extracellular matrix synthesis and remodelling	£5600 /mg**	Gordon and Blobe (2008)
Insulin-like growth factor-1 (IGF-1)	7,600 g/mol	70 (3)	Mitogenic influence on endothelial cells and fibroblasts	$270 / mg*	Edmondson *et al* (2003)
Vascular endothelial growth factor (VEGF)	38,200 g/mol	165 (11)	Angiogenesis	$3510 / mg*	Tonneson *et al* (2000)
Hepatocyte growth factor (HGF)	83,000 g/mol	728 (48)	Motogenic and mitogenic influences on fibroblasts	$4400 / mg*	Nakamura (1991)

*ProSpec-Tany Technogene (Rehovot, Israel) **Peprotech EC (London, UK)
(catalogues accessed, September ,2008)

identified for these receptors in mammals are EGF, transforming growth factor-α (TGF-α), HB-EGF (heparin binding), betacellulin, amphiregulin, epiregulin, epigen and the neuregulins (NRGs) 1–4 (Olayioye *et al*, 2000).

In the absence of ligand, monomeric receptors reside within the cell membrane in an inactive state, distributed evenly over the cell membrane (Bazley and Gullick, 2005). However, when ligand is present in the surrounding milieu, the receptor sites become occupied by monomeric EGF. Provided two stable 1:1 EGF:EGFR intermediate complexes persist, sequential receptor dimerisation and oligomerisation ensue (Ferguson *et al,* 2003). Receptor dimers, which have greater stability and ligand-binding affinity than their corresponding monomers (Ben-Levy *et al,* 1992; Zhou *et al,* 1993), are increasingly considered to be necessary for activation (Alroy and Yarden, 1997). Consequent to ligand binding and receptor dimerisation, intracellular tyrosine kinase catalytic activity is increased (Hubbard and Till, 2000; Dibb *et al,* 2004).

Subsequent to the transphosphorylation of the receptor dimer, secondary messenger proteins, possessing one of the two main classes of domains that recognise site-specific phosphorylation ("docking sites"), can interact with the receptors (Bazley and Gullick, 2005). An example of a well-characterised second messenger/receptor interaction, is the recruitment of the enzyme phospholipase C gamma (PLCγ) (Wang *et al,* 2001). In its inactive state, PLCγ is normally found in the cytosol. However, upon phosphorylation of the EGFR, PLCγ is able to interact with the phosphorylated receptor. This causes, not only tyrosine phosphorylation by the activated receptor, but also relocation to the plasma membrane, where it ultimately generates the secondary messengers, inositol 1,4,5-triphosphate (IP_3) and diacylglycerol (Falasca *et al,* 1998), required for calcium/calmodulin-dependent kinases and the stimulation of protein kinase C. Additional targets of signaling are the JAK-STAT pathway (Janus kinases - Signal Transducers and Activators of Transcription; Schindler *et al,* 2007). These transduce the signal carried by extracellular polypeptides (e.g. growth factors) to the cell nucleus, where activated STAT proteins modify gene expression (Henson and Gibson, 2006). This pathway plays a central role in principal cell fate decisions, regulating the processes of cell proliferation, differentiation and apoptosis (Bazley and Gullick, 2005).

Within the 53 amino acid polypeptide structure of EGF, are two lysine residues (K_{28}, K_{48}), which would permit conjugation to succinoylated dextrin (Figure 3.1). Lysine 28 is located within the 3-D structure of EGF and thus, may not allow polymer conjugation, due to steric inhibition (Lu *et al*, 2001). Lysine 48, however, is located peripherally and may, therefore, allow site-specific conjugation to succinoylated dextrin. Leucine 47 is implicated in EGFR binding, so this action should be inhibited by conjugation of the polymeric macromolecule to the adjacent amino acid. This would be dependent upon the site of conjugation, as site specific conjugation at the N-terminus would still permit EGFR binding, due to the increased distance from the binding moiety (Lee *et al*, 2003; Zeng *et al*, 2006).

Chronic wound proteinases and reactive oxygen species have been shown to degrade growth factors, including EGF, involved in normal dermal wound healing (Yager *et al*, 1997; Wlashek *et al*, 1997; James *et al*, 2003; Moseley *et al*, 2004; Wlashek and Scharfetterr-Kochanek, 2005). Therefore, the application of the PUMPT concept may provide protection and stabilisation of the recombinant EGF (rhEGF) protein, in a simulated chronic wound environment. Indeed, the conjugation of macromolecules, such as poly(ethylene glycol), dextran, polyamidoamine dendrimers, to EGF has previously been shown in other studies, to reduce bioactivity and the receptor binding ability of EGF (Gedda *et al*, 1996; Lee *et al*, 2003; Zeng *et a;*, 2006; Hee Na *et al*, 2006; Thomas *et al*, 2008; summarised in Table 3.3).

3.1.2.2 Recombinant human epidermal growth factor

RhEGF was one of the first growth factors to be synthesised, using recombinant DNA technology, in *Saccharomyces cerevisiae* (Brake *et al,* 1984). In the present Study, the rhEGF that was used in the synthesis of the polymer-protein conjugate was purchased commercially, following expression in *Escherichia coli.* RhEGF is a single, non-glycosylated, polypeptide chain, having a molecular mass of 6,222 g/mol. The rhEGF was purified by proprietary chromatographic techniques, resulting in a purity greater than 98 %, as determined by analysis by reverse-phase-high performance liquid chromatography (RP-HPLC) and analysis by sodium dodecyl sulfate-polyacrylamide gel electrophoresis (SDS-PAGE). The sequence of the first five N-terminal amino acids was determined and found to be Asn-Ser-Asp-Ser-Glu, which agrees with the sequence of native human EGF. rhEGF quantification

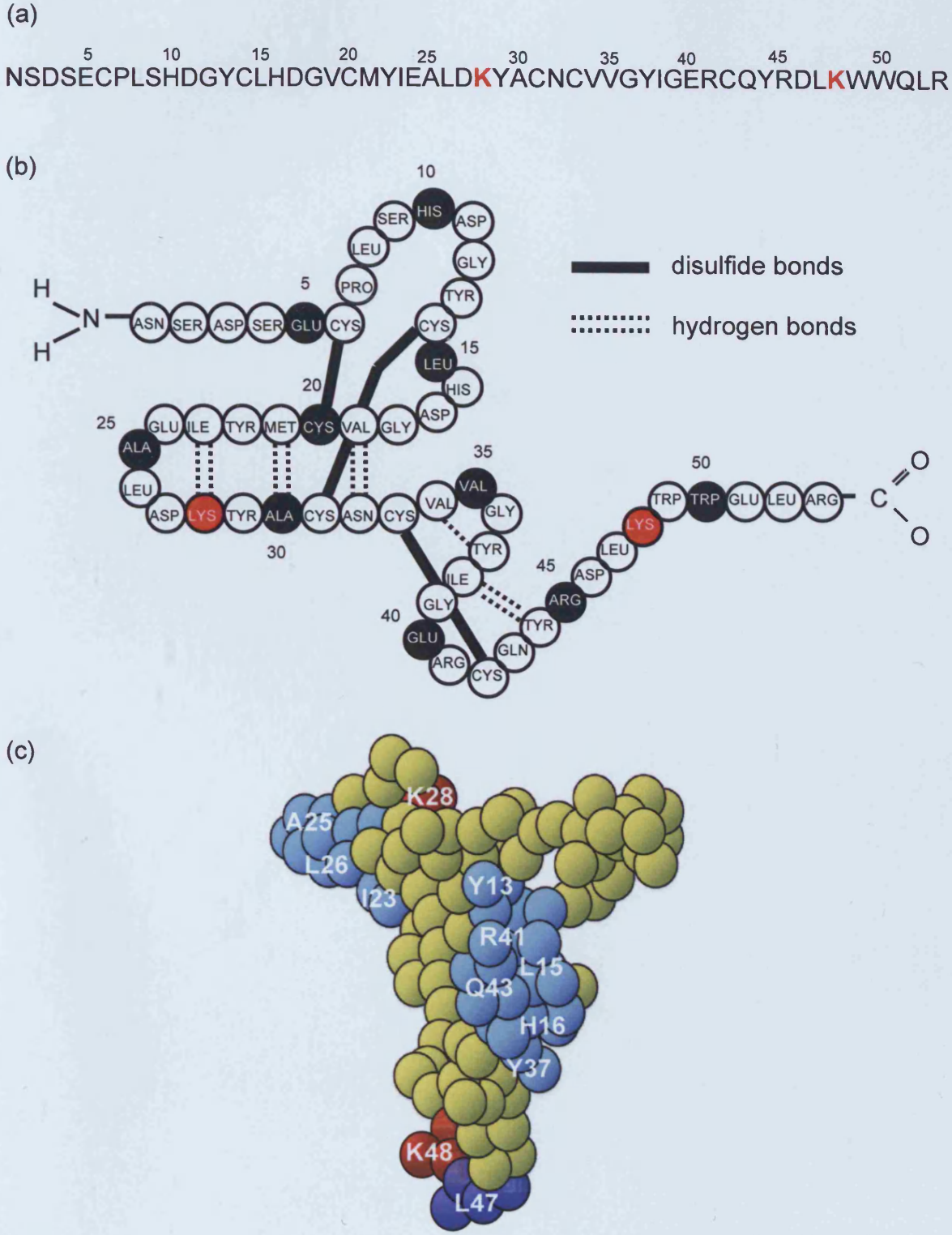

Figure 3.1 **Human epidermal growth factor (EGF).** Panel (a) shows the amino-acid sequence, panel (b) shows the protein primary structure with locations of potential disulfide bonds and hydrogen bonds (adapted from Boonstra *et al*, 1995), and panel (c) shows the space-filling model of the EGF molecule, with surface residues known to be important in dimerization (I23, A25, L26, Y13, L15, H16, Y37, R41, Q43) and receptor binding (L47), highlighted in blue, and lysine residues (K28, K48), highlighted in red (adapted from Lu *et al*, 2001).

Table 3.3 Literature review of polymer-EGF conjugates

Polymer (molecular weight)	Polymer : protein	EGF origin	*In vitro* model	Reduction in EGF activity (% of unmodified EGF)	Reference
Dextran (70,000 g/mol)	1 : 356	Mouse	U343 human glioma	37 - 75%	Gedda *et al* (1996)
Poly(ethylene glycol)					
(2000 g/mol)	3 : 1	Recombinant human	NRK47F	No reduction*	Lee *et al* (2003)
(5000 g/mol)	3 : 1		(Rat renal interstitial fibroblasts)		
Poly(ethylene glycol)-*block*-poly(δ-valerolactone) micelles					
(2,000 g/mol)	1 : 1552	Unknown	MDA-MB-468 human breast cancer	No reduction*	Zeng *et al* (2006)
Poly(ethylene glycol)					
(2000 g/mol)	3 : 1	Recombinant human	NRK49F	71%	Hee Na *et al* (2006)
(5000 g/mol)	3 : 1		(Rat renal interstitial fibroblasts)	67%	
(20,000 g/mol)	3 : 1			61%	
Poly(amidoamine) dendrimer					
(26,530 g/mol)	1 : 3	Mouse	SCC15 (Human head & neck squamous cell carcinoma)	25%	Thomas *et al* (2008)

*N-terminus conjugation

was performed by two independent methods, using ultra-violet spectroscopy at 280 nm, using the absorbance value of 2.858, as the molar extinction coefficient for a 0.1% (1mg/ml) solution and analysis by RP-HPLC, using a calibrated solution of rhEGF, as a reference standard (Manufacturer's data sheet; Prospec-Tany Technogene, Rehovot, Israel).

3.1.3 Experimental aims

The aims of this Chapter were the:

1. Synthesis and characterisation of succinoylated dextrin.
2. Synthesis and characterisation of dextrin-rhEGF conjugate batches.
3. Purification of dextrin-rhEGF batches.
4. Analysis of the degradation of dextrin, succinoylated dextrin and dextrin-rhEGF, in response to physiologically relevant α-amylase concentrations, using gel permeation chromatography (GPC).
5. Assessment of the stability of dextrin-rhEGF in an α-amylase-free environment.
6. Assessment of the stability of dextrin-rhEGF in response to proteinases, using fast-protein liquid chromatography (FPLC).
7. Quantification of the rate and amount of rhEGF released from the dextrin-rhEGF conjugate, in response to physiologically relevant α-amylase concentrations, using FPLC and enzyme-linked immunosorbant assay (ELISA).

3.2 Methods

A number of general methods (Chapter 2) were used for the characterisation of the dextrin-rhEGF conjugates synthesised; the BCA protein assay (Section 2.6.2.3), SDS-PAGE (Section 2.6.2.2), FPLC and GPC (Section 2.6.2.1.).

3.2.1 Succinoylation of dextrin

Succinoylated dextrin was synthesised, according to the method of Hreczuk-Hirst *et al* (2001b). The reaction scheme is summarised in Figure 3.2. Dextrin (51,000 g/mol; 1g, 19.6 μmol) was added to DMAP (80 mg, 655 μmol) in a 50 mL

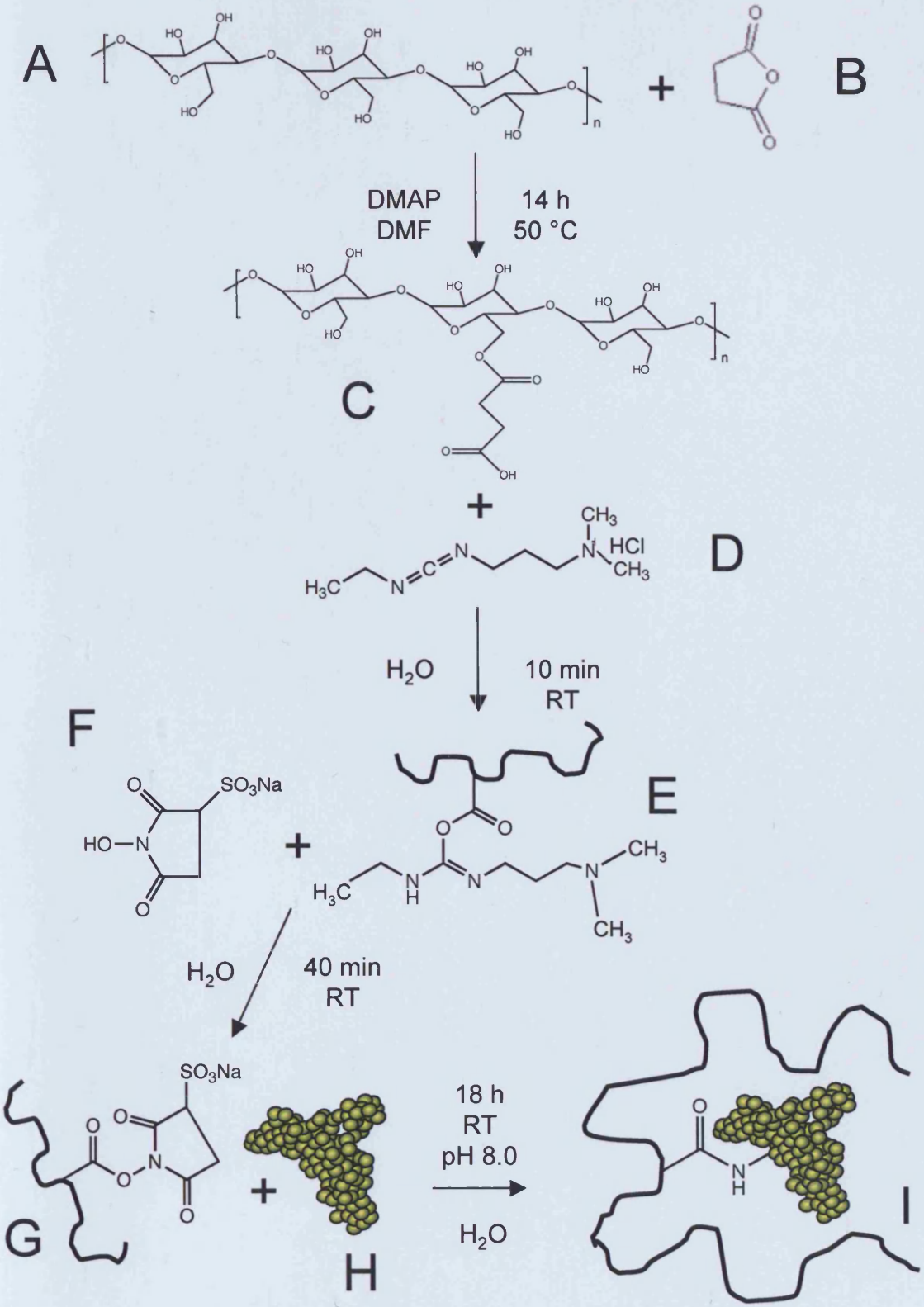

Figure 3.2 **Dextrin-rhEGF synthesis**. Dextrin (A) was functionalised with succinic anhydride (B), in combination with DMAP and DMF, to produce succinoylated dextrin (C). This was reacted with EDC (D), to form an amine reactive, *O*-acylisourea intermediate (E). Reaction with sulfo-NHS (F) then formed an amine-reactive sulfo-NHS ester (G). Lysine residues within the rhEGF molecule (H), formed stable amide bonds, resulting in the dextrin-rhEGF conjugate (I).

round bottom flask. This mixture was purged with nitrogen and anhydrous dimethylformamide (DMF) (7.5 mL), added to the stirred mixture. Succinic anhydride (182.5 mg, 1.825 mmol) was dissolved in DMF (2.5 mL) and added to the reaction mixture. The resultant mixture was stirred under nitrogen, at 50 °C for 14 h.

The DMF was evaporated under high vacuum, to leave a few drops of the reaction mixture. The remaining reaction mixture was added, drop-wise, to 250 mL of vigorously stirred, diethyl ether and left for 10 h, under continual stirring. The resulting mixture was filtered under vacuum and dissolved into a minimal amount of double-distilled water (ddH_2O). This solution was purified by dialysis (molecular weight cut-off 10,000 g/mol), to remove free reactants (succinic anhydride, DMAP, DMF) in 5 L of ddH_2O for approximately 8 water changes, allowing 1-2 h between each water change. The remaining product was then collected, froze and lyophilised for two days, and stored at 4 °C, for subsequent characterisation.

3.2.2 Confirmation and quantification of dextrin functionalisation

3.2.2.1 Titration

The degree of carboxylic acid group incorporation into the dextrin polymer, from succinic anhydride, was quantified by titration (Hreczuk-Hirst *et al*, 2001a). Solutions of succinoylated dextrins (1.5 mg/mL, 2 mL) were titrated against sodium hydroxide (NaOH; 50 μM), using a bromothymol blue indicator (1 % w/v in ethanol, pH range 6 - 7.6). The end point of the titration was indicated by a change in the solution colour from yellow to blue, at pH 7.6. Titrations were performed in triplicate, and the mean mol % modification, i.e. the number of carboxylic acid groups incorporated, was calculated (Figure 3.3).

3.2.2.2 Fourier transform infrared (FTIR) spectroscopy

The extent of the functionalisation of the succinoylation dextrin was determined by Fourier transform infrared (FTIR) spectroscopy. FTIR is a measurement technique, whereby spectra are collected based on measurements of the temporal coherence of a radiative source, using time-domain measurements of the electromagnetic radiation or other type of radiation. It can be applied to a variety of types of spectroscopy, including optical spectroscopy, infrared spectroscopy (IR),

- Dextrin (51,000 g/mol) = approximately 283 glucose monomers (180 g/mol)
- Succinoylated dextrin is a mixture of unmodified glucose monomers (***U***) + succinoylated monomers (***S***) (280 g/mol)

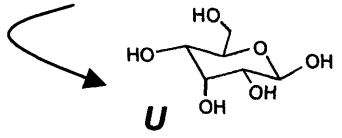

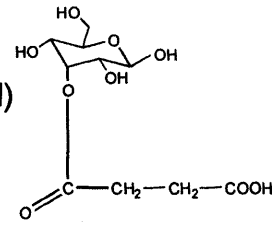

molecular weight (**Mw**) = (180***U***) + (280***S***) ***U*** = 283 - ***S*** therefore, **Mw** = ((283 - ***S***) x 180) + (280***S***)
succinoylated detxrin

$$\text{succinoylated dextrin (mol)} = \frac{\text{mass of succinoylated dextrin (g) } (\boldsymbol{SD})}{((283 - \boldsymbol{S}) \times 180) + (280\boldsymbol{S}))} = \frac{\boldsymbol{SD}}{50{,}940 + 100\boldsymbol{S}} = \frac{\boldsymbol{SD}}{\text{Mw dextrin } (\boldsymbol{DEX}) + 100\boldsymbol{S}}$$

TITRATION → moles NaOH (***Na***) = ***S*** x moles succinoylated dextrin

$$\boldsymbol{Na} = \boldsymbol{S}\left(\frac{\boldsymbol{SD}}{\boldsymbol{DEX} + 100\boldsymbol{S}}\right) \quad \text{therefore} \quad \boldsymbol{S} = \frac{\boldsymbol{DEX}}{\left(\frac{\boldsymbol{SD}}{\boldsymbol{Na}}\right) - 100}$$

*calculate **S** by titration*

Mw = (283 - ***S***) x 180) + (280***S***) Weight % succinoylation = $\frac{280\boldsymbol{S}}{\boldsymbol{Mw}} \times 100$

Mol % succinoylation = $\frac{\boldsymbol{S}}{283} \times 100$

Figure 3.3 **Calculation of % modification of succinoylated dextrin.** Modification was expressed as mean mol % succinoylation (n = 3). *U* = number of unmodified glucose monomers; *S* = number of modified (succinoylated) glucose monomers; *DEX* = molecular weight of unmodified dextrin (g/mol); *SD* = mass of succinoylated dextrin (g), analysed via titration; *Na* = moles of sodium hydroxide (NaOH), used in titration; *Mw* = molecular weight (g/mol).

nuclear magnetic resonance, and electron spin resonance spectroscopy (Ellis and Goodacre, 2006).

Succinoylated dextrins were analysed, usually using 64 scans, over the mid-infrared (400 – 4000 cm^{-1}) and near-infrared (4000^{+} cm^{-1}) regions, with background interferences being subtracted. Scanning in these two regions enabled the detection of both specific molecules and combination bands, respectively. Where spectra were unresolved, the number of scans was increased from 64 to 300. This improved the signal to noise ratio, to give much clearer spectra. Qualitative analysis of the FTIR spectra was conducted by interpretation of the peaks in the double-bond region, 2000 – 1500 cm^{-1}.

3.2.3 Molecular weight and polydispersity determination of succinoylated dextrin, by GPC

Dextrin and succinoylated dextrin, solubilised in phosphate buffered saline (PBS; 3 mg/mL), were injected (60 µL) onto the GPC column, as described in Section 2.6.2.1. Elution profiles were monitored over 30 min, at a flow rate of 1 mL/min. Weight average, the number average molecular weights and the polydispersity of the succinoylated dextrin samples, were derived from the polysaccharide molecular weight standard curve, obtained as previously described.

3.2.4 Ninhydrin assay

Prior to conjugation of rhEGF to dextrin, it was firstly important to determine the number of available amine groups available for conjugation. The ninhydrin assay was selected for this purpose. Ninhydrin is a powerful oxidising agent, with the ability to react with all primary amino acids, between pH 4 and 8, resulting in a purple colour, which forms the basis of the quantitative measurement of amine content (Plummer, 1978).

A 4 M lithium acetate buffer solution was prepared by dissolving lithium acetate dihydrate (102.02 g) in ddH_2O (150 mL). Acetic acid (glacial) was added, until pH 5.2 was reached. The volume was made up to a final volume of 250 mL with ddH_2O. Ninhydrin (0.8 g) and hydrindantin (0.12 g) were dissolved in 30 mL DMSO and 10 mL lithium acetate buffer, respectively.

DL-amino-2-propanol was dissolved in ddH_2O to provide amino acid

standards with concentrations in the range of 12.9 – 90.4 μM. A sample of rhEGF (250 μg/mL in PBS) was prepared. Buffered ninhydrin reagent (86 μL) was added to an equal quantity of sample/standard solution and heated in a water bath, at 100 °C for 15 min. The mixtures were subsequently cooled to room temperature, and 130 μL of 50 % v/v ethanol added, prior to spectrophotometric analysis at 570 nm. A typical calibration curve is shown in Figure 3.4.

3.2.5 Succinoylated dextrin-rhEGF conjugation and characterisation

Conjugation of the rhEGF to succinoylated dextrin was optimally performed at a 2:1 molar ratio (rhEGF : succinoylated dextrin), based on preliminary data. rhEGF was supplied in 1 mg aliquots of lyophilised powder. Succinoylated dextrin (8.2 mg) was dissolved in 500 μL of ddH_2O and added to EDC (1.12 mg), in a 10 mL round bottomed flask and stirred for 10 min, at room temperature. To this, sulfo-NHS (1.2 mg) was added and stirred for a further 40 min, under identical conditions. rhEGF (2 mg) was dissolved in ddH_2O (300 μL) and added to the reaction mixture. NaOH (0.5 M) was added drop-wise, until the mixture reached pH 8. The resulting mixture was stirred for 18 h. The conjugate was purified using FPLC and ultra-filtration as described in Section 2.6.1. The purified conjugate was characterised by GPC, FPLC, SDS-PAGE and BCA protein assay, as described in Section 2.6.

3.2.6 Degradation of dextrin, succinoylated dextrin and the dextrin-rhEGF conjugate, by α-amylase

Human salivary α-amylase (Type XIII-A) was supplied as units (U) per mg of protein. One U will liberate 1 mg of maltose from starch, in 3 min, at pH 6.9, 20 °C. Human plasma amylase is normally quoted as international units (i.u.), or Somogyi units, where one i.u. will liberate 1 mg of glucose from starch, in 30 min, at pH 7.4, 40 °C (equivalent to 0.0167 μkatals/L). A calibration curve was constructed using known concentrations of salivary amylase, assayed using the Phadebas® amylase assay (Section 6.2.3.2) to equate U to i.u. (Figure 3.5). All values herein are quoted as human plasma equivalents (i.u.).

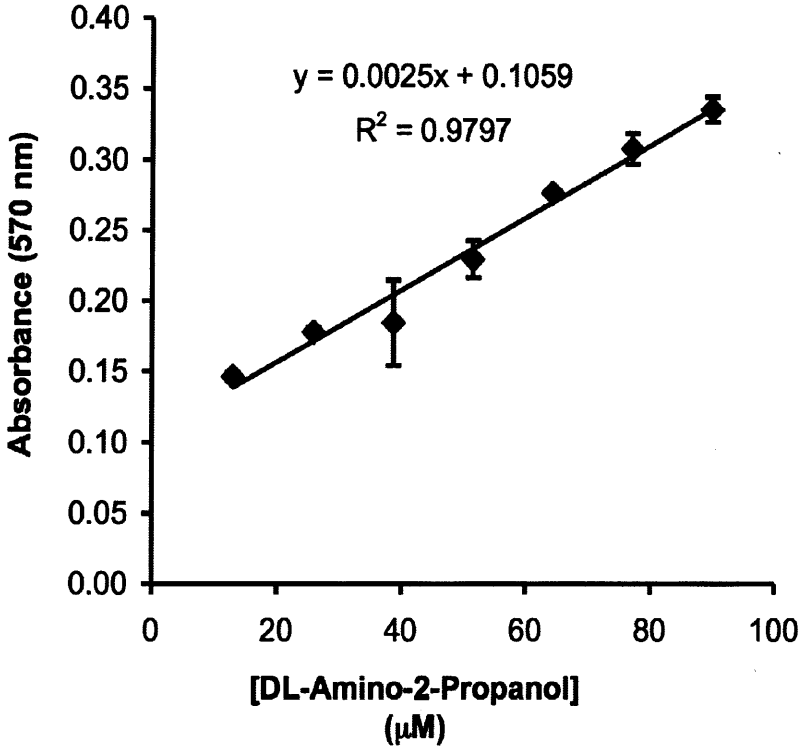

Figure 3.4 **Ninhydrin assay.** Typical calibration curve obtained for the quantification of the number of primary amines in rhEGF, available for polymer-protein conjugation, using DL-amino-2-propanol standards (mean ± S.D., n = 3).

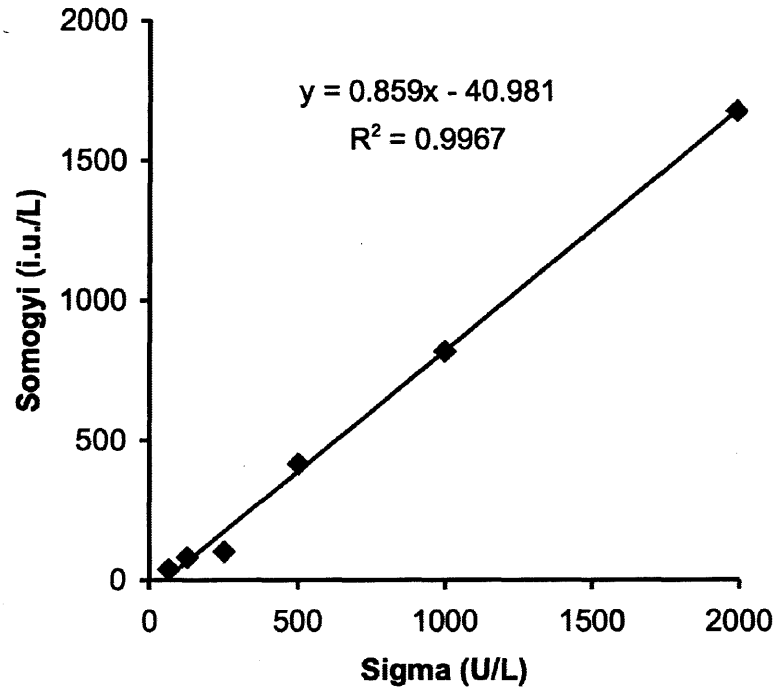

Figure 3.5 **α-Amylase conversion.** A typical batch calibration to convert Sigma units (U) to Somogyi international units (i.u.) (mean ± S.D., n = 3, error bars are within data points).

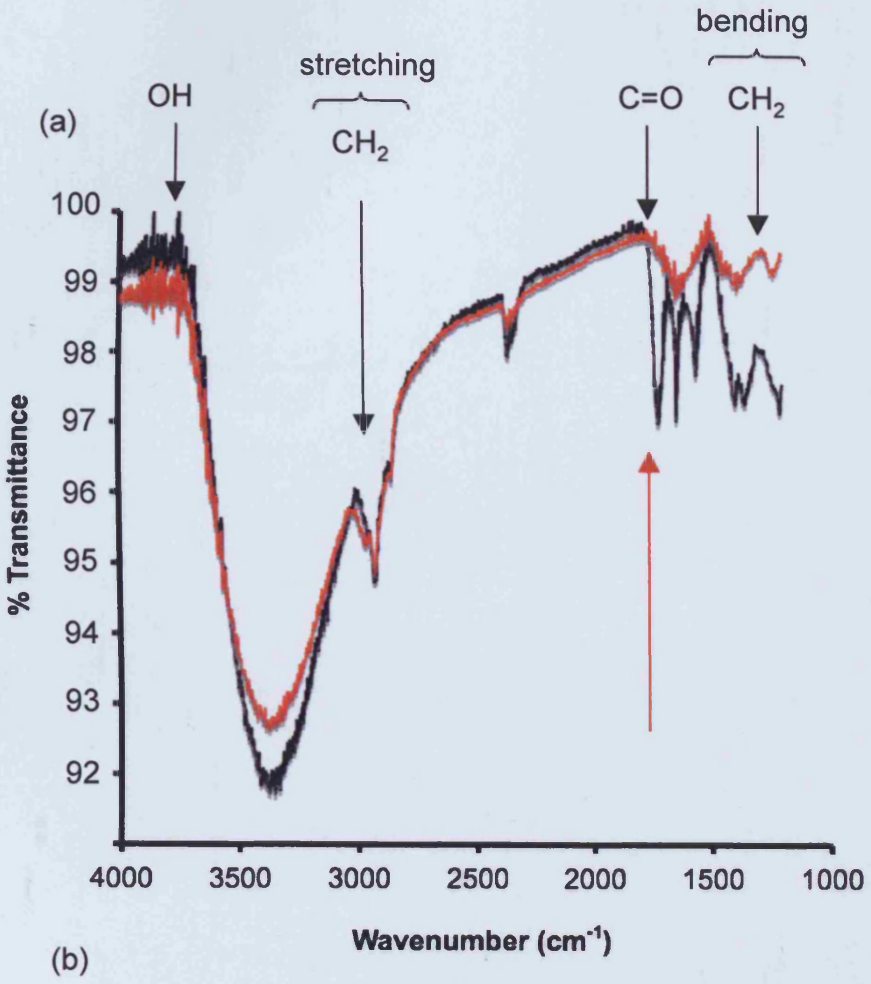

Group	Frequency Range (cm^{-1})
OH stretching vibrations	
OH	3610-3645
CH Stretching vibrations	
CH2	2843-2863, 2916-2936
CH	2880-2900
C=O Stretching Vibrations	
Nonconjugated	1700-1900
Conjugated	1590-1750
CH Bending Vibrations	
CH2	1405-1465

Figure 3.6 **Fourier transform infrared (FTIR) spectroscopy analysis of dextrin and succinoylated dextrin.** Panel (a) shows typical spectrum of dextrin is shown in red, and succinoylated dextrin, in black. Infrared band positions for relevant chemical groups are arrowed. Succinoylation was confirmed by the presence of the non-conjugated C=O groups at the characteristic wavenumber (1720 cm^{-1}; arrowed in red). Panel (b) shows characteristic infrared band positions for different chemical groups (Adapted from Advanced Light Source, 2008).

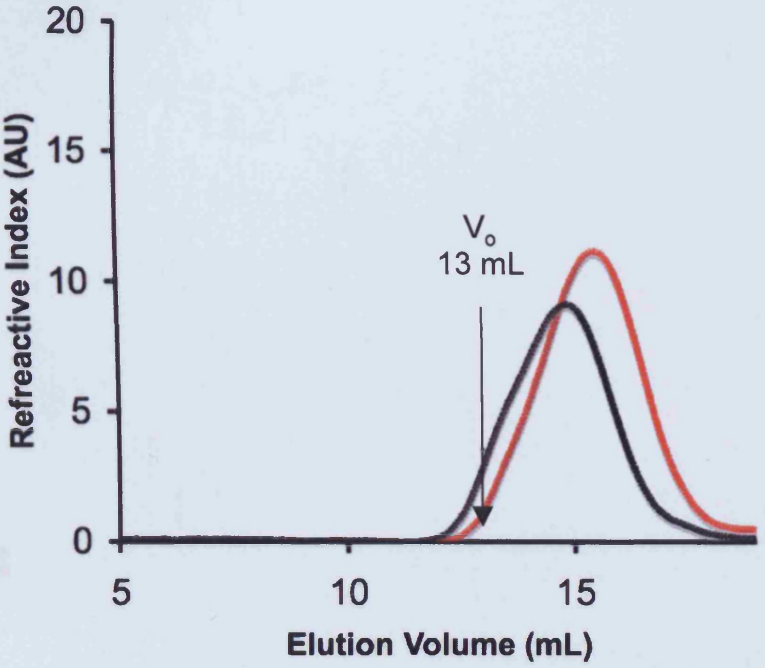

Figure 3.7 **Gel permeation chromatography (GPC) analysis of dextrin and succinoylated dextrin**.A typical chromatogram of dextrin is shown in red, and succinoylated dextrin, in black. The shift in elution volume results from the succinoylation, leading to an increase in hydrodynamic volume and approximate molecular weight (dextrin approximately 57,000 g/mol, succinoylated dextrin approximately 84,000 g/mol). V_0 represents the void volume.

dark smearing appearing between approximately 197,000 to 37,000 g/mol, corresponding to the presence of a polydisperse conjugate. Prior to purification, there was also a band present within the conjugate reaction mixture at approximately 6,000 g/mol, corresponding to free rhEGF (Figure 3.8a). This band was absent following purification, by FPLC (Figure 3.8b).

Similarly, FPLC analysis of the conjugation reaction mixture, prior to purification, showed a peak corresponding to the dextrin-rhEGF conjugate, in the void volume (V_o) region (7.7 mL) (Figure 3.9a). Other peaks, corresponding to free rhEGF (14-16 mL) (Figure 3.9b), and the reactants DMAP (Figure 3.9c) and sulfo-NHS (Figure 3.9d), were also identified. Following FPLC purification, the conjugate was free of these reactants and free rhEGF (Figure 3.9e). Estimation of molecular weight by comparison to the FPLC protein standard curve, was 147, 000 ± 17, 000 g/mol (mean ± S.D. n = 5 batches). GPC was also used to estimate molecular weight, by comparison to the polysaccharide standard curve, and polydispersity (106, 000 ± 1000 g/mol and 1.53, respectively; mean ± S.D. n = 3).

Various batches of dextrin-rhEGF were synthesized and characterized to optimise the reaction conditions (Table 3.4). The optimum conditions for synthesis of the dextrin-rhEGF conjugates were concluded to be a 2:1 molar ratio of rhEGF:dextrin, with an 18 h reaction time. Synthesis was reproducible, with the mean rhEGF content being 16.3 ± 4.4 wt % protein, as determined by BCA assay (n = 5 batches, mean ± S.D.). This equated an rhEGF incorporation of approximately 2 moles of rhEGF to every mole of succinoylated dextrin.

3.3.2 Degradation of dextrin, succinoylated dextrin and the dextrin-rhEGF conjugate, by α-amylase

Dextrin, succinoylated dextrin and the dextrin-rhEGF conjugate were degraded by physiological levels of α-amylase (93 i.u./L), which produced a shift in molecular weight over time, as evident by GPC (Figure 3.10a). Minimal degradation occurred in α-amylase-free conditions (Figure 3.10b). Succinoylated dextrin ($T_{1/2}$ = 79.7 h) was degraded at a much slower rate than native dextrin ($T_{1/2}$ = 6 min). The dextrin-rhEGF conjugate was degraded in a similar fashion to succinoylated dextrin ($T_{1/2}$ = 55.4 h) (Figure 3.10c), indicating that protein conjugation did not affect polymer degradation.

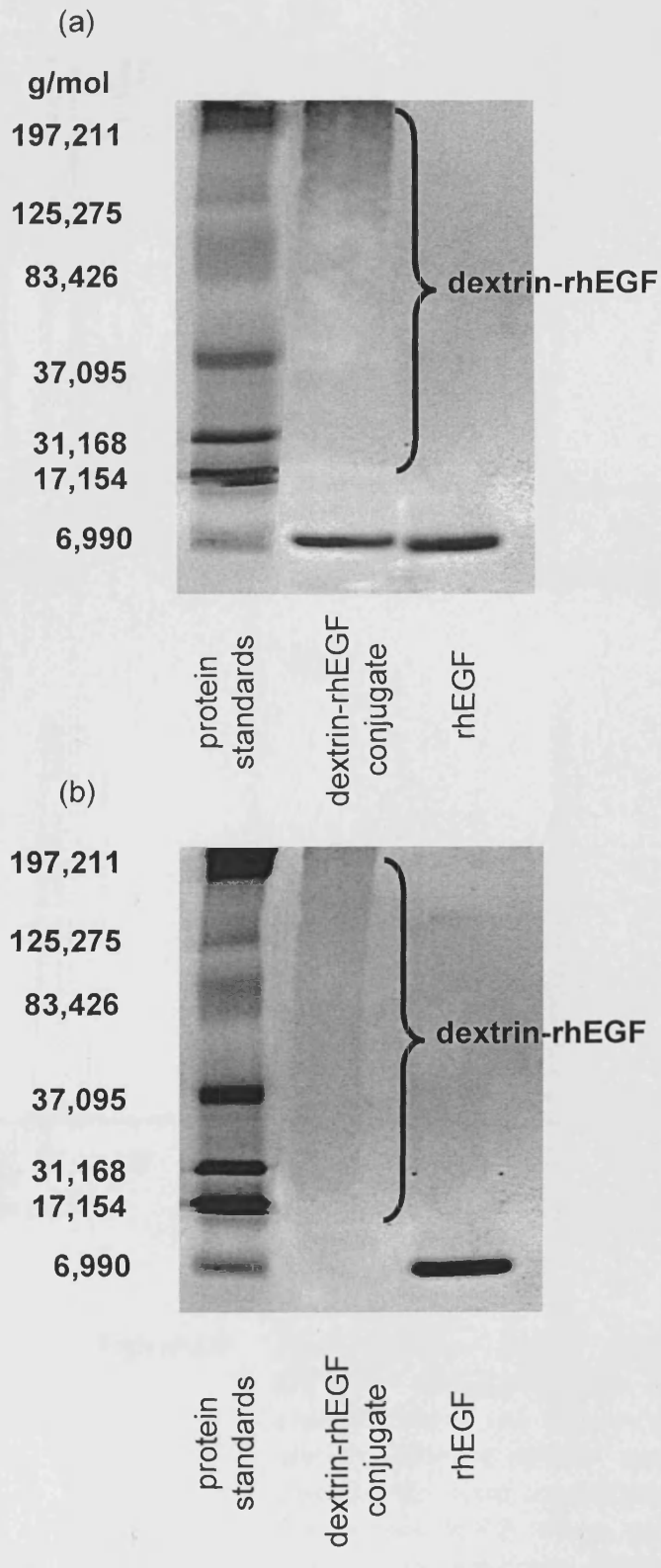

Figure 3.8 **Sodium dodecyl sulfate-polyacrylamide gel electrophoresis (SDS-PAGE) analysis of dextrin-rhEGF.** Panel (a) shows the dextrin-rhEGF reaction mixture, prior to FPLC purification and panel (b) shows the same sample post-FPLC purification. Free rhEGF (at approximately 6,000 g/mol) was below the limit of detection (< 200 ng) in the purified sample.

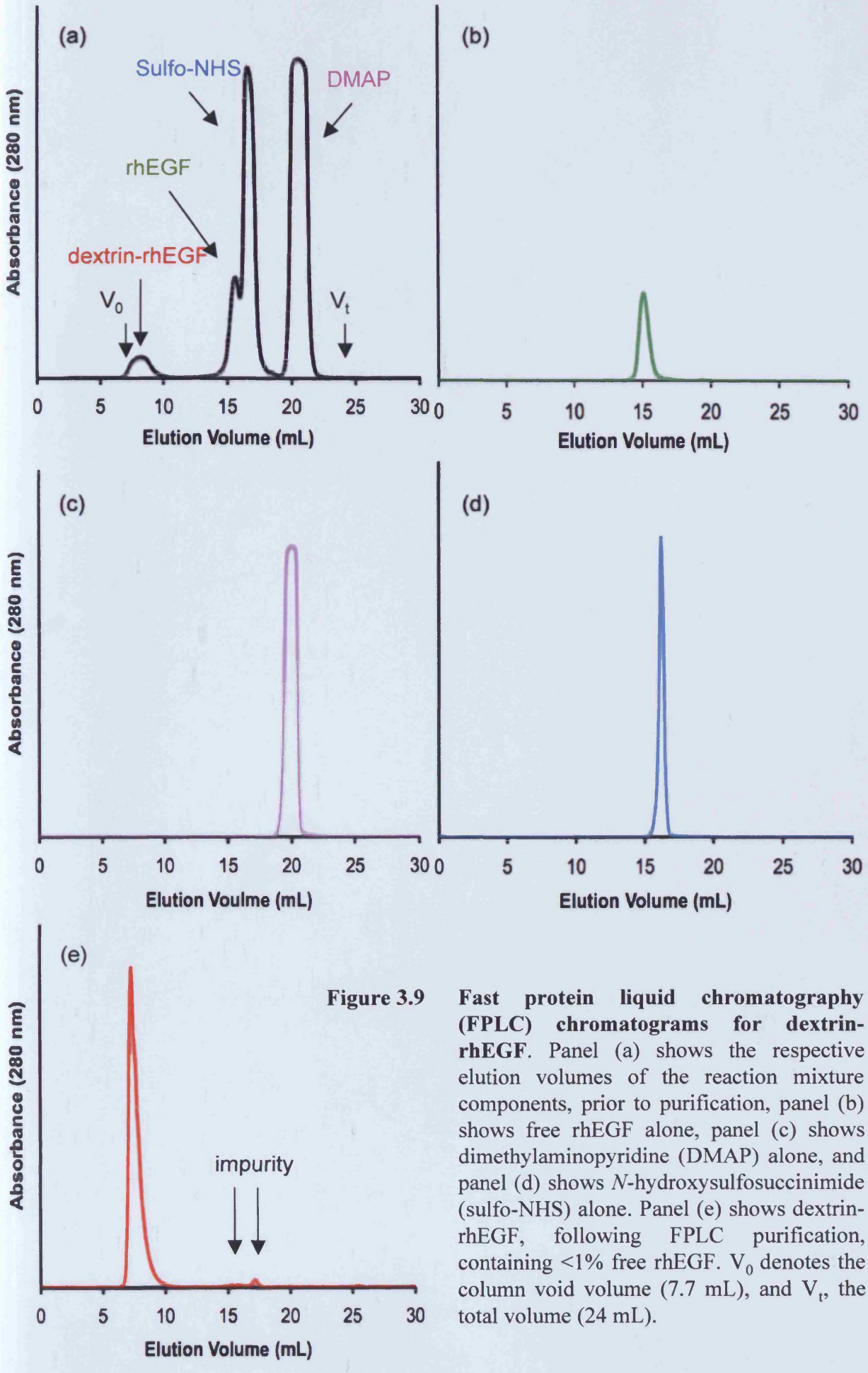

Figure 3.9 **Fast protein liquid chromatography (FPLC) chromatograms for dextrin-rhEGF.** Panel (a) shows the respective elution volumes of the reaction mixture components, prior to purification, panel (b) shows free rhEGF alone, panel (c) shows dimethylaminopyridine (DMAP) alone, and panel (d) shows *N*-hydroxysulfosuccinimide (sulfo-NHS) alone. Panel (e) shows dextrin-rhEGF, following FPLC purification, containing <1% free rhEGF. V_0 denotes the column void volume (7.7 mL), and V_t, the total volume (24 mL).

Table 3.4 Dextrin-rhEGF conjugate, batch summary

Batch	Reaction mixture (dextrin : rhEGF)	Reaction time	% conjugation of rhEGF (weight %)	Estimation of molecular weight (FPLC)	Ratio of dextrin : rhEGF	% yield rhEGF**
JTH001	1 : 1	18 h	6 %	126,000 g/mol	2 : 1	12 %
JTH002	2 : 1	18 h	7 %	137,000 g/mol	1 : 1	17.3 %
JTH003	2 : 1	30 h	4 %	134,000 g/mol	3 : 1	2.4 %
JTH004	2 : 1	18 h	16.8%	137,000 g/mol	1 : 2	47.9 %
JTH005	2 : 1	18 h	14.3 %	157,000 g/mol	3 : 4	37.2 %
JTH006	2 : 1	18 h	11 %	172,000 g/mol	1 : 1	23.1 %
JTH007	2 : 1	18 h	23.1 %	131,000 g/mol	2 : 5	31.2 %
JTH008	2 : 1	18 h	16.5 %	140,000 g/mol	1 : 2	19.8 %
		* average	16.3 %	147,000 g/mol	1 : 2	31.8 %

*batches JTH001 - JTH003 were for reaction optimisation purposes only. Subsequent batch calculations were based upon JTH004 - JTH008
** weight % x mass of conjugate

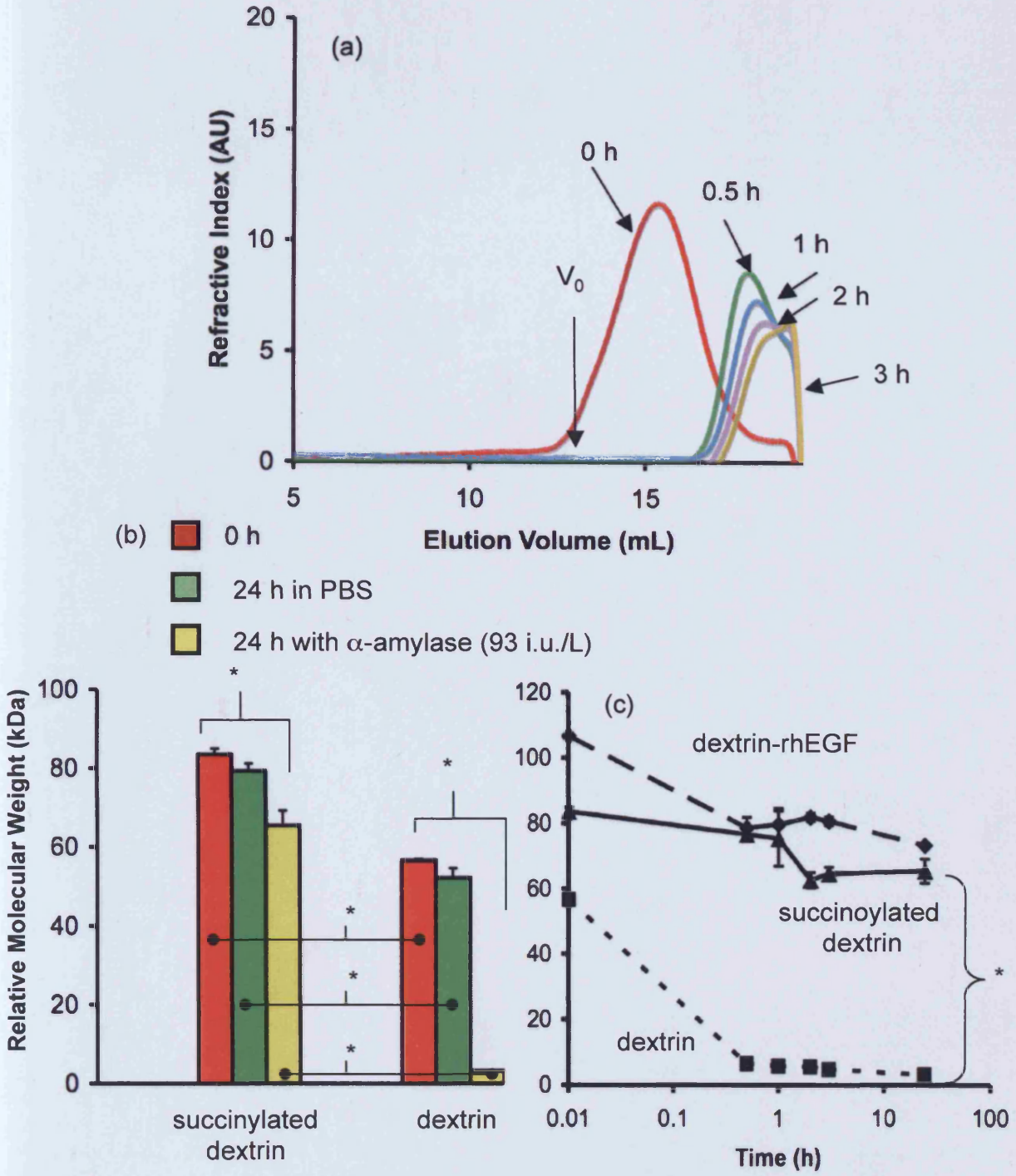

Figure 3.10 GPC analysis of the degradation of dextrin, succinoylated dextrin and dextrin-rhEGF. Panel (a) shows the typical shift in elution volume (and approximate molecular weight) of dextrin, in response to α-amylase (93 i.u./L) over a 3 h period. V_0 denotes the void volume (13 mL). Panel (b) shows the degradation of succinoylated dextrin and dextrin, over a 24 h period, in the absence (PBS) and presence of α-amylase (93 i.u./L) (n = 3; mean ± S.D., * $p < 0.001$, ANOVA and Bonferroni *post hoc* test). Panel (c) shows the change in relative molecular weight (GPC analysis) of dextrin (- - ■ - -), succinoylated dextrin (—▲—), and dextrin-rhEGF (- - ◆ - -), in the presence of α-amylase (93 i.u./L), over a 24 h period (n = 3; mean ± S.D., * $p = 0.0012$, ANOVA and Bonferroni *post hoc* test).

3.3.3 Dextrin-rhEGF conjugate degradation assays

When the dextrin-rhEGF conjugate was exposed to α-amylase (93 i.u./L), the polymer was degraded and free rhEGF was released (Figure 3.11). FPLC analysis showed the characteristic reduction in peak area, corresponding to the dextrin-rhEGF conjugate (6-9 mL), when exposed to α-amylase at 37 °C, as the dextrin polymer was degraded. In a reciprocal fashion, the FPLC peak corresponding to free rhEGF (14-16 mL) increased as rhEGF was released into solution. In α-amylase-free conditions, at 37 °C, the conjugate remained stable, with minimal degradation of the dextrin-rhEGF conjugate and little or no release of free rhEGF, calculated as the ratio of the peak heights of rhEGF : dextrin-rhEGF. The conjugate was thus verified to be resistant to hydrolytic degradation. The conjugate remained stable, both in solution at 4 °C and lyophilised with later reconstitution. Upon addition of α-amylase (93 i.u./L), rhEGF was liberated over a 168 h period. As rhEGF was released and the conjugate degraded, there was a shift in the rhEGF : dextrin-rhEGF ratio, in favour of the released growth factor. A biphasic pattern, with an episode of released rhEGF over 0-3h, followed by sustained release from 3 - 168 h was evident.

The ELISA method was sensitive to the human isoform of EGF (including rhEGF). The dextrin-rhEGF conjugate that had not been exposed to α-amylase, was shown not to stimulate the antigen-antibody response required for the ELISA reaction. In contrast, following α-amylase exposure, free rhEGF released into solution did stimulate the antigen-antibody complex formation (Figure 3.12). After 168 h, 61.2 % of the total rhEGF content of the conjugate was released. However, α-amylase and succinoylated dextrin controls did not produce a recordable response. Again, the biphasic pattern of rhEGF release that was noted by FPLC analysis, was also evident, with rhEGF release reaching a plateau after 24 h and increasing during the final 144 h.

3.3.4 Stability of rhEGF and the dextrin-rhEGF conjugate, in response to proteinases

As a proof of concept study, free rhEGF was degraded at a greater rate ($T_{1/2}$ = 45min), than the dextrin-rhEGF conjugate ($T_{1/2}$ > 3h), following trypsin (0.025%) exposure (Figure 3.13a). FPLC analysis of rhEGF and dextrin-rhEGF, in response to neutrophil elastase (at physiologically relevant concentrations), exhibited marked

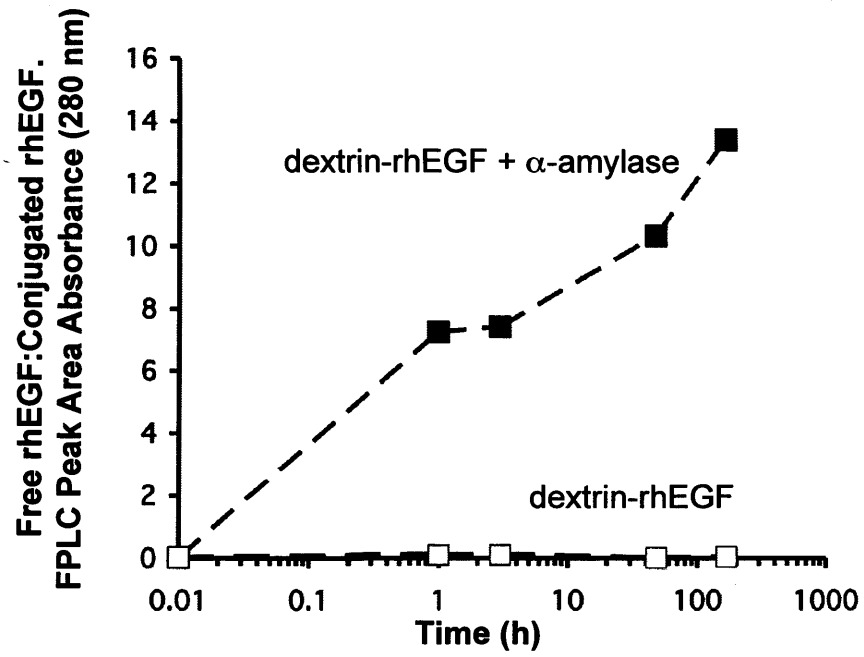

Figure 3.11 **FPLC analysis of rhEGF released from dextrin-rhEGF,** in the presence (- - ■- -) and absence (- - □ - -) of α-amylase (93 i.u./L), shown as the ratio of FPLC chromatogram peak areas, corresponding to dextrin-rhEGF and free rhEGF (n = 1).

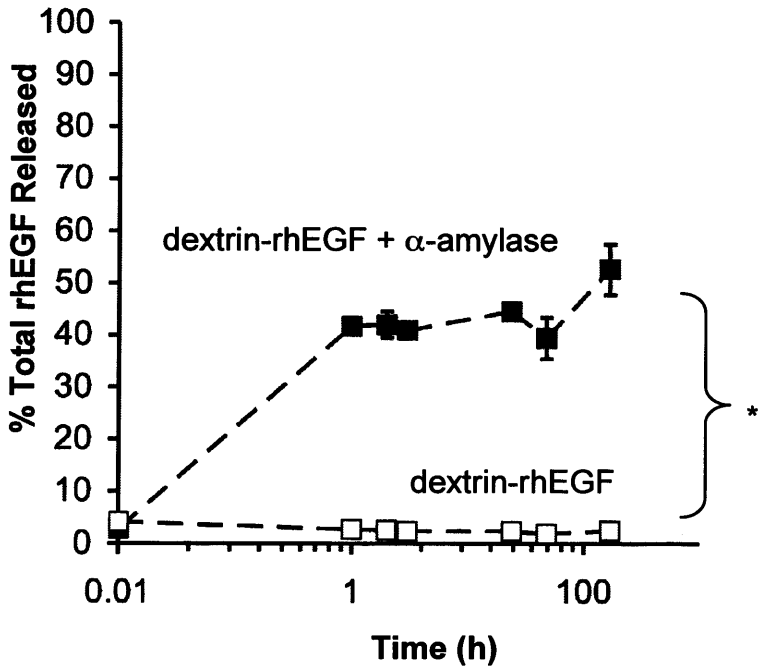

Figure 3.12 **Enzyme-linked immunosorbant assay (ELISA) analysis of rhEGF release from dextrin-rhEGF.** The release of rhEGF from dextrin-rhEGF, in the presence (- - ■- -) and absence (- - □- -) of α-amylase (93 i.u./L). The results are shown as the amounts of rhEGF released (pg/mL), as a percentage of the total protein content of dextrin-rhEGF (n = 3; mean ± S.E.M., * p = 0.0012, Student's t-test).

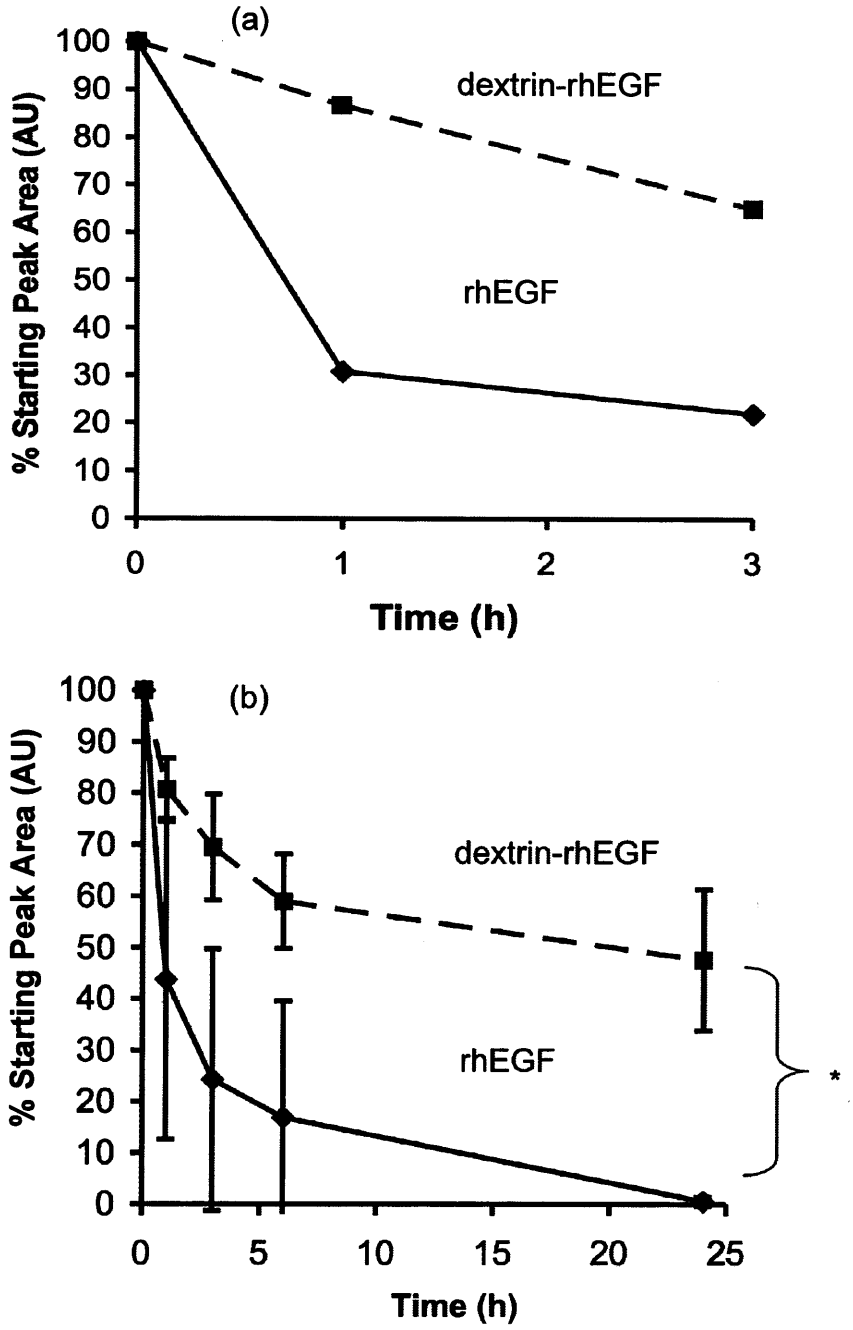

Figure 3.13 **FPLC analysis of dextrin rhEGF (--■--) and free rhEGF (—◆—) degradation, in response to proteinases.** Panel (a) shows a proof of concept experiment, in response to trypsin-EDTA (0.025%) (n=1) and panel (b) shows the stability of rhEGF and dextrin-rhEGF, in the presence of neutrophil elastase (100 μg/mL) (n = 2; mean ± S.D., * p = 0.0401, Student's t-test).

degradation of rhEGF ($T_{1/2}$ < 2h),when compared to conjugated rhEGF ($T_{1/2}$ > 24h) (Figure 3.13b). Indeed, nearly 70% of the dextrin-rhEGF conjugate remained, following 6h exposure to neutrophil elastase.

3.4 Discussion

The Chapter aimed to synthesise and characterise a dextrin-rhEGF conjugate. Quantification of the amine groups available for polymer conjugation, via the ninhydrin assay, estimated a different number (mean = 1.2), from the actual value (three: two lysine residues and the N-terminus). The discrepancy between the actual and calculated amine groups may be a consequence of the inaccessibility of the amine groups, within the tertiary structure of the protein. Although there appeared to be only one accessible amine group for conjugation, probably lysine 48 (K_{48}), site-specific conjugation was still possible. Furthermore, with the close locality of K_{48} to a residue implicated in EGF-receptor binding (leucine 47) (Lu *et al,* 2001), it can be postulated that conjugation may reduce receptor-binding capability and therefore, permit "masking" of rhEGF bioactivity, in keeping with the PUMPT concept.

3.4.1 Dextrin-rhEGF conjugation

Succinoylation of dextrin is a reliable, reproducible and cost-effective mechanism for the "activation" of the dextrin polymer. The introduction of reactive pendant groups to the polymer chain allowed chemical modification, without inducing instability in the polymer, that can be associated with other forms of modification, involving functional group introduction into the polymer backbone (Hreczuk-Hirst *et al*, 2001a). The chemicals used in this process are also less toxic than those highlighted, associated with other such processes (Bruneel and Schacht, 1993a; 1993b; Table 3.1).

The variable succinoylation of dextrin has been previously reported to be between 5% to 34% (Hreczuk-Hirst *et al*, 2001a; Ferguson *et al*, 2006; Duncan *et al*, 2008) as determined by titration. With the introduction of biologically active carboxylic groups to the dextrin polymer, it was possible to form polymer-protein conjugates. The reaction efficiency was optimised with the use of cross-linking agents (EDC, sulfo-NHS), resulting in up to 23.1% incorporation of rhEGF, by weight.

Reproducible conjugation was evident, using reliable methods of protein assay (SDS-PAGE, FPLC and the BCA protein assay), which detected both free- and conjugated rhEGF. The conjugate product was characterised and purified, to remove both free rhEGF and excess cross-linking agents from the reaction mixture, resulting in < 1 % contamination with free rhEGF or cross-linkers.

3.4.2 Challenges to the dextrin-rhEGF conjugate characterisation

There was a significant difference in the estimated average molecular weight of the dextrin-rhEGF conjugate by GPC (106, 000 ± 1000 g/mol) and FPLC (147, 000 ± 17, 643 g/mol).

Characterisation of a polymer-protein conjugate is generally difficult, as it does not behave like either individual component. This is especially significant when using GPC to determine molecular weight. Pullulan, like dextrin, is a polysaccharide that would be expected to take on a random coil structure in solution (Shingel, 2004), and therefore, is expected to behave similarly to dextrin. For these studies, pullulan was deemed the most appropriate choice as a molecular weight standard. However, it was recognised that the estimation of the conjugate molecular weight was likely to be difficult, by GPC.

Similarly, it remained impossible to obtain an absolute molecular weight for the conjugate, using FPLC, due to the structural and chemical properties of the conjugate, compared to the protein standards. Proteins have a unique tertiary structure that is, not only, dependent on their molecular weight, but also their charge, thus making accurate calibration of the FPLC column difficult. The presence of the polymer would, therefore, influence the molecular weight and charge of the conjugate and the polydispersity, making accurate determinations of molecular weight impossible.

SDS-PAGE was used to confirm the increase in rhEGF protein molecular weight, suggesting successful conjugation of succinoylated dextrin and rhEGF. Free rhEGF was compared to the pre- and post-purification reaction products, in relation to a series of molecular weight markers. The smearing observed for the dextrin-rhEGF conjugates, indicated that polydisperse dextrin-rhEGF conjugates were produced, due to the random coil nature of dextrin, in addition to uneven protein distribution along the polymer chain and between different chains. There are numerous conformations in which the dextrin-rhEGF conjugate could exist, as a

result of the multiple binding sites on succinoylated dextrin. The potential for cross-linking was reduced, by the fact that rhEGF had only one potential binding site. Using the weight % rhEGF incorporation, in conjunction with the estimation of dextrin-rhEGF molecular weight (FPLC), the ratio of dextrin : rhEGF, on average per batch, was calculated to be 1 : 2 (dextrin : rhEGF). This matched the initial ratio in the optimum reaction mixture, and although free rhEGF was also noted in typical pre-purification FPLC chromatograms, it must also be assumed that an equivalent amount of unconjugated, succinoylated dextrin, must also be present.

3.4.3 Dextrin-rhEGF degradation

The present Chapter demonstrated that dextrin, succinoylated dextrin and the dextrin-rhEGF conjugate, are all susceptible to α-amylase-mediated degradation, and therefore, are suitable as the degradable carrier component of a polymer-protein conjugate. Modification of dextrin by succinoylation, not only allowed activation of the polymer chain, thus permitting conjugation to rhEGF or other proteins/peptides, but also reduced the rate of α-amylase-mediated degradation. Degradation was slowed nearly 800-fold, by the addition of carboxylic acid side chains to the dextrin molecule. As the polymer was degraded, the degree of polydispersity was reduced as the chain lengths shortened and began to normalise to limit-dextrin and smaller maltose and isomaltose disaccharide units.

Hreczuk-Hirst *et al* (2001b) demonstrated that the rate of dextrin degradation was proportional to the degree of succinoylation, as unmodified dextrin had a half-life of 1-5 min, following exposure to rat plasma-derived α-amylase (approximately 12,000 to 23,000 i.u./L), or porcine plasma α-amylase (approximately 2,000 i.u./L). These findings are similar to those obtained in the present Study, even though a much lower concentration of human, salivary α-amylase was used (93 i.u./L; $T_{1/2} = 6$ minutes). The greater the mol % carboxylic acid groups incorporated, the slower the degradation rate. Rapid degradation was apparent at < 15 mol %, but at greater degrees of succinoylation, a slower degrading polymer, capable of sustained release over several days was produced.

As one of the aims of this Study, was to assess the dextrin-rhEGF conjugate as a therapy for human chronic wounds, the majority of the subsequent studies were performed under physiological concentrations of human plasma α-amylase.

Although the α-amylase employed herein was from a human source, it is not pancreatic in origin (as human plasma α-amylase would be). Nevertheless, any further experimentation using human pancreatic amylase would yield similar results.

The ELISA did not detect any free rhEGF in the purified dextrin-rhEGF conjugate, unless the polymer had been degraded by α-amylase. Therefore, it can be concluded that the succinoylated dextrin polymer is likely to reduce the immunogenicity of rhEGF, again increasing the potential half-life of the rhEGF protein, as in the conjugated form, rhEGF and the active EGF-receptor binding domains are "masked". The use of a polyclonal detection system may have allowed the detection of the rhEGF, prior to complete polymer degradation, as sites away from the conjugation may be detected. However, it must be considered that without proteolysis, the amide bond between the polysaccharide remnant and the rhEGF protein will remain. The "masking" effect does have a drawback, however, in that an accurate measure of the quantity of rhEGF incorporated into the dextrin-rhEGF cannot be directly quantified by ELISA, although degradation studies, as shown herein, have been demonstrated to liberate over 60 % of the calculated rhEGF from the dextrin-rhEGF conjugate, on exposure to α-amylase, for 168 h.

The controlled release phenomenon, described here would theoretically enhance the stability of the rhEGF protein, in both plasma and chronic wound fluid. Indeed, increased resistance to proteolytic degradation, as would occur in a chronic wound environment, is apparent by the resistance of the dextrin-rhEGF conjugate, to degradation in both the trypsin, proof-of-concept model, and the neutrophil elastase model (a proteinase in chronic wound fluid; Trengove *et al*, 1999). Subsequently, the half-life of rhEGF, when conjugated to succinoylated dextrin, was observed to increase over 12-fold, after exposure to neutrophil elastase.

In all studies of α-amylase-mediated degradation, a biphasic pattern was evident, with rapid initial enzymatic hydrolysis, followed by a slower, more sustained pattern of release. This phenomenon was also reported by Hreczuk-Hirst *et al* (2001b). The initial hydrolysis would quickly produce large polymer chains (10,000 – 20,000 g/mol), which would then undergo slower degradation to the limit-dextrin, and then to maltose and isomaltose disaccharide units.

3.5 Conclusions

In summary, the succinoylation of dextrin produced an activated polymer that allowed reversible protein conjugation, via α-amylase-mediated degradation. The half-life of succinoylated dextrin (and of the dextrin-rhEGF conjugate), under physiological concentrations of human plasma α-amylase, was sufficient to permit effective, controlled, rhEGF release. Whereas traditional controlled release agents combine the active ingredient in a carrier vehicle, there is no chemical binding between the vehicle and therapeutic agent. Thus, the therapeutic agent is open to immunogenic reactions and degradation. This Chapter has demonstrated that the dextrin-rhEGF conjugate can "mask" the conjugated rhEGF from both an immunogenic response and proteolytic degradation. Upon polymer degradation by α-amylase, immunogenic rhEGF is released. The inactivation ("masking") must be reversible ("unmasking") to allow delivery of bioactive rhEGF to the site of action. The large molecular size of dextrin-rhEGF, which has been determined by GPC and FPLC, may also allow targeting of specific tissues, via the enhanced permeability and retention (EPR) effect (Matsumura and Maeda, 1986).

The bioactivity of rhEGF and "unmasked" dextrin-rhEGF conjugate, will now be established, in addition to the reduction in conjugate bioactivity, when in an α-amylase-free environment. Samples of the dextrin-rhEGF conjugate, that have been exposed to wound proteinases, will also be analysed, to ensure bioactivity is retained and restored, as part of the PUMPT hypothesis. Further evaluation included assessment of the rhEGF bioactivity, with *in vitro* cell-based models of wound healing.

Chapter Four

In Vitro Evaluation of The Stimulation of Cellular Activity by The Dextrin-rhEGF conjugate

Chapter Four: *In Vitro* Evaluation of The Stimulation of Cellular Activity by The Dextrin-rhEGF Conjugate

Contents

4.1 Introduction

The main cell types involved in the structural process of wound healing, i.e. collagen synthesis, and extracellular matrix (ECM) remodelling and re-epithelialisation, are the fibroblasts and keratinocytes (Martin, 1997). Therefore, the stimulatory effects of recombinant human epidermal growth factor (rhEGF) and the dextrin-rhEGF conjugate on these cells, will be the focus of the present Chapter. Specifically, cellular migration into the wound space and cellular proliferation, to replace and repair lost or dysfunctional tissues, will be examined.

4.1.1 Fibroblasts

Fibroblasts synthesise and maintain the ECM of the dermis, and provide a structural framework for normal skin function. Embryologically, these cells are derived from the mesenchyme (Desmoulliere and Gabbiani, 1996). Fibroblasts are the most common cell type in the connective tissue of animals and secrete the precursors of the ECM, including collagen, elastin, proteoglycans and glycoproteins (Doljanski, 2004).

Morphologically, fibroblasts have a branched cytoplasm, surrounding an elliptical nucleus (Desmoulliere and Gabbiani, 1996). Although disjointed and scattered at low cellular density, fibroblasts, when at a high cellular density, often locally align in parallel clusters. Active fibroblasts can be recognized by their abundant rough endoplasmic reticulum. Inactive fibroblasts, which are also known as fibrocytes, are smaller and spindle shaped (Bucala *et al*, 1994). They have a reduced rough endoplasmic reticulum. Tissue injury stimulates fibrocyte activity, and the induction of fibroblasts mitosis (Quan *et al*, 2004).

Fibroblasts are morphologically heterogeneous with diverse appearances depending on their location and activity. While epithelial cells form the lining of body structures, it is fibroblasts and related connective tissues that sculpt the form of an organism (Grinnell *et al*, 2003). Although, similar in structure, such fibroblasts can retain their individual phenotype (Sorrell and Caplan, 2004). For example, chronic wound fibroblasts undergo cellular senescence (irreversible entry into the G_0 phase of the cell cycle), at an earlier stage than their patient-matched, normal dermal counterparts (Telgenhoff and Shroot, 2005; Wall *et al*, 2008).

As an early response to injury, local dermal fibroblasts begin to proliferate and migrate to the site of injury, where they synthesise a collagen-rich ECM

(McClain *et al*, 1996). Many of the growth factors present at the wound site act as mitogens or as chemotactic factors for fibroblasts, including platelet-derived growth factor (PDGF), EGF, fibroblast growth factor (FGF), insulin-like growth factor-1 (IGF-1) and transforming growth factor-β (TGF-β) (Martin, 1997). After one week, a proportion of the fibroblast population will have differentiated into myofibroblasts, due to TGF-β_1 and mechanical cues, related to the forces resisting contraction (Desmouliere *et al*, 1996; Grinnell and Ho, 2002; Hinz, 2007; Hinz *et al*, 2007). Expression of α-smooth muscle actin, allows the generation of contractile forces to reduce the wound area.

The fibroblasts that will be used in the present Study were derived from biopsies of the edge of a chronic venous leg ulcer and of the ipsilateral thigh, from a single patient. These cells were hTERT (human telomerase, reverse transcriptase) immortalized and donated by Dr Ivan Wall and Dr Mathew Caley (Tissue Engineering and Reparative Dentistry, School of Dentistry, Cardiff University). These chronic wound and normal dermal fibroblast cell lines have been established to mimic impaired and normal wound healing responses, *in vitro*.

4.1.2 Keratinocytes

Keratinocytes are structured in a laminar form that makes up the five layers of the epidermis (*strata basalis; spinosum; granulosum; lucidum;* and *corneum*). Keratinocytes originate in the *stratum basalis* from keratinocyte stem cells, which migrate up through the dermis, undergoing differentiation as they progress. On reaching the *stratum corneum*, these become flattened or *squamous* in morphology and are highly keratinized (Eckert, 1989), providing the skin with it's barrier characteristics to infective or toxic vectors, and minimizes moisture loss (Madison, 2003). Keratinocytes are continuously shed from the *stratum corneum* and replaced by cells from below (Houben *et al*, 2007). The transit time from *stratum basalis* to *stratum corneum* is approximately one month, although this can be accelerated in hyperproliferative keratotic conditions, such as psoriasis (Weinstein *et al*, 1984).

Keratinocytes are responsible for the process of re-epithelialisation, which occurs during the late-inflammatory and proliferative phases of wound healing (Patel *et al*, 2006, Gurtner *et al*, 2008). Upon re-epithelialisation of the wound, the normal barrier function of the skin (to moisture and pathogens) is restored, allowing the

proliferation of sub-epidermal fibroblasts and ECM remodeling (Patel *et al*, 2006; Sivamani *et al*, 2007). Unlike fibroblasts, the keratinocytes migrate in a group-wise fashion, producing a "sliding sheet" of cell migration (Zhao *et al*, 2003).

In unwounded skin, basal keratinocytes are attached to the specialised basal lamina via hemidesmosomes, which bind to laminin in the basal lamina via $\alpha 6\beta 4$ integrins, which have intracellular links to the keratinocyte cytoskeleton (Haapasalmi *et al*, 1996). For keratinocyte migration to occur, these hemidesmosomes are degraded and the expression of new integrins ($\alpha 5\beta 1$), collagen receptors and fibronectin/tenascin receptors, allows the cells to "crawl" over the wound matrix (Cavani *et al,* 1993; Breuss *et al*, 1995; Haapasalmi *et al*, 1996). Forward locomotion involves the contraction of actinomysin filaments within the cytoskeleton, which insert into the new adhesion complexes (Mitchison and Cramer, 1996). This activity is not limited solely to basal cells, as suprabasal cells can "leapfrog" the basal cells, during migration, in combination with "sliding sheet" migration (Zhao *et al*, 2003).

In order to migrate through the provisional wound matrix, keratinocytes at the leading edge of the sheet of migration, must degrade the fibrin barrier ahead of them by plasmin activation (from the plasminogen precursor within the clot), via expression of tissue-type plasminogen activator (tPA) or urokinase-type plasminogen activator (uPA) (McNeill and Jensen, 1990). Various matrix metalloproteinases (MMPs) are up-regulated by keratinocytes. MMP-9 (gelatinase B) is believed to be released from basal cells from the basal lamina (Salo *et al,* 1994), whilst MMP-1 (interstitial collagenase) aids degradation of collagens I and III in the wound matrix, allowing migration (Saarialho-Kere *et al*, 1994; Moseley *et al*, 2004). Once the skin defect has been covered by a cell monolayer, a new stratified epidermis is established from the wound edge, inwards, allowing the restoration of normal cellular activity (Martin, 1997).

In the present Study, a spontaneously immortalised human keratinocyte cell line (HaCaT; Boukamp *et al*, 1988) was used. The HaCaT cell line mimics many of the properties of normal epidermal keratinocytes, is not invasive and can differentiate, under appropriate experimental conditions. Indeed, cell migration assays with primary human keratinocytes and HaCaT cells have proved to have similar results (Koivisto *et al*, 2006). Both of these cells have been shown to be sensitive to EGF stimulation, at nanogram concentrations (Kim and Kim, 2008).

4.1.3 Human epidermoid carcinoma (HEp2) cells

For proof of concept studies, a human epidermoid carcinoma (HEp2) cell line was used. This cell line is known to over-express EGF-receptor on the cell surface (Salomon *et al*, 1995) and be sensitive to EGF stimulation (Raspaglio *et al*, 2003). The HEp2 cell line was established in 1952 (Moore *et al*, 1955), from tumours that had been produced in irradiated-cortisonised, weanling rats, following injection with epidermoid carcinoma tissue, from the larynx of a 56-year-old male (Toolan, 1954). The HEp2 cell line has supported the growth of measles virus (Black *et al*, 1956), and it has been used for experimental studies of tumor production in rats, hamsters, mice, embryonated eggs and volunteer terminal cancer patients (Moore, 1958).

4.1.4 EGF stimulation

Both fibroblasts and keratinocytes are sensitive the EGF stimulation (Nickoloff *et al*, 1988; Shiraha *et al*, 2000). Their culture requires the addition of exogenous EGF, in the form of foetal calf serum (FCS). As the present Study will involve the addition of exogenous rhEGF, either free, or in the form of the dextrin-rhEGF conjugate. A cell type that was highly responsive to EGF stimulation, that could be maintained in serum-free media, was also implemented (HEp2), allowing the effects of free rhEGF, the dextrin-rhEGF conjugate or EGF present in FCS, to be distinguished.

4.1.5 Experimental aims

A series of assays of cell proliferation and migration, were developed, involving the aforementioned cell lines. The efficacy of rhEGF and the dextrin-rhEGF conjugate, were assessed in these models, as was the "masking" of rhEGF bioactivity via succinoylated dextrin conjugation, and "unmasking", in response to physiological levels of α-amylase.

The aims of this Chapter were the:

1. Optimisation of the cell proliferation assay with rhEGF.
2. Assessment of cell proliferation, in response to the dextrin-rhEGF conjugate in HEp2 cells, keratinocytes, and patient-matched normal dermal and chronic wound fibroblasts.

3. Evaluation of "masking/unmasking" of the dextrin rhEGF conjugate, by α-amylase, on the cellular response.
4. Optimisation of the cell migration assay with keratinocytes and fibroblasts.

4.2 Methods

Cells were cultured, as described in Section 2.6.3.1.

4.2.1 Cell viability/proliferation assay

HEp2 cells, HaCaT keratinocytes and normal and chronic wound fibroblasts were seeded into 96-well microtitre plates at a cell density of 2.5 x 10^3 cells/well in 10 % foetal calf serum-containing media (SCM 10%). Cells were maintained at 37 °C/5% CO_2 for 24 h. Cell-type specific media was used (summarised in Table 4.1). The optimum cell density was determined from the cellular growth curves (Figures 2.7 – 2.9, Section 2.6.3.7). The MTT assay (Section 2.6.3.7) used for assessment of cellular viability and proliferation.

4.2.1.1 Optimisation

All cell types were serum-starved, in serum-free media (SFM), for 24 h. To assess optimum proliferation, in response to exogenous rhEGF, cells were maintained in media with differing FCS content (0, 1 and 10 %), with the aim of determining the minimum concentration of endogenous EGF (present in FCS), to enable cell proliferation. It was first necessary to prepare the stock solutions of rhEGF. RhEGF (400 ng/mL) in either SCM 10%, SCM 1% or SFM, for each specific media (Table 4.1), were prepared and serially diluted, upon addition to the cells. Cells were maintained at 37 °C/5% CO_2 for 72 h, upon which, cell proliferation was assayed using the MTT assay (Section 2.6.3.7).

4.2.1.2 Addition of the dextrin-rhEGF conjugate

In the case of the dextrin-rhEGF conjugate, media was prepared, as shown in Table 4.2, and maintained at 37 °C/5% CO_2 with, or without, α-amylase (29 - 521 i.u./L) for 24 h. In parallel, samples of rhEGF or the dextrin-rhEGF conjugate were also exposed to trypsin-EDTA (0.025%) (Section 3.2.7), purified using FPLC (Section 2.6.1), and exposed to α-amylase (93 i.u./L), at 37 °C, for 24 h.

Table 4.1 Cell culture media composition

Cell line	10% FCS-containing media	1% FCS-containing media	Serum-free media
Human epidermoid carcinoma (HEp2)	***H-SCM 10%:*** EMEM penicillin G (100 U/mL) streptomycin sulphate (100 μg/mL) amphotericin B (0.25 μg/mL) 10 % v/v FCS	***H-SCM 1%:*** EMEM penicillin G (100 U/mL) streptomycin sulphate (100 μg/mL) amphotericin B (0.25 μg/mL) 1 % v/v FCS	***H-SFM:*** EMEM penicillin G (100 U/mL) streptomycin sulphate (100 μg/mL) amphotericin B (0.25 μg/mL)
HaCaT keratinocyte	***K-SCM 10%:*** DMEM 67.5% Ham's F12 nutrient media 22.5% penicillin G (100 U/mL) streptomycin sulphate (100 μ g/mL) amphotericin B (0.25 μg/mL) hydrocortisone (400 ng/mL) adenine (0.089 mM) cholera toxin (0.08 μg/mL) insulin (5 μg/mL) 10% v/v FCS	***K-SCM 1%:*** DMEM 67.5% Ham's F12 nutrient media 22.5% penicillin G (100 U/mL) streptomycin sulphate (100 μ g/mL) amphotericin B (0.25 μg/mL) hydrocortisone (400 ng/mL) adenine (0.089 mM) cholera toxin (0.08 μg/mL) insulin (5 μg/mL) 1% v/v FCS	***K-SFM:*** Epilife® medium, plus HKGS kit: bovine pituitary extract (0.2% v/v) bovine insulin (5 μg/mL) hydrocortisone (0.18 μ g/mL) bovine transferrin (5 μg/mL)
Normal dermal fibroblasts and chronic wound fibroblasts	***F-SCM 10%:*** DMEM penicillin G (100 U/mL) streptomycin sulphate (100 μg/mL) amphotericin B (0.25 μg/mL) L-glutamine (2 mM) puromycin (1 μg/ml) 10% v/v FCS	***F-SCM 1%:*** DMEM penicillin G (100 U/mL) streptomycin sulphate (100 μg/mL) amphotericin B (0.25 μg/mL) L-glutamine (2 mM) puromycin (1 μg/ml) 1% v/v FCS	***F-SFM:*** DMEM penicillin G (100 U/mL) streptomycin sulphate (100 μg/mL) amphotericin B (0.25 μg/mL) L-glutamine (2 mM) puromycin (1 μg/ml)

FCS = foetal calf serum, EMEM = Eagle's minimum essential medium,
DMEM = Dulbecco's modified Eagle's medium, HKGS = human keratinocyte growth supplement

Table 4.2 Stock solutions of the dextrin-rhEGF conjugate

Cell line	[dextrin-rhEGF] ng/mL (rhEGF-equivalent)	Cell culture medium	+/- α-amylase (i.u./L)
Human epidermoid carcinoma (HEp2)	50	H-SFM	29 - 521
HaCaT keratinocyte	400	K-SFM	93
Normal dermal fibroblasts	400	F-SCM 1%	93
Chronic wound fibroblasts	400	F-SCM 1%	93

On commencing the proliferation assay, either the dextrin-rhEGF conjugate, without prior α-amylase exposure or dextrin-rhEGF conjugate, exposed to α-amylase (and in one experimental run, trypsin-EDTA, 0.025%), were added to the each cell-type, and serially diluted. Cell cultures were maintained at 37 °C/5% CO_2, for 72 h, upon which cell proliferation was assayed, using the MTT assay (Section 2.6.3.7). In additional experiments, similar cell proliferation assays were performed with HEp2 cells, seeded at 2.5 x 10^3 cells/well, with the addition of dextrin-rhEGF (50 ng/mL rhEGF equivalent) and α-amylase (521 i.u./L). However, in this case cell proliferation was assessed daily, over 8 days to investigate any sustained rhEGF release effects from the dextrin-rhEGF conjugate.

4.2.1.3 Controls

HEp2 cells were seeded into 96-well microtitre plates, at a cell density of 2.5 x 10^3 cells/well, in H-SCM 10 %, and maintained at 37 °C/5% CO_2, for 24 h. The cells were serum-starved in H-SFM, and maintained at 37 °C/5% CO_2, for 24 h. To assess possible cell proliferation induced by dextrin, succinoylated dextrin or α-amylase, stock solutions were also prepared:

- Dextrin (400 μg/mL in H-SFM)
- Succinoylated dextrin (400 μg/mL in H-SFM)
- α-amylase (93 i.u./mL in H-SFM)

Dextrin and succinoylated dextrin were serially diluted upon addition to cells. Cells were maintained at 37 °C/5% CO_2, for 72 h, upon which an MTT assay was performed (Section 2.6.3.7).

4.2.2 Cell migration in monolayer culture

A variety of methods have been used in the measurement of cell migration, including the transwell assay (Boyden, 1962), often modified by fluorescence quantitation (Spessotto *et al,* 2002). Other techniques include the under agarose migration assay (Nelson *et al*, 1975), the soft-agarose drop method (Silva *et al,* 2003), and the phagokinetic track motility assay for phagocytic cell types (Albrecht-Buehler, 1977). Wound healing can be assessed using time-lapse video microscopy (Providence *et al*, 2000). Although the transwell assay has been applied to random migration (Huttenlocher *et al*, 1996), video time-lapse microscopy provides

advantages by yielding actual speeds of individual cells and additional features of motion (Bahnson *et al*, 2005). The introduction of video imaging and computer-assisted methods of tracking, have further aided this approach (Huttenlocher *et al*, 1998; Shutt *et al*, 2000).

4.2.2.1 Scratch wound model assay

Normal dermal fibroblast, chronic wound fibroblast and HaCaT keratinocyte cellular migration, on exposure to rhEGF or the dextrin-rhEGF conjugate, in the presence and absence of α-amylase (93 i.u./L), were assessed, using an *in vitro* "scratch wound model assay", according to Stephens *et al* (2004). Following trypsinisation, cells were seeded in 24-well tissue culture plates, in cell-type specific SCM 10% (1ml), at a cell density of $2.5x10^4$ cells/well. Cells were maintained at 37°C/5% CO_2, for 48 h, to reach 95 – 100% confluence. A single scratch was made with a sterile pipette across the cell layer and following washing (x 2) in PBS, the SCM 10% was replaced with culture medium (1ml), containing rhEGF or the dextrin-rhEGF conjugate, in the presence and absence of α-amylase (93 i.u./L), and control media (Table 4.3). The rhEGF and the dextrin-rhEGF conjugate were added at optimum concentrations to respective culture media, using data obtained from the MTT cell proliferation assays, previously described (Section 4.2.1). All experiments were performed in duplicate.

4.2.2.2 Time-lapse microscopy

Cell migration was visualised over a 48 h period (in a controlled atmosphere at 37 °C/5% CO_2), using automated time-lapse microscopy. Digital images were captured at 20 min intervals and image sequences saved as QuickTime® movie files, for further analysis (QuickTime®, version 7.1.5, Apple Computer Inc, Cupertino, USA).

4.2.2.3 Image analysis – wound area estimation (HaCaT keratinocytes only)

QuickTime® movie files were opened using Openlab 5® software, and images at time points: 0h, 24h or 48h, selected and copied into a photo-processing package (Adobe Photoshop® CS3; Adobe Systems Incorporated, San Jose, USA). Files were processed as shown in Figure 4.1. The files were further processed using ImageJ®

Table 4.3 Cell culture medium composition for the scratch wound model assay

Cell line	Media description	[rhEGF] ng/mL	[dextrin-rhEGF] ng/mL (rhEGF-equivalent)	[Succinoylated dextrin] µg/mL	Cell culture medium	α-amylase (i.u./L)
HaCaT keratinocyte	rhEGF	0 - 10	0	0	K-SFM	0
	Dextrin-rhEGF	0	0 - 100	0	K-SFM	+/- 93
	Succinoylated dextrin control	0	0	1.56	K-SFM	0
	α-amylase control	0	0	0	K-SFM	93
Normal dermal fibroblasts and chronic wound fibroblasts	rhEGF	0 - 3.13	0	0	F-SCM 1%	0
	Dextrin-rhEGF	0	0.1	0	F-SCM 1%	+/- 93
	Succinoylated dextrin control	0	0	1.56	F-SCM 1%	0
	α-amylase control	0	0	0	F-SCM 1%	93

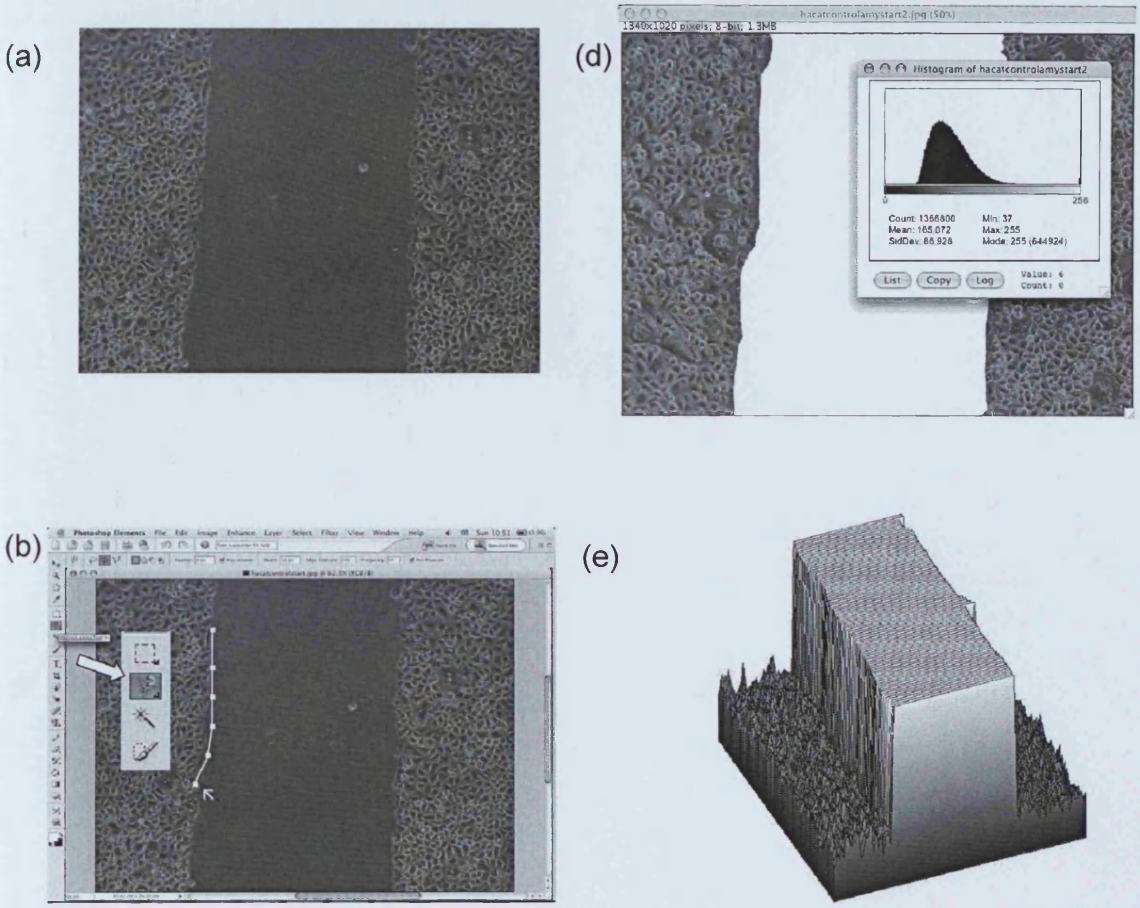

Figure 4.1 Image analysis

Wound area calculation

An image file of keratinocytes (a) was processed by manual selection of the wound area (b) and filling with a contrasting colour (white) (c). A histogram of the colours present was produced and the number of pixels (in white) detemined, allowing wound size as a percentage of the total, to be calculated (d). A 3-D representation surface plot was further generated (e).

(f)

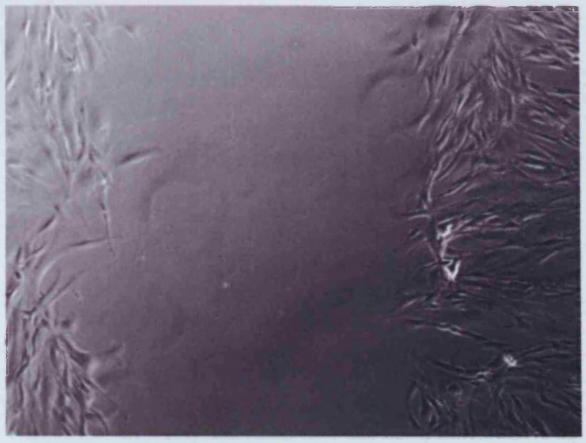

(g)

(h)

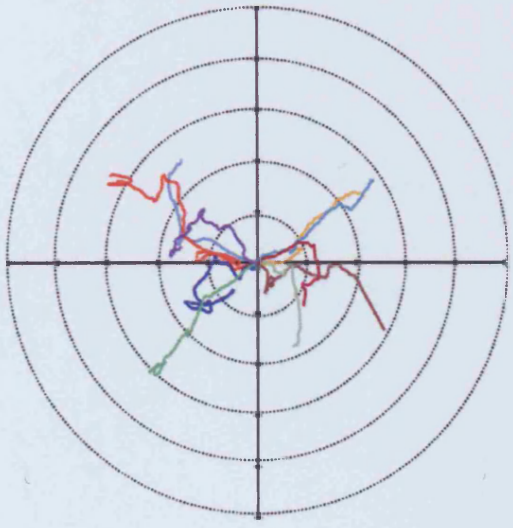

Figure 4.1 (continued)

Cell Tracking
A example still image from a movie file of normal dermal fibroblasts (f) was processed, by tracking individual cells (g) and the resulting vectors (h) and velocities calculated.

software (ImageJ 1.37v; http://rsb.info.nih.gov/ij/).

4.2.2.4 Image analysis – cell tracking (all cell types)

Image processing and cell tracking were performed with ImageJ® software, including MTrackJ plugin software (Erik Meijering; http://www.imagescience.org /meijering/ software/mtrackj/). 10 cells of characteristic movement were selected per movie, the tracks recorded and the velocities calculated, based upon total distance travelled/ time (1 pixel = 1.03374 μm).

4.2.3 Statistical analysis

Statistical analyses were undertaken, using GraphPad Prism®, version 4.00 (GraphPad Software, San Diego, USA). Data were compared using a Student's t-test or a one-way ANOVA, with a Bonferroni post-test. Results were expressed as a mean and standard deviation (S.D.), or standard error of the mean (S.E.M.). Statistical significance was considered at a probability of $p < 0.05$.

4.3 Results

4.3.1 Cell viability/proliferation

4.3.1.1 Optimisation of the cell viability/proliferation assay

The selection of optimum conditions (% FCS and the range of [rhEGF]) for each cell type, was based on the lowest % FCS necessary, to maintain cell proliferation and thus, reduce the influence of endogenous EGF, within FCS. HaCaT proliferation was most pronounced in response to rhEGF, in K-SCM 10%. A similar result was also obtained with K-SFM ($p > 0.05$) (Figure 4.2). Therefore, the K-SFM was shown to support cell proliferation, without exogenous rhEGF interference and was, therefore, used in subsequent experiments. Significant ($p < 0.01$) fibroblast (normal dermal and chronic wound) proliferation occurred in F-SCM 1%, in the fibroblast assays (Figure 4.3). HEp2 cells were observed to proliferate in serum-free conditions, thus free from endogenous EGF interference (Figure 4.4).

4.3.1.2 Addition of rhEGF and the dextrin-rhEGF conjugate, to all cell types

In the HEp2 model, rhEGF displayed a biphasic pattern of activity, causing stimulation of proliferation at lower concentrations, but inhibition of proliferation at

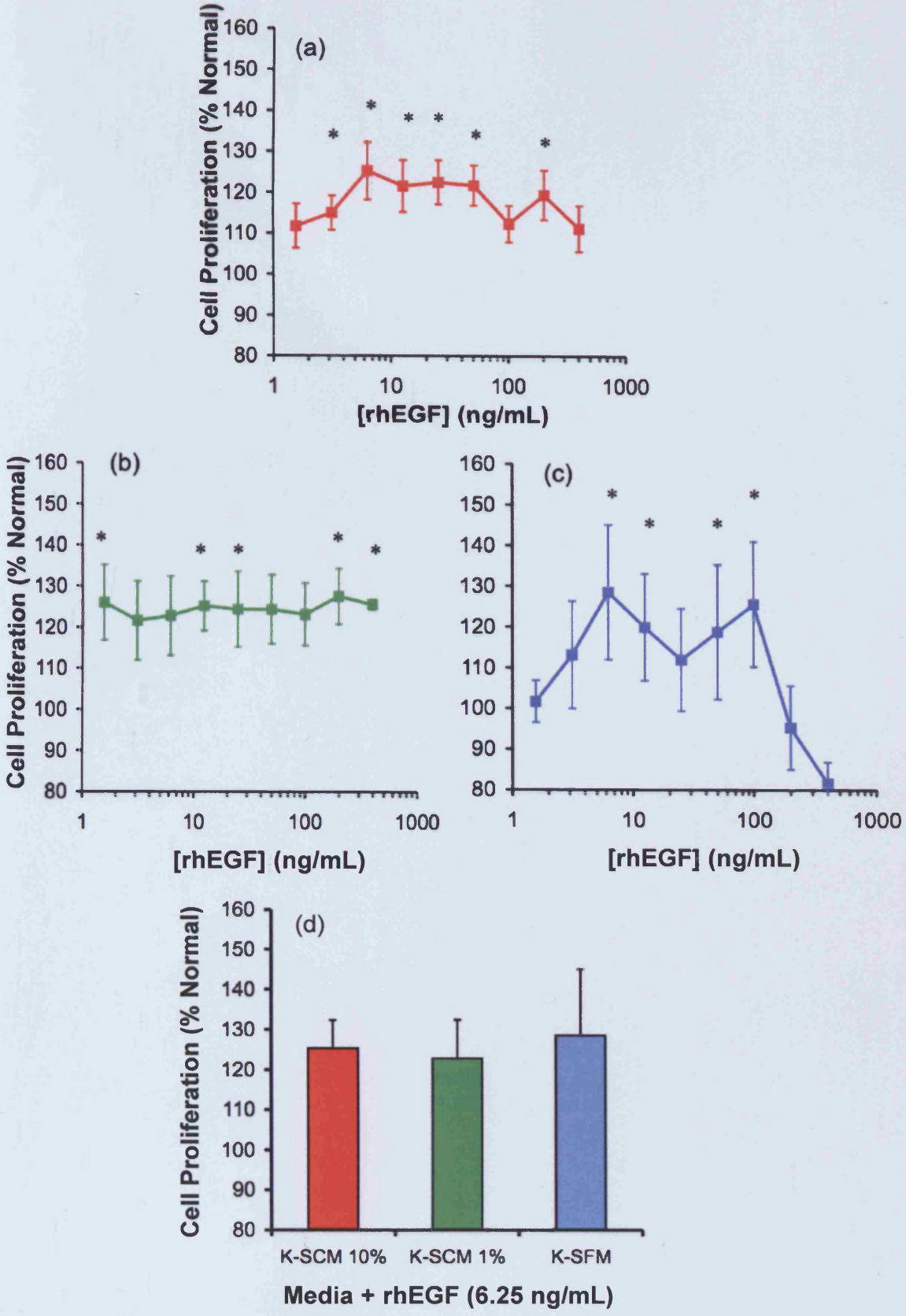

Figure 4.2 **HaCaT proliferation assay optimisation.** Panel (a) demonstrates HaCaT responses to rhEGF, in K-SCM 10%, panel (b) in K-SCM 1% and panel (c) in K-SFM (mean ± S.D., n = 6; * $p < 0.01$, ANOVA and Bonferroni *post hoc* test).Panel (d) shows no significant difference in cell proliferation, between media compositions, with the addition of rhEGF (6.25 ng/mL). Normal = rhEGF-free control.

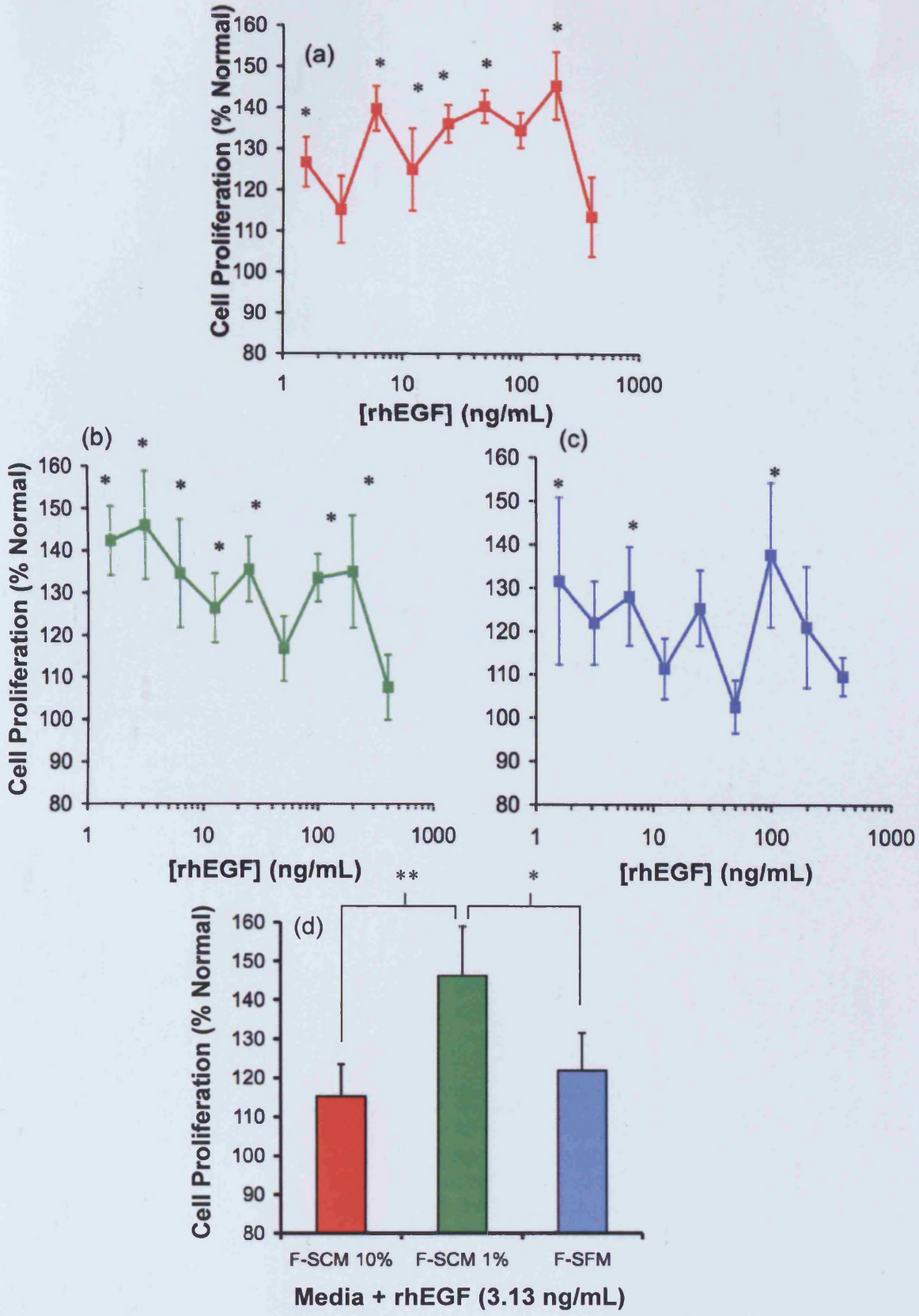

Figure 4.3 **Dermal fibroblast proliferation assay optimisation.** Panel (a) demonstrates normal dermal fibroblast responses to rhEGF, in F-SCM 10%, panel (b) in F-SCM 1% and panel (c) in F-SFM. Panel (d) shows a significant increase in cell proliferation in F-SCM 1%, with the addition of 3.13 ng/mL rhEGF (mean ± S.D., n = 6; * $p <$ 0.01, ** $p < 0.001$ ANOVA and Bonferroni *post hoc* test). Normal = rhEGF-free control.

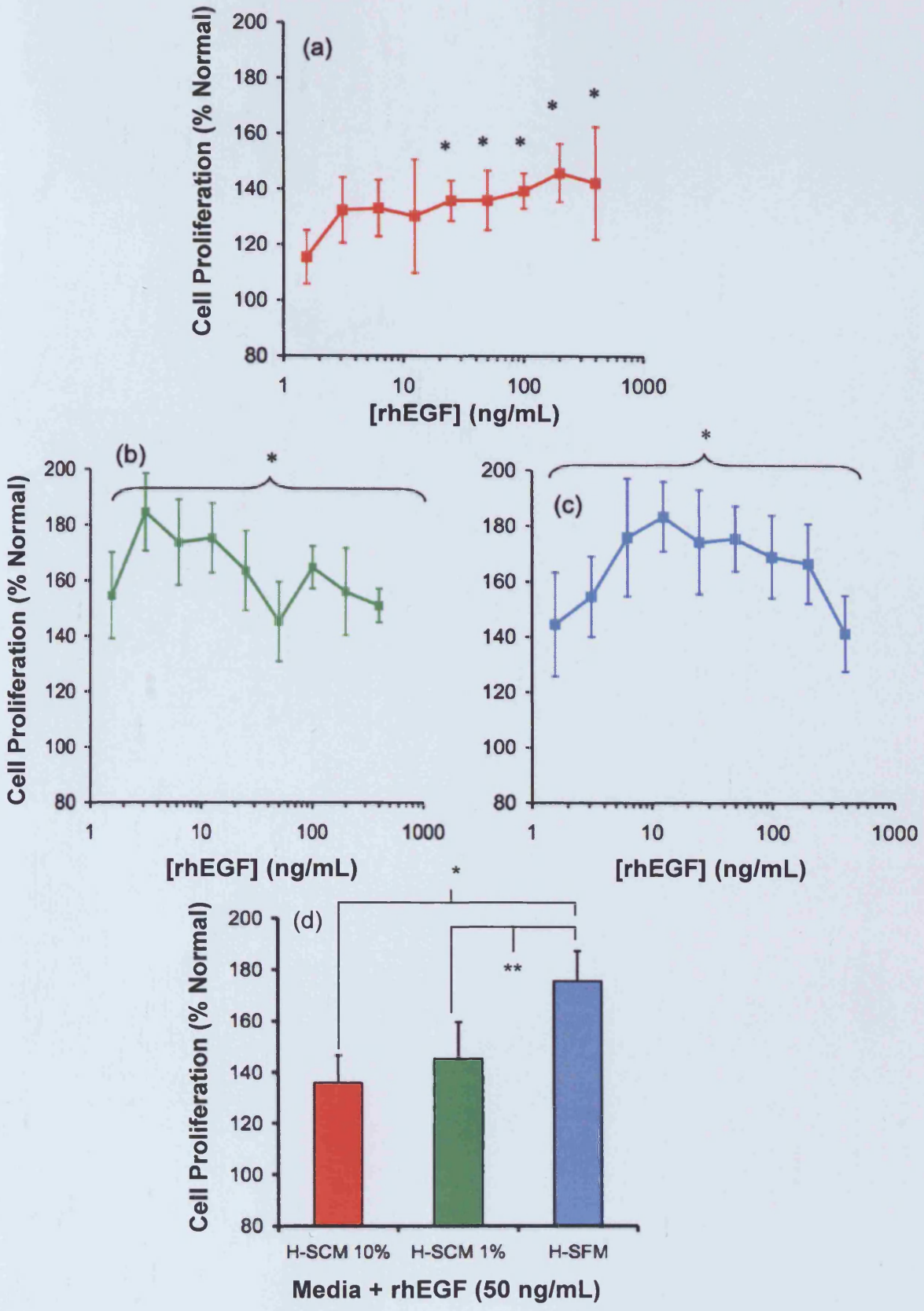

Figure 4.4 **HEp2 proliferation assay optimisation.** Panel (a) demonstrates HEp2 responses to rhEGF, in H-SCM 10%, panel (b) in H-SCM 1% and panel (c) in H-SFM. Panel (d) shows a significant increase in cell proliferation in H-SFM, with the addition of 50 ng/mL rhEGF (mean ± S.D., n = 6; * $p < 0.001$, ** $p < 0.01$, compared to normal, ANOVA and Bonferroni *post hoc* test). Normal = rhEGF-free control.

higher concentrations (>400ng/mL; Figure 4.5). The peak concentration for activity with the dextrin-rhEGF conjugate, following 24 h α-amylase exposure (93 i.u./L), was 0.19 - 6.25 ng/mL, compared with free rhEGF, which displayed highest activity at 3.13 – 100 ng/mL (Figure 4.5a). In the HaCaT, normal dermal and chronic wound fibroblast models (Figures 4.5b and 4.6), this biphasic response was less pronounced, but cells were sensitive to rhEGF stimulation at a wider range of concentrations (i.e. HaCaT at 0.1 – 100 ng/mL and fibroblasts at 0.006 – 6400 ng/mL). The dextrin-rhEGF conjugate consistently stimulated proliferation at lower equivalent concentrations, compared to free rhEGF. In the HEp2 model, no significant increase in cell proliferation occurred with dextrin, succinoylated dextrin or α-amylase controls (Figure 4.7a).

In the HEp2 model, the dextrin-rhEGF conjugate activity (without the addition of α-amylase), was not significantly different to controls ($p > 0.05$). When α-amylase (93 i.u./L) was added to the incubation medium, HEp2 cell proliferation was restored to a level equivalent to that observed with free rhEGF, at 72 h ($p < 0.001$) (Figure 4.7b). The extent of proliferation, induced by the dextrin-rhEGF conjugate was clearly related to the amount of α-amylase added (Figure 4.7c). In the study of sustained release, when HEp2 cells were exposed to rhEGF or the dextrin-rhEGF conjugate (± α-amylase), native rhEGF caused the greatest increase in proliferation, over the initial 5 days of exposure, prior to proliferation returning to baseline levels. In contrast, the dextrin-rhEGF conjugate promoted sustained cell proliferation over 8 days, initially at lower levels compared to free rhEGF, but by day 5, maximum proliferation was equivalent to that of free rhEGF, at day 2. RhEGF caused a significant increase in proliferation, compared to proliferation on day 0, on days 2 to 4 ($p < 0.005$), whereas the dextrin-rhEGF conjugate retained a significant stimulation of proliferation, compared to proliferation on day 0, until day 6 ($p < 0.005$). Moreover, this stimulation was significantly more active than rhEGF on days 5, 6 and 8 ($p < 0.0002$) (Figure 4.8).

Following successive exposure of rhEGF or the dextrin-rhEGF conjugate, to trypsin-EDTA (0.025%), followed by α-amylase (93 i.u./L), activity of the free rhEGF was reduced to that of the control ($p > 0.05$), whereas dextrin-rhEGF retained its bioactivity and thus, exhibited resistance to proteolytic degradation (Figure 4.9).

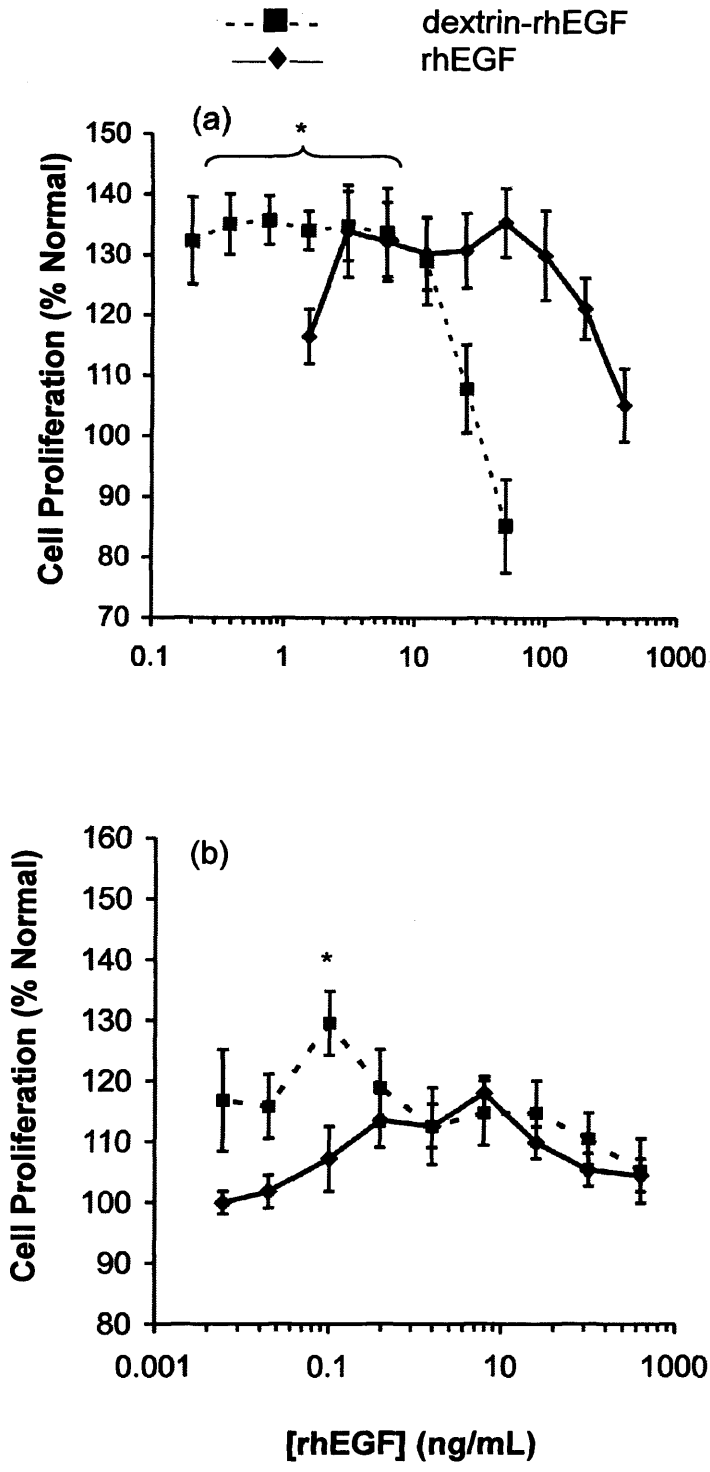

Figure 4.5 **HEp2 and HaCaT responses to rhEGF and dextrin-rhEGF (+ α-amylase).** Panel (a) shows proliferation of HEp2 cells, at 72 h, in the presence of rhEGF (—◆—) and α-amylase-activated, dextrin-rhEGF (- -■- -), at the rhEGF concentrations shown (mean ± S.E.M., n = 3; * $p < 0.001$, ANOVA and Bonferroni *post hoc* test). Panel (b) shows proliferation of HEp2 cells, at 72 h, in the presence of rhEGF (—◆—) and α-amylase-activated, dextrin-rhEGF (- -■- -), at the rhEGF concentrations shown (mean ± S.E.M., n = 3; * $p < 0.05$, ANOVA and Bonferroni *post hoc* test). Normal = rhEGF-free control.

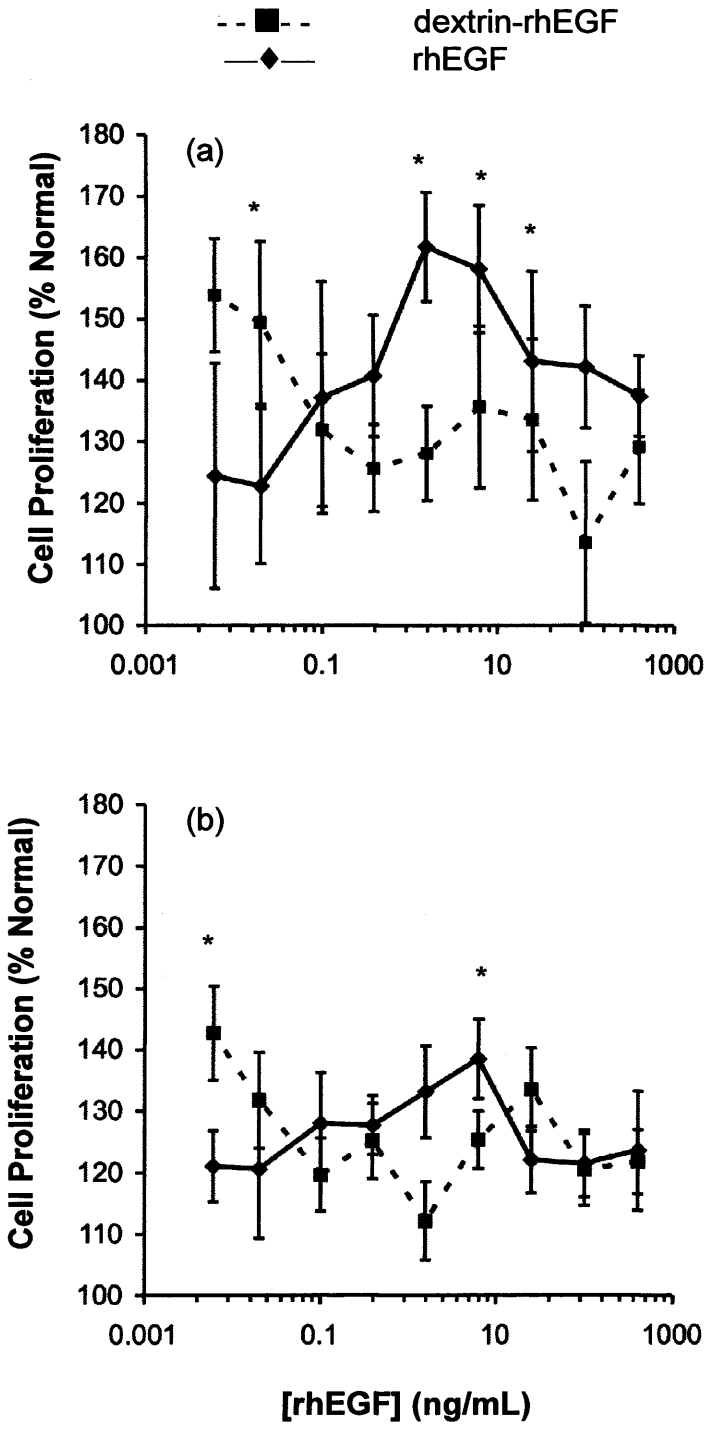

Figure 4.6 **Fibroblast response to rhEGF and dextrin-rhEGF (+ α-amylase).** Panel (a) shows proliferation of normal dermal fibroblasts, at 72 h, in the presence of rhEGF (—◆—) and α-amylase-activated, dextrin-rhEGF (- -■- -), at the rhEGF concentrations shown (mean ± S.E.M., n = 3; * $p < 0.01$, ANOVA and Bonferroni *post hoc* test). Panel (b) shows proliferation of chronic wound fibroblasts, at 72 h, in the presence of rhEGF (—◆—) and α-amylase-activated, dextrin-rhEGF (- -■- -), at the rhEGF concentrations shown (mean ± S.E.M., n = 3; * $p < 0.05$, ANOVA and Bonferroni *post hoc* test). Normal = rhEGF-free control.

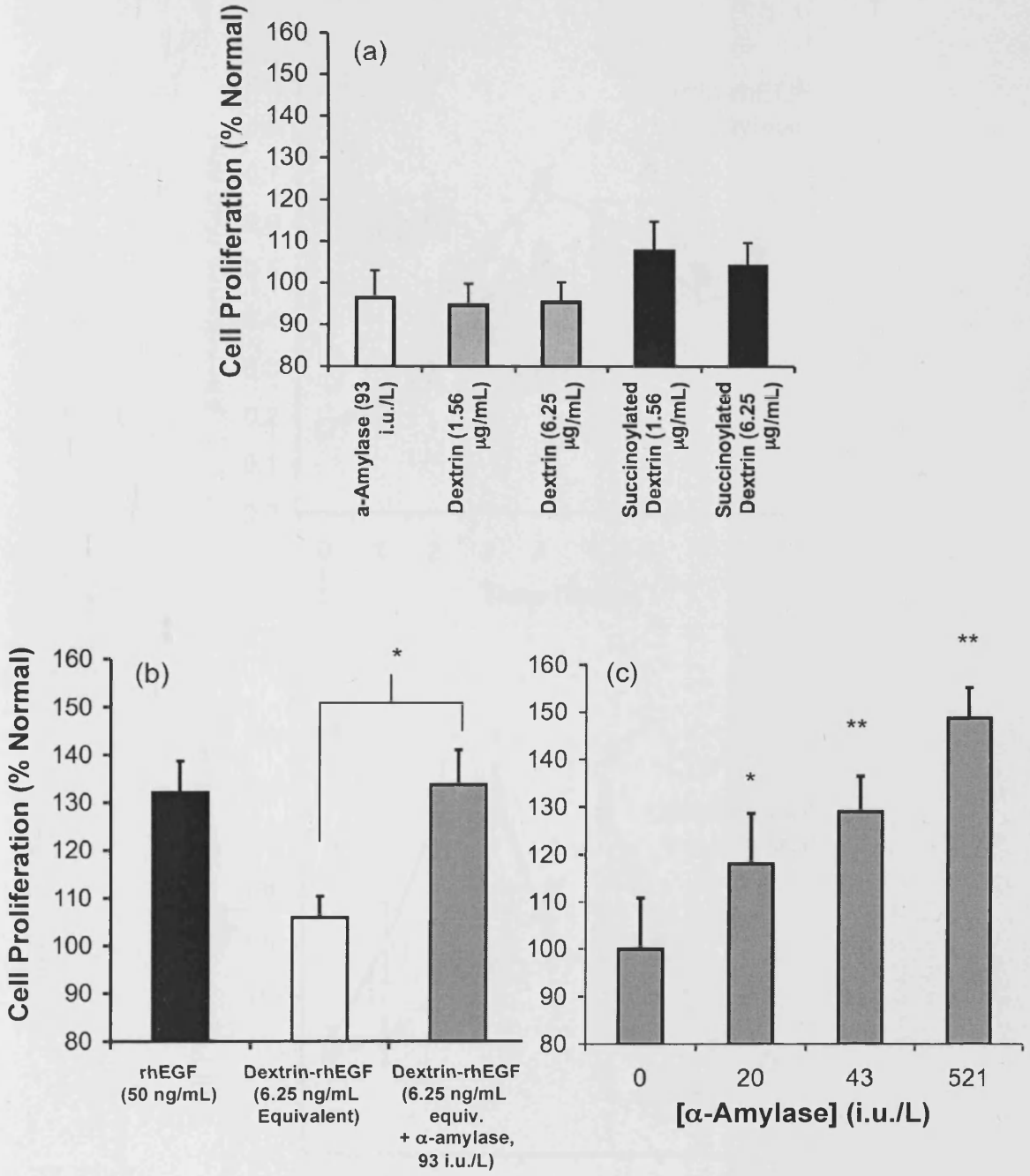

Figure 4.7 **Controls and "masking/unmasking" in HEp2 cells.** Panel (a) shows controls have no significant effect ($p > 0.05$, ANOVA and Bonferroni *post hoc* test) on cell proliferation. Panel (b) compares the proliferation of HEp2 cells, at 72 h, in the presence of rhEGF and the dextrin-rhEGF conjugate, in the presence and absence of α -amylase (93 i.u./L) (mean ± S.E.M.; n = 3; * $p = 0.0035$, ANOVA and Bonferroni *post hoc* test). Panel (c) shows restoration of rhEGF activity was related to the concentration of α -amylase added (mean ± S.D., n = 6, * $p < 0.01$, ** $p < 0.001$, ANOVA and Bonferroni *post hoc* test). Normal = rhEGF-free control.

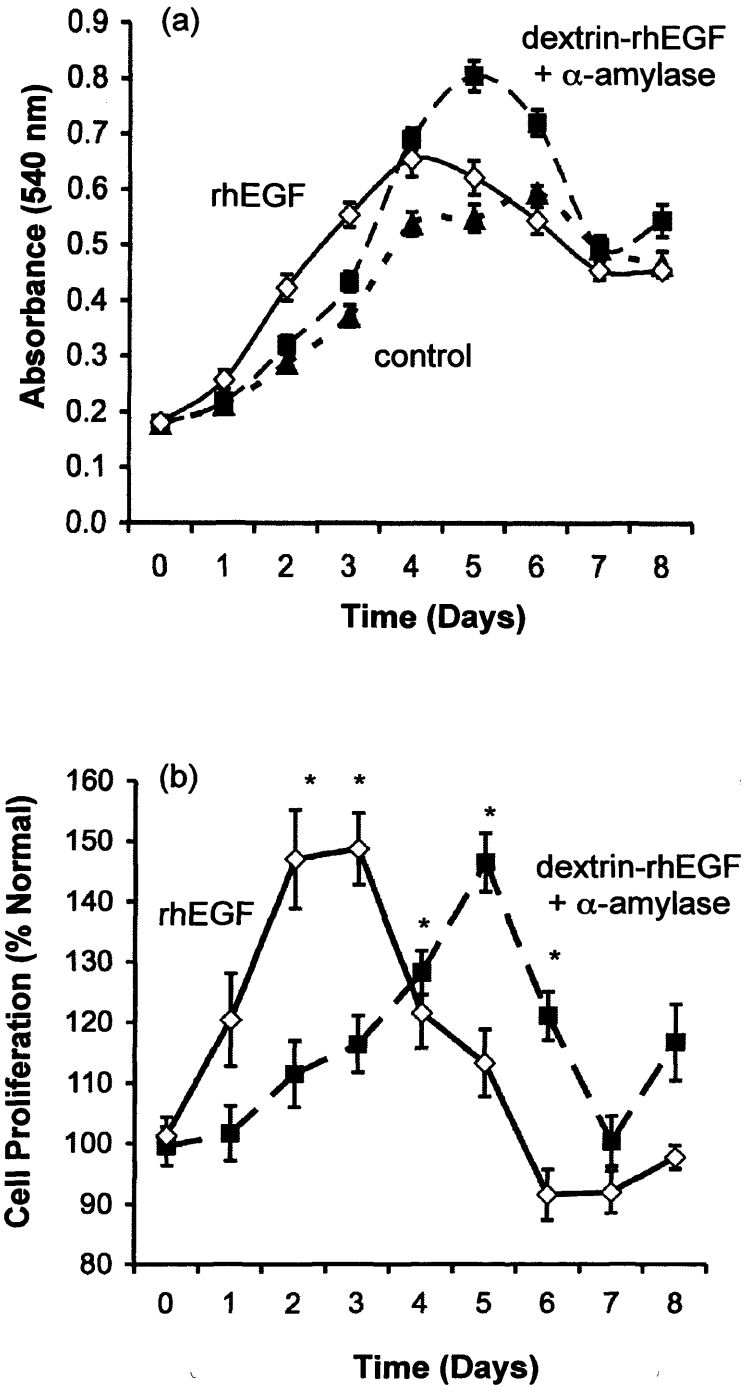

Figure 4.8 **Sustained release effects of dextrin-rhEGF.** Panel (a) shows HEp2 proliferation curves over 8 days, when HEp2 cells were grown in serum-free conditions (control), or in the presence of rhEGF (50 ng/mL) or dextrin-rhEGF (6.25 ng/mL rhEGF equivalent), following exposure to α-amylase (521 i.u./L). Panel (b) shows sustained proliferation of HEp2 cells, compared to controls (mean ± S.E.M., n = 4; * $p < 0.001$, ANOVA and Bonferroni *post hoc* test). Normal = rhEGF-free control.

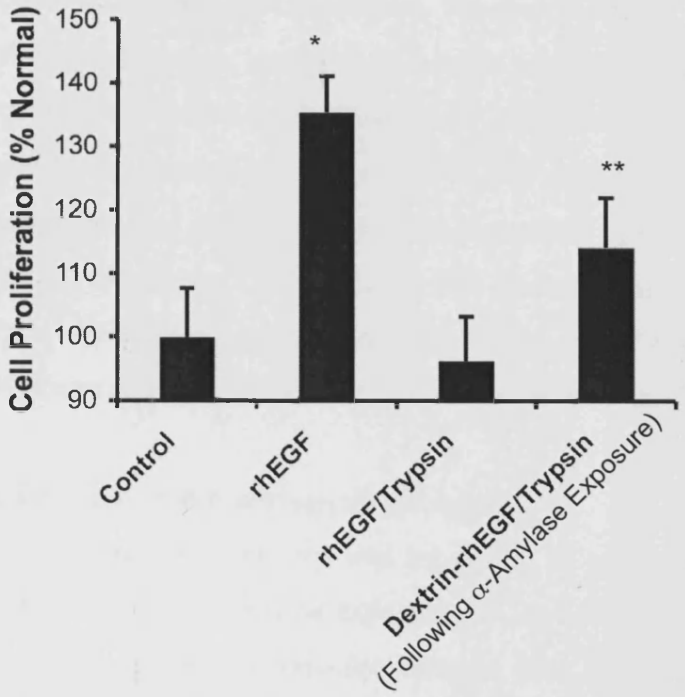

Figure 4.9 **Dextrin-rhEGF conjugate resistance to proteolysis.** Proliferation of HEp2 cells, in response to rhEGF, following trypsin exposure, was reduced to that of rhEGF-free controls, whereas dextrin-rhEGF retained bioactivity, compared to rhEGF-free controls (mean ± S.D., n = 6, * $p < 0.001$, ** $p < 0.05$, ANOVA and Bonferroni *post hoc* test). Normal = rhEGF-free control.

4.3.2 Cell migration

4.3.2.1 Image analysis – wound area estimation (HaCaT keratinocytes only)

Under rhEGF-free conditions, wound closure did not occur over 48 h (Figure 4.10). Optimum wound closure occurred in the presence of rhEGF (6.25 ng/mL). At a higher concentration of rhEGF (10 ng/mL), complete wound closure was suppressed. Under α-amylase-free conditions, the dextrin-rhEGF conjugate did not cause complete wound closure, resulting in wounds of a similar area to rhEGF-free controls, (dextrin-rhEGF = 20.8 ± 1.5 %, K-SFM = 25.3 ± 7.9 %; mean ± S.D., n = 2; $p > 0.05$). Upon the addition of α-amylase (93 i.u./L), rhEGF activity was restored, resulting in wound closure. Again, at higher concentrations of rhEGF (> 10 ng/mL), wound closure was suppressed (Figure 4.11). 3-D surface plots illustrated the time course of a typical wound closing, in response to dextrin-rhEGF conjugate, following the addition of α-amylase (full movies can be found in Appendix - DVD).

4.3.2.2 Image analysis – cell tracking (all cell types)

HaCaT cell migration velocity was increased, in response to the dextrin-rhEGF conjugate, following α-amylase exposure (93 i.u./L) ($p = 0.0001$). There was no significant difference in cell velocity between free rhEGF and "unmasked" dextrin-rhEGF ($p > 0.05$) (Figure 4.12). Both normal dermal fibroblast and chronic wound fibroblast migration velocity was increased, in response to the dextrin-rhEGF conjugate, following α-amylase exposure (93 i.u./L), and rhEGF (Figures 4.13 - 4.15). Normal dermal fibroblasts migrated at a greater velocity, in response to rhEGF (both free and that released from the dextrin-rhEGF conjugate, $p = 0.0098$). Chronic wound fibroblasts migrated at a similar velocity to their patient-matched normal dermal fibroblast counterparts, 15.6 ± 2.2 μm/h (chronic) versus 14 ± 3.3 μm/h (normal) (mean ± S.D., n=10, $p > 0.05$). Again, cell migration velocity was increased, in response to the dextrin-rhEGF conjugate, following α-amylase exposure (93 i.u./L) ($p = 0.0012$). HaCaT migration velocity increased by over 300%, in response to rhEGF (released from the dextrin-rhEGF conjugate, upon α-amylase exposure, 93 i.u./L), whilst both normal dermal and chronic wound fibroblasts increased by just over 50%.

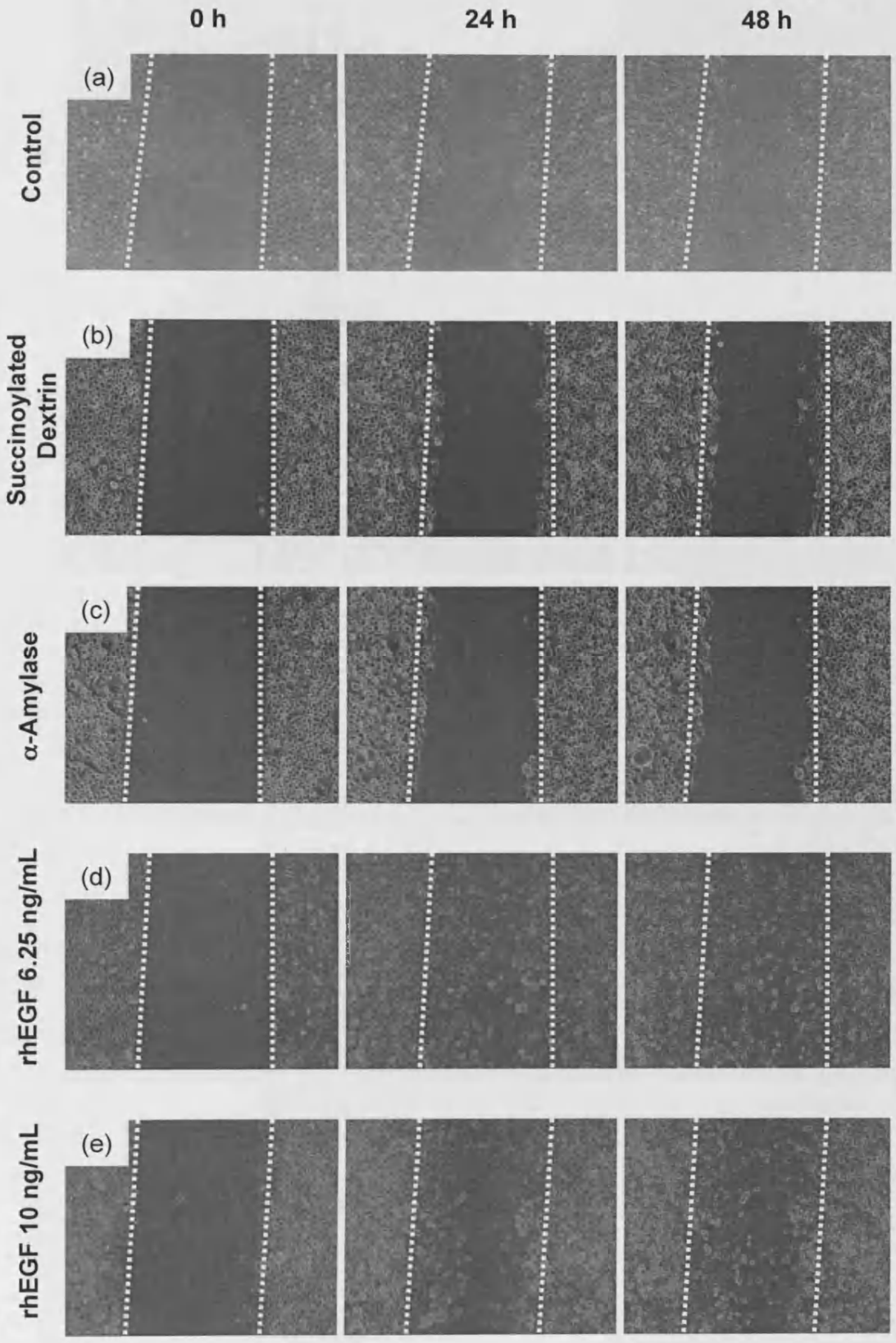

Figure 4.10 **HaCaT cell migration (i).** Cellular migration over a 48 h period, in response to (a) rhEGF-free media, (b) succinoylated dextrin (1.56 μg/mL), (c) α-amylase alone (93 i.u./L), (d) rhEGF (6.25 ng/mL) and (e) rhEGF (10 ng/mL). Healing was optimum, in response to rhEGF 6.25 ng/mL.

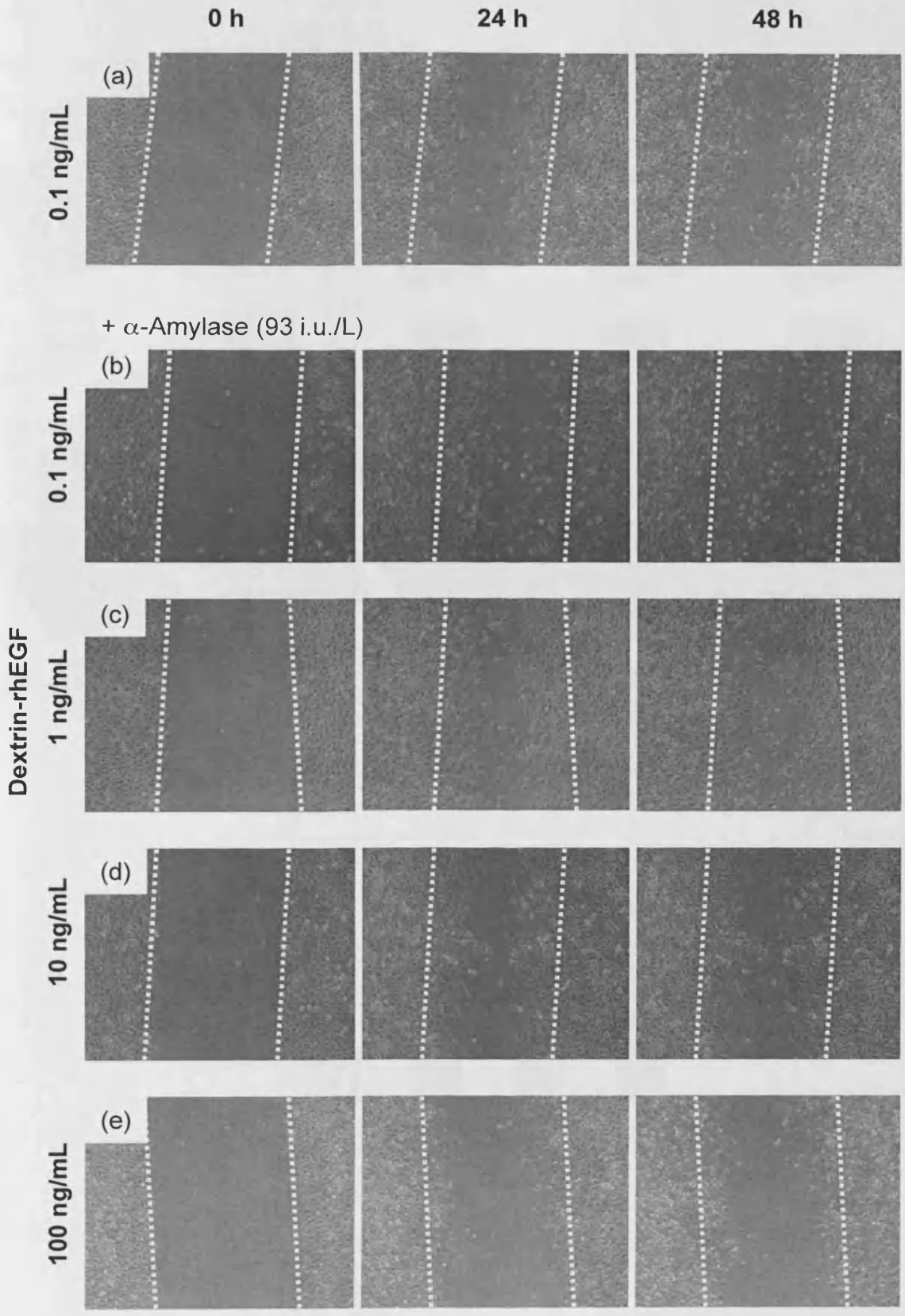

Figure 4.11 **HaCaT cell migration (ii).** Cellular migration, over a 48 h period, in response to (a) dextrin-rhEGF (0.1 ng/mL rhEGF equivalent), in the absence of α-amylase, and dextrin-rhEGF, following 24 h exposure to α-amylase (93 i.u./L) (b) 0.1 ng/mL, (c) 1 ng/mL, (d) 10 ng/mL and (e) 100 ng/mL (rhEGF equivalent).

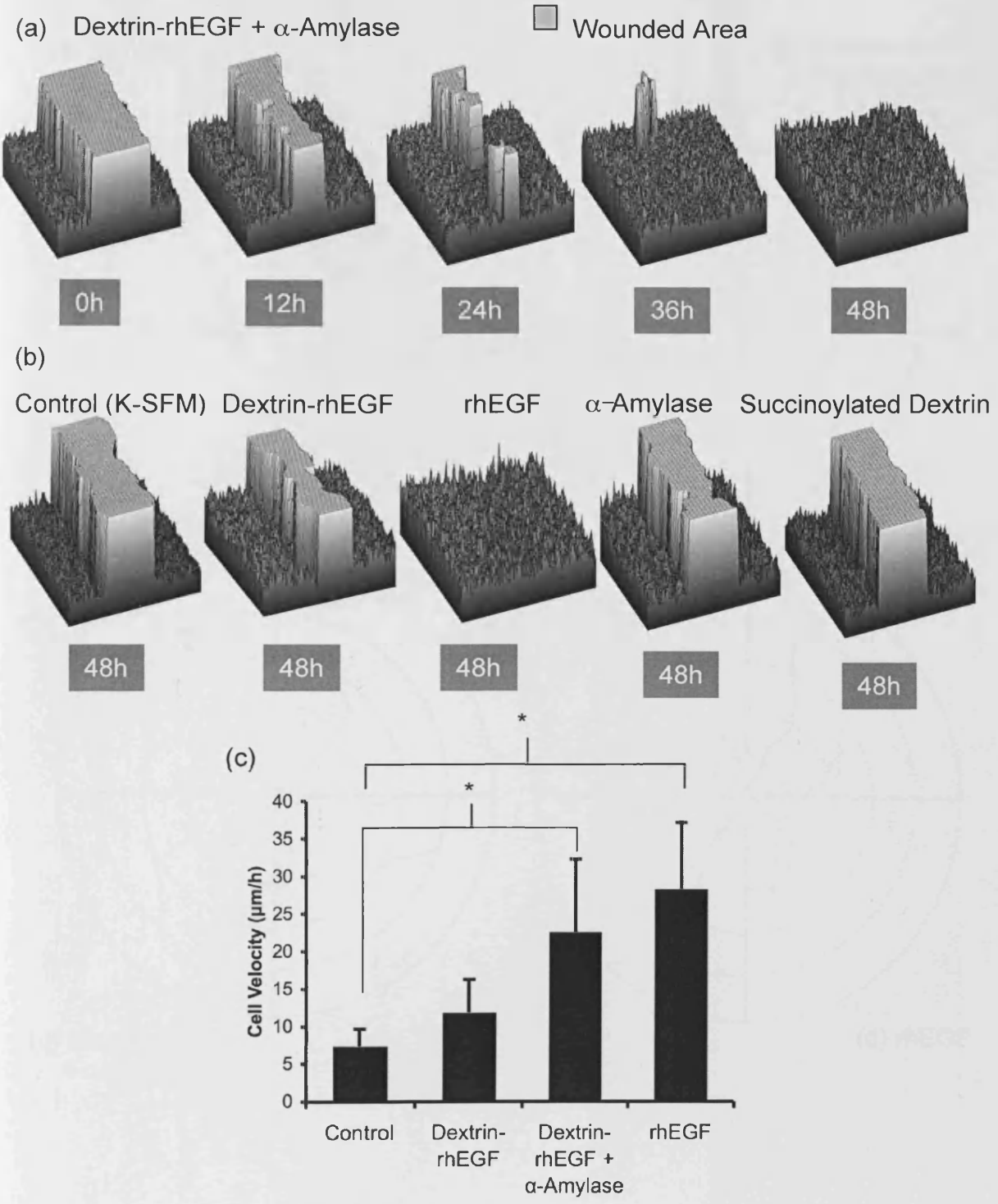

Figure 4.12 **HaCaT cell migration (iii).** Panel (a) shows 3-D representative surface plots of wound healing over 48 h, in response to dextrin-rhEGF (0.1 ng/mL equivalent), in the presence of α-amylase (93 i.u./L). Panel (b) shows surface plots of positive and negative control samples, as described above. Panel (c) shows HaCaT cell migration velocity, in response to rhEGF-free conditions, dextrin-rhEGF (0.1 ng/mL equivalent), in the presence and absence of α-amylase (93 i.u./L), and rhEGF (6.25 ng/mL) (mean ± S.D., n = 10; * p = 0.0001, Student's t-test).

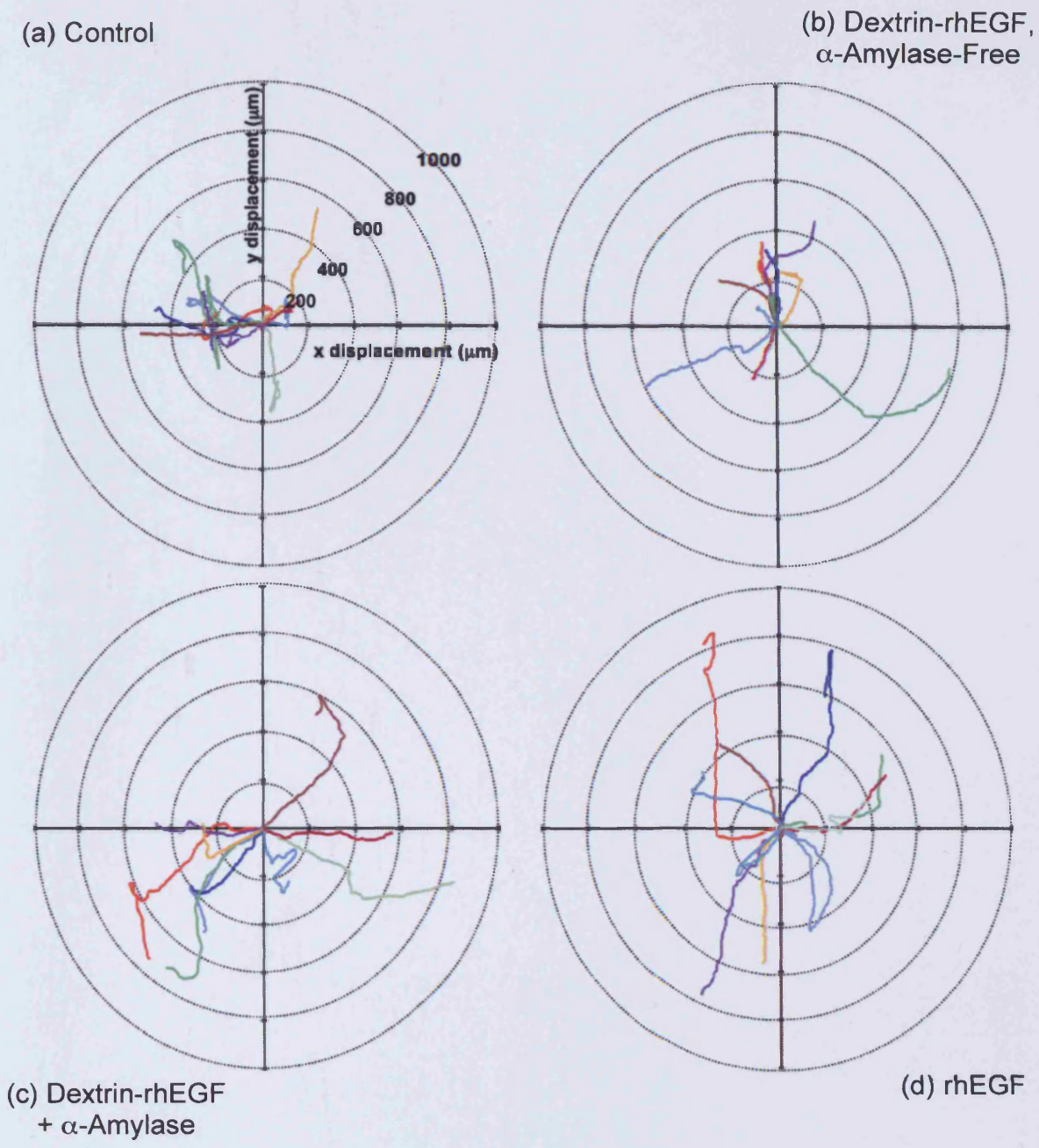

Figure 4.13 **Normal dermal fibroblast migration.** Cell tracking for 10 typical dermal fibroblasts per movie, over a 48 h period. Panel (a) shows control cells in F-SCM 1%, panel (b) shows a typical response to the addition of dextrin-rhEGF (0.1 ng/mL rhEGF equivalent), in the absence of α-amylase, panel (c) shows increased migration, in response to dextrin-rhEGF (0.1 ng/mL rhEGF equivalent), following the addition of α-amylase (93 i.u/L) and panel (d) shows fibroblast migration, in response to free rhEGF (3.125 ng/mL).

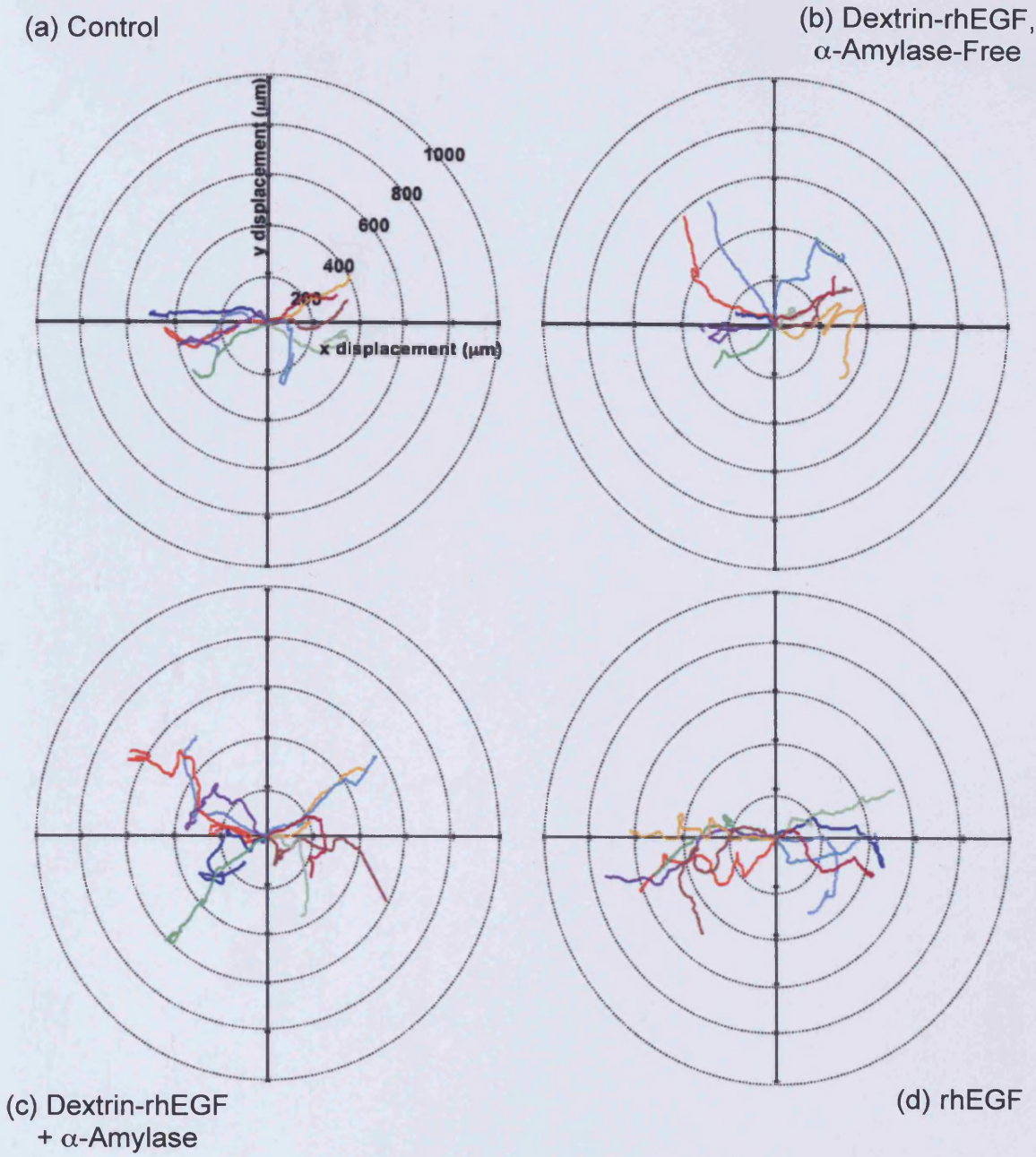

Figure 4.14 **Chronic wound fibroblast migration.** Cell tracking for 10 typical chronic wound fibroblasts per movie, over a 48 h period. Panel (a) shows control cells in F-SCM 1%, panel (b) shows a typical response to the addition of dextrin-rhEGF (0.1 ng/mL rhEGF equivalent), in the absence of α-amylase, panel (c) shows increased migration, in response to dextrin-rhEGF (0.1 ng/mL rhEGF equivalent), following the addition of α-amylase (93 i.u/L) and panel (d) shows fibroblast migration, in response to free rhEGF (3.125 ng/mL).

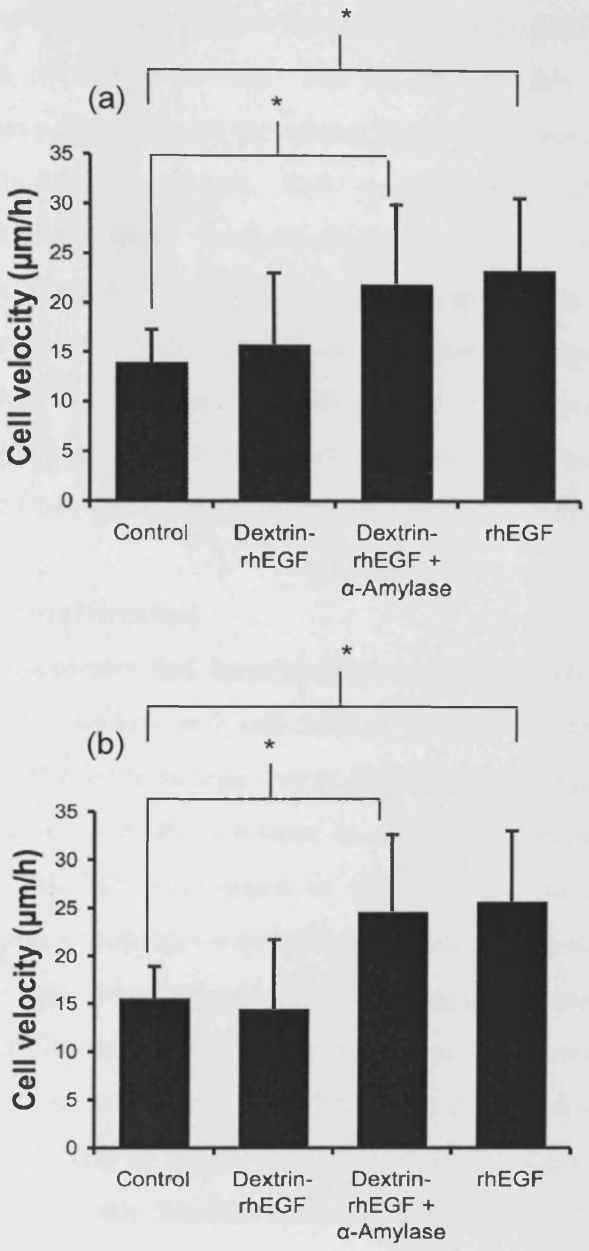

Figure 4.15 **Fibroblast migration velocities.** Panel (a) shows normal dermal fibroblast migration velocities, in response to dextrin-rhEGF (0.1 ng/mL equivalent), dextrin-rhEGF, in the presence of α-amylase (93 i.u./L) and rhEGF (3.125 ng/mL) (mean ± S.D., n = 10; * p = 0.0098, Student's t-test). Panel (b) shows chronic wound fibroblast migration velocities, under the same conditions (mean ± S.D., n = 10; * p = 0.0012, Student's t-test).

4.4 Discussion

This chapter aimed to investigate the bioactivity of rhEGF and dextrin-rhEGF in *in vitro* models of wound healing. The *in vitro* models of wound healing, described herein, have demonstrated the effects that rhEGF has on normal cells and those derived from chronic wounds. This promotion of cell proliferation and migration was evident using well-established assays, and appears highly reproducible. Although the HEp2 cell line is only a model for the subsequent work, it was reliable and predictable with the cellular proliferation responses induced, and importantly, was able to be successfully cultured, in rhEGF-free conditions. Thus, this facilitated the analysis of the action of rhEGF and the dextrin-rhEGF conjugate without interference from the action of endogenous rhEGF, within the culture media.

4.4.1 Cell viability/proliferation

The dermal fibroblasts and keratinocytes required rhEGF in normal culture medium, for successful culture and sub-culture. Data from the HEp2 model, in combination with data from the normal dermal fibroblasts, chronic wound fibroblasts and HaCaT keratinocytes, provided evidence to support the "proof of concept", that rhEGF could be successfully conjugated to succinoylated dextrin, released in a controlled manner upon succinoylated dextrin degradation by α-amylase, and further retain the bioactivity upon release (equivalent to that of the unmodified rhEGF). The concentration of α-amylase used in the majority of these studies was within the range found in normal human serum (Branca *et al*, 2001) and chronic wounds (Chapter 6).

Whilst the bioactivity of rhEGF was effectively "masked" when conjugated to succinoylated dextrin, these Studies demonstrated that the rhEGF activity was restored upon "unmasking" of the dextrin, by the application of α-amylase, at human physiological concentrations, it showed an increase in bioavailability. This was evident in cell proliferation experiments at lower equivalent concentrations of rhEGF, compared to unmodified, "free" rhEGF and protein stabilisation in the presence of a model proteinase. Thus, the need for high concentration of rhEGF was reduced.

Current products that are available in the wound healing field that contain rhEGF are at a high rhEGF concentration (ReGenD150; 150μg rhEGF/g of carrier matrix, resulting in mg quantities of rhEGF being applied to a large wound area), to

account for the protein degradation in chronic wounds (Krishna-Mohan, 2007). At such high levels of rhEGF administration, the systemic uptake may be increased, potentially leading to peripheral side effects, due to rhEGF. EGF promotes tumour invasion in EGFR positive cancer cells (Zolfaghari and Djakiew, 1996; Kondapaka *et al*, 1997; Angelucci *et al*, 2006). These findings highlight the potential of the dextrin-rhEGF conjugate, to effectively deliver a bioactive dosage of rhEGF. Indeed, stimulation of cells in these experiments occurred at pg/L concentrations; at levels which are similar to that of normal serum EGF levels (317 pg/mL ± 31 pg/mL; Savage *et al*, 1986). The dextrin-rhEGF conjugate affords the opportunity to effectively deliver a bioactive dosing at normal physiological levels.

The biphasic response identified at various concentration of rhEGF, with suppression at high concentrations, has been previously reported in both *in vitro* and *in vivo* studies (Lai *et al*, 1989; Breuing *et al*, 1997). It has been postulated that down-regulation of the EGFR in the presence of high concentrations of EGF may account for this (Lai *et al*, 1989). In the cell proliferation studies described here (particularly in the HEp2 cell line), the effects of high concentrations (400 ng/mL) of rhEGF were most pronounced.

The conjugation to the degradable polymer, succinoylated dextrin, also permitted the controlled release of rhEGF, into the "wound environment". Over an 8-day period, rhEGF activity was prolonged after conjugation, when compared to unmodified, free rhEGF. With sustained release, rhEGF could be released, whilst still remaining within the narrow therapeutic range, to promote cell proliferation. In a clinical setting, this may reduce the need for repeated applications, and reduce the amount of rhEGF applied to a wound.

4.4.2 Cell migration

The migration of fibroblasts and keratinocytes was enhanced by rhEGF (in both free and conjugated forms, following α-amylase exposure). The action of conjugation caused "masking" of the rhEGF bioactivity, which was restored upon "unmasking", by polymer degradation, by α-amylase.

Fibroblasts and keratinocytes exhibit very distinct morphological characteristics, both in appearance and cell motility (Desmoulliere and Gabbiani, 1996; Zhao *et al*, 2003). As such, the analysis by time-lapse microscopy had to be

adapted to account for these differences. The presence of very little inter-cellular space, and reduced contact inhibition between keratinocytes *in vitro*, is related to their structural dynamics in the epidermis, *in vivo*, where they form a waterproof, protective barrier (Werner *et al*, 2007). The most appropriate methods of image analysis were based around the subtraction of cell-free background (the *in vitro* scratch wound) and the analysis of the mass movement of the body of cells, which act together to form a "sliding sheet" of cell movement to rapidly repair wounds (Zhao *et al*, 2003).

In contrast, fibroblasts in cell culture, have a much larger amount of inter-cellular space than keratinocytes. As such, the most appropriate method to examine fibroblast cell migration *in vitro*, was time-lapse microscopy, which focuses on individual cells, rather than a cohort of cells. Therefore, individual fibroblast cell tracking and velocity calculations, were implemented. Indeed, it is recognised that the motility of fibroblasts is an indirect measure of their ability to produce and re-organise the ECM (Grinnell *et al*, 2003).

Both fibroblasts and keratinocytes were responsive to the action of free rhEGF. Keratinocyte wound healing and migration velocity were markedly increased in response to rhEGF, when compared to rhEGF-free controls. Although normal and chronic wound fibroblasts did show increased migration velocity, when stimulated by rhEGF (both free rhEGF, and that released from the dextrin-rhEGF conjugate, following α-amylase exposure), the magnitude of the effects on keratinocyte average migration velocity was marked (up to 300% increase over rhEGF-free controls). This may reflect that the activity of the HaCaT keratinocyte cell line was more dependent upon rhEGF alone, compared to fibroblasts, whose activity is known to be more closely regulated *in vivo* by other growth factors (e.g. TGF-β) (Hinz, 2007; Hinz *et al*, 2007).

4.5 Conclusions

The *in vitro* data, detailed in this Chapter, obtained from cells involved in normal and pathological wound healing, demonstrated that rhEGF significantly stimulated both cellular proliferation and migration of all the target cell populations. The cellular proliferation data (from cells leaving G_0 of the cell cycle and increasing the metabolic activity), exhibited increased cellular activity and migration, both of

which are essential to normal wound healing. The present Chapter has shown that the dextrin-rhEGF conjugate can "mask" the activity of rhEGF, which can be fully restored, following polymer degradation by α-amylase ("unmasking"), under physiological conditions. With this established "proof of concept", further *in vitro* studies were undertaken to investigate the intracellular mechanisms by which rhEGF signalling in the cell types was induced.

5.1 Introduction

The epidermal growth factor receptor (EGFR; erbB-1), belongs to the family of ErbB receptor tyrosine kinases (Bazley and Gullick, 2005), which also includes c-erbB-2/HER2, c-erbB3-/HER3 and c-erbB4/HER4. The 11 mammalian ligands currently identified for these receptors are epidermal growth factor (EGF), transforming growth factor-α (TGF-α), HB-EGF (heparin binding-EGF), betacellulin, amphiregulin, epiregulin, epigen and the neuregulins (NRGs) 1–4 (Olayioye *et al*, 2000).

EGFR is a 170,000 g/mol transmembrane glycoprotein, that normally plays important roles in cell proliferation, differentiation and growth, and was the first receptor tyrosine kinase (RTK) to be discovered (Carpenter *et al*, 1978). The study of RTKs has subsequently yielded an insight into the underlying mechanisms by which these kinases function (Schlessinger 2000), including the recruitment and activation of secondary messengers (Jorissen *et al*, 2003). Each member of the ErbB family comprises a conserved protein tyrosine kinase domain, that resides within the cytoplasmic domain, a transmembrane domain and a glycosylated, extracellular ligand-binding domain (Marques *et al*, 1999; Bazley and Gullick, 2005) (Figure 5.1).

5.1.1 EGFR activation

In the absence of ligand, monomeric receptors reside within the cell membrane in an inactive state, distributed fairly evenly over the cell membrane (Bazley and Gullick, 2005). However, when ligand is present in the surrounding milieu, the receptor sites become occupied by monomeric EGF. The EGF sidechain of leucine 47 (next to lysine 48, the potential conjugation site for succinoylated dextrin, Chapter 3), projects into a hydrophobic domain, consisting of leucine 382, phenylalanine 412, isoleucine 438 and alanine 415, at it's base (Jorissen *et al*, 2003). Provided two stable 1:1 EGF:EGFR intermediate complexes persist, sequential receptor dimerisation and oligomerisation ensue (Ferguson *et al*, 2003). Receptor dimers, which have greater stability and ligand-binding affinity than their corresponding monomers (Ben-Levy *et al*, 1992; Zhou *et al*, 1993), are increasingly considered to be necessary for activation (Alroy and Yarden, 1997). Ligand binding and receptor dimerisation, subsequently, induce intracellular tyrosine kinase catalytic activity (Hubbard and Till, 2000; Dibb *et al*, 2004).

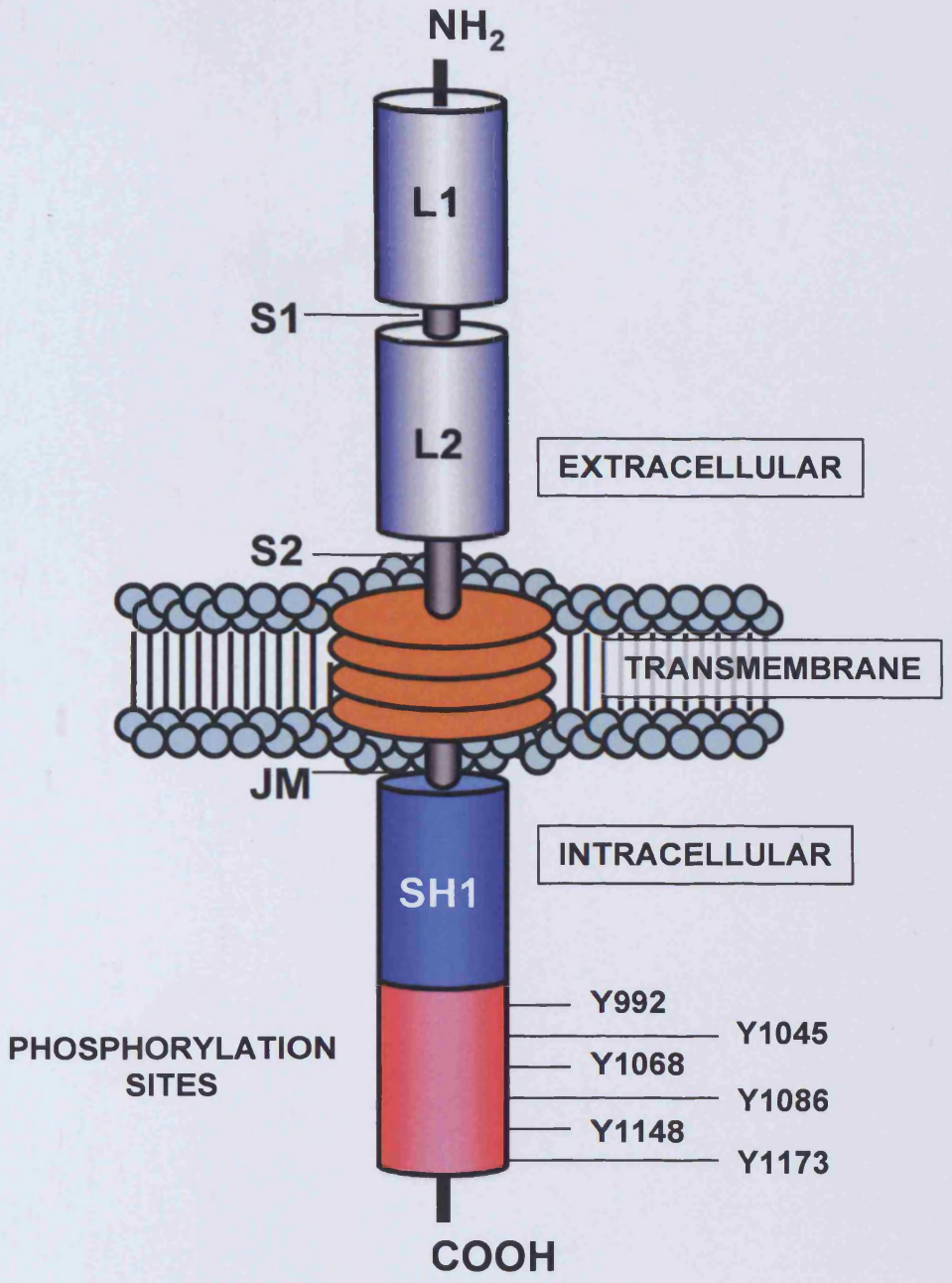

Figure 5.1 **Schematic representation of the EGFR monomer.** The extracellular domain consists of two ligand-binding subdomains (L1, L2) and two cysteine-rich domains (S1, S2). S1 permits EGFR dimerisation. SH1 is the protein tryrosine-kinase and exist above the six tyrosine residues available for phosphorylation. The transmembrane and juxtamembrane (JM) domains target the EGFR to caveolae (adapted from Bazley and Gullick, 2005).

5.1.1.1 EGFR phosphorylation

Subsequent to the transphosphorylation of the receptor dimer, at Y1173, secondary messenger proteins, possessing one of the two main classes of domains that recognise site-specific phosphorylation ("docking sites"), can interact with the receptors (Bazley and Gullick, 2005). An example of a well-characterised secondary messenger/receptor interaction, is the recruitment of the enzyme phospholipase C gamma (PLCγ) (Wang *et al,* 2001). In its inactive state, PLCγ is normally found in the cytosol. However, upon phosphorylation of the EGFR, PLCγ is able to interact with the phosphorylated receptor. This causes tyrosine phosphorylation by the activated receptor and its relocation to the plasma membrane, where it ultimately generates the second messengers, inositol 1,4,5-triphosphate (IP_3) and diacylglycerol (DAG) (Falasca *et al,* 1998), required for calcium/calmodulin-dependent kinases and the stimulation of protein kinase C. Additional targets of signaling are the JAK-STAT pathway (Janus kinases – Signal Transducers and Activators of Transcription; Schindler *et al,* 2007). These transduce the signal carried by extracellular polypeptides (e.g. growth factors) to the cell nucleus, where activated STAT proteins modify gene expression (Henson and Gibson, 2006). This pathway plays a central role in principal cell fate decisions, regulating the processes of cell proliferation, differentiation and apoptosis (Bazley and Gullick, 2005).

5.1.1.2 Signal transducers and activators of transcription (STATs)

Seven STATs have been identified in mammals (Sano *et al,* 1999). Each of these is differentially activated by various extracellular ligands. Many investigators have demonstrated that growth factors, including EGF, TGF-α and platelet-derived growth factor (PDGF), activate members of the STAT family, including STAT1 and STAT3 (Hernandez-Sotomayor and Carpenter, 1992; Ihle, 1996; Darnell, 1997). EGF has been shown to activate STAT1 and STAT3, in EGFR over-expressing cells (e.g. HEp2 cells) (Sadowski *et al,* 1993, Zhong *et al,* 1994; Park *et al,* 1996). The EGFR can activate STATs, in a JAK-independent manner, due to the presence of an intrinsic tyrosine kinase (Ihle, 1996). The phosphorylated STAT then forms dimmers, which translocate to the nucleus, where it binds to DNA-response elements in promoter regions, thus regulating growth factor/cytokine-directed gene expression (Zhong *et al,* 1994; Ihle, 1996; Darnell, 1997). Strategies which down-regulate

EGFR can inhibit cell proliferation and abrogate STAT3 activation (Song and Grandis, 2000). Indeed, studies which have demonstrated that STAT3 gene disruption leads to mutant mice with no apparent abnormalities; with normal epidermal and hair follicle development. In this model, however, wound healing was markedly retarded. An *in vitro* study with cultured keratinocytes, revealed that this phenotype was attributed to impaired migration, as a consequence of impaired STAT3 activation (Kira *et al*, 2002; Sano *et al*, 2008).

5.1.2 Intracellular studies

For the study of the EGF-activation pathway, many techniques have been employed, including immunocytochemistry, Northern blotting, Western blot analysis, microarrays and bioinformatics (Harper *et al*, 2002; Liu *et al*, 2005; Hurtado *et al*, 2007). In this Chapter, the presence and activation of the EGFR, by rhEGF and the "unmasked" dextrin-rhEGF conjugate, were examined using fluorescence and chemiluminescence techniques. Fluorophores are functional groups within molecules that absorb energy at a specific wavelength (excitation), and re-emit it, again at a specific wavelength (Lichtman and Conchello, 2005). These are used widely in cell biology, but some are sensitive to pH, resulting in quenching of the fluorescence (Lattanzio, 1990; Takahashi *et al*, 1999). Alexa488 is a green emitting fluorophore (absorption = 495 nm, emission = 519 nm), which has been reported to fluoresce, in a pH-independent manner (Thorn and Parker, 2004).

5.1.3 Experimental aims

A series of assays were developed to examine the mechanism of action of rhEGF and rhEGF, released from the dextrin-rhEGF conjugate, in response to α-amylase. The distribution of EGFR and EGF-endocytosis, in the HEp2 epidermoid carcinoma cells, HaCaT keratinocytes, normal dermal fibroblasts and chronic wound fibroblasts, were established, using fluorescence-labelled EGF, in conjunction with fluorescence-activated cell sorting (FACS) and fluorescence microscopy techniques. EGFR-activation and intracellular secondary messenger activation were examined, using sodium dodecyl sulphate-polyacrylamide gel electrophoresis (SDS-PAGE) (Section 2.6.2.2), and Western blot analysis.

The aims of this chapter were the:

1. Detection of EGFR in the different cell lines.
2. Optical imaging of EGFR, using confocal microscopy.
3. Quantification of relative EGFR density between the different cell lines using FACS analysis.
4. Analysis of EGFR activation, by the dextrin-rhEGF conjugate, following α-amylase exposure.

5.2 Methods

A number of general methods (Chapter 2) were utilised in the present Chapter, including the SDS-PAGE (Section 2.6.2.2), the BioRad protein assay (Section 2.6.2.4), cell culture (Section 2.6.3.1) and FACS analysis (Section 2.6.3.8).

To assess the pH-dependent quenching of Alexa488, EGF-Alexa488 was diluted to a range of concentrations (0 – 100 μg/mL) in a range of phosphate buffers (Table 5.1), and fluorescence was recorded using a Fluostar Optima microplate reader, equipped with a 520 nm filter.

5.2.1 Confocal microscopy

HEp2 cells, HaCaT cells and normal dermal and chronic wound fibroblasts, from subculture, were seeded at a density of 5 x 10^3 cells/well on CultureSlides in cell-specific, 10 % serum-containing media (SCM 10%; 200μL). After 24 h, cells were serum-starved, in cell-specific, serum-free media (SFM; 200 μL) for a further 24 h. Leupeptin (50 μM) was added to the media and the cells maintained at 37 °C/5 % CO_2 for 10 min. Culture media was aspirated and EGF-Alexa488 (10 μg/mL, in phosphate buffered saline, PBS; 100 μL), added to cells, with additional leupeptin (50 μM), for between 0 and 60 min, at 4 °C or 37 °C. Cells were washed (x 3) with PBS and fixed with 4 % paraformaldehyde (in PBS, pH 6.8; 100 μL), for 20 min, at room temperature, in the dark. Slides were mounted with Vectashield™ mounting medium ± DAPI and examined by Confocal Microscopy (Section 2.5.2.9).

Table 5.1 Phosphate buffer compositions

Buffer molarity (mM)	Monosodium phosphate monohydrate (mg)	Disodium phosphate heptahydrate (mg)	ddH_2O (mL)	pH
100	1270	212	100	5.8
100	1028	684	100	6.4
100	312	2075	100	7.4

5.2.2 Fluorescence-activated cell sorting (FACS)

HEp2 cells, HaCaT cells, normal dermal and chronic wound fibroblasts, were seeded at 1.5 x 10^5 cells, in a 75 cm^2 tissue culture flask and maintained at 37 °C/5 % CO_2 in SCM 10 % (10 mL cell-specific media) until 90 % confluent. Cells were washed (x 3) in PBS and serum-starved in SFM (10 mL) for 24 h. Media was then aspirated and EGF-Alexa488 (10 μg/mL in PBS; 1 mL) added to cells at 4 °C and 37 °C, in the dark, for 0 to 30 min. Cells were washed (x 3) with PBS and trypsin-EDTA (0.025 %) added for 5 min, at 37 °C/5 % CO_2. When the cells had detached from the tissue culture flask, SCM 10 % (9 mL) was added and the cell suspensions aspirated and centrifuged at 1500 *g* for 1 min using a Precision Durafuge 200 centrifuge. The supernatants were removed and the resulting cell pellets re-suspended in ice-cold PBS (1 mL), and re-centrifuged, as described above. This process was repeated twice more. The cells were finally re-suspended in ice-cold PBS (200 μL) and the samples stored on ice, until required for FACS analysis (Section 2.6.3.8).

5.2.3 Western blotting

5.2.3.1 Cell culture - EGFR expression

HEp2 cells, HaCaT keratinocytes, and patient-matched, normal and chronic wound fibroblasts, were seeded at 5 x 10^5 cells/100mm sterile Petri dish and maintained in 5mL of SCM 10 %, until 90 % confluent. Cells were serum-starved for 24h, in SFM, prior to protein extraction.

5.2.3.2 Cell culture - EGFR and STAT3 phosphorylation

HEp2 cells and HaCaT keratinocytes were seeded at 5 x 10^5 cells/100 mm sterile Petri dish and maintained at 37 °C / 5% CO_2, in 5 mL SCM 10 %, until 90 % confluent. Cells were serum-starved for 24 h, in SFM, prior to the addition of rhEGF (400 ng/mL, in H-SFM, for HEp2 cells; 6.25 ng/mL, in K-SFM, for HaCaT cells), the dextrin-rhEGF conjugate (400 ng/mL rhEGF equivalent, in H-SFM, for HEp2 cells; 0.1 ng/mL rhEGF equivalent, in K-SFM, for HaCaT cells), or α-amylase-exposed, dextrin-rhEGF conjugate (400 ng/mL rhEGF equivalent, in H-SFM, for HEp2 cells; 0.1 ng/mL rhEGF equivalent, in K-SFM, for HaCaT cells; both samples contained α-amylase, 93 i.u./L, pre-incubated at 37°C for 24 h). Samples were

selected at regular intervals between 0 and 40 min to study phosphorylated EGFR expression (following 2.5 min rhEGF/dextrin-rhEGF exposure and subsequently washed (x3) with PBS), or 0 and 24 h for analysis of phosphorylated STAT3 expression, and the cellular proteins extracted.

5.2.3.3 Protein extraction

Cells were washed (x3) with ice-cold, PBS and the cellular proteins extracted by scraping into ice-cold extraction buffer (1 mL; 50 mM Tris-HCl buffer, pH 7.5, containing 5 mM EDTA and 1 mM dithiothreitol) and sonicated (5 x 20 s). Cell suspensions were harvested, centrifuged at 15,000 *g* (4 °C) (Section 2.5.2), for 20 min, and the protein content of the resulting supernatants determined, using the BioRad DC Protein Assay (Section 2.5.3.4). Samples (70 μg protein) were lyophilised, and stored at -20 °C, until required.

5.2.3.4 Sodium dodecyl sulphate-polyacrylamide gel electrophoresis (SDS-PAGE)

Protein samples and positive controls (A431 cell lysate for EGFR analysis; K562 whole cell lysate for STAT3 phosphorylation analysis) were suspended in non-reducing, Laemmli loading buffer (1mL 0.5 M Tris-HCl, pH 6.8, containing 0.8 mL glycerol, 1.6 mL 10% SDS, 0.32 mL 0.05 % bromophenol blue, 4.18 mL ddH2O; 20μL) and loaded onto pre-formed, 4-15 % gradient gels, along with molecular weight markers (Section 2.6.2.2). Electrophoresis was performed at a constant 18 mA, for 3 h.

5.2.3.5 Western blot analysis

SDS-PAGE gels underwent electroblotting onto PVDF membranes, using a Trans-Blot Semi-Dry Electrophoretic Transfer Cell System (Section 2.5.2), at a constant 15 V, for 30 min. On transfer, PVDF membranes were blocked with blocking buffer (5 % skimmed milk powder, in 0.05 % Tween 20 / PBS, pH 7.2) overnight.

5.2.3.6 Immunodetection

The PVDF membranes were immuno-probed with primary antibodies, anti-EGFR (phosphoY1173; anti-human, polyclonal IgG antibody, raised in rabbit), anti-STAT3 (phospho Y705; anti-human, polyclonal IgG antibody, raised in rabbit), anti-actin (C-2; anti-human, monoclonal IgG antibody, raised in mouse), and anti-EGFR (F4; anti-human, monoclonal IgG, raised in mouse), all diluted 1 : 200 in blocking buffer, at room temperature for 1 h. The membranes were rinsed in blocking buffer (1 x 15 min, followed by 2 x 5 min), prior to incubation with horse-radish peroxidase conjugated secondary antibodies, anti-rabbit, polyclonal IgG antibody, raised in goat; and anti-mouse, polyclonal IgG antibody, raised in goat, diluted 1 : 3000 in blocking buffer, at room temperature, for 1 h. The membranes were rinsed in blocking buffer, at room temperature (1 x 15 min, followed by 2 x 5 min), prior to incubation in chemiluminescent reagent (ECL Plus Western Blotting Detection Reagent Kit), for 1 min, at room temperature. Membranes were analysed with autoradiographic film (Hyperfilm-ECL) for 15 s to 5 min. Films were developed with an Autodeveloper (Section 2.5.2).

5.2.4 Statistical analysis

Statistical analyses were undertaken using GraphPad Prism®, version 4.00 (GraphPad Software, San Diego, USA). Data were compared using a Student's t-test or a one-way ANOVA, with a Bonferroni post-test. Results were expressed as a mean and standard deviation (S.D.). Statistical significance was considered at a probability of $p < 0.05$.

5.3 Results

5.3.1 Confocal microscopy

No significant pH-dependent quenching of Alexa488 occurred, over a pH range 5.8 – 7.4 (Figure 5.2). EGFR binding by EGF-Alexa488 occurred more efficiently at 37 °C, than at 4 °C, in HEp2 cells, over a 30 min period (Figure 5.3). The increase in green signal, corresponded to increased EGFR binding. At a typical single-cell level, EGFR binding at 37 °C, in HEp2 cells, occurred in a time-dependent manner, from 1 min (Figure 5.4a). Cell surface receptor binding increased, as did the apparent uptake of the fluorophore (conjugated to EGF). The EGFR was

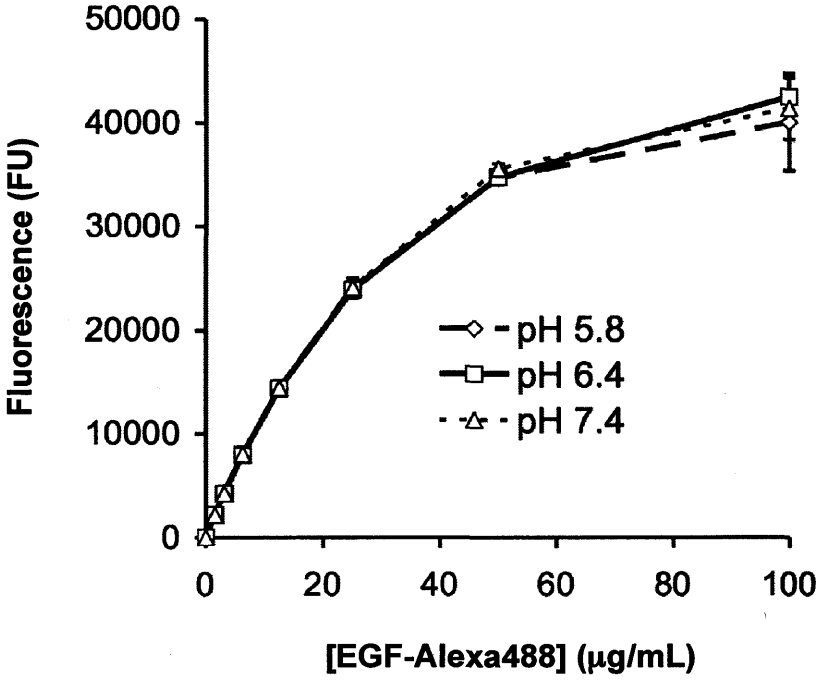

Figure 5.2 **Fluorescence of EGF-Alexa488 at various pHs.** The fluorescence of EGF-Alexa488 was not dependent upon pH, either at physiological pH (7.4) or intracellular pH (5.8) (mean ± S.D., n = 3, $p > 0.05$).

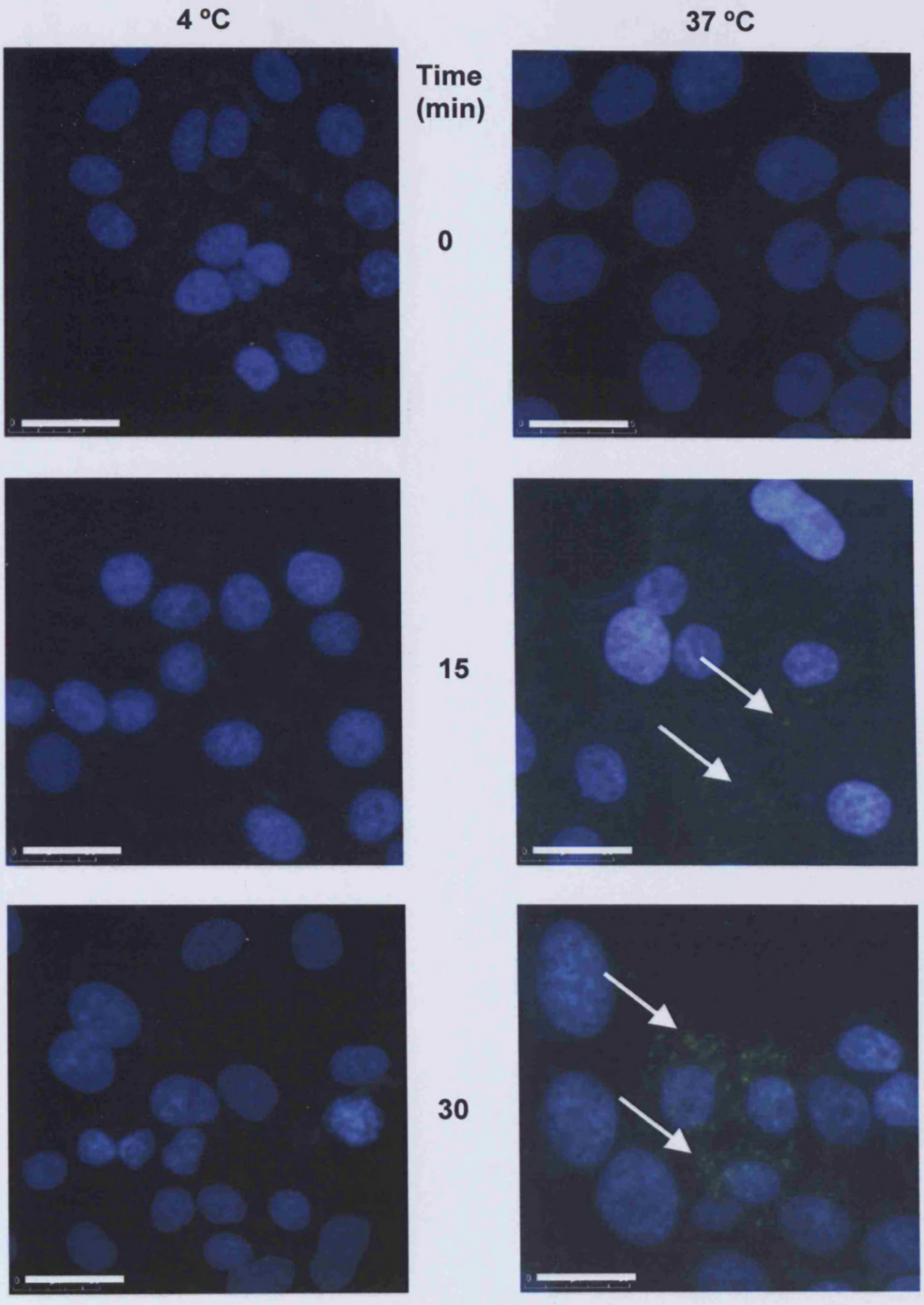

Figure 5.3 **Confocal microscopy of HEp2 cells.** The images to the left, demonstrate minimal receptor binding and uptake at 4 °C, whilst binding was increased (arrowed) in a time-dependent manner at 37 °C. Scale bar = 25 μm. Blue = DAPI, green = EGF-Alexa488.

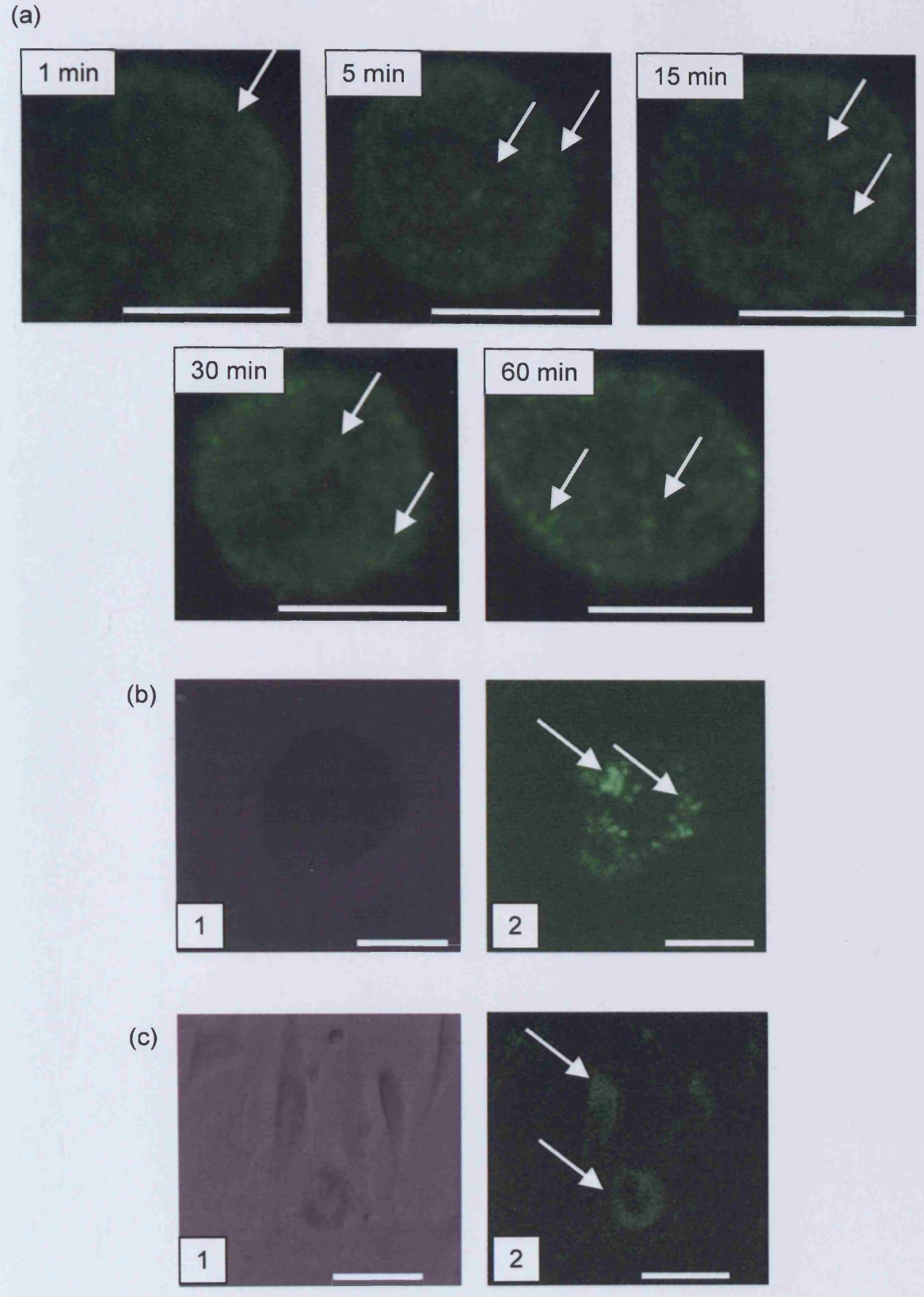

Figure 5.4 **Confocal microscopy of HEp2, HaCaT and normal dermal fibroblasts.** Panel (a) demonstrates the typical time-dependent binding of EGF-Alexa488 to HEp2 cells, at 37 °C. Panel (b) demonstrates a typical HaCaT keratinocyte, viewed in brightfield (1) and fluorescence (2) at 15 min, 37 °C/5% CO_2. Panel (c) demonstrates typical normal dermal fibroblasts, viewed in brightfield (1) and fluorescence (2) at 15 min, 37 °C. Scale bar = 25 μm.

also present on HaCaT keratinocytes and normal dermal fibroblasts, as indicated by confocal microscopy (Figures 5.4b and 5.4c).

5.3.2 Fluorescence-activated cell sorting (FACS)

FACS analysis demonstrated ligand-specific binding occurring at a maximum rate after only 1 minute in HEp2 cells, which was sustained over a 30 minute period. Dot plots (Figure 5.5a) showed the evolution of population of non-viable after 30 min in the 4 °C control. Although specific uptake increased over 30 minutes (Figure 5.5b), non-specific binding also increased (Figure 5.5c), but significantly more binding occurred at 37 °C (p = 0.0058). Different cell types bound and endocytosed the EGF-Alexa488, at contrasting rates/quantities. HEp2 cells and HaCaT keratinocytes bound significantly more EGF, than both the normal dermal and chronic wound fibroblasts ($p < 0.01$). There was no significant difference between geometric mean fluorescence of the normal and chronic wound fibroblasts ($p > 0.05$) (Figure 5.6). There was also no significant difference between the geometric mean fluorescence of the HEp2 cells and the HaCaT keratinocytes ($p > 0.05$).

5.3.3 Western blot analysis

EGFR was identified to be differentially expressed amongst the different cell types examined. A band was detected at approximately 170,000 Da, corresponding to the EGFR. There was greater expression of EGFR in the HEp2 and HaCaT keratinocytes, than in the normal dermal fibroblasts and chronic wound fibroblasts (Figure 5.7). In the HEp2 cells, the EGFR was phosphorylated at Y1173, in response to rhEGF (400 ng/mL), with maximal phosphorylation at 20 min (Figure 5.8a). When rhEGF activity was "masked" by conjugation to succinoylated dextrin (the dextrin-rhEGF conjugate), in the absence of α-amylase, the degree of phosphorylation was markedly reduced (Figure 5.8b). Upon the addition of α-amylase (93 i.u./L) and incubation for 24 h at 37 °C / 5% CO_2, rhEGF was released from the conjugate, causing activation and phosphorylation of EGFR, with maximal effect at 40 min (Figure 5.8c). Similarly, STAT3 phosphorylation (at Y705) occurred, in the presence of rhEGF (400 ng/mL), with a detectable band present at 92,000 Da (Figure 5.9a). Again, activity was "masked" by the dextrin-rhEGF conjugate, in the absence of α-

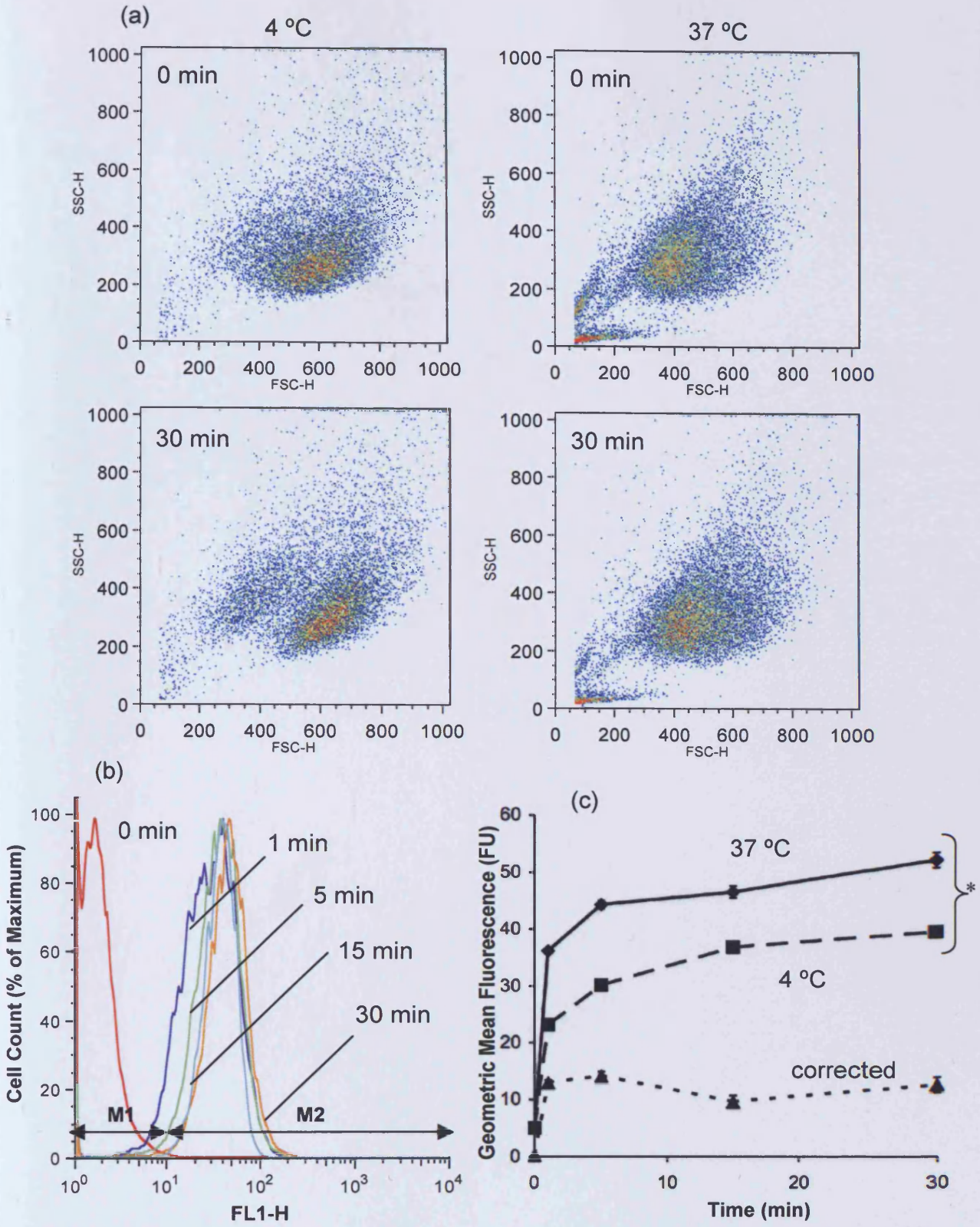

Figure 5.5 **Fluorescence-activated cell sorting (FACS) of HEp2 cells**. Panel (a) shows dot-plots of a typical distribution of EGF-Alexa488 labelled HEp2 cells, at 0 and 30 min. Panel (b) shows a histogram of the distribution of fluorescence at 37 °C, over 30 min. Panel (c) shows the corrected geometric mean fluorescence (- - ▲ - -), calculated by subtracting non-specific binding at 4 °C (-- ■ --) from specific, active EGFR binding, at 37 °C (—◆—) (mean ± S.D., n = 2, * p = 0.0058, Student's t-test)

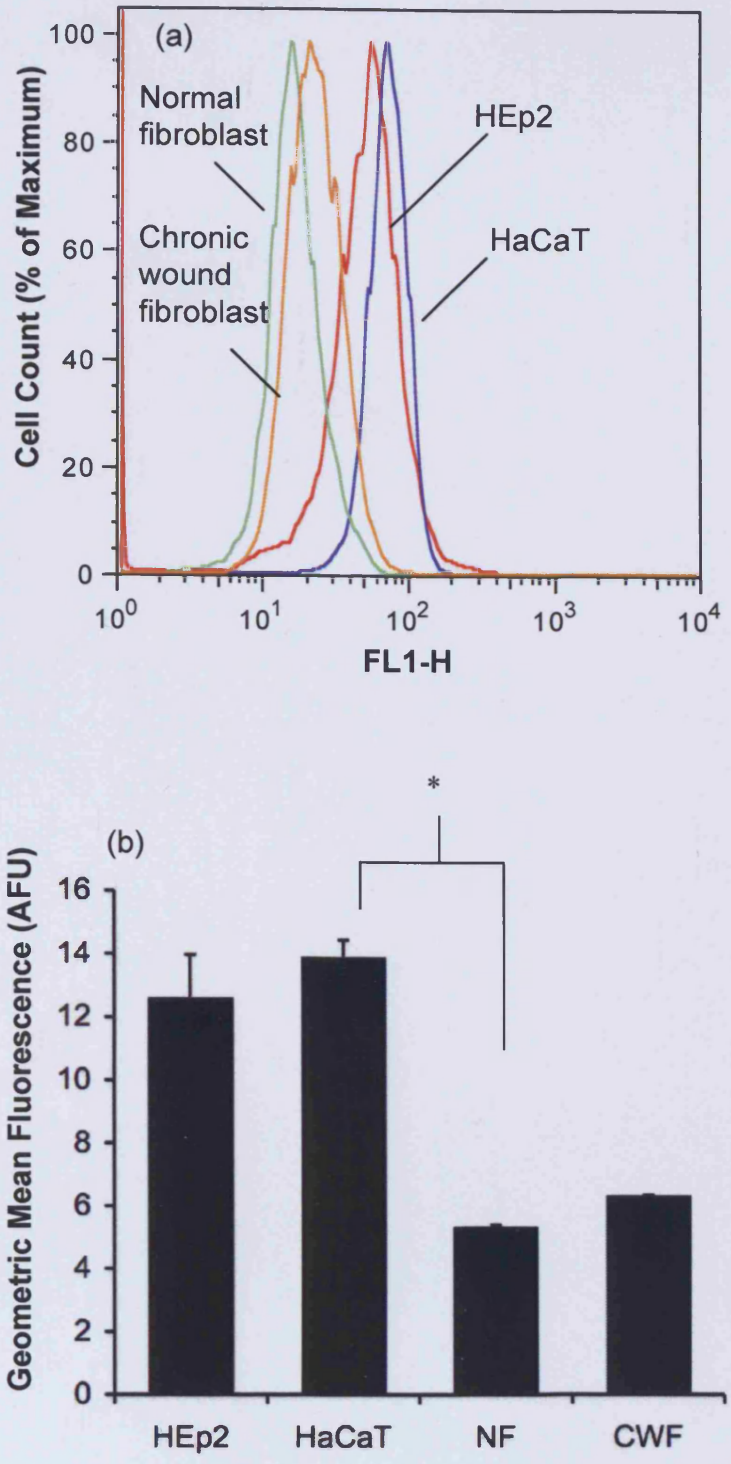

Figure 5.6 **Fluorescence-activated cell sorting (FACS) of all cell types.** Panel (a) shows a histogram of the fluorescence distribution amongst the different cell types. Panel (b) shows the geometric mean fluorescence amongst the different cell types: HEp2, HaCaT keratinocytes, normal dermal fibroblasts (NF) and chronic wound fibroblasts (CWF), (mean ± S.D., n = 2; * $p < 0.01$, ANOVA and Bonferroni *post hoc* test).

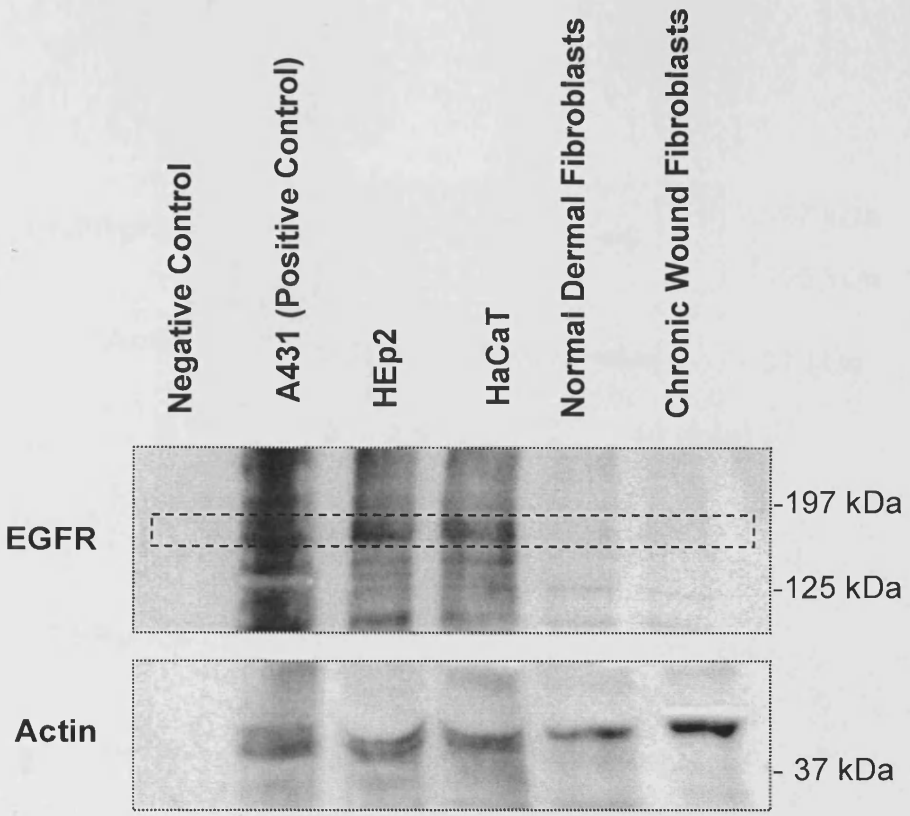

Figure 5.7 **Western blot analysis of the EGFR.** A band was present at 170 kDa for A431 whole cell lysate (positive control), HEp2 and HaCaT keratinoycte, representing, the EGFR. A very weak band was present in this region, in the normal dermal fibroblasts and chronic wound fibroblasts. Actin was used as a loading control.

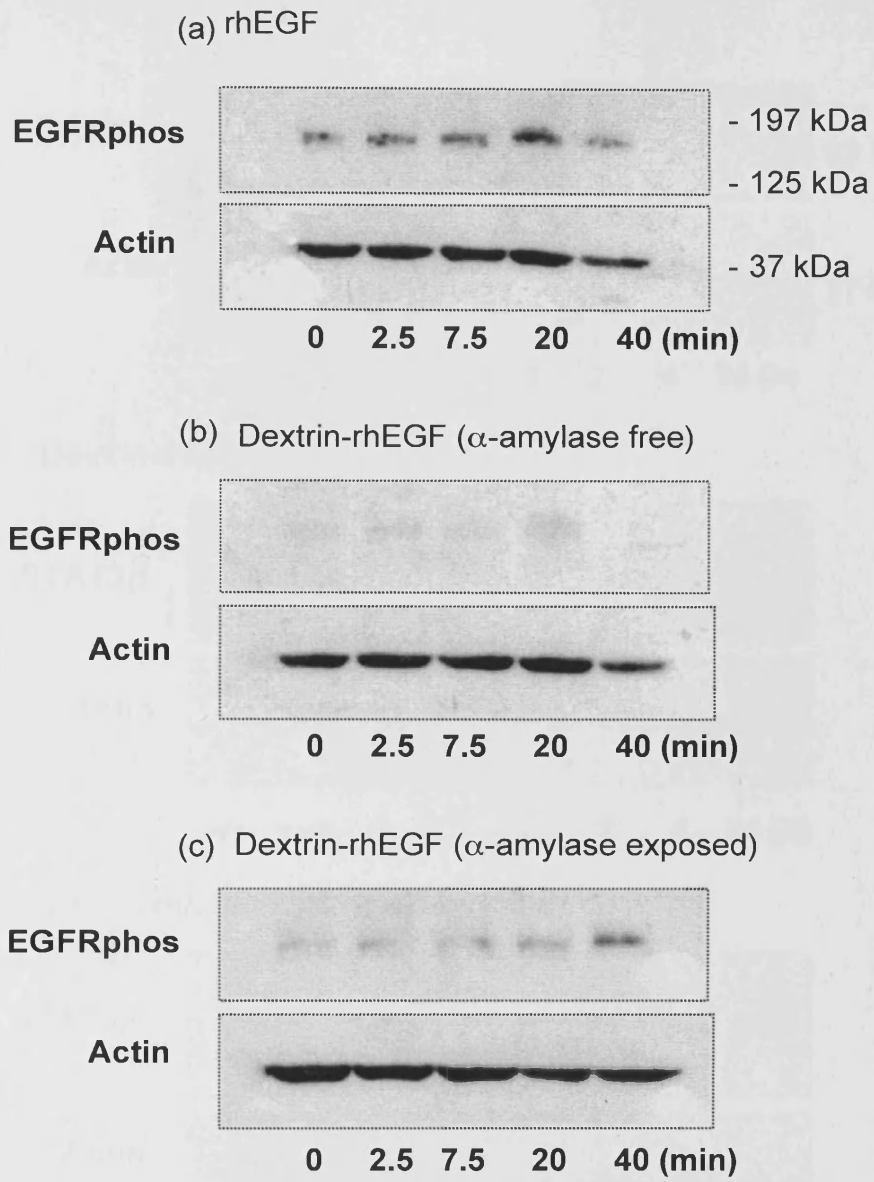

Figure 5.8 **Western blot analysis of phosphorylated EGFR in HEp2 cells.** Panel (a) shows the presence of EGFR (phospho Y1173) at approximately 170 kDa with actin loading controls, in response to rhEGF (400 ng/mL). Panel (b) shows minimal phosphorylation in response to dextrin-rhEGF (400 ng/mL equivalent) in the absence of α-amylase and panel (c) shows the restoration of rhEGF activity with the dextrin-rhEGF (400 ng/mL equivalent), following 24 h exposure to α-amylase (93 i.u./L). Actin was used as a loading control.

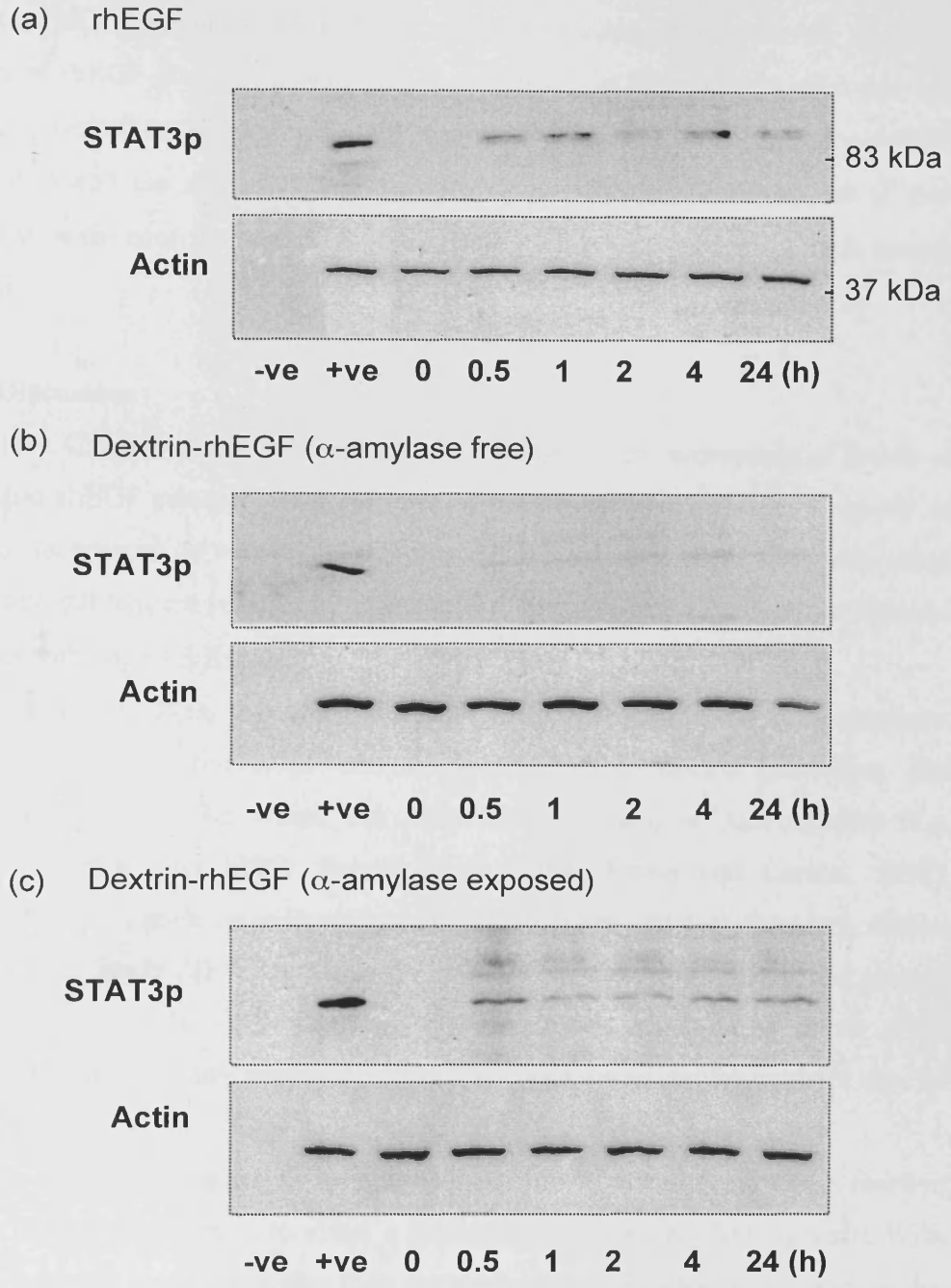

Figure 5.9 **Western blot analysis of the phosphorylated STAT3 in HEp2 cells.** Panel (a) shows the presence of STAT3 (phospho Y705) at approximately 92 kDa, with actin loading controls, in response to rhEGF (400 ng/mL). Panel (b) shows minimal phosphorylation, in response to dextrin-rhEGF (400 ng/mL equivalent) in the absence of α-amylase and panel (c) shows the restoration of rhEGF activity with the dextrin-rhEGF (400 ng/mL equivalent), following 24 h exposure to α-amylase (93 i.u./L). K562 whole cell lysate was a positive control (+ve). Actin was used as a loading control.

amylase (Figure 5.9b), and "unmasked" upon the addition of α-amylase (Figure 5.9c). In HaCaT keratinocytes, STAT3 phosphorylation was observed upon the addition of rhEGF and the dextrin-rhEGF conjugate, in the presence of α-amylase (93 i.u./L), following 2 h exposure. EGFR phosphorylation was absent in the rhEGF-free control and the dextrin-rhEGF conjugate, not exposed to α-amylase (Figure 5.10). The actin controls confirmed the equality of loaded protein in each sample analysed.

5.4 Discussion

This Chapter aimed to investigate the intracellular mechanism of action of rhEGF and rhEGF released from the dextrin-rhEGF conjugate. Using a variety of analytical techniques, it was confirmed that conjugation of rhEGF to succinoylated dextrin, and subsequent release, in response to α-amylase did not affect the classical signalling pathway of rhEGF.

Fluorescent dyes, that can be used to investigate intracellular mechanisms, are known to be sensitive to pH and can undergo pH-dependent quenching. The intracellular pH is acidic, which can cause the quenching of fluorophores (e.g. fluorescein isothyanate, FITC; Palmer *et al*, 1994; Kwon and Carson, 1998). Alexa488 has been reported to be resistant to such activity and was, therefore, chosen for the present Study (Thorn and Parker, 2004). This was confirmed in the present Chapter (Section 5.3). Quenching of the fluorescent signal may have given misleading results, and any potential intracellular tracking of the fluorophore may be affected by this.

As already discussed in Section 3.4, rhEGF possesses only one reactive amine to permit conjugation, to either a fluorophore or succinoylated dextrin. With only one potential conjugation site, then the production of co-conjugates, such as the fluorescent labelling of an EGF molecule, prior to conjugation, to permit tracking of the EGF molecule, following α-amylase mediated release from the polymer conjugate, was not be possible. A series of experiments proved this to be correct (data not shown). Oregon Green™ (OG)-labelled dextrin could be conjugated to rhEGF (via the reactive lysine group), to produce an OG-dextrin-rhEGF conjugate that could be potentially tracked, using fluorescence analysis (FACS, Confocal Microscopy). However, with only one binding site, a dextrin-rhEGF-OG conjugate

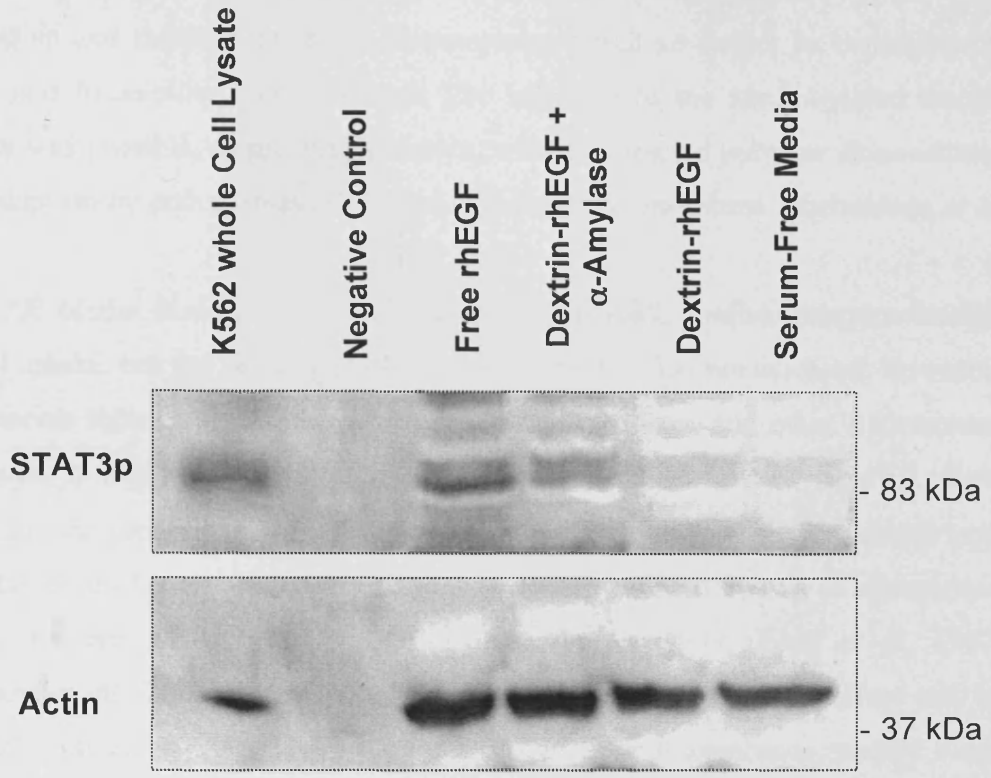

Figure 5.10 **Western blot analysis of the phosphorylated STAT3 in HaCaT cells,** after 2 h exposure to rhEGF, dextrin-rhEGF and dextrin-rhEGF exposed to α-amylase. A band corresponding to STAT3 (phospho Y705), is observed at approximately 92 kDa, in the K562 whole cell lysate positive control. It is also observed, after 2 h, in the presence of free rhEGF (6.25 ng/mL), and dextrin-rhEGF (0.1 ng/mL rhEGF equivalent), exposed to α-amylase (93 i.u./L). There is a weak or absent band when exposed to dextrin-rhEGF, in the absence of α-amylase, or rhEGF-free media, for 2 h. Actin was used as a loading control.

could not be synthesised. The synthesis of dextrin-rhEGF-OG would have allowed the tracking of rhEGF whilst conjugated (as could OG-dextrin-rhEGF), but upon degradation and rhEGF release, the fluorescence would no longer be conjugated to rhEGF and traceability would be lost. The labelling of the succinoylated dextrin polymer was possible, as previously shown, with the labelled polymer demonstrated to be taken up by endocytosis and sorted, via the early endosome (Richardson *et al*, 2008).

All of the studies here, involving EGF-Alexa488, confirm receptor-binding and cell uptake, but the bioactivity of fluorescent rhEGF was not assessed. To enable a fluorescent signal to be detected by Confocal Microscopy, and other fluorescence techniques, a high concentration of rhEGF was used (0.5 – 10 μg/mL). Cells involved in the process of dermal wound healing (keratinocytes and fibroblasts) have been shown to be sensitive to EGF-stimulation, at much lower concentrations ranging between 10 – 50 ng/mL (Ando and Jensen, 1993; Yang *et al*, 1997; Sutherland *et al*, 2005). At high a high concentrations, a cytotoxic effect can be observed (Gill and Lazar, 1981; Barnes, 1982). These fluorescence studies were, therefore, useful for the imaging of receptor binding and EGF uptake, but it must be emphasised that this was not a true reflection of the events may be encountered *in vivo*.

5.4.1 Epidermal growth factor distribution

The EGFR is present on the majority of cell types (Lopez *et al*, 1992). It is found at different densities upon the cell surface of these different cells (Krupp *et al*, 1982; Engstrom *et al*, 1985; Falette *et al*, 1989; Lopez *et al*, 1992). The expression of EGFR may predict the behaviour of cells to EGF stimulation (Jorissen *et al*, 2003). Upon ligand-binding and receptor dimerisation, the EGFR is taken up into the cell by endocytosis and processed at an intracellular level, resulting in receptor recycling and degradation, and the up- or down-regulation of cell surface receptors (Yarden and Ullrich, 1988; Gruenberg and Maxfield, 1995; Levkowitz *et al*, 1998; Bao *et al*, 2008). Cells which over-express EGFR (e.g. epithelial carcinomas) are known to be susceptible to EGF-stimulation, as receptor blocking can reduce the cells' ability to proliferate and migrate *in vivo* (Bundred *et al*, 2001; Chan *et al*, 2002).

The literature reports typical cell surface EGFR densities for fibroblasts (7 x 10^4 per cell; Krupp *et al*, 1982) and keratinocytes (9.2 x 10^3 to 8.5 x 10^4 per cell;

Lopez *et al*, 1992). These numbers of cell-surface receptors represent 85 – 95 % of the total receptors per cell (Krupp *et al*, 1982). In the present Study, the EGFR was more significantly expressed in HaCaT keratinocytes (immortalised, adult human cells) than in the fibroblasts, although the receptor was still present in both the fibroblast cell types. Interestingly, there were no significant differences in the EGFR expression between the normal dermal and chronic wound fibroblasts. It has been suggested that cells from burn wound margins may under-express specific cell surface receptors (Wenczak *et al*, 1992), as do aged (senescent) cells (Shirahara *et al*, 2000). In the proteolytic chronic wound environment, cell surface receptors may be prone to degradation, and whilst still being expressed, their longevity may be reduced. The present Study confirmed that patient-matched, fibroblasts from different dermal origin, expressed a similar number of receptors when removed from the normal dermal or chronic wound environments. Consequently, the down-regulation of the EGFR, or possibly, the reduced half-life of the EGFR, in the chronic wound environment (Wenczak *et al*, 1992), is not reflected, *ex vivo*.

5.4.2 EGFR activation and intracellular signalling

The EGFR was differentially expressed amongst the model cell line (HEp2), compared to the keratinocytes and normal dermal and chronic wound fibroblasts. The levels detected by Western blotting, were in accordance with those detected by FACS analysis.

Western blot analysis of specific proteins involved in the EGFR signalling cascade, demonstrated that the model HEp2 cell line was sensitive to rhEGF stimulation, with phosphorylation of the EGFR occurring within 2.5 minutes of exposure, with maximal stimulation after 20 minutes. This confirmed the ability of rhEGF to activate this specific pathway. In the wound model, involving HaCaT keratinocytes, STAT3 phosphorylation occurred in the presence of both free rhEGF, or that derived from α-amylase-exposed, dextrin-rhEGF. The activation of the EGFR signalling cascade was, therefore, demonstrated to occur in both cell line models. With the activation of this cascade in the epidermal-derived cell line, it confirms the observations in the *in vitro* models of cell proliferation and migration (Chapter 4).

In accordance with the polymer masking-unmasking protein therapy (PUMPT) hypothesis, the activity and ability of rhEGF to bind to the EGFR should be "masked" by the conjugation to the succinoylated dextrin macromolecule.

Western blot analysis confirmed this, as minimal expression of the phosphorylated EGFR was evident, in response to the dextrin-rhEGF conjugate in the absence of α-amylase exposure, with an equivalent quantity of rhEGF present. Upon the addition of α-amylase (at physiological concentrations), for 24 hours, rhEGF was released, inducing activation (phosphorylation) of the EGFR. Interestingly, there was a slight delay in the induction of maximal activity (40 minutes versus 20 minutes) between the free rhEGF and rhEGF released ("unmasked") from the dextrin conjugate. This may be a consequence of growth factor conjugation to succinoylated dextrin, resulting in an amide bond between the reactive residue and carboxylic side-chain, which would be resistant to polysaccharide degradation. Such events may lead to delayed receptor binding. Alternatively, the total rhEGF was not completely released by α-amylase exposure, as was observed by ELISA (Section 3.3.3). With potentially only 40 – 50 % of the available rhEGF released, a weaker, or delayed response, as apparent by Western blot analysis, may have resulted.

Following EGFR phosphorylation, the intracellular pathway was activated, resulting in STAT3 phosphorylation, which continued over a 24-hour period. In the presence of the "masked" dextrin-rhEGF conjugate, there was minimal activation. Phosphorylated STAT3 was examined, as STAT3 is normally latent within the cytoplasm and may not be affected by EGFR activation (Kira *et al*, 2002). Under all conditions where the EGFR had been phosphorylated, subsequent phosphorylation of the STAT3 was demonstrated to occur. Again, the activation of these intracellular pathways confirms the bioactivity of the dextrin-rhEGF conjugate observed in Chapter 4.

5.5 Conclusions

These preliminary *in vitro* studies, involving cells found in the normal and wound dermis and epidermis, in addition to a model cell line (HEp2), demonstrate that the EGFR was present upon the surface of all cells types examined. However, the EGFR was accessible to the binding of labelled EGF and rhEGF, both as free rhEGF and as that released from the dextrin-rhEGF conjugate. Following receptor-ligand binding, normal intracellular pathways were activated. It can, therefore, be concluded that rhEGF conjugation to succinoylated dextrin, and subsequent rhEGF release by α-amylase (at physiological concentrations) does not affect the inherent

bioactivity of the rhEGF. The next line of investigation involved the development and optimisation of an *ex vivo* model of wound healing, and the examination of rhEGF and the dextrin-rhEGF conjugate, in this *ex vivo* model.

Chapter Six

Dextrin-rhEGF Conjugate Evaluation in an Ex Vivo Model of Wound Healing And Wound Fluid Analysis

Chapter Six: Dextrin-rhEGF Conjugate Evaluation in an *Ex Vivo* Model of Wound Healing And Wound Fluid Analysis

Contents

6.1 INTRODUCTION

Ex vivo organ culture is the maintenance of multiple cell types in an organ-specific structured manner. The majority of skin that can be cultured *in vitro*, is *ex vivo* derived, but is grown as an organotypic model (e.g. human skin equivalents, HSE). Organotypic skin culture, *in vitro*, can involve the development of an artificial matrix, seeded with multiple cell types found together in a specific organ, *in vivo*, to mimic the appearance and/or function of the organ. HSEs consist of a dermis, epidermis and partially differentiated, *stratum corneum*, but are deficient in skin appendages, such as pilosebaceous units and hair follicles (Godin and Touitou, 2007). However, such skin appendages, themselves have been cultured *in vitro* (Philpott *et al*, 1990). In recent years, the development of organotypic skin has allowed advances in wound healing investigation *ex vivo*, prior to *in vivo* assessment (Godin and Touitou, 2007). Examples of these two subtypes of *ex vivo* model and how they apply to wound healing and the assessment of the dextrin-recombinant human epidermal growth factor (dextrin-rhEGF) conjugate, are considered below.

Another *ex vivo* model routinely used, has involved the collection of acute and chronic wound fluid. Wound fluid was utilised for both analytical and experimental purposes, for example to confirm the presence of α-amylase in wound fluid, which was essential for fulfilment of the Polymer masking-UnMasking Protein Therapy (PUMPT) hypothesis. Wound fluid was also used in the assessment of the stability of the dextrin-rhEGF conjugate, in the presence of chronic wound proteinases. These are vital steps, prior to the commencement of *in vivo* evaluation of the dextrin-rhEGF conjugate.

6.1.1 *Ex vivo* organ culture and models of wound healing

6.1.1.1 Organotypic skin culture

The first organotypic models of skin were based upon human keratinocytes, cultured upon an irradiated fibroblast layer, supported on plastic (Rheinwald and Green, 1975). Cultured sheets of keratinocytes were first applied to burn wounds as a skin substitute, as opposed to autologous skin grafting, in 1981 (O'Connor *et al*, 1981). Recent developments in the synthesis of artificial skin substitutes has involved the use of 3-D scaffolds, to mimic the extracellular matrix (ECM), on which cellular or dermal and/or epidermal equivalents can be cultured and applied to

wounds. Acellular dermal equivalents can also be used in the trauma setting to provide a dermal template for endogenous cellular ingrowth.

With the development of tissue-engineered, skin equivalents, for *in vivo* application, these have also been applied to *in vitro* studies of transdermal drug permeation (Pasonen-Seppänen *et al*, 2001; Ajani *et al*, 2007) and skin irritancy testing (Ponec, 2002), prior to *in vivo* assessment. With reference to cutanous wound healing, the development of HSEs has provided biologically meaningful experimental systems, to study epidermal biology and epithelial–mesenchymal cross talk, in an *in vivo*-like tissue context (Andriani *et al*, 2003; Abraham *et al*, 2004; Margulis *et al*, 2005). These 3-D tissues allow direct determination of key response parameters of wounded epithelium, including cell proliferation, migration, differentiation, growth factor responses and proteinase expression (Singer and Clark, 1999). As such, these systems provide a valuable model to study cell interactions in complex tissues (Egles *et al*, 2008).

However, the true *in vivo* architecture is lost with these models, and although an artificial representation can be synthesized and seeded with multiple organ derived cell lines, these systems are not a perfect model in which to examine the wound healing potential of the dextrin-rhEGF conjugate. HSEs are an ideal candidate for skin replacement *in vivo* (Dini *et al*, 2006; Pham *et al*, 2007), but for the assessment of the dextrin-rhEGF conjugate, an established organ culture model will be utilised.

6.1.1.2 Corneal re-epithelialisation

Organ culture models, involving *ex vivo* corneas, have been successfully developed for the assessment of gene therapy (Mohan *et al*, 2005), immunomodulatory drugs (Flueckiger *et al*, 2005) and corneal wound healing (Zhao *et al*, 2006; Castro-Combs *et al*, 2008). Either the whole eye, or cornea alone, can be maintained outside if the body, resulting in the *in vivo* architecture of the cornea being retained, along with the endogenous cell types (Figure 6.1).

Corneal epithelial wound closure models have been employed by many investigators. They involve inducing a defined, central epithelial wound (and excision of the anterior stratified squamous epithelium) and characterising the kinetics of the wound healing response. Healing occurs in distinct phases involving the "sliding" of cells to cover the denuded surface, cell proliferation and stratification

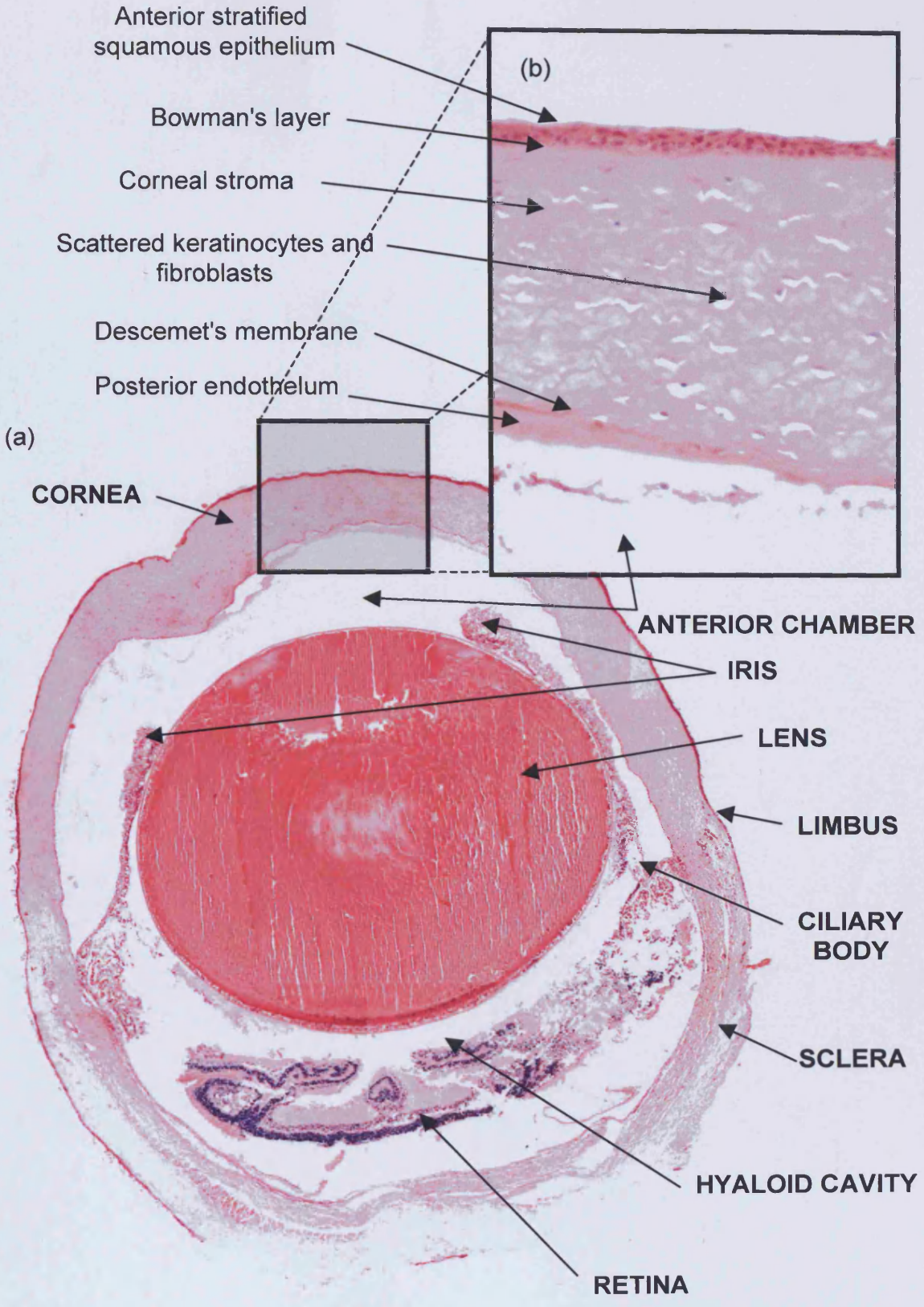

Figure 6.1 **Cross-section through the murine eye.** Panel (a) shows a 4 x magnification of a haematoxylin and eosin (H&E) stained cornea, with structures labelled. Panel (b) shows a 20 x magnification of the cornea, with structures labelled.

(Zhao *et al*, 2003). Prior to the onset of these events, there is a lag phase of about five hours, *in vivo*. Cells migrate at a constant rate of approximately 60 to 80 μm/hour, until wound closure is completed (Pfister, 1975; Kuwabara *et al*, 1976; Matsuda *et al*, 1985; Crosson *et al*, 1986). Agents that have selective effects on epithelial growth, migration, adhesion, and differentiation have been identified. These include topically applied growth factors, such as EGF, fibroblast growth factor (FGF), transforming growth factor-β_1 and -β_2 (TGF-β_1 and -β_2), keratinocyte growth factor (KGF), hepatocyte growth factor (HGF), platelet-derived growth factor (PDGF), insulin-like growth factor (IGF), interleukins (IL) -1 and -6, tumour necrosis factor-α (TNF-α), endothelin-1 (ET-1) and retinoids (Elliott, 1980; Kandarakis *et al*, 1984; Ubels *et al*, 1985; Takagi *et al*, 1995; Imanishi *et al*, 2000).

Ex vivo models of corneal re-epithelialisation, include the culture of the whole eye (Reid *et al*, 2005), submerged in tissue culture medium, or models that mimic the *in vivo* arrangement of the eye, by isolating the cornea and maintenance at the air-fluid interface. Such models can also further imitate the *in vivo* situation, by perfusion of the anterior chamber, at a defined pressure, producing a constant tear film to maintain corneal moisturisation, which can also deliver experimental compounds to the cornea (Zhao *et al*, 2006). Various animal species have been used for these experiments, such as rat (Reid *et al*, 2005), cow (Zhao *et al*, 2006), rabbit (Castro-Combs *et al*, 2008) and pig (Flueckiger *et al*, 2005).

An *ex vivo* rat corneal model will be utilised herein, for assessment of the dextrin-rhEGF conjugate. Although it is a model of acute wound healing, and the tissue architecture is dissimilar to skin, this model will be employed, prior to the investigation of the dextrin-rhEGF conjugate with an *in vivo* model of impaired dermal wound healing (Chapter 7). In the pre-clinical development of the dextrin-rhEGF conjugate, from *in vitro* repopulation of a wounded monolayer culture, to *ex vivo* organ culture, these vital further steps that have established the potential of the dextrin-rhEGF conjugate to enhance wound healing.

6.1.2 Wound fluid

It is widely assumed that wound fluid is a reflection of the wound environment (Trengove *et al*, 1996; Mani, 1999). As such, it may provide important clues regarding the status of the wound itself. Wound fluids/exudates can be

collected using minimally invasive methods and have the potential to provide important biochemical information in the healing status of a wound. Numerous methods for wound fluid collection have been reported (Moseley *et al*, 2004; Yager *et al*, 2007).

6.1.2.1 Acute wound fluid

The majority of studies examining acute wound fluid have relied upon peri-operatively-placed suction drains, such as the Jackson-Pratt® (American Heyer Schulte Corp., Santa Barbara, USA), or Portavac™ drains (Howmedica International Incorporated, Pfizer Medical Technology Group, Shannon, Ireland), or from blister fluid (Ortega *et al*, 2000). Although drainage fluids are relatively easy to obtain, these will only reflect the early stages of acute wound repair. During this phase, the levels of cytokines and growth factors differ. Studies have shown that growth factors, such as EGF, PDGF and FGF are initially high, and then progressively fall, whilst vascular endothelial growth factor (VEGF) and IL-1 rise during the first post-operative week. TGF-β remains relatively constant during this time, although all these levels vary between studies (Vogt *et al*, 1998; Baker *et al*, 2003; Di Vita *et al*, 2006). This temporal variation can reflect the underlying wound healing processes. No studies have reported the α-amylase content in acute wound fluids.

6.1.2.2 Chronic wound fluid

Fluid obtained from chronic wounds can be aspirated from underneath occlusive dressings (James *et al*, 2003) or by extraction from wound dressing materials, placed upon wounds (Moseley *et al*, 2004). Studies that have compared the biomarker profile of acute and chronic wound fluids have shown, consistently, that pro-inflammatory cytokines, such as the interleukins; tissue proteinases, including the matrix metalloproteinases (MMP-2 and -9) and serine proteinases (e.g. neutrophil elastase); and reactive oxygen species (ROS), are present at significantly higher levels in non-healing wounds, as opposed to healing wounds (Moseley *et al*, 2004; Yager *et al*, 2007). A consensus on the levels of growth factors in acute and chronic wounds, has not yet been reported, with variable levels of EGF, PDGF and TGF-β, found in these contrasting wound fluids. Decreased levels of growth factors, or inappropriate localisation may also be a factor (Cooper *et al*, 1994; Higley *et al*,

1995; Trengove *et al*, 2000). A consistent finding is that when acute or chronic wound fluid is applied to cells, acute wound fluids promote dermal fibroblast proliferation and ECM synthesis, whilst chronic wound fluids suppressed this response (Katz *et al*, 1991; Bucalo *et al*, 1993; Mendez *et al*; 1999). No studies have reported the α-amylase content within chronic wound fluids.

6.1.3 Amylase

The amylases are a group of enzymes found in all living organisms, that breakdown starches into disaccharides, by acting upon α-1,4-glycosidic bonds. α-amylase is found in humans, although not exclusively, whereas β- and glucoamylase are found exclusively in plants and microorganisms (Janacek, 1997; Pandey *et al*, 2000).

6.1.3.1 α-Amylase

The α-amylases act at random locations along the polysaccharide chain, yielding intermediate length dextrins, shorter limit dextrins, maltotetraoses and maltotrioses, and ultimately the dissacharides, maltose and isomaltose (isomaltose retains an α-1,6-glycosidic bond) (Burkart, 2004) (Figure 6.2). In humans, α-amylase occurs in two isoforms (pancreatic- and salivary-α-amylase), which are produced in the pancreas and parotid glands, respectively (Abrams *et al*, 1987; Whitcomb and Lowe, 2007). Approximately 5 - 6 % of the total protein in pancreatic secretions, is α-amylase (Whitcomb and Lowe, 2007). α-Amylase is a 512 amino acid glycoprotein, of approximately 57,600 g/mol (Abrams *et al*, 1987). α-Amylase acts at an optimum pH of 6.7 – 7.0, in the proximal ileum and, on starch hydrolysis, as described above, the resulting limit dextrins and disaccharides are further digested by intestinal brush border enzymes (maltase, isomaltase). The resulting monosaccharides are subsequently absorbed (Alpers, 1994). The predicted amino acid sequences of the salivary and pancreatic isoforms differ by only 6 % (Abrams *et al*, 1987). These have nearly identical crystal structures (Ramasubbu *et al*, 1996) and have the same mechanisms of action. The two isoforms can be distinguished by electrophoresis (Lott and Lu, 1991).

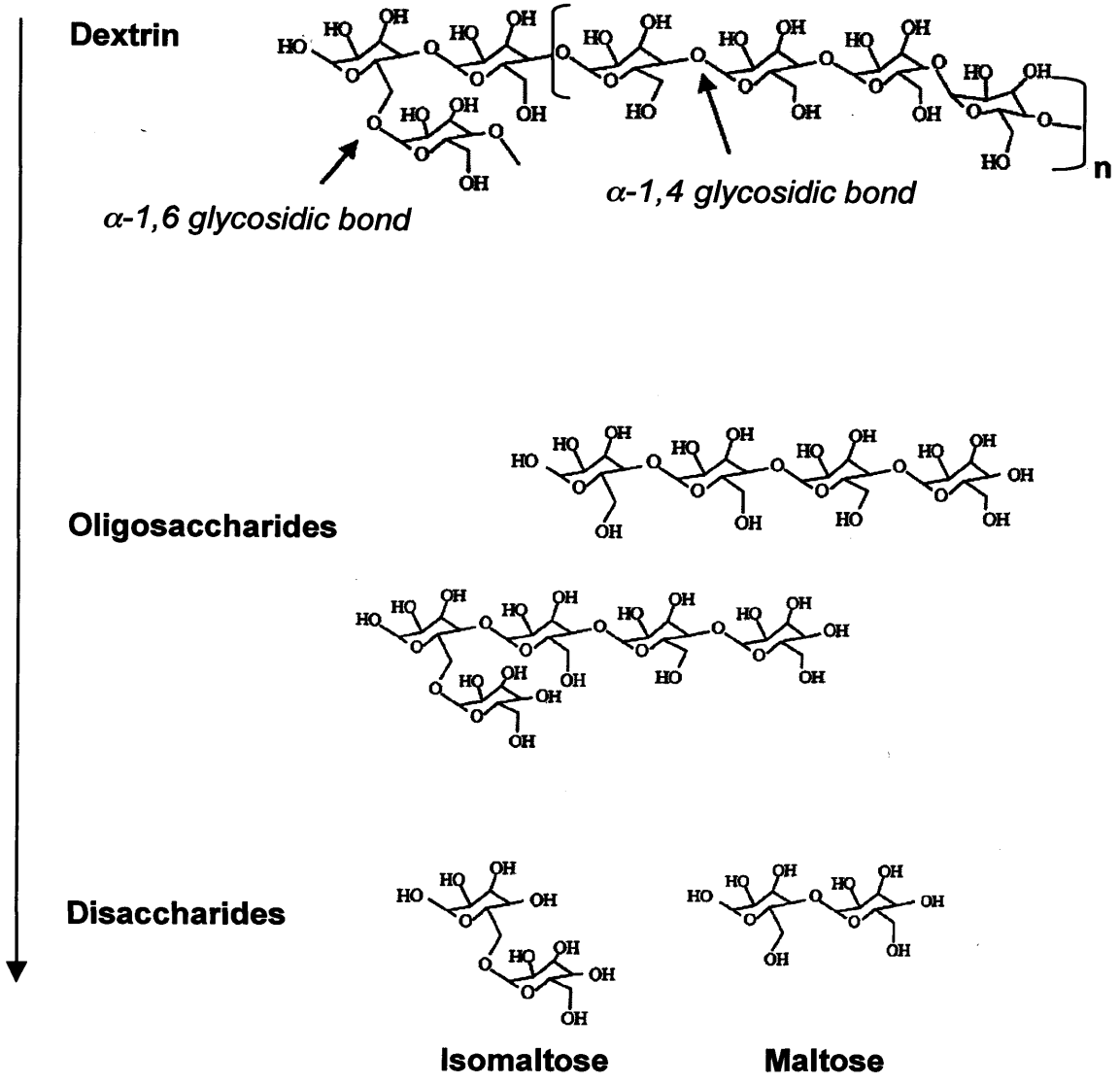

Figure 6.2 **The degradation of polysaccharides by α-amylase.** Polysaccharides are degraded by the random hydrolysis of α-1,4 glycosidic bonds, initially to medium length dextrins (n = 200 - 300) and subsequently to oligosaccharides and component disaccharides. α-1,6 glycosidic bonds (< 5 % in dextrin) are not degraded by α-amylase thus, ultimately, resulting in isomaltose liberation. Final degradation of the disaccharides is mediated by maltase and isomaltase, present at the intestinal brush border.

6.1.4 Experimental aims

The efficacy of the dextrin-rhEGF conjugate, has been established with *in vitro* models of wound healing, involving cells (fibroblasts, keratinocytes) known to be important in the normal response to injury, as well as those derived from chronic wounds (Chapters 4 and 5). Prior to investigation in an *in vivo* model of impaired wound healing (Chapter 7), the dextrin-rhEGF conjugate was evaluated in an *ex vivo* organ culture model of acute wound healing. The composition of wound fluid was also established, with respect to α-amylase and elastase activities.

The aims of this Chapter were the:

1. Establishment of an *ex vivo* model of acute corneal wound healing.
2. Assessment of the effectiveness of the dextrin-rhEGF conjugate, to induce corneal repair, *ex vivo.*
3. Collection of *ex vivo* wound fluid from acute and chronic wounds.
4. Analysis of wound fluids, for α-amylase and elastase activities.

6.2 Methods

6.2.1 *Ex vivo* corneal organ culture model of acute wound healing

6.2.1.1 Corneal wounding

Two-month old male Wistar Han rats (250-300g; Charles River Laboratories, Margate, UK), were sacrificed by CO_2 asphyxiation, confirmed by cervical dislocation. A medial and lateral canthotomy was performed to allow access to the globe, using a surgical scalpel (15-blade). The globe was irrigated with balanced salt solution (1 mL, BSS Plus®), containing 0.1% ethylenediaminetetraacetic acid (EDTA). The irrigation remained *in situ* on the cornea for 5 min. Excess irrigation solution was removed with a cotton swab. Using a binocular Operating Microscope (Stemi 2000-C), at 1.25x magnification, the cornea was scored with an ultra-fine micro-knife (15° cutting angle, 5mm blade). A circular abrasion was developed and the corneal anterior epithelium denuded, to produce a full-thickness corneal abrasion of 2mm diameter (Figure 6.3). The globe was then enucleated and placed in a 12-well tissue culture plate, secured on a bleb of cyanoacrylate adhesive gel (Loctite Super Glue). Prior to the addition of culture medium, the globe was maintained in

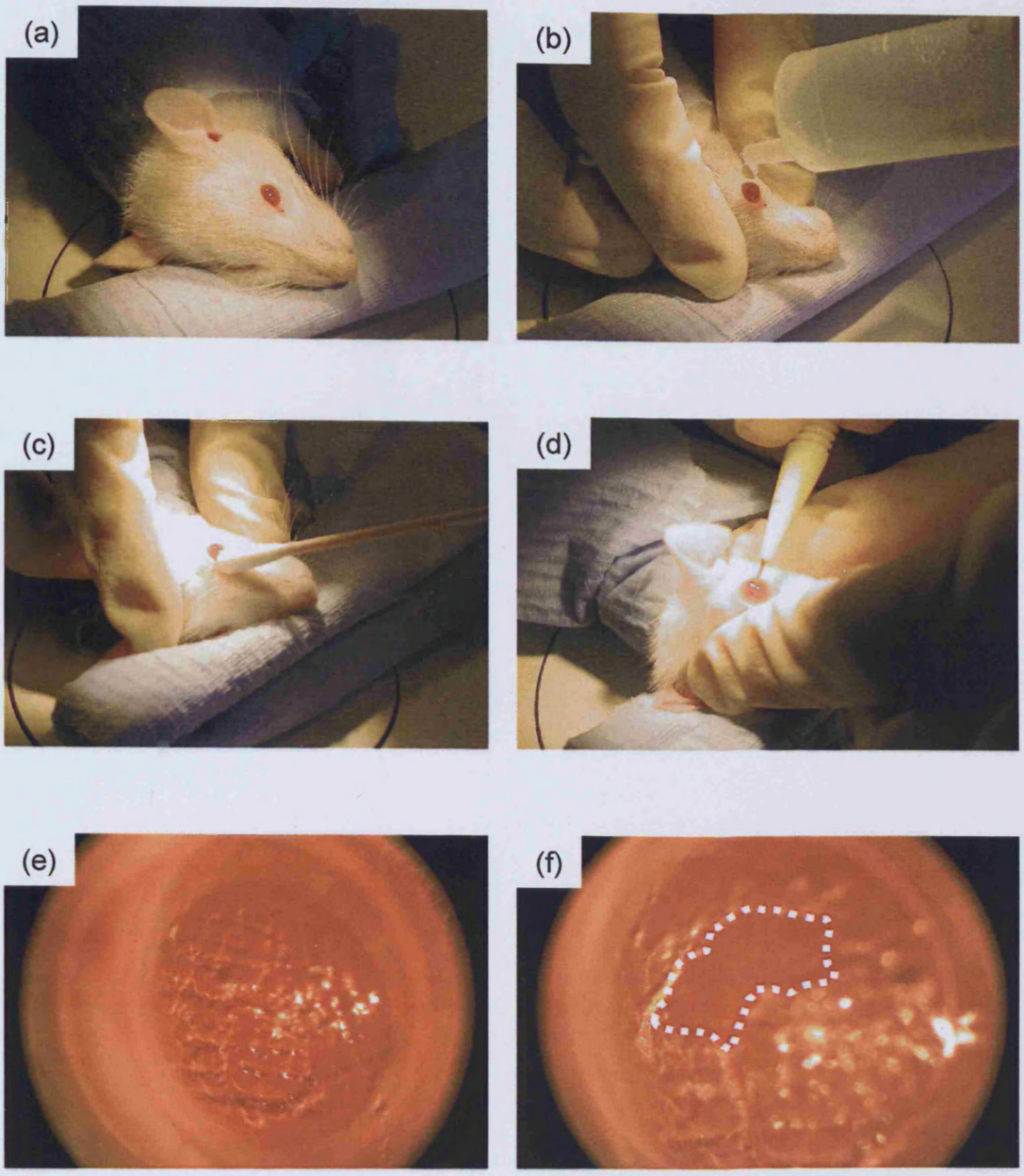

Figure 6.3 ***Ex vivo*** **corneal wound healing - specimen preparation.** (a) Male Wistar Han rat were sacrificed. (b) Eyes were irrigated with BSS Plus® solution, containing 0.1% EDTA, for 5 min. (c) The excess irrigation fluid was swabbed from the eyes. (d) The eyes were abraded with a micro-knife, to produce a scored cornea (e). (f) The abrasions were developed, by progressive removal of the epithelium (as indicated by the dotted line).

BSS Plus® (3 mL) solution. 4 specimens were assigned to each Control and Study Group.

6.2.1.2 Addition of tissue culture medium and study compounds

Tissue culture medium, Dulbecco's modified Eagle's medium (DMEM) supplemented with penicillin G, 100U/mL; streptomycin sulphate, 100μg/mL; amphotericin B, 0.25μg/mL; puromycin, 1μg/mL; L-glutamine, 2mM (serum-free media; SFM), was applied to the Control Group (Group 1). For the Study Groups, the SFM was supplemented, as follows:

- Group 2 - 10% foetal calf serum (FCS) (serum containing media; SCM).
- Group 3 - α-amylase (93 i.u./L).
- Group 4 – rhEGF (1 μg/mL).
- Group 5 - rhEGF (10 μg/mL).
- Group 6 - dextrin-rhEGF (1 μg/mL rhEGF equivalent)
- Group 7 - dextrin-rhEGF (1 μg/mL rhEGF equivalent) and α-amylase (93 i.u./L) (pre-incubated for 24 h, at 37 °C).
- Group 8 - dextrin-rhEGF (10 μg/mL rhEGF equivalent) and α-amylase (93 i.u./L) (pre-incubated for 24 h, at 37 °C).

Supplemented tissue culture medium (3 mL), as described above, was added to each well, containing the *ex vivo* globes, and the specimens maintained at 37 °C / 5% CO_2, for 64 h.

6.2.1.3 Corneal imaging

Corneal wounds were recorded using digital photography. Images from the Operating Microscope (at 2.5x magnification), were recorded with a digital camera (Nikon Coolpix 4500). For each specimen, tissue culture medium was aspirated from the well and excess fluid removed from the cornea, using a cotton swab. Following imaging, the tissue culture medium was replaced, as described above. Images were recorded at time points between 0 and 64 h. To confirm corneal wound healing, fluorescein staining was performed, using a Fluorets® Sterile Ophthalmic Strip,

activated with phosphate buffered saline (PBS), and images recorded at 1.25x magnification, under an ultraviolet light source, at 365nm.

6.2.1.4 Image analysis

Digital images were contrast enhanced in Adobe® Photoshop® CS3 (Adobe Systems Incorporated, San Jose, USA) and size-normalised. Wound edges were delineated in Microsoft® PowerPoint® (2004 for Mac; Microsoft Corporation, Washington, USA) and wound sizes (as a percentage of the image size) calculated, using Image J software (ImageJ 1.40g; http://rsb.info.nih.gov/ij/) (Figure 6.4).

6.2.2 Wound fluid collection

Informed consent was obtained for all procedures, which were performed under Local Research Ethics Committee (LREC) approval. Patient undergoing mastectomy surgery (acute wound fluid) or with venous leg ulcers (chronic wound fluid), were recruited from inpatient (Department of Surgery) and outpatient (Wound Healing Research Unit) populations, at the University Hospital of Wales, Cardiff, UK.

6.2.2.1 Acute wound fluid collection

Acute wound fluid samples (n = 5 patients) were obtained using peri-operatively placed, sub-cutaneous suction drains (Jackson-Pratt), over a 24 h period. Samples (1 mL) were clarified by centrifugation (15,000 *g*, 5 min at 4°C) and the supernatants stored at -80°C, until required.

6.2.2.2 Chronic wound fluid collection

Each venous leg ulcer or diabetic foot ulcer (n = 5 patients) was dressed with Release® and covered with a Bioclusive® film dressing. These dressings remained *in situ* > 4h. Upon wound dressing saturation, the Bioclusive® film was removed, the saturated Release® dressing removed, using sterile forceps, and placed in a sterile vial on dry ice, for transfer. Any non-saturated regions within the Release® dressings were removed with sterile scissors. In order to elute the wound fluids, dressings were immersed in 0.1M Tris-HCl buffer, pH 7.4, containing 0.1% Triton X-100 (wound fluid elution buffer; 500 μL buffer/cm^2 dressing). Chronic wound fluids were eluted

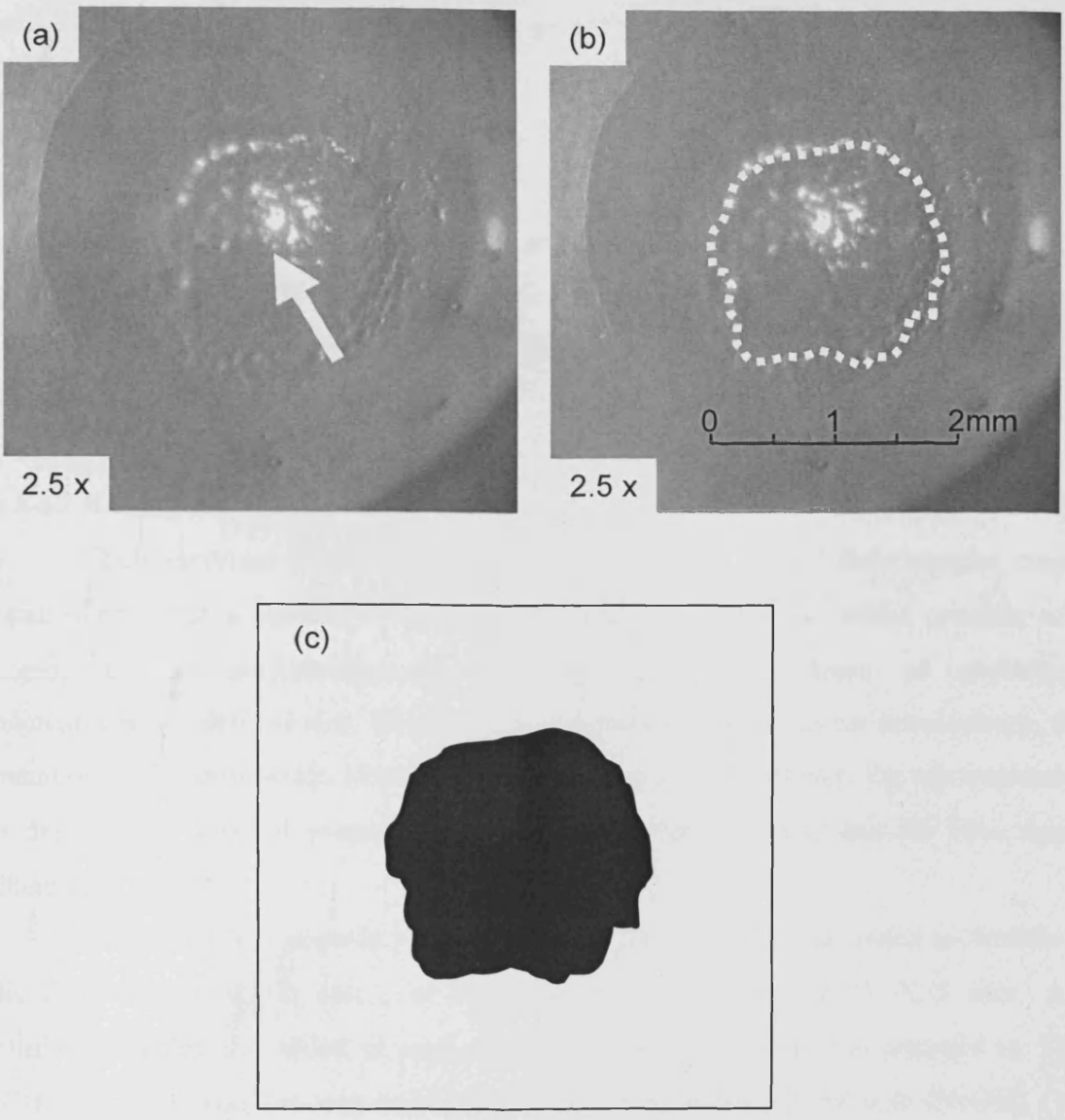

Figure 6.4 **Corneal abrasion - image analysis.** (a) The corneas were digitally imaged at 2.5 x magnification. (b) The wound areas were highlighted (as indicated by white dotted line). (c) The wound areas were calculated, as a percentage of the whole image size (black pixels : white pixels). Serial measurements were taken for each abrasion, at specified time points, up to 64 h.

for 2 h, at 4°C, under constant agitation (Cullen *et al*, 2002). Eluted wound fluid samples were aliquoted (1 mL) and stored at -80°C, until required.

6.2.3 Wound fluid analysis

6.2.3.1 Protein content determination

The total protein content of each acute and chronic wound fluid sample, was quantified, using the Bio-Rad DC Protein Assay (Section 2.6.2.4). Total protein content was determined, with reference to a standard calibration curve, as described previously.

6.2.3.2 α-Amylase activity assay

The α-amylase content of each acute and chronic wound fluid sample, was established using a starch-dye assay (Phadebas®). A Phadebas® tablet consists of homogeneously interlinked starch polymers, taking the form of globular microspheres of defined size. When a blue dye becomes bound to the microsphere, it remains insoluble in water. However, in the presence of α-amylase, the microsphere is degraded at a speed proportional to the α-amylase activity, and the blue dye liberated.

Each acute and chronic wound fluid sample (200 μL) was added to double-distilled water (ddH_2O; 4mL), in triplicate, and prewarmed at 37 °C/5 min. A Phadebas® tablet was added to each sample, vortexed for 10 s, and returned to 37 °C/15 min. The reaction was terminated with 0.5 M sodium hydroxide (NaOH) (1 mL), the sample vortexed and centrifuged (1500 *g*, 5 min). An aliquot of each supernatent (200 μL) was placed in a 96-well microtitre plate. The absorbance of each well was assessed using a Dynex MRX Spectrophotometer, equipped with a 620 nm filter. Absorbance results (patient result – blank = absorbance) were compared to the supplied, Phadebas® batch-matched, standard calibration curve, for calculation of α-amylase content. α-Amylase activities were expressed as i.u./L and per mg of protein, for each acute and chronic wound fluid sample.

6.2.3.3 Elastase activity assay

The elastase activity in each acute and chronic wound fluid sample was determined, using the EnzChek® elastase assay (Section 2.6.2.6). The activity, over a

1 h period, was determined (relative fluorescence units (RFU)/min), as was the activity with reference to the protein content of each wound fluid sample (RFU/min/mg protein). Activity at 1 h was established, with reference to a standard calibration curve, and the units (U) and concentration (ng/mL) of elastase calculated. I U was defined as the amount of enzyme necessary to solubilize 1 mg of elastin in 20 min, at pH 8.8 and at 37 °C (defined by the manufacturer).

6.2.3.4 EGF content of wound fluid

Each acute, and chronic, wound fluid sample was analysed by ELISA (200 μL, in triplicate), and compared to a rhEGF standard curve, as previously described (Section 2.6.2.5).

6.2.3.5 rhEGF and dextrin-rhEGF stability, in chronic wound fluid

rhEGF (250 pg/mL) and the dextrin-rhEGF conjugate (250 pg/mL equivalent), were diluted in chronic wound fluid (patient C, the highest elastase activity; 6 mL), and incubated at 37 °C. Aliquots (600 μL) were taken at time points between 0 and 72 h, snap-frozen and stored at -80 °C. On termination of the experiment, samples defrosted and analysed by ELISA (200 μL, in triplicate) and compared to a rhEGF standard curve, as described previously (Section 2.6.2.5).

6.2.4 Statistical analysis

Statistical analyses were undertaken using GraphPad Prism® version 4.00 (GraphPad Software, San Diego, USA). Data were compared using a Student's t-test. Results were expressed as a mean and standard deviation (S.D.). Statistical significance was considered at a probability of $p < 0.05$.

6.3 Results

6.3.1 Corneal wound healing

In the establishment of the *ex vivo* organ culture model of acute wound healing, wounds (2 mm) were observed to remain unhealed, when cultured in SFM (Group 1), but did heal, in response to media, supplemented with 10 % FCS (Group 2). Fluorescein staining confirmed the presence of a corneal abrasion in Group 1, after 64 h, and the absence of any unhealed area, in Group 2 at 24-48 h. Corneal

abrasions remained in Group 3 (α-amylase alone, 93 i.u./L), Group 4 (rhEGF, 1 μg/mL), and Group 5 (rhEGF, 10 μg/mL), at 64 h. Group 6 (dextrin-rhEGF, 1 μg/mL rhEGF equivalent, in the absence of α-amylase), remained unhealed at 64 h, but upon exposure to of α-amylase (93 i.u./L), the abrasions were observed to have healed, in response to the dextrin-rhEGF conjugate, at both 1 μg/mL rhEGF equivalent (Group 7) and 10 μg/mL rhEGF equivalent (Group 8), by 48 h (Figure 6.5).

There was a significant improvement in wound healing (p = 0.0098), in response to SCM (Group 2), compared to the SFM (Group 1) and α-amylase (Group 3)controls, at 24 h. All wounds in the SCM group (Group 2) had fully re-epithelialised by 48 h, whilst the average wound areas in the serum-free controls (Groups 1 and 3), were 24.5 % ± 8.1 % and 31.4 % ± 5 %, respectively, of that at time 0 h (mean ± S.D.) (Figure 6.6a).

In the free rhEGF Groups (Groups 4 and 5), there were no significant effects on wound re-epithelialisation (p > 0.05), and neither resulted in total wound re-epithelialisation. Wound areas, at 64 h, were 5.6 % ± 11.3 % and 23.4% ± 21.4 %, of the total wound area at time 0 h, for the 10 μg/mL rhEGF, and 1 μg/mL rhEGF Groups, respectively (mean ± S.D.) (Figure 6.6b).

In the dextrin-rhEGF conjugate Study Groups (Groups 6 to 8), there was failed re-epithelialisation, in the absence of physiological concentrations of α-amylase (Group 6), with an abrasion of 23.4% ± 5.5% of that at time 0, persisting at 64 h (mean ± S.D.). This was not significantly different to the SFM control (Group 1) (p > 0.05). Upon the addition of α-amylase (93 i.u./L), there was a significant decrease in the wound area, at 24 h, in both the 1 μg/mL rhEGF equivalent (Group 7) and 10 μg/mL rhEGF equivalent (Group 8) Groups (p = 0.0004). The dextrin-rhEGF conjugate was significantly more effective, at decreasing the wound area, at 24 h, at the lower dose (1 μg/mL rhEGF equivalent), than at the higher dose (10 μg/mL rhEGF equivalent) (p = 0.0067) (Figure 6.6c).

6.3.2 Wound fluid analysis

6.3.2.1 Protein content determination

The protein contents of the acute (4.76 ± 0.89 mg/mL) and chronic wound fluid (1.27 ± 0.35 mg/mL) samples (n = 5 patients for both; mean ± S.D.), were significantly higher in the acute wound fluid specimens (p < 0.0001, n = 5). The

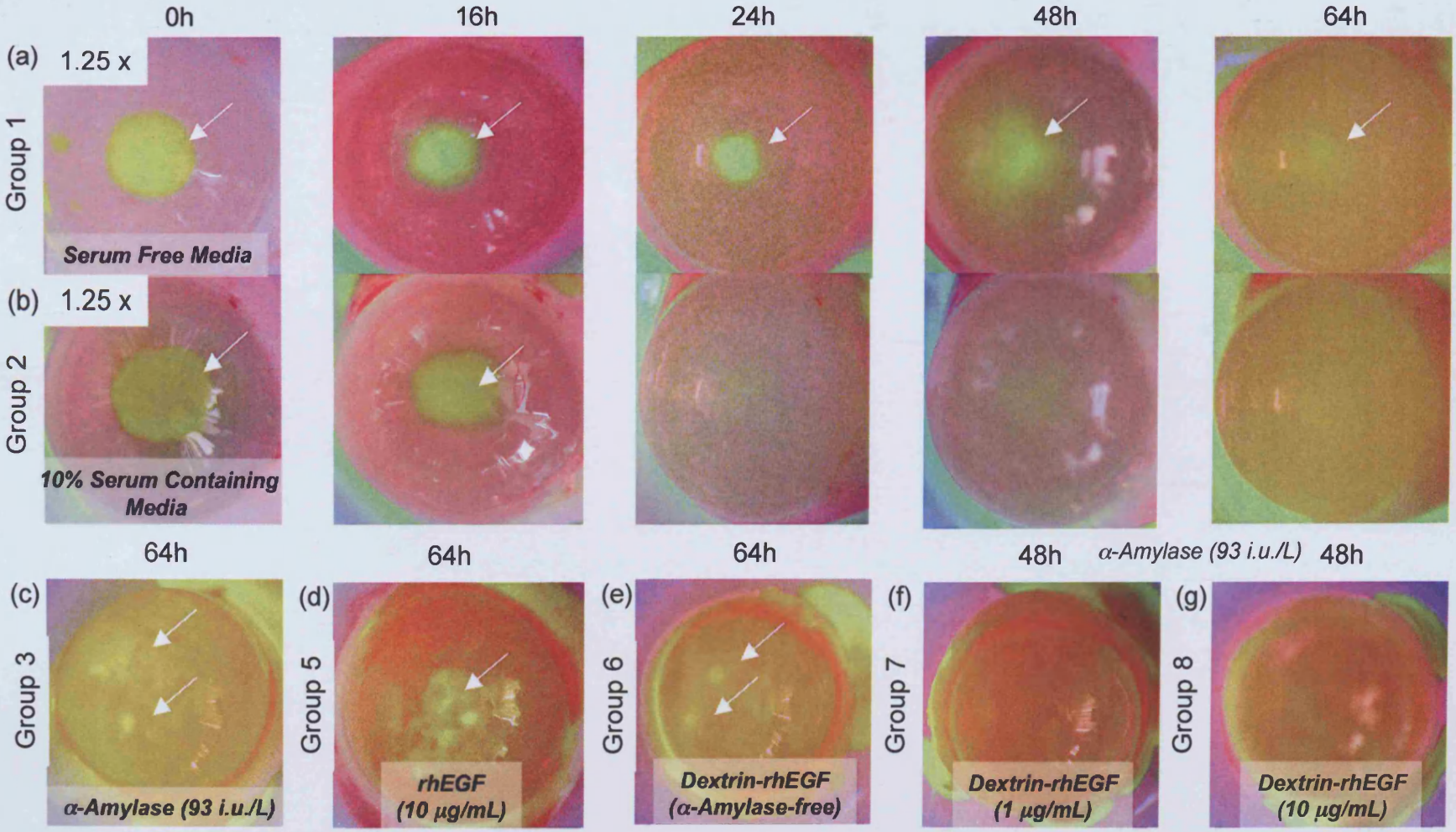

Figure 6.5 **Fluorescein staining of the *ex vivo* corneal abrasion.** Panel (a) shows a typical corneal abrasion, serially stained with fluorescein (arrowed) over a 64 h period, in serum free media. Panel (b) shows the corneal abrasion, healing in response to 10% serum containing media, over a 64 h period. Panels (c-e) show the persistence of the abrasion (arrowed) at 64 h in response to α-amylase (93 i.u./L), free rhEGF (10 μg/mL), and dextrin-rhEGF (α-amylase-free) respectively. Panel (f) shows the corneal abrasion healed, at 48 h, in response to α-amylase (93 i.u./L) exposed dextrin-rhEGF (1 μg/mL rhEGF equivalent) and panel (g) shows the corneal abrasion healed, at 48 h, in response to α-amylase (93 i.u./L) exposed dextrin-rhEGF (10 μg/mL rhEGF equivalent).

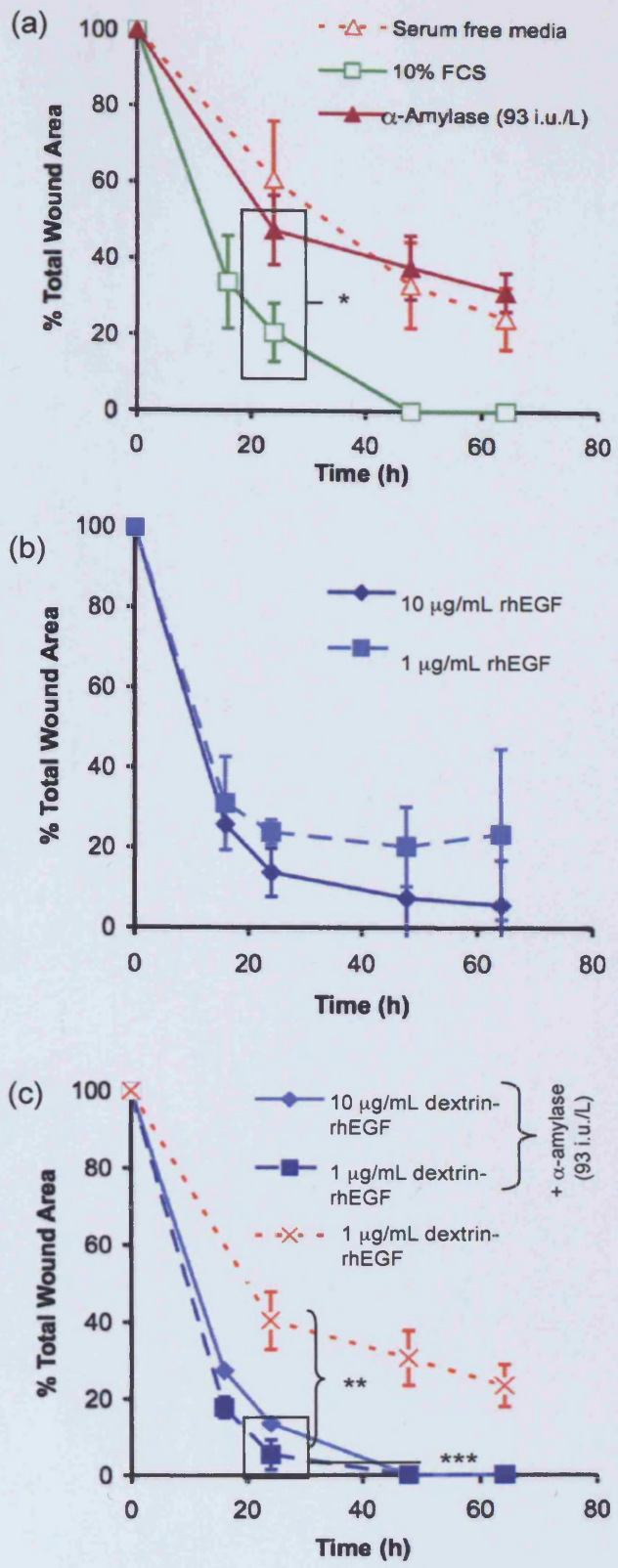

Figure 6.6 ***Ex vivo* corneal wound healing.** Panel (a) shows corneal wound closure in response to controls (Groups 1-3) (* $p = 0.0098$). Panel (b) shows corneal wound healing, in response to epidermal growth factor (rhEGF) (Groups 4 and 5), with no significant difference in efficacy ($p > 0.05$). Panel (c) shows corneal wound healing, in response to dextrin-rhEGF, in the presence and absence of α-amylase (93 i.u./L) (Groups 6-8) (** $p = 0.0004$, *** $p = 0.0067$).

protein contents, α-amylase activity and elastase activity of each acute and chronic wound fluid sample, is summarised in Table 6.1.

6.3.2.2 α-Amylase activity assay

α-Amylase was observed to be present in all samples of acute and chronic wound fluid. There was significantly greater activity in acute wound fluid samples, than the chronic wound fluid samples ($p < 0.0001$). There was also greater variation in activity in the acute wound fluid samples, with an average activity of 188 ± 73 i.u./L (n = 5, mean ± S.D.). The chronic wound fluid samples had an average α-amylase activity of 52 ± 5 i.u./L (n = 5, mean ± S.D.) (Figure 6.7). When the α-amylase activity was calculated per mg of protein, there was no significant difference between the acute (208 ± 88 i.u./L, mean ± S.D.) and chronic (217 ± 67 i.u./L, mean ± S.D.) wound fluid samples ($p > 0.05$).

6.3.2.3 Elastase activity assay

There was no elastase activity observed in any of the acute wound fluid samples examined. Elastase activity was detected in the chronic wound fluid samples, with a mean activity of 2.1 ± 1.2 RFU/min (n = 5, mean ± S.D.). When activity was calculated per mg of protein analysed, the mean activity was 17 ± 8.8 RFU/min/mg protein (n = 5, mean ± S.D.). (Table 6.1). The mean activity at 1 h was 126 ± 74 RFU, which equated to an average elastase activity of 0.004 ± 0.002 U/mL, or an average elastase concentration of 30 ± 18 ng/mL.

6.3.2.4 EGF content of wound fluids

EGF was not detected by ELISA in any chronic wound fluid samples examined (limit of detection is approximately 3.9 pg/mL human EGF). In the acute wound fluid samples, EGF was detected in all samples, except patient 1 (Figure 6.8a), with an average of 34 ± 22 pg/mL (n = 4, mean ± S.D.).

6.3.2.5 rhEGF and dextrin-rhEGF stability, in chronic wound fluid

When rhEGF and the dextrin-rhEGF conjugate were exposed to chronic wound fluid (Patient C; elastase activity = 30.7 RFU/min/mg protein), over a 72 h period, rhEGF was degraded. As such, rhEGF was undetected by the polyclonal,

Table 6.1 Wound fluid analysis - α-amylase and elastase contents

Wound fluid	Patient	Protein content (mg/mL) (mean ± S.D.)	α-Amylase activity (i.u./L) (mean ± S.D.)	α-Amylase activity / mg protein (i.u./L/mg)* (mean ± S.D.)	Elastase activity at 60 min (RFU)	Elastase activity (RFU/min) (mean ± S.D.)	Elastase activity / mg protein (RFU/min/mg)** (mean ± S.D.)
ACUTE	1	4.28 ± 0.05	172 ± 19	201 ± 22	NO ELASTASE ACTIVITY DETECTED		
	2	4.13 ± 0.16	166 ± 34	201 ± 41			
	3	4.47 ± 0.12	256 ± 27	286 ± 30			
	4	4.57 ± 0.10	261 ± 35	286 ± 38			
	5	6.33 ± 0.13	83 ± 39	66 ± 30			
CHRONIC	A	1.42 ± 0.01	48 ± 2	168 ± 7	116	1.93 ± 0.18	13.7 ± 1.3
	B	1.15 ± 0.07	51 ± 4	221 ± 17	82	1.37 ± 0.37	11.8 ± 3.2
	C	1.40 ± 0.14	55 ± 5	195 ± 18	257	4.28 ± 0.54	30.7 ± 3.9
	D	1.67 ± 0.05	57 ± 3	169 ± 9	85	1.42 ± 1.24	8.5 ± 7.5
	E	0.74 ± 0.02	49 ± 8	332 ± 55	91	1.52 ± 0.31	20.3 ± 4.2

* Measured using 200 μL samples ** Measured using 100 μL samples

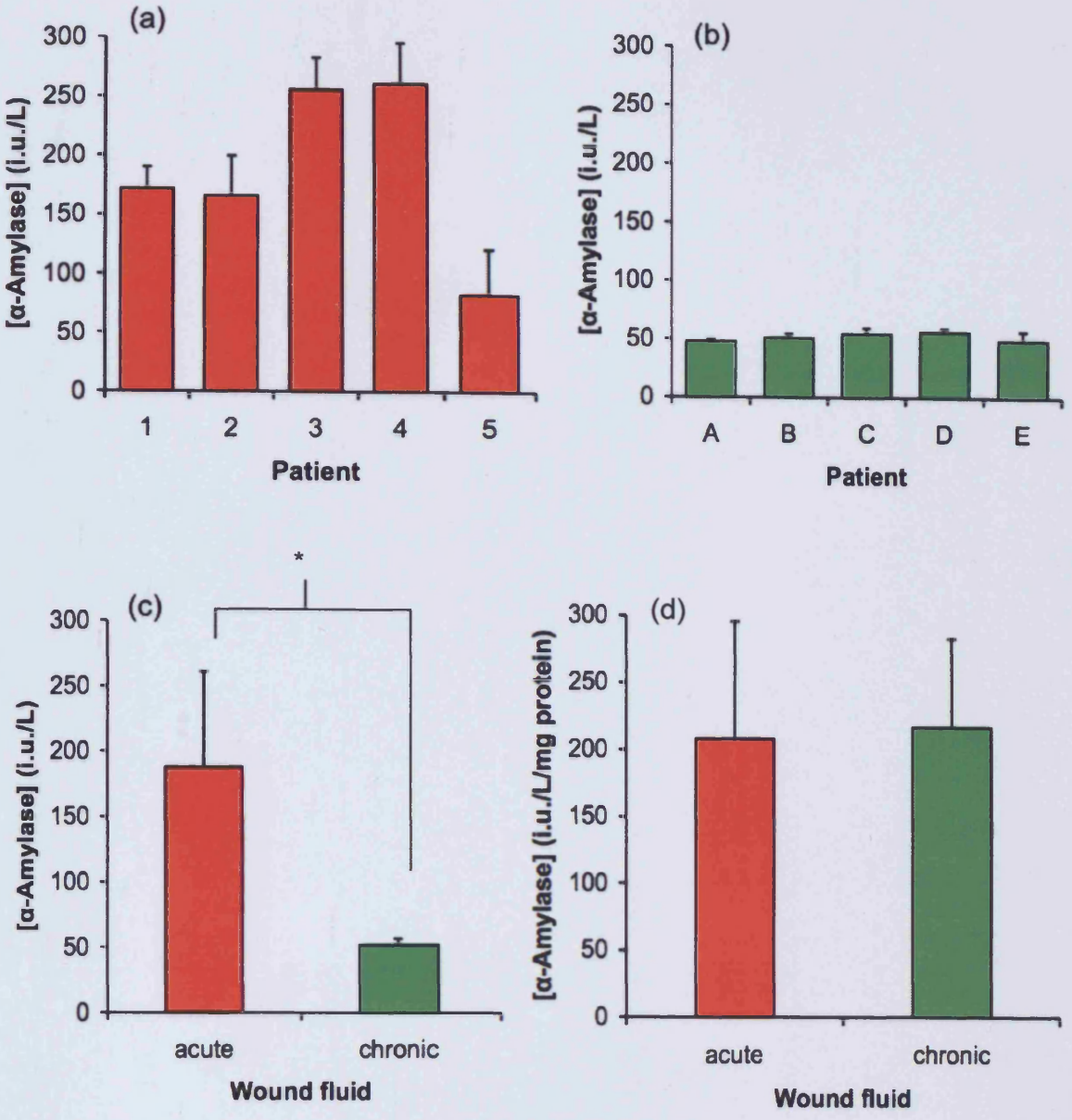

Figure 6.7 ***Ex vivo* wound fluid analysis.** Panel (a) shows the activity of α-amylase in samples of acute wound fluid, from mastectomy patients (n = 5, mean ± S.D.). Panel (b) shows the α-amylase activity in samples of chronic wound fluid, derived from venous leg ulcers (n = 5, mean ± S.D.). Panel (c) shows a significant difference between the α-amylase activity in acute and chronic wound fluids (mean ± S.D., * $p < 0.0001$, Student's t-test). Panel (d) shows α-amylase activity, when corrected for protein content (mg), with no significant difference ($p > 0.05$) between acute and chronic wound fluid samples (mean ± S.D.).

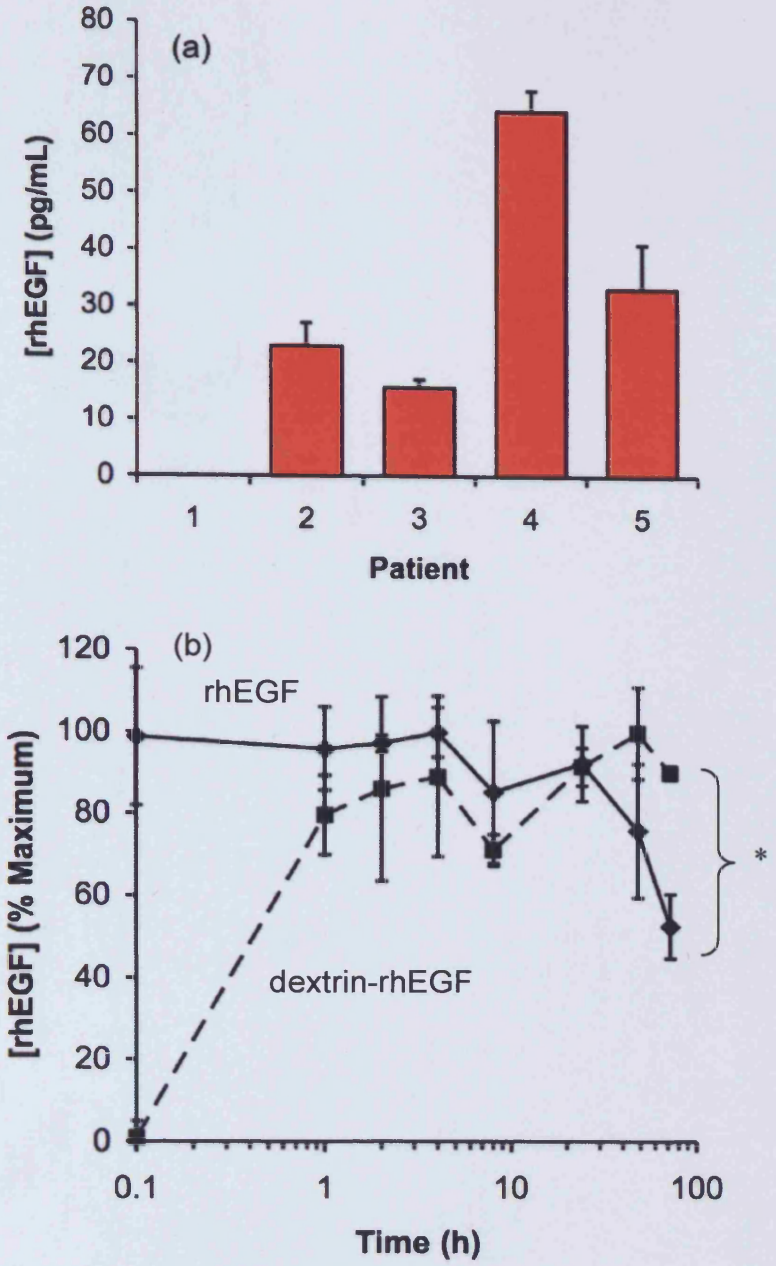

Figure 6.8 **EGF, rhEGF and dextrin-rhEGF conjugate stability in wound fluid.** Panel (a) shows the concentration of EGF in acute wound fluid samples (n = 5, mean ± S.D.). Panel (b) shows the stability of free rhEGF and dextrin-rhEGF in chronic wound fluid (Patient C), as a percentage of the maximum concentration of rhEGF, over time (mean ± S.D.). There was a significant difference in the amounts of rhEGF detected at 72 h, between free rhEGF and rhEGF, released from the dextrin-rhEGF conjugate (* $p = 0.0013$, Student's t-test).

anti-EGF ELISA, with 52.7% of the maximum concentration of rhEGF remaining, at 72h ($T_{1/2}$ is approximately 76 h) (Figure 6.8b). The dextrin-rhEGF conjugate was degraded by endogenous α-amylase within the chronic wound fluid sample (195 i.u./L/mg protein), releasing rhEGF that was detectable by ELISA, resulting in a maximal rhEGF concentration, at 48 h (Figure 6.8c). There was a significant increase in rhEGF concentration in the chronic wound fluid, following rhEGF release from the dextrin-rhEGF conjugate, after 72 h, compared to free rhEGF ($p = 0.0013$).

6.4 Discussion

This Chapter aimed to establish an *ex vivo* model of wound healing in the rat cornea, and assess the ability of rhEGF and the dextrin-rhEGF conjugate to promote wound healing. Samples of acute and chronic wound fluid were also collected and analysed for α-amylase and elastase activity.

6.4.1 Corneal re-epithelialisation

The *ex vivo* model of corneal wound healing, established herein, was sensitive to stimulation by FCS and by rhEGF (in the form of the dextrin-rhEGF conjugate). Although, it was a model of acute wound healing, rather than impaired, chronic wound healing, valuable information about the efficacy of the dextrin-rhEGF conjugate was provided. In the conjugated form, the rhEGF promoted a significant increase in the rate of corneal wound healing, with wound closure by 48 hours, compared to free rhEGF, which, although was more effective than rhEGF-free controls, did not always permit wound closure, by 64 hours. As was shown *in vitro* (Chapter 4), in both the cellular proliferation and migration assays, the ability of conjugation to "mask" the activity of the rhEGF, was reproducible in this *ex vivo* model. With the addition of exogenous α-amylase, at physiological concentrations, rhEGF was released, or "unmasked" from the polymer, thereby restoring bioactivity.

The increased efficacy of the dextrin-rhEGF conjugate, in enhancing corneal wound healing, may be due to the sustained release phenomena (Chapter 4). In the *ex vivo* model described herein, the rhEGF was applied as a single dose at the outset of the experiment, and the free rhEGF may have been degraded, due to the short half-life of EGF. The half-life of EGF in the cornea (rabbit) is 78 minutes (Chan *et al*, 1991), which is identical to the plasma elimination half-life (rat) (Kuo *et al*, 1992).

In the *ex vivo* organ culture model, the pharmacokinetics of EGF will differ, but the sustained release of rhEGF, from the α-amylase-mediated, degradation of the dextrin-rhEGF conjugate ($T_{1/2}$ = 55.4 hours, Chapter 3), may account for the enhanced wound healing in the dextrin-rhEGF Study Groups.

This *ex vivo* model was reproducible and allowed the assessment of the Study compounds. Although, it did not mimic the corneal environment as closely as air-fluid interface models, with topical tear-flow and controlled anterior chamber pressure (Zhao *et al*, 2006), it did allow an effective evaluation of acute wound healing. With complete wound closure, at approximately 48 hours, in the dextrin-rhEGF Study Groups, the rate of wound closure is similar to that observed *in vivo* (Pfister, 1975; Kuwabara *et al*, 1976; Matsuda *et al*, 1985; Crosson *et al*, 1986).

The injured corneal epithelium is sensitive to rhEGF stimulation (Pastor and Calonge, 1992; Lu *et al*, 2001; Hori *et al*, 2007), and therefore, this *ex vivo* model is suited to the evaluation of the dextrin-rhEGF conjugate. There are no reported *ex vivo* models of a chronic corneal abrasion, or ulcer. Thus, the present evaluation had to be performed in an acute wound healing model.

6.4.2 Wound fluid analysis

The acquisition of acute and chronic wound fluid samples, by standard clinical collection techniques, allowed the quantification of α-amylase activity within these fluids. There are no published reports of α-amylase activity within such body biofluids. In the pre-clinical development of the dextrin-rhEGF conjugate, degradation studies have involved the use of physiological levels of α-amylase (typically 93 i.u./L), based upon published serum α-amylase concentrations (Raftery, 1998; Branca *et al*, 2001). Serum α-amylase activity can vary greatly, especially in the presence of diseases, such as acute pancreatitis or a perforated peptic ulcer (Raftery, 1998).

The α-amylase activity in acute wound fluids was within the normal serum range (50-300 i.u./L). The α-amylase activity in chronic wound fluids was significantly reduced, but this may be due to a dilution effect of the collection technique, resulting in a lower protein content in the chronic wound fluids, when compared to acute wound fluids (Moseley *et al*, 2004). The protein concentrations of wound fluids from non-healing wounds is lower than that from healing wounds

(James *et al*, 2000), but the elution of the saturated dressings into a buffer, may have further resulted in a reduced total protein content. When α-amylase activity was corrected for protein content, there was no significant difference in the α-amylase activity between the acute and chronic wound fluid samples. The corrected α-amylase activity, in chronic wound fluids was higher than the majority of the α-amylase (93 i.u./L) used in the present investigation of the PUMPT concept. In can, therefore, be inferred that similar degradation results would be expected to be observed *in vivo*, to those observed *in vitro* (Chapters 3 and 4).

Elastase activity was below the limit of detection in all of the acute wound fluid samples analysed. This was also observed by Trengove *et al* (1999). There was a large variation in the elastase activity in the chronic wound fluids, in agreement with previous reports (Trengove *et al*, 1999; Cullen *et al*, 2002). The elastase activity reported in this Chapter (8.5 – 30.7 RFU/min/mg protein) is significantly less than reported by Cullen *et al* (2002) (13 – 49,456 RFU/min/mg protein), despite similar wound fluid collection and elastase assay protocols, being employed. When the elastase activity in the chronic wound fluid samples was referred to a standard calibration curve, the average concentration of elastase reported in this Chapter (30 ng/mL), was much lower than that reported by Trengove *et al* (1999) (100,000 ng/mL), although, in this incidence, different wound fluid collection and elastase assay techniques were utilised. Therefore, these results may not be directly comparable. Wound fluid composition is variable, and can be influenced by the presence of infection and the pathogenesis and duration of the wound (Yager *et al*, 2007).

To assess the stability of rhEGF and the dextrin-rhEGF conjugate, in a chronic wound environment (Section 3.2.7), the highest reported concentration of neutrophil elastase was utilised (100,000 ng/mL). The dextrin-rhEGF conjugate was shown to be more resistant to proteolytic degradation ($T_{1/2}$ > 24 hours), compared to free-rhEGF ($T_{1/2}$ < 2 hours) (Section 3.3.4). On exposure to chronic wound fluid, free rhEGF was degraded, but in slower manner ($T_{1/2}$ was approximately 76 hours) than when exposed to exogenous neutrophil elastase ($T_{1/2}$ < 2 hours). α-Amylase activity in chronic wound fluids was great enough to permit degradation of the dextrin-rhEGF conjugate and release rhEGF, which remained stable in the chronic wound fluid. This was evident by a significant increase in rhEGF at 72 hours from

Chapter Seven: Dextrin-rhEGF Conjugate Evaluation in an *In Vivo* Model of Impaired Wound Healing

Contents

7.1 Introduction

Many *in vivo* models of wound healing, both acute and chronic, have been reported in the literature (Kiritsy *et al*, 1993; Davidson, 1998). These have involved various species of animal and have been used in evaluation of different growth factors, in the dermal wound healing process (Kiritsy *et al*, 1993; LeGrand, 1998). In this Chapter, *in vivo* models will be reviewed, as will previous studies involving epidermal growth factor (EGF), while the model employed for the evaluation of the dextrin-rhEGF conjugate will be described.

7.1.1 *In vivo* models of wound healing

7.1.1.1 Acute wound healing models

In vivo models of acute wound healing involve the introduction of an injury and a relatively rapid course of repair. These are designed to mimic the response to injury, after surgery or trauma (Davidson, 1998). Incisional wounds can be produced with a surgical scalpel, laser or electrocautery, with minimal collateral damage. The wounds can then be closed by mechanical means (e.g. surgical sutures), referred to as primary closure, or left open to heal by secondary closure. Excisional wounds involve the removal of a volume of the target tissue, which can subsequently heal by secondary closure (Davidson, 1998). The larger wound void, when compared to incisional wounds, affords greatest ability to analyse material for biochemical or histological analysis. Experimental wounds can be covered by an occlusive dressing, allowing the collection of wound fluids. Examples of such excisional wounds (from superficial to deep), include the stripping of the epidermis, with adhesive tape (Tammi *et al*, 2005); the formation of sub-epidermal blisters, by mechanical suction devices, chemicals or heat (Saarialho-Kere *et al*, 2002); partial thickness (split thickness) dermal injury, by shaving with a blade or dermatome, or by chemical or thermal means (Davis *et al*, 2007); or full-thickness, dermal injury, by complete full-thickness excision of an area of skin with a blade or dermatome (Nanney *et al*, 2008).

In animals with skin that has a *panniculus carnosus* (a muscular layer underneath and attached to the skin, e.g. rodents, rabbits, guinea pigs), excisional wounds can be splinted open, to reduce the effect of contraction on wound healing (Michaels *et al*, 2007). Contraction is the centripetal movement of the wound margins, due to the compaction of granulation tissue, within the "body" of the wound (Farahani and Kloth, 2008). Contraction involves the rapid shrinkage of the wound

area by the loose skin, reducing the need for re-epithelialisation, as is found in tight-skinned species (e.g. pig, human). It must be differentiated from contracture, which is a myofibroblast-induced, pathological process, involved in hypertrophic scarring (Shin and Minn, 2004). Other models of acute wound healing, include dead-space models, which can be used to investigate subcutaneous wound healing; wound chambers to allow continuous analysis of wound progression, and burns, produced by chemical or thermal means (Davidson, 1998).

7.1.1.2 Impaired / chronic wound healing models

The chronic non-healing wound is uncommon in laboratory animals. As such, there is no accurate animal model corresponding to the chronic skin wounds in humans (venous leg ulcer or diabetic foot ulcers), due to anatomical, postural, age and cultural conditions, only found in humans. Human cutaneous anatomy is also markedly different from most laboratory species, except the pig (tight-skinned, with strong fascial attachment). Whilst many animal models have been employed, the majority of models of non-healing wounds are impaired or delayed acute wound healing models (Davidson, 1998).

7.1.1.3 Impaired wound healing

Impaired wound healing can be induced in experimental animals by metabolic defects, such as chemically induced diabetes mellitus, via streptozotocin or alloxan administration; or by genetic diabetes (db/db), or obesity (ob/ob) (Goodson and Hunt, 1979a; Klingbeil *et al*, 1991; Tsuboi *et al*, 1992). Malnutrition, such as vitamin A, vitamin C, or zinc-deficiency, has also been investigated in the rat and guinea pig (Levenson and Demetriou, 1992). Immunosuppression, via the administration of corticosteroids, or genetically immunodeficient rodent strains (severe combined immune deficiency (SCID), nude mouse/rat), can further be used to suppress the wound healing response, or to allow human xenografting, to produce a humanised skin model (Escamez *et al*, 2004; Garcia *et al*, 2007). Antiproliferative chemotherapeutic agents (adriamycin, hydroxyurea), can impair wound healing, by direct inhibition of cellular proliferation, or by indirect action on the propagation of immune cells (Winn *et al*, 1987; Curtsinger *et al*, 1989; Pearse and Sylvester, 1992). Radiation, either locally or total body irradiation, can also reduce local or systemic populations of cells, critical for wound repair (Cromack *et al*, 1993). Local infection,

with bacterial suspensions of between 10^6 and 10^9 colony-forming units/g, have also been used to retard wound healing (Heggers *et al*, 1992).

7.1.1.4 Chronic wound healing

In vivo models of chronic wound healing cannot accurately represent the venous ulcer or diabetic ulcer, but the ischaemia associated with all of the pathologies underlying chronic wounds, can be simulated. Cutaneous ischaemia has been demonstrated in the guinea pig, using a skin banding technique (Constantine and Bolton, 1986; Skrabut *et al*, 1996). Other models of ischaemia have involved vascular ligation, e.g. the rabbit ear model (Ahn and Mustoe, 1990; Mustoe *et al*, 1991), and skin flap techniques (McFarlane *et al*, 1965; Quirinia *et al*, 1992; Chen *et al*, 1999). Pressure sores have also been modelled in multiple species (Hyodo *et al*, 1995; Salcido *et al*, 2006). In addition to necrosis caused by local ischemia, chemicals can induce local skin necrosis and ulceration. Doxorubicin is a chemotherapeutic agent that can cause ulceration (Rudolph *et al*, 1979), and Brown Recluse spider (*Loxosceles* spp.) venom contains sphingomyelinase, which can induce dermal necrosis (Davidson, 1998). The various *in vivo* models available, are summarised in Table 7.1.

7.1.2 The genetically diabetic (db/db) mouse

Venous leg ulcers and diabetic foot ulcers are a significant cause of morbidity in the elderly population (Price and Harding, 2004). However, these pathological processes have no animal equivalent. The genetically diabetic mouse, although a model of impaired acute wound healing, can exhibit delayed healing in skin wounds, similar to that found in patients with diabetes, so offers a useful model for studying wound repair (Kawanabe *et al*, 2007).

The genetically diabetic mouse was developed by Hummel *et al* (1966), by discovering a Lepr db mutation on a C57BLKS background. It experiences a hyperinsulinaemic phase, followed by a hypoinsulinaemic phase, at 2 - 3 months of age. The homozygous diabetic mouse (db/db) is also obese and has several advantages as a compromised wound healing model. The heterozygous littermates do not exhibit either diabetes or obesity. The homozygous animals develop many of the clinical and metabolic symptoms that resemble human adult onset diabetes, including

Table 7.1 ***In vivo*** **animal models of wound healing**

Acute Wound Healing	Impaired Wound Healing	Chronic Wound Healing
Incisional - Primary closure (a) - Secondary closure (b) Excisional - Split thickness (c) - Full thickness (d) Dead space models - Sub-cutaneous healing (e) Wound chambers - Serial measurements Burns (f) - Chemical - Thermal (hot/cold)	*Metabolic defects* - Chemical diabetes - Genetic diabetes - Obesity - Malnutrition Immune system - Corticosteroids - SCID / nude mouse - Chemotherapeutics - Radiation - Local infection	*Ischaemia* - Vessel ligation - Skin banding - Skin flaps Pressure sores - Friction - Mechanical loading - Plaster casts Dermonecrosis - Doxorubicin - Spider venom

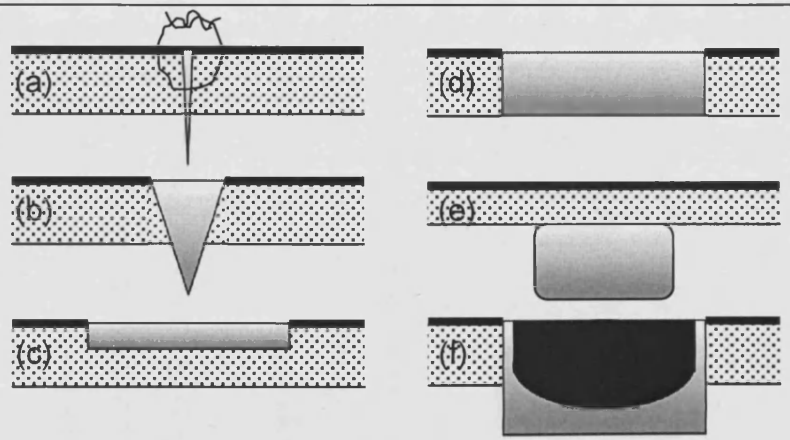

(a) - (f) Schematic diagrams of acute wounding procedures, which can be extended into impaired healing and chronic wound healing animal models. Adapted from Davidson, 1998.

peripheral neuropathy, microvascular lesions, basement membrane thickening, glomerular filtration abnormalities, immune complex deposition, immunodeficiency, obesity, and severe hyperglycemia (Coleman *et al*, 1982). In addition, the full-thickness wounds in these mice exhibit a marked delay in inflammatory cell infiltration, granulation tissue formation and wound closure, when compared with their non-diabetic counterparts (Greenhalgh *et al*, 1990).

The spontaneous diabetic mouse has advantages over drug-induced diabetes (as mentioned earlier), which utilize steroids or cytotoxic agents, such as alloxan or streptozotocin, to induce the diabetic state, as these can be toxic, not only to the pancreatic beta cells, but also the urinal tubules, liver and exocrine pancreas (Rerup, 1970). In addition, alloxan and streptozotocin alter macrophage phagocytosis and depress T-cell function (Goodson and Hunt, 1979b).

Limitations of the db/db model, include the presence of the *panniculus carnosus* and predilection for wound closure by contraction, rather than re-epithelialisation, and the underlying pathophysiology of the diabetes contrasts with the human. These animals are not only hyperglycemic, but also hyperinsulinaemic, which is dissimilar to what is observed in human diabetes, with respect to insulin. Often, human diabetics are hypoinsulinaemic. Elevated levels of insulin within the wound fluid of these mice could potentially interact with other exogenous growth factors, to yield different effects than those observed with growth factors alone (Kiritsy *et al*, 1993).

The role of EGF in cutaneous wound healing in the diabetic mouse has been studied by Choi *et al* (2008) (streptozotocin-induced diabetes), and the efficacy of exogenous EGF to promote wound healing in the db/db mouse has not been shown to be significant, whilst other growth factors, such as platelet-derived growth factor (PDGF) and transforming growth factor-α (TGF-α), have been shown to improve wound healing in the db/db mouse (Brown *et al*, 1994). Examples of studies involving the db/db mouse, are summarised in Table 7.2.

7.1.3 *In vivo* animal studies involving EGF

EGF has been applied to wounds in various *in vivo* models of wound healing. Franklin and Lynch (1979), applied EGF suspended in a saline-albumin / Aquaphor ointment, to an acute wound in rabbit ears, and demonstrating apparent improvement

Table 7.2 ***In vivo*** **studies involving the genetically diabetic (db/db) mouse model**

Study	Active agent	Age (weeks)	Dressing	Application	Dosing Regimen
Greenhalgh *et al*, 1990	Platelet-derived growth factor (PDGF-BB), fibroblast growth factor (FGF)	8 - 12	OpSite®	Injection through dressing	Days 0 - 5 Sacrificed day 14
Brown *et al*, 1994	PDGF-BB, epidermal growth factor (EGF*), transforming growth factor-β (TGF-β)	8 - 12	OpSite®	Injection through dressing	Days 0 - 4 Sacrificed day 21
Ishikawa *et al*, 2003	EGF-fibronectin collagen binding domain	9 - 11	Bioclusive®	Injection through dressing	Days 0 and 3 Sacrificed day 6
Kirchner *et al*, 2003	Vascular endothelial growth factor (VEGF)	8 - 12	OpSite®	Injection through dressing	Days 0 - 4 Sacrificed day 21
Deiters *et al*, 2004	Macrophage-activating lipopeptide-2 (MALP-2)	12 - 15	Hydrofilm®	Injection through dressing	Single dose day 0 Sacrificed day 25
Kawanabe *et al*, 2007	Sphingosine-1-phosphate	8 - 10	None	Peripheral intradermal injection	Daily for 13 days Sacrificed day 14
Pietramaggiori *et al*, 2008 * 10 μg/mL	Poly-*N*-acetyl glucosamine	8 - 12	Microalgal nanofibre patch	Patch applied to wound	Patch for 1h or 24h per day Sacrificed day 10 or 21

in wound healing and scar maturation. A sustained-release EGF pellet was subcutaneously implanted into Sprague-Dawley rats (Buckley *et al*, 1985), leading to an increase in granulation tissue and collagen synthesis, in this acute wound model. Mustoe *et al* (1991), in an acute wound healing model in rabbit ears, demonstrated that EGF significantly promoted re-epithelialisation. The first Study involving EGF, in the db/db mouse, did not show any efficacy in wound closure (Brown *et al*, 1994). This may be due to growth factor instability in the *in vivo* diabetic wound. Different vehicles have been used to optimise EGF-delivery to acute wounds, such as gelatins (Ulubayram *et al*, 2001; Tanaka *et al*, 2005), petroleum-based ointments (Kwon *et al*, 2006), chitosan (Alemdaroglu *et al*, 2006), liposomes (Alemdaroglu *et al*, 2008), and nanofibres (Choi *et al*, 2008), using rat, rabbit, dog and diabetic mouse models (summarised in Table 7.3).

Dextrin conjugates have not been tested *in vivo,* in animal wound healing models, to date. The dextrin-rhEGF conjugate was applied topically (dissolved in phosphate buffered saline (PBS), to excisional wounds in genetically diabetic mice in the present Study. Although EGF application has only been reported in this model once before, and the impaired acute wound of the mouse is substantially different from a human chronic ulcer, it is a robust model for evaluation, prior to clinical trials. Indeed, the pre-clinical assessment of the recombinant human platelet-derived growth factor (rhPDGF) containing gel, Regranex® (Johnson & Johnson, Gargrave, UK), involved the genetically diabetic (db/db) mouse (Brown *et al*, 1994; LeGrand, 1998).

In the present Study, dextrin-rhEGF conjugate application was by injection through an occlusive wound dressing onto the wound bed, at delayed intervals, due to the sustained release nature of the conjugate. Unmodified rhEGF was used in one of the Control Groups, at the same 1 μg per dose, as per Brown *et al* (1994). The dextrin-rhEGF was also applied at a 1 μg per dose, and also at a 0.1 μg per dose, to examine the increased efficacy at a lower dose, as was highlighted in previous *in vitro* Studies (Chapter 4), and *ex vivo* Studies (Chapter 6). The presence of α-amylase in mouse serum was further established, in order to "unmask" the dextrin-rhEGF conjugate. Mouse plasma was also analysed, to investigate any systemic absorption of rhEGF, from these topical applications.

Table 7.3 ***In vivo*** **assessment of epidermal growth factor (EGF), utilising various animal wound healing models**

Study	Animal	Vehicle	EGF dose	Wound	Dressing	Dosing Regimen
Franklin & Lynch, 1979	Rabbit (acute wound)	Ointment (Aquaphor, saline-albumin)	0.5 μg/mL	Full thickness 20 - 30 mm diameter (314 mm^2 - 700 mm^2)	Not reported	Every 12h Sacrificed day 42
Buckley *et al*, 1985	Sprague-Dawley rat (acute wound)	Cholesterol-methylcellulose-lactose pellets	10 - 20 μg/day	Subcutaneous implantation	N/A	Single dose Sacrificed day 3, 7 or 14
Mustoe *et al*, 1991	Rabbit (acute wound)	Bovine collagen suspension	5 μg per dose	Full thickness 6 mm diameter (10 mm^2)	Tegaderm® applied over wound	Single dose Skin biopsy day 7
Brown *et al*, 1994	Genetically diabetic (db/db) mouse (impaired wound)	5 % poly-ethylene glycol solution	1 μg per dose	Full thickness 15 x 15 mm (225 mm^2)	OpSite® Injection through dressing	Days 0 - 4 Sacrificed day 21
Ulubayram *et al*, 2001	Rabbit (acute wound)	Gelatin microspheres	0.5 or 7.5 μg per dose	Full thickness 8 mm diameter (50 mm^2)	Gelatin applied to wound and covered with OpSite®	Every 12h Sacrificed day 7, 14 or 21
Tanaka *et al*, 2005	Hairless dog (acute wound)	Gelatin film	18 μg per dose	Partial thickness 30 x 30 mm (900 mm^2)	Gelatin film covered with Perme-Aid®	Daily for 15 days Skin biopsy day 30
Alemdaroglu *et al*, 2006	Sprague-Dawley rat (acute wound)	Chitosan gel	10 μg/mL	Partial thickness burn 20 mm diameter (314 mm^2)	Chitosan gel	Daily for 14 days Skin biopsy day 3, 7 or 14

7.1.4 Experimental aims

The activity and mechanisms of action of the dextrin-rhEGF conjugate, has previously been confirmed *in vitro* (Chapters 4 and 5) and *ex vivo* (Chapter 6). The next stage of the pre-clinical evaluation was the assessment of the dextrin-rhEGF conjugate *in vivo*, in a model of impaired dermal wound healing.

The aims of this Chapter were the:

1. Quantification of α-amylase in mouse serum.
2. Establishment of an *in vivo* model of impaired dermal wound healing, utilising the db/db mouse model.
3. Evaluation of the dextrin-rhEGF conjugate *in vivo*, via gross wound and histological image analysis.
4. Determination of systemic rhEGF absorption *in vivo*.

7.2 Methods

7.2.1 Animal husbandry

70 male diabetic mice (C57BLKs/Bom db/db), aged approximately 12-13 weeks, were used in this Study. On arrival in the UK, the mice were housed in Groups of 4 to 5 animals, according to Home Office Regulations. On experimental wounding, animals were housed in individual cages (cage dimensions 35 x 15 x 15 cm, with sawdust bedding, changed twice weekly), in an environment maintained at an ambient temperature of 23°C, with 12-hour light/dark cycles. Mice were provided with food (Standard Rodent Diet, B&K Universal, Grimston, UK) and water *ad libitum*. To acclimatise the animals to their surroundings, prior to experimentation, animals were housed for a period of 5 days without disturbance, other than to refresh their bedding and to replenish their food and water provisions. Following all anaesthetic events, animals were placed in a warm environment and monitored until fully recovered from the procedure. All animal procedures were carried out in a Home Office Licensed Establishment, under Home Office Licences (PCD: 50/2505; PPL: 40/2650; PIL: 50/3482; PIL: 70/4934; PIL:40/7904). The health of animals was monitored on a daily basis, throughout the Study.

7.2.2 Creation of full-thickness excisional wounds

On day 0, animals were anaesthetised (isofluorane and air, National Vet Services, Stoke-on-Trent, UK) and the dorsum shaved and cleaned, with saline-soaked gauze. A single, standardised full-thickness wound (10 mm x 10 mm), was created in the left dorsal flank skin of each experimental animal. Wounds in all treatment Groups were subsequently dressed with a circumferential band of the film dressing, Bioclusive® (Figure 7.1). This was performed by Dr. Jeff Hart (Cica Biomedical, Knaresborough, UK).

7.2.3 Application of Study compounds

Animals were assigned to each Study Group, which received treatments (100 μL, day 0), solublised in PBS. All treatments were administered through the Bioclusive® film, using a 27-gauge needle (Tyco Healthcare, Gosport, UK).

- Group 1 received the free succinoylated dextrin polymer (50 μg/mL, 10 animals).
- Group 2 received rhEGF (10 μg/mL, 10 animals).
- Group 3 received the dextrin-rhEGF conjugate (1 μg/mL rhEGF equivalent, 10 animals).
- Group 4 received the dextrin-rhEGF conjugate (10 μg/mL rhEGF equivalent, 20 animals).
- Group 5 (no treatment) were dressed with Bioclusive® alone (20 animals).

Animals in all Groups were re-anaesthetized, their film dressings and any free debris removed, and their wounds cleaned, using saline-soaked sterile gauze on post-wounding, day 3. Following photography (see below), animals in all Groups were re-dressed with a circumferential band of Bioclusive® and the treatments reapplied, as a 100 μL injection through the Bioclusive® dressing. On post- wounding, day 8, animals from all Groups were re-anaesthetized, their film dressings removed, wounds cleaned (as above), wounds photographed, and the treatments reapplied, as a 25 μL injection, through the Bioclusive® dressing.

Immediately following wounding, and subsequently on days 3, 8, 11 and 16, wounds were digitally photographed (Nikon Coolpix 4500), together with an image

Figure 7.1 **Creation of the wound.** Panel (a) shows the 10 x 10 mm template marked onto the shaved dorsal skin. Panel (b) shows the full- thickness excisional wound. Panel (c) shows the circumferential Bioclusive® film dressing, overlaying the wound area. Each test agent was then injected through the film dressing, onto the wound bed.

calibration scale and wound identity plate. The condition of each wound and peri-wound tissues were examined at each of these time points, and any effects, beneficial or adverse, were documented. In all cases, the condition of the dressing materials were examined daily throughout the Study and were replaced, as necessary. On post-wounding, day 16, all remaining animals were sacrificed, using CO_2 asphyxiation (confirmed by cervical dislocation). The animals were weighed, blood samples taken via cardiac puncture, and the wound tissues harvested, for histological analysis. The protocol employed is summarised, in Figure 7.2. These procedures were performed on my behalf, by Dr. Jeff Hart.

7.2.4 Image analysis of wound closure

Image Pro Image Analysis Software (version 4.1.0.0, Media Cybernetics, Bethesda, USA), was used to calculate the wound closure from wound images, in each of the experimental Groups. For each wound, at each time point, open wound area was measured and expressed in terms of % wound area remaining, relative to that immediately on wounding, at day 0. As the process of wound closure results from the combined effects of wound contraction (the inward movement of marginal tissue) and re-epithelialisation (wound resurfacing by the inward the migration of epithelial cells), wound closure, over time, was also considered with respect to these components (Figure 7.3).

7.2.5 Tissue processing of wounds

Wounds and surrounding normal tissue (5 mm) were excised and fixed in 10% buffered formalin (Bios Europe, Skelmersdale, UK), for routine histological assessment. Excised tissues were sandwiched between two pieces of filter paper, prior to being placed in fixative, to reduce the extent of tissue curling. Fixed specimens were trimmed and bisected, generating two half wounds, per site. Both halves were processed and embedded in paraffin wax. Specimens were orientated in such a fashion, as to ensure that appropriate transverse sections of the wound were taken.

7.2.6 Histological evaluation

Wax embedded tissues were sectioned (6 μm), with a microtome (Leica Microsystems (UK) Ltd., Milton Keynes, UK) and representative sections stained

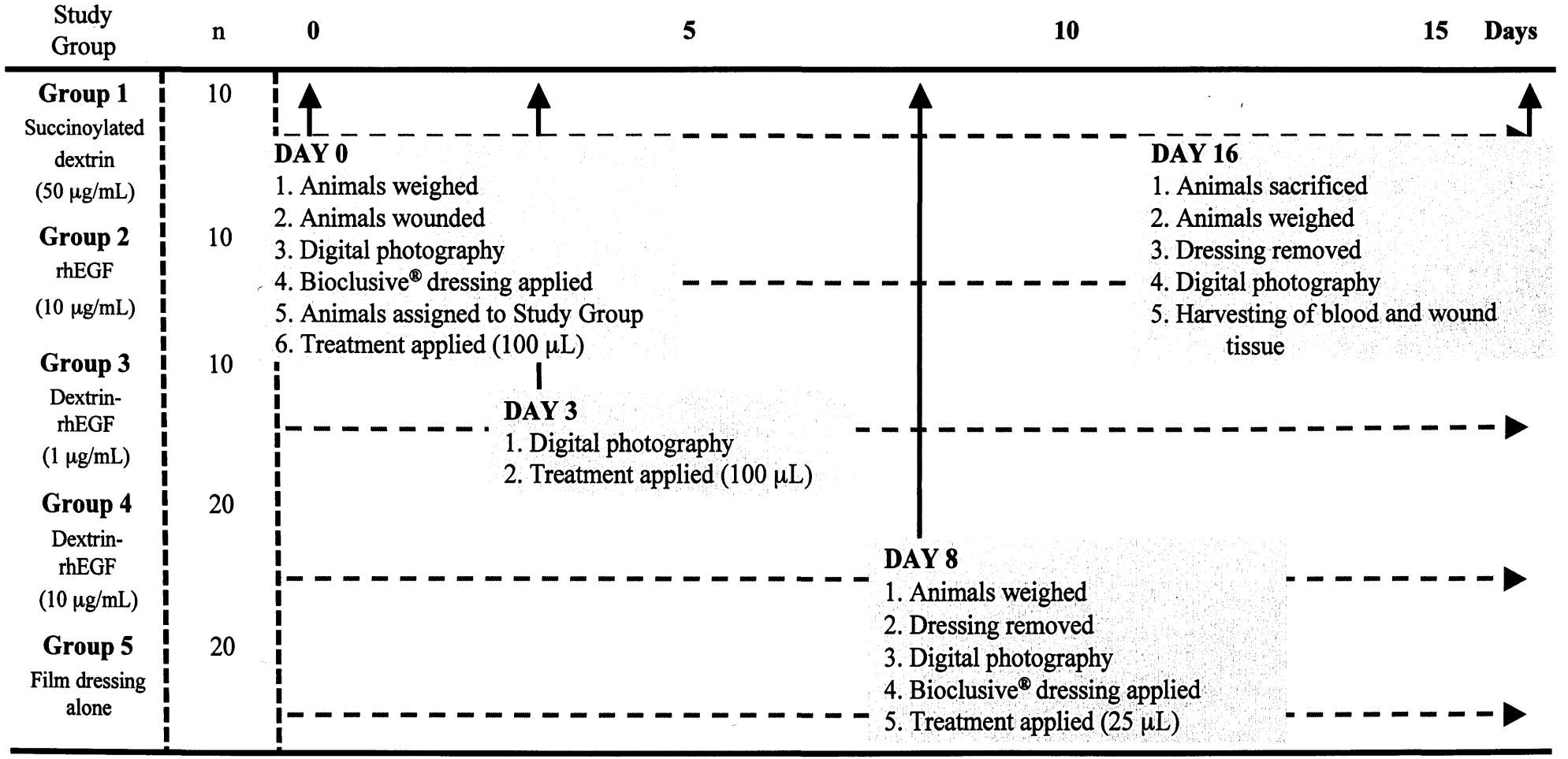

Figure 7.2 **Study protocol.** The experimental steps that were applied for the evaluation of the dextrin-rhEGF conjugate, in the genetically diabetic (db/db) mouse, impaired wound healing model. Each Group was investigated until day 16. At time-points of wound photography, changing of dressings, or application of treatments, the animals were anaesthetised.

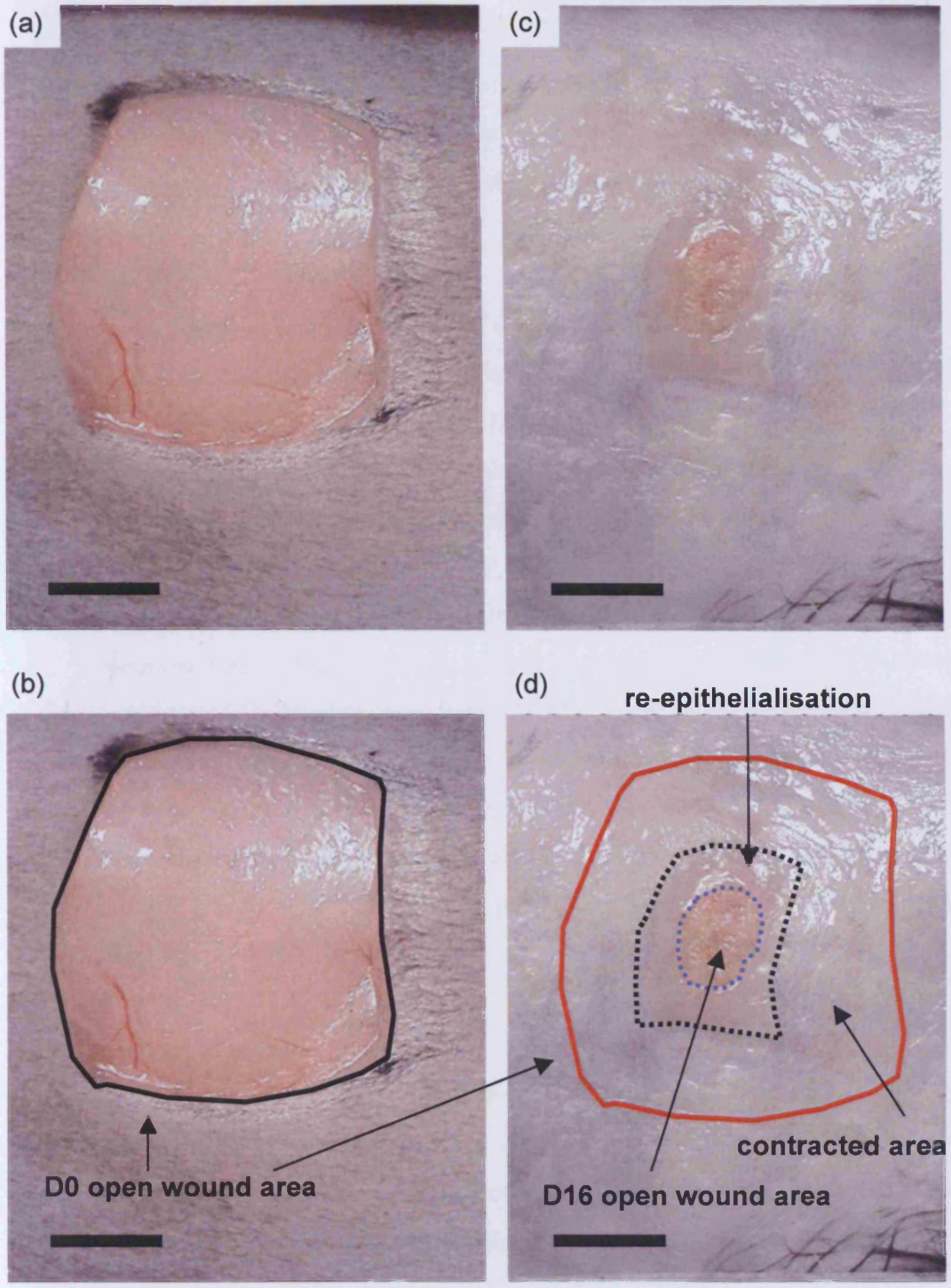

Figure 7.3 **Image analysis of wound closure.** Panel (a) shows a typical 10 x 10 mm dorsal excisional wound at day 0. Panel (b) shows the wound area highlighted (black line). Panel (c) shows the same wound at day 16. Panel (d) shows the wound at day 16, with the wound area at D0, overlaid (red line), the day 16 open wound area (dotted blue line), and the limit of wound contraction (dotted black line). The area of re-epithelialisation lies between the limit of contraction, and open wound area. Scale bar = 5 mm.

with haematoxylin and eosin (H & E). A further set of sections of each wound were taken and immunostained for CD-31, an antigen constitutively expressed on endothelial cells. Tissue harvesting and histological processing was performed by Dr. Jeff Hart.

7.2.6.1 Assessments on haematoxylin and eosin (H & E) stained sections

The following evaluations were undertaken, using Image Pro Image Analysis Software, on representative H & E sections from each wound:

(a) Quantitative assessment of granulation tissue formation (Figure 7.4).

(b) Quantitative assessment of wound maturity (Figure 7.5).

7.2.6.2 Assessments on CD31-immunostained sections

The impact of each treatment on wound angiogenesis, was assessed in terms of the prevalence of endothelial cells, within wound tissue sections. Sections (6 μm) were stained with anti-CD31. CD-31 is an antigen constitutively expressed on endothelial cells (Albelda *et al*, 1991). Angiogensis was studied in 5 high-powered fields of view (hpfov), from representative sections of each wound, and expressed as the number of CD31 positive areas counts, per hpfov. An example of CD31 staining and vessel counting, is shown in Figure 7.6.

7.2.7 Analysis of mouse plasma rhEGF

At sacrifice (day 16), blood samples were taken from mice in each Group, by cardiac puncture. Blood was centrifuged, at 15,000 *g*/5 min, at 4°C, the plasma aspirated and stored at -80 °C. At the time of analysis, samples were defrosted, and a human EGF ELISA performed, on each plasma sample. Results were compared to a rhEGF standard curve, as described previously (Section 2.6.2.5).

7.2.8 Analysis of mouse plasma α-amylase

A pooled sample of mouse serum (from eight mice), was kindly donated by Dr. Alastair Sloan, Tissue Engineering and Reparative Dentistry, School of Dentistry, Cardiff University. α-Amylase activity was established, using the Phadebas® assay (Section 6.2.3.2).

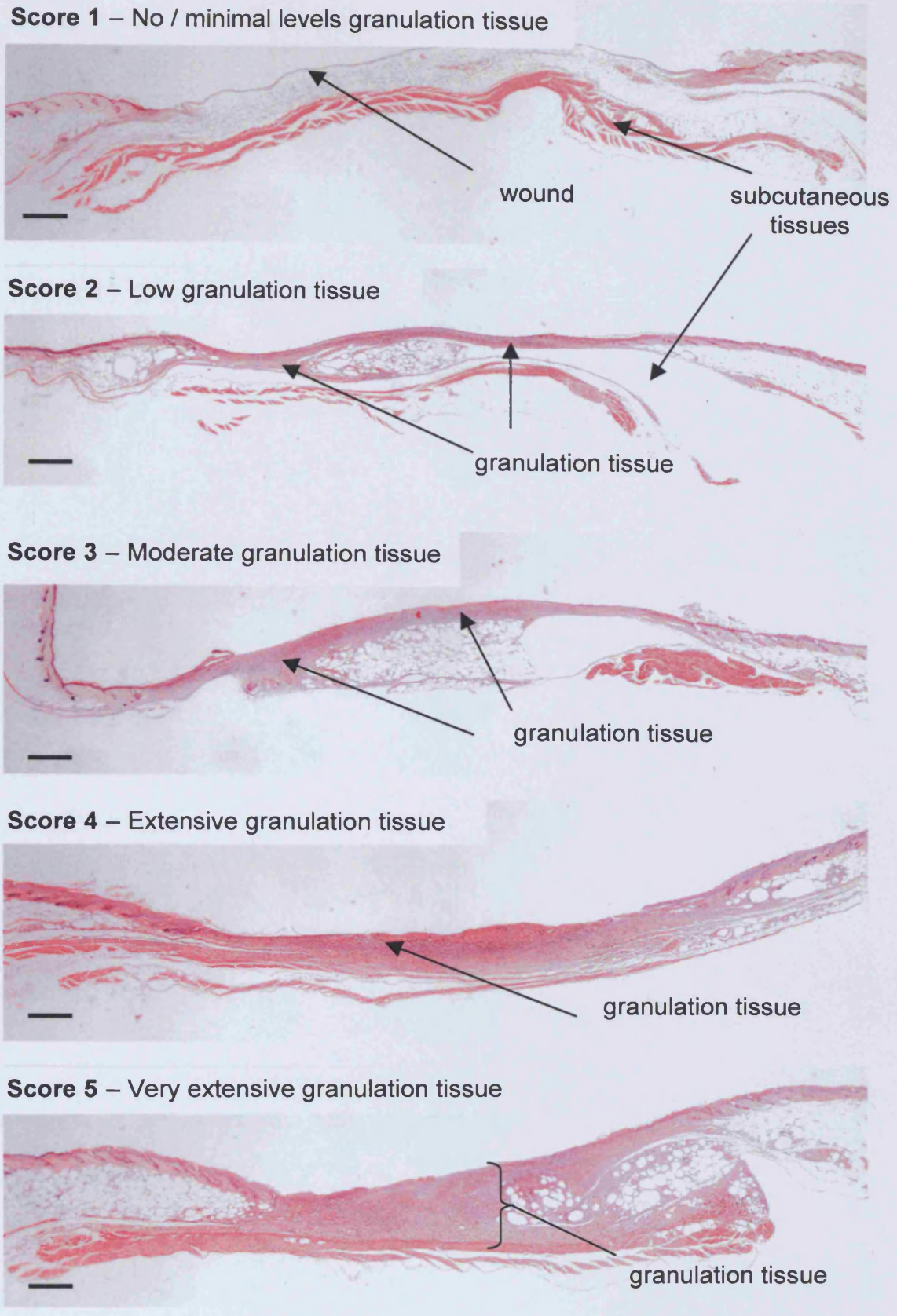

Figure 7.4 **Qualitative assessment of granulation tissue formation.** Histological sections were scored, based upon the formation of granulation tissue, in H & E stained sections (scale bar - 500 μm).

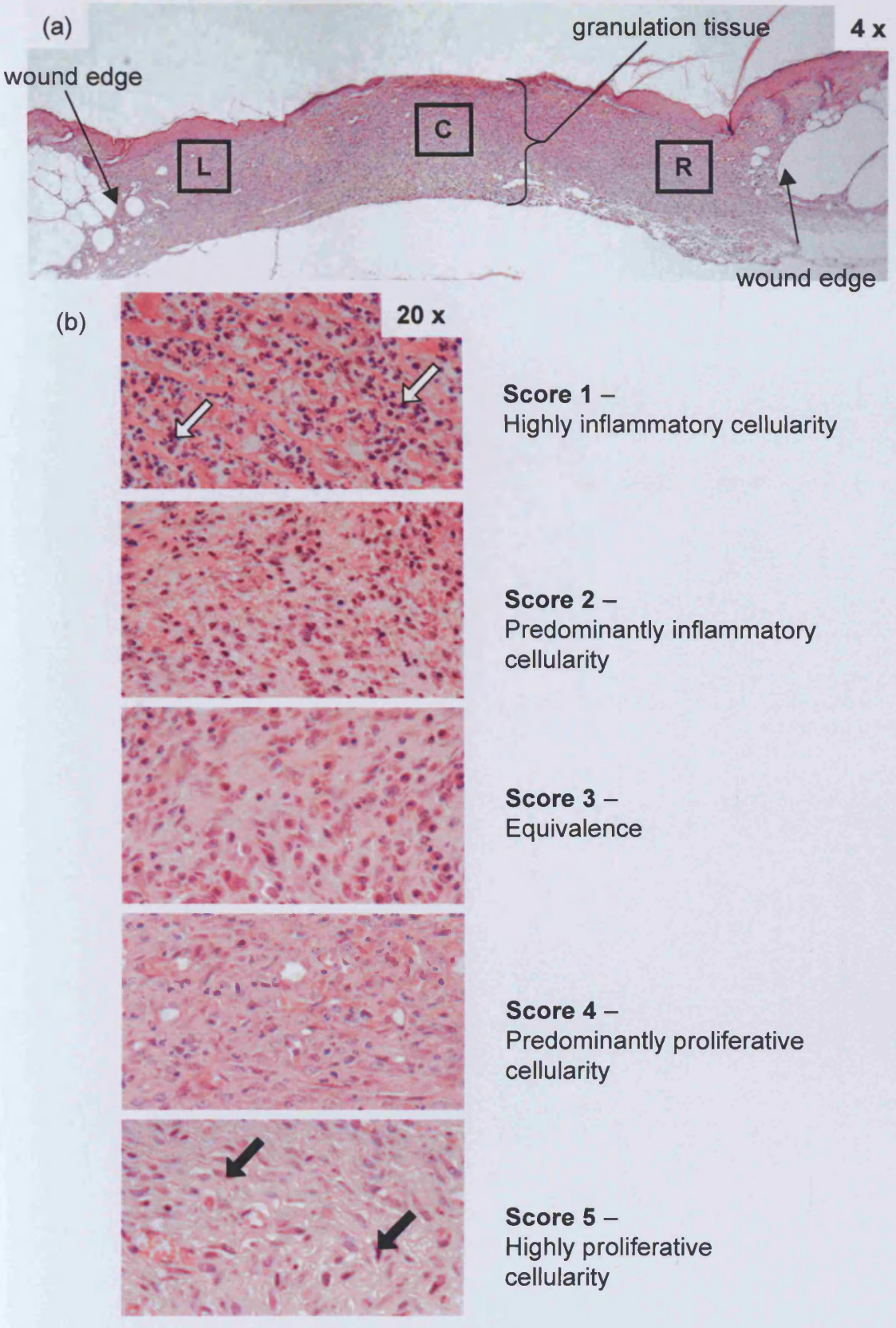

Figure 7.5 **Wound maturity scoring.** Panel (a) shows a typical histological cross-section of a wound, at day 16, with areas selected for scoring, from the wound centre (C), and the left (L) and right (R) margins. Panel (b) shows the wound maturity scoring scale. During the inflammatory phase of wound healing, the more predominant cells are of the inflammatory sub-type (arrowed white). As wound healing progresses into the proliferative phase, the inflammatory cells are replaced (e.g. with fibroblasts - arrowed black).

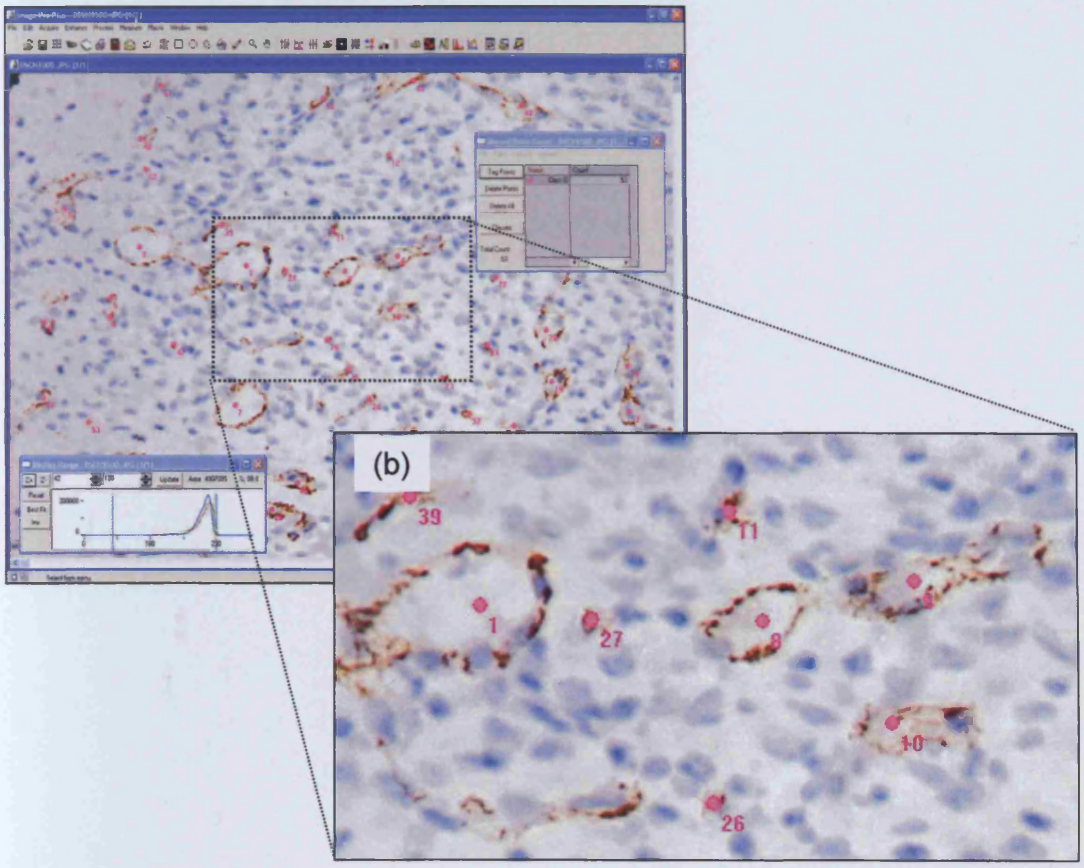

Figure 7.6 **Assessment of CD31 stained histological sections.** (a) Angiogensis was studied in 5 high powered fields of view (hpfov), from representative sections of each wound and expressed as the number of CD31 positive areas counts, per hpfov. Panel (b) shows an area of higher magnification with the areas labelled and numbered (• focal area of CD31 staining).

7.2.9 Statistical analysis

Statistical analyses were undertaken using GraphPad Prism®, version 4.00 (GraphPad Software, San Diego, USA). Mean values (with standard errors), for all live and post-mortem histological assessments, were calculated for each treatment Group. Data was tested for normality, using the Shapiro-Wilk test. If data failed this normality test, non-parametric analysis (Kruskal Wallace, Multivariate Analysis followed by *ad hoc* two sample Mann Whitney U-test analysis), was used to test the significance of any inter-Group differences in each of the study parameters investigated. If data for all treatment Groups was deemed to be normal for a given parameter, parametric analysis (ANOVA – Multivariate Analysis, followed by *ad hoc* two sample student t-test), was also performed. Results were expressed as a mean and standard deviation (S.D.), or standard error of the mean (S.E.M.). Statistical significance was considered at a probability of $p < 0.05$.

7.3 Results

One animal was excluded from the *in vivo* Study due to faecal impaction, at day 2, post-wounding (succinoylated dextrin Control, Group 1). The remaining 69 animals completed the Study, to day 16.

7.3.1 Wound closure

Data concerning wound closure in diabetic (C57BLKs/Bom db/db) mice, from two different sources ("American" C57BLKs/Bom db/db, The Jackson Laboratory, Bar Harbor, USA, n = 20; "European" C57BLKs/Bom db/db, M&B, Ry, Denmark, n = 17) and the European non-diabetic litter-mates (M&B, Ry, Denmark, n = 9), was kindly donated by Dr. Jeff Hart. The wound closure rates were significantly reduced in the American model, under control conditions (transparent wound dressing only), when compared to the European model ($p < 0.0001$), at day 16, under the same conditions (Figure 7.7). Both diabetic models remain unhealed at day 16, whilst the non-diabetic, European model healed by day 13. The European diabetics underwent significantly more re-epithelialisation ($p = 0.0056$), by day 16, compared to the American diabetics, whilst wound contraction analysis exhibited no significant difference between the two diabetic Study Groups ($p > 0.05$).

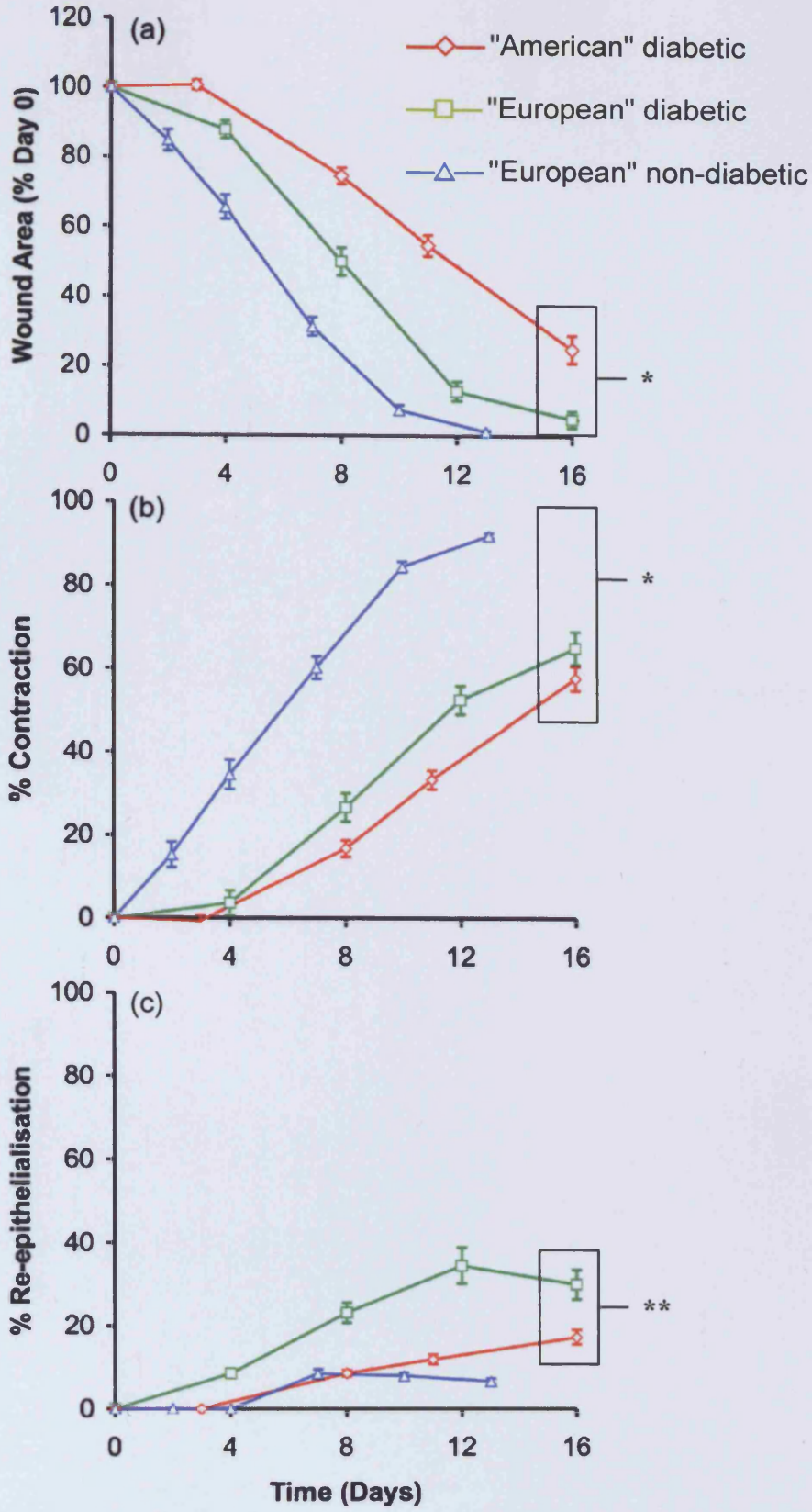

Figure 7.7 ***In vivo* wound healing in diabetic and non-diabetic mice.** Panel (a) shows the total wound area reduction, over 16 days, compared to the wound size, at day 0. The American diabetic mice had significantly larger wounds, compared to their European counterparts, at day 16. Panel (b) shows the percentage of wound healing by contraction, and panel (c) shows the percentage of wound healing by re-epithelialisation (mean ± S.E.M., $*p < 0.0001$ $**p = 0.0056$, Mann-Whitney U-test).

7.3.1.1 Animal body weights

The body weights of the animals did not significantly differ ($p > 0.05$), between day 0 and day 8, in any of the Study Groups. In Group 1, animals were weighed, prior to cardiac puncture, on day 16, and there was no significant change in the body weights, over the 16-day period ($p > 0.05$). In the remaining Sample Groups, blood samples were taken, prior to weighing, to reduce the formation of blood clots. This resulted in significant decreases ($p < 0.05$) in body weights, at day 16, in all Groups, except Group 3 ($p > 0.05$).

7.3.1.2 Assessment of the dextrin-rhEGF conjugate

Typical digital wound photography demonstrated a reduction in wound area in response to the dextrin-rhEGF conjugate (Figure 7.8; Appendix DVD). At day 11, post-wounding, the dextrin-rhEGF conjugate, at both 1 and 10 μg/mL rhEGF equivalent (Groups 3 and 4, respectively), induced a significant reduction in wound area ($p \leq 0.035$), compared to the untreated Controls (Group 5) ($p < 0.05$) (Figure 7.9a). Free rhEGF, 10 μg/mL (Group 2), had no significant effect on wound area reduction ($p > 0.05$), whilst free, succinoylated dextrin polymer (Group 1) retarded wound area reduction ($p = 0.02$) (Figure 7.9b). When conjugated to succinoylated dextrin, rhEGF significantly increased the ability to promote wound area reduction (Groups 3 and 4), and therefore wound closure, when compared to free rhEGF, 10 μg/mL (Group 2) ($p \leq 0.011$). At the higher dose, 10 μg/mL rhEGF equivalent (Group 4), the dextrin-rhEGF was most effective ($p = 0.002$) (Figure 7.9c).

Wound contraction increased in response to the dextrin-rhEGF conjugate (Groups 3 and 4), when compared to the untreated Controls (Group 5), and was most effective at 1 μg/mL rhEGF equivalent (Group 3) ($p = 0.012$), at day 11. A significant increase in re-epithelialisation was observed with the dextrin-rhEGF conjugate, at 10 μg/mL rhEGF equivalent (Group 4) ($p = 0.001$), at day 11 (Figure 7.10). At day 16, post-wounding, a significant decrease in wound area reduction was observed in the succinoylated dextrin polymer and free rhEGF Control Groups (Groups 1 and 2, respectively) ($p < 0.001$). The dextrin-rhEGF conjugate promoted a significant decrease in wound area, at 10 μg/mL rhEGF equivalent (Group 4) ($p = 0.028$). The lower dose dextrin-rhEGF (1 μg/mL rhEGF equivalent; Group 3) was

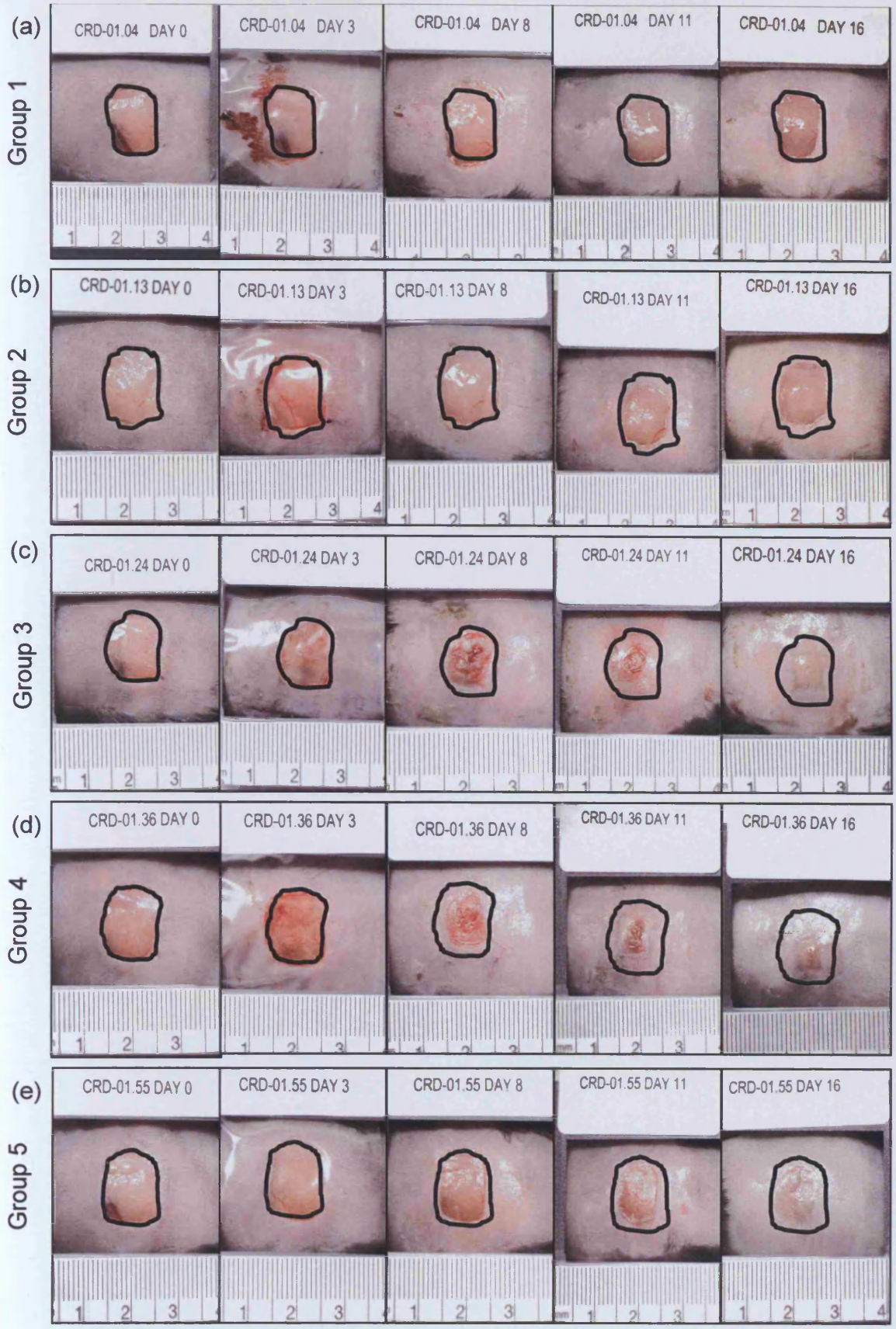

Figure 7.8 **Digital wound photography.** The images show the typical *in vivo* wound healing, in response to (a) free succinoylated dextrin polymer (Group 1), (b) free rhEGF (10 μg/mL; Group 2), (c) the dextrin-rhEGF conjugate (1 μg/mL rhEGF equivalent; Group 3), (d) the dextrin-rhEGF conjugate (10 μg/mL rhEGF equivalent; Group 4), or (e) no treatment. The wound area at day 0 is represented by the black line. All images are included in Appendix DVD.

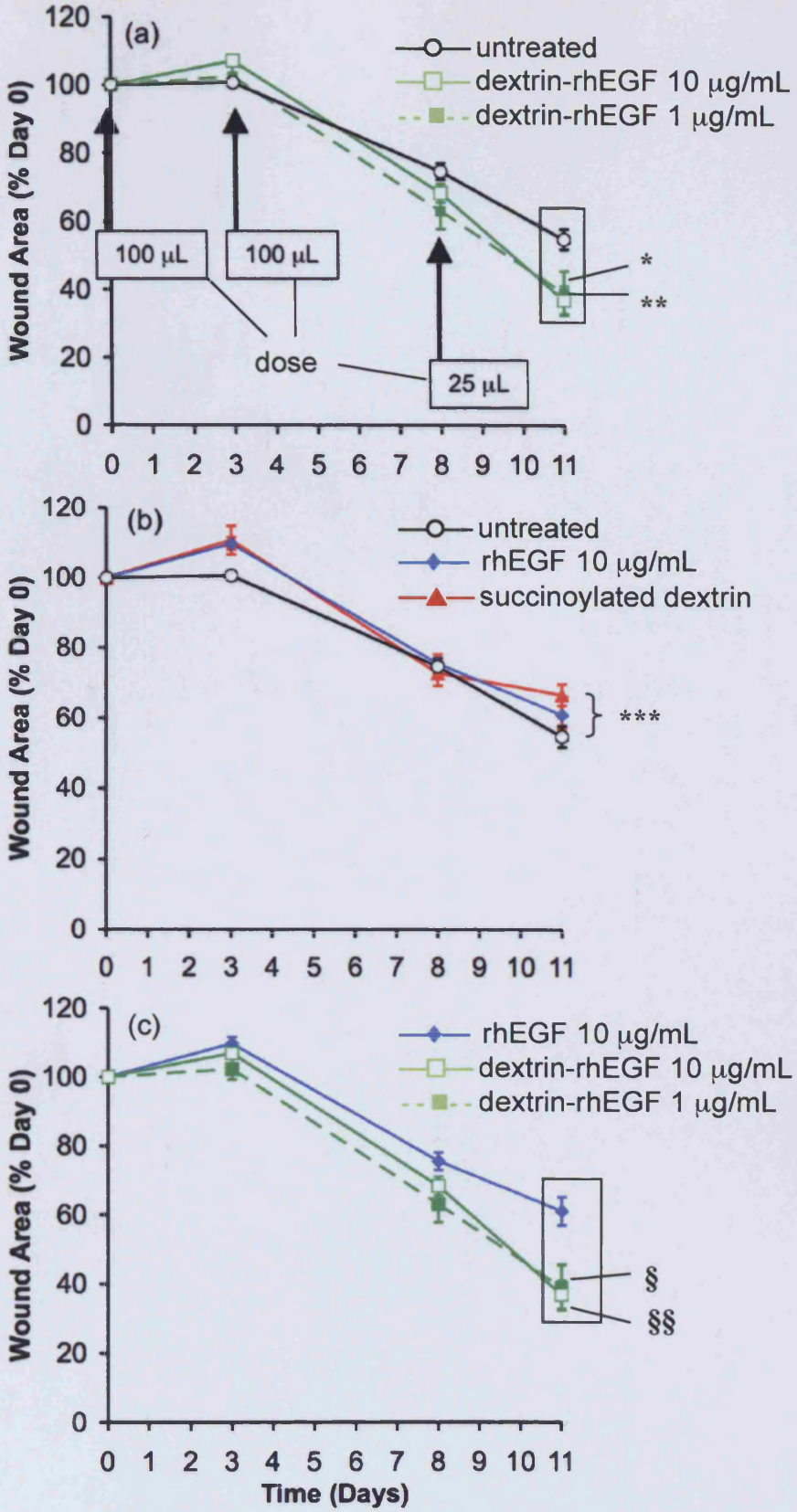

Figure 7.9 **Wound area reduction, in response to the dextrin-rhEGF conjugate.** Panel (a) shows the wound area reduction, in response to the dextrin-rhEGF conjugate, the dosing schedule is indicated in the overlay (mean ± S.E.M., * $p = 0.035$ ** $p = 0.002$, Mann-Whitney U-test). Panel (b) shows the wound area reduction in response to the controls (free rhEGF and succinoylated dextrin) (mean ± S.E.M., *** $p = 0.02$, Mann-Whitney U-test). Panel (c) compares free rhEGF with the dextrin-rhEGF conjugate, at 1 and 10 μg/mL rhEGF equivalents (mean ± S.E.M., § $p = 0.011$, §§ $p = 0.002$, Mann-Whitney U-test).

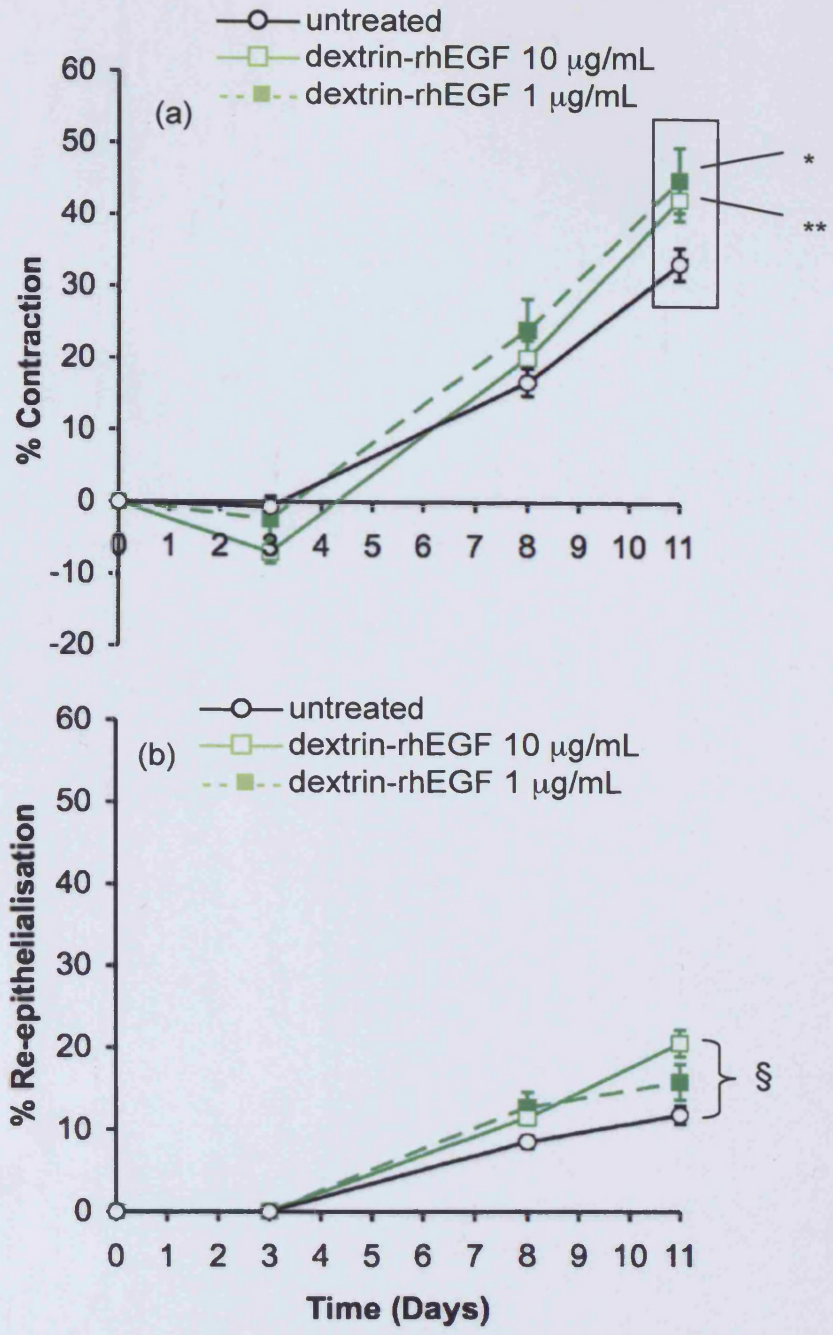

Figure 7.10 **Wound contraction and re-epithelialisation, in response to the dextrin-rhEGF conjugate.** Panel (a) shows that wound contraction was increased, in response to the dextrin-rhEGF conjugate, at both 1 and 10 μg/mL, compared to untreated controls (mean ± S.E.M., * p = 0.012, ** p = 0.031, Mann-Whitney U-test). Panel (b) shows increased re-epithelialisation, in response to the 10 μg/mL dextrin-rhEGF conjugate (mean ± S.E.M., § p = 0.001, Mann-Whitney U-test), but not 1 μg/mL dextrin-rhEGF conjugate ($p > 0.05$).

not significantly different to the untreated Control (Group 5), by day 16 ($p > 0.05$) (Figure 7.11).

7.3.2 Histological analysis

7.3.2.1 Granulation tissue

Granulation tissue deposition was significantly increased in all dextrin-rhEGF Groups, compared to the free rhEGF and succinoylated dextrin Controls ($p < 0.05$). (Figure 7.12; Appendix DVD). In the high-dose (10 μg/mL rhEGF equivalent), dextrin-rhEGF conjugate Study Group 4, the granulation tissue score was significantly higher than the untreated Controls (Group 5) ($p = 0.006$), but in the low-dose (1 μg/mL rhEGF equivalent), dextrin-rhEGF conjugate Study Group 3, there was no significant difference between the dextrin-rhEGF conjugate and untreated Control Groups ($p > 0.05$). There was also no significant difference between free rhEGF and no treatment Control Group 5 ($p > 0.05$).

7.3.2.2 Wound maturity

Sections from the central wound area were consistently scored significantly lower (more inflammatory cells), compared to those from the wound margin ($p < 0.0001$), irrespective of Study Group. The maturity of the wounds were not significantly affected by the dextrin-rhEGF conjugate, at either concentration (Groups 3 and 4), compared to the untreated Controls (Group 5), at either the central or marginal wound areas. An inflammatory stimulus was observed in the free rhEGF (Group 2) and free succinoylated dextrin (Group 1) specimens, at the central wound area ($p \leq 0.004$) (Figure 7.13).

7.3.2.3 Angiogenesis

Quantitative assessment of angiogenesis within the wound (at the central, intermediate and marginal zones), at day 16, was performed by quantifying the number of angiogenic events, per hpfov. The marginal and intermediate hpfovs were each from the right and left side of the wound, and the mean calculated (± S.E.M.). In the central wound area, there was a significant difference in angiogenic events between the dextrin-rhEGF conjugate Group 4 (10 μg/mL rhEGF equivalent), compared to the untreated Controls (Group 5) ($p = 0.011$).

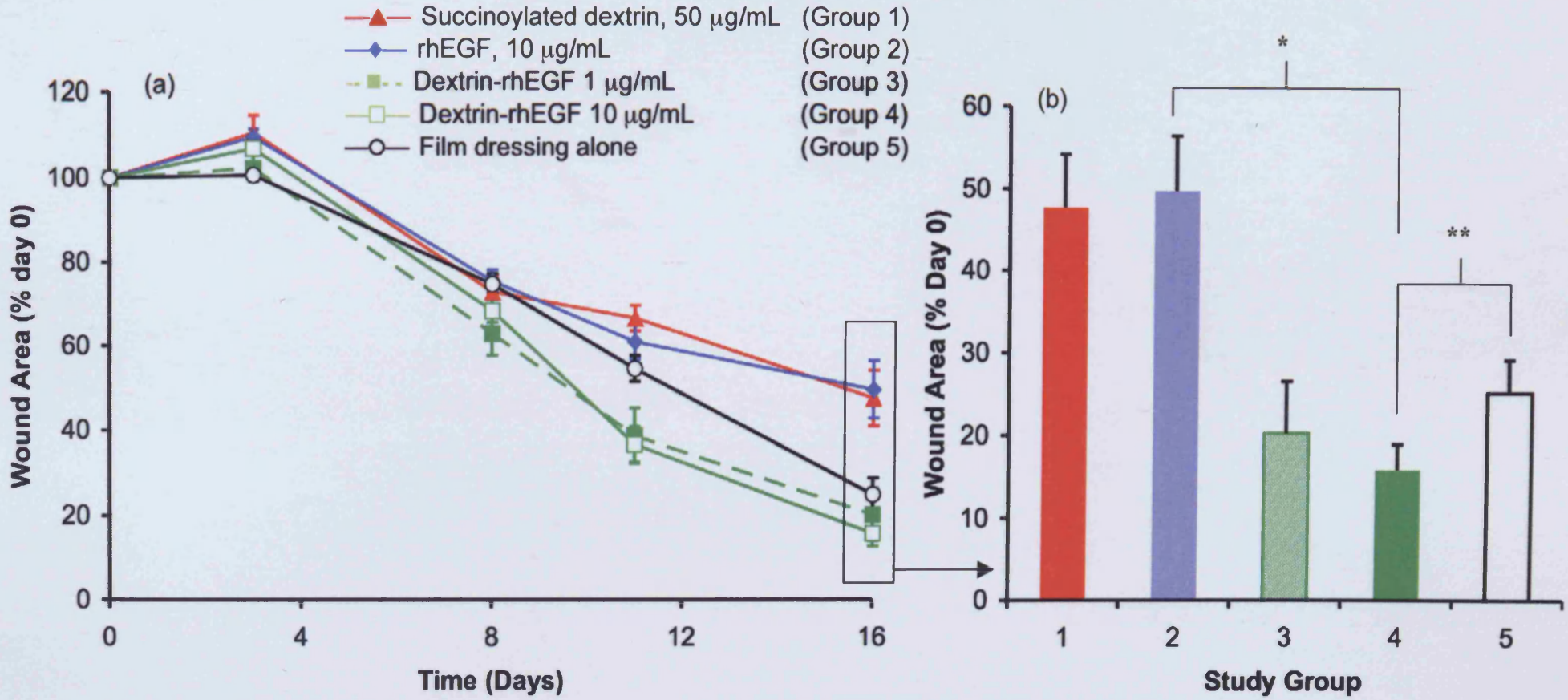

Figure 7.11 **Wound area reduction, over 16 days.** Panel (a) shows the wound area reduction in all 5 Study Groups over the 16 day, Study period. Panel (b) shows the wound area, on day 16, as a percentage of the wound size, on day 0 (mean ± S.E.M., * $p < 0.001$, ** $p = 0.028$, Mann-Whitney U-test).

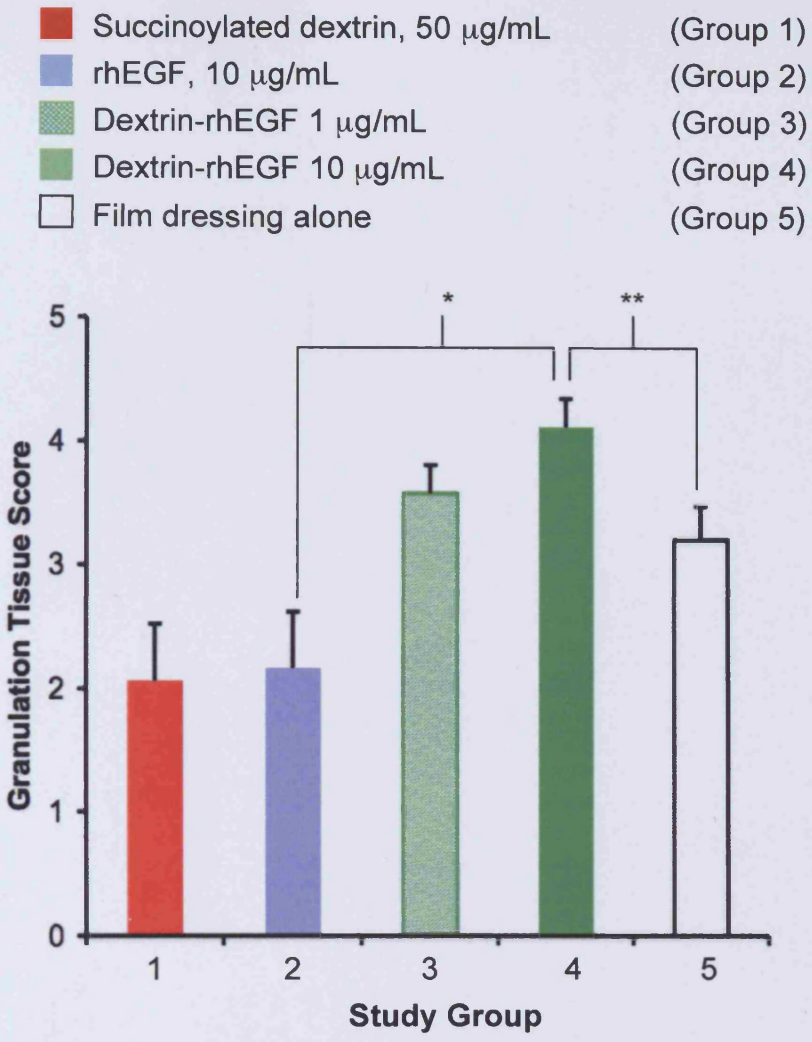

Figure 7.12 **Granulation tissue formation, at day 16.** The granulation tissue scores for each Study Group, at day 16 (mean ± S.E.M., * $p = 0.004$, ** $p = 0.006$, Mann-Whitney U-test).

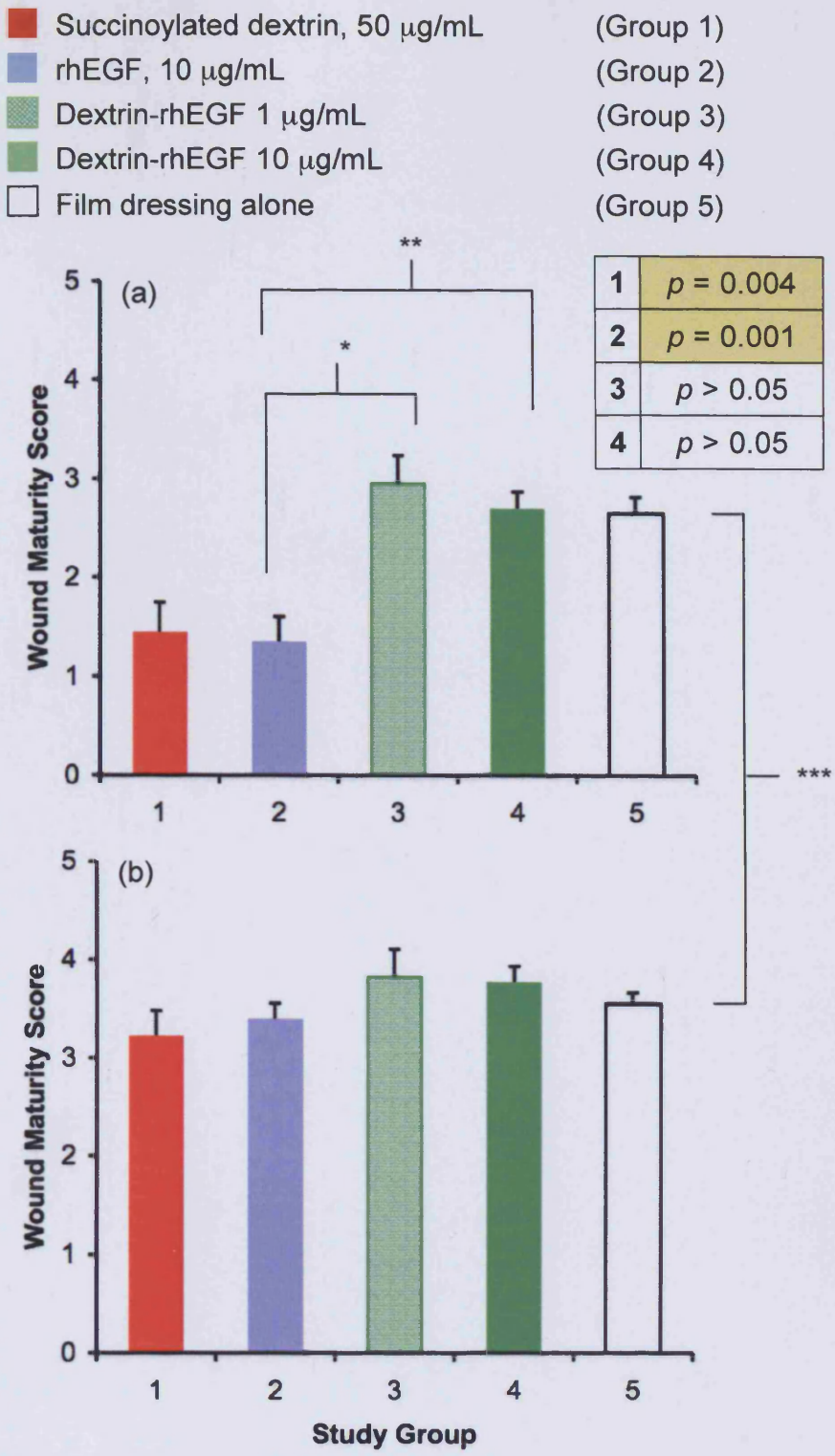

Figure 7.13 **Wound maturity.** Panel (a) shows the wound maturity scores for samples selected from the wound centre. The Table shows Group comparison with untreated controls (Group 5) and panel (b) from the wound margin (mean ± S.E.M.) The dextrin-rhEGF conjugate (at both 1 and 10 μg/mL), did not significantly effect wound maturity, compared to untreated controls ($p > 0.05$), at either the centre or wound margin. Free rhEGF induced an inflammatory response (low wound maturity score), at the wound centre (*$p = 0.002$, ** $p = 0.004$, Mann-Whitney U-test), compared to the dextrin-rhEGF conjugate (1 μg/mL). All wounds were significantly more mature at the wound margin, than the central wound (*** $p < 0.0001$, Mann-Whitney U-test).

In contrast, free rhEGF (Group 2) significantly reduced the number of angiogenic counts (p = 0.035). At the intermediate wound zone, angiogenesis was significantly enhanced by the dextrin-rhEGF conjugate Group 4 (10 μg/mL rhEGF equivalent; p = 0.001). At the marginal wound zone, significant angiogenesis was also observed in the 10 μg/mL rhEGF equivalent, dextrin-rhEGF conjugate Group 4, compared to the untreated Controls (Group 5) (p = 0.010). Overall, angiogenic events in the wound were significantly increased by rhEGF, released from the dextrin-rhEGF conjugate (10 μg/mL rhEGF equivalent; Group 4), compared to untreated Controls (Group 5) (p = 0.017), or free rhEGF (10 μg/mL; Group 2) (p = 0.005) (Figure 7.14).

The results of the digital wound analysis and histological evaluation of the wounds, are summarised in Table 7.4.

7.3.3 Mouse serum rhEGF content

Analysis of the rhEGF content of mouse serum, derived from mice in each study group, at day 16, was performed with a human EGF ELISA, which is sensitive to rhEGF (Section 2.6.2.5). No rhEGF was detected in any of the samples of mouse serum, from any of the Study Groups.

7.3.4 Mouse serum α-amylase content

The pooled sample of mouse serum contained 1800 ± 20 i.u./L α-amylase (n = 3, mean ± S.D.). This was approximately ten-times the concentration of α-amylase in human serum, or acute or chronic wound fluids (Section 6.3.2).

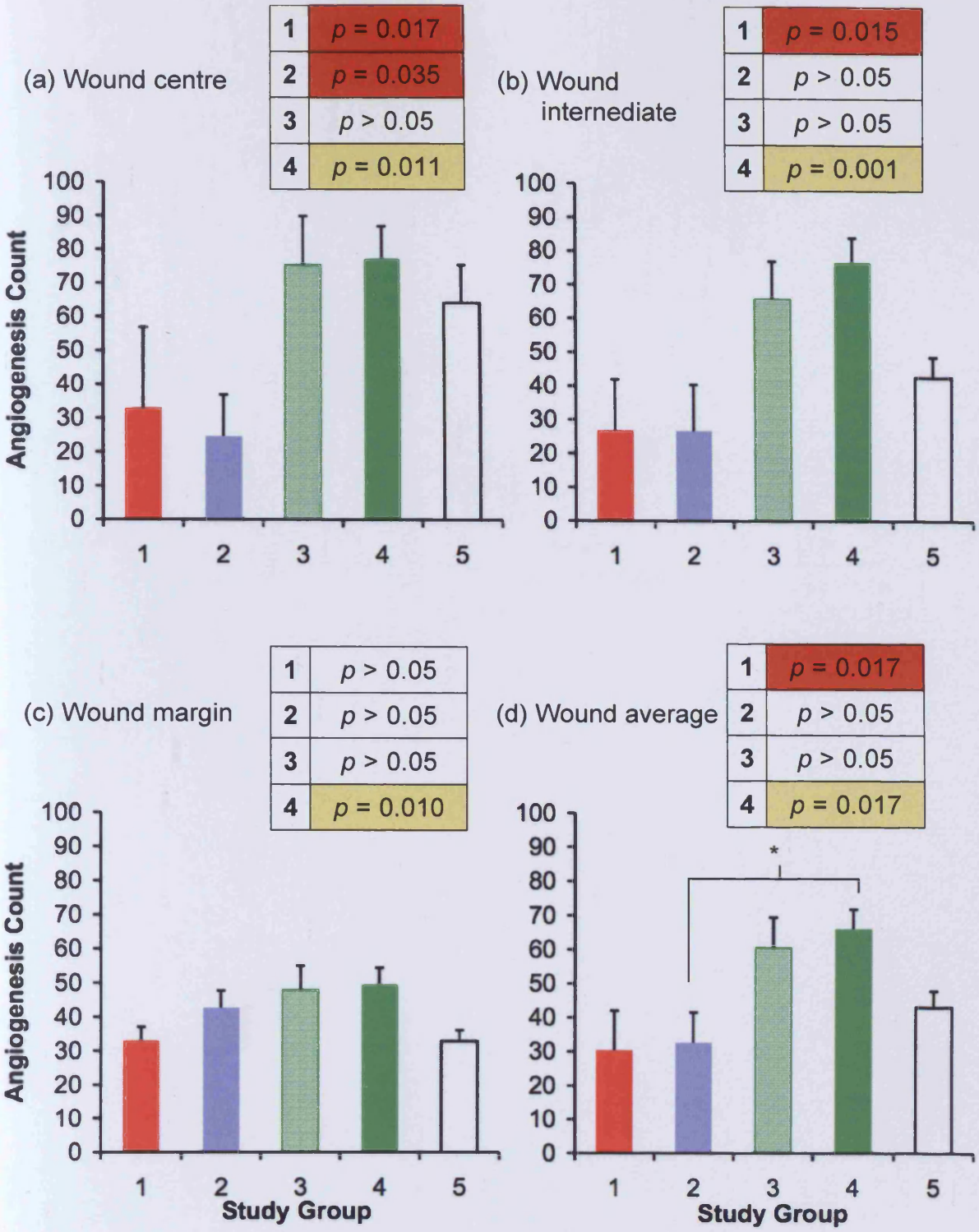

Figure 7.14 **Wound angiogenesis.** Panel (a) shows the number of angiogenic counts per high power field of view (hpfov), at the wound centre. The Table shows the significance of each Study Group compared to the untreated control (Group 5). Free rhEGF (Group 2) significantly retarded angiogenesis (highlighted red). Panel (b) shows equivalent data from the intermediate wound, with a significant increase in angiogenic counts in the 10 μg/mL dextrin-rhEGF conjugate Group (Group 4; highlighted yellow). Panel (c) shows similar data for the wound margin, with a significant increase in angiogenic counts in the 10 μg/mL dextrin-rhEGF conjugate Group (Group 4). Panel (d) shows the average number of angiogenic counts throughout the wound, with a significant increase in angiogenic counts in the 10 μg/mL dextrin-rhEGF conjugate Group (Group 4). The dextrin-rhEGF conjugate significantly stimulated angiogenesis more than free rhEGF, * $p = 0.005$. All p values were calculated by Mann-Whitney U-test.

Table 7.4 **Summary of the significance of the effects of the dextrin-rhEGF conjugate on db/db mouse wound healing *in vivo*, compared to untreated controls**

	Dextrin-rhEGF (1 μg/mL rhEGF equivalent)	**Dextrin-rhEGF (10 μg/mL rhEGF equivalent)**
Wound area reduction		
DAY 11	$p = 0.035$	$p = 0.002$
DAY 16	$p > 0.05$	$p = 0.028$
Wound contraction		
DAY 11	$p = 0.012$	$p = 0.031$
Re-epithelialisation		
DAY 11	$p > 0.05$	$p = 0.001$
Granulation tissue score	$p > 0.05$	$p = 0.006$
DAY 16		
Wound maturity	$p > 0.05$	$p > 0.05$
DAY 16		
Angiogenesis (mean)	$p > 0.05$	$p = 0.017$
DAY 16		

7.4 Discussion

This Chapter aimed to evaluate the dextrin-rhEGF conjugate in an *in vivo* model of impaired wound healing. Other biochemical parameters, such as basic pharmacokinetic data and mouse serum α-amylase activity, were also established.

7.4.1 Model selection

The confirmation of the presence of α-amylase within mouse serum, even though at a much higher level than in humans, permitted the selection of an *in vivo* murine model. Dawra *et al* (2007) reported similar levels of serum α-amylase, in C57BL/6 mice. The genetically diabetic (db/db) mouse is an established model of impaired dermal wound healing, and although, not a true representation of the human chronic wound, it has been used in studies of wound healing, involving rhEGF (Brown *et al*, 1994).

The db/db mice selected in the present Study, from a North American Supplier, showed significantly impaired wound healing, when compared to European db/db and non-diabetic mice, of the same strain. Wound area and re-epithelialisation were both slower in the North American db/db mice. Wound contraction was similar in both models. These findings established the North American diabetic mouse as the slowest model of wound healing, from those available. Therefore, these mice were selected for use in the present Study. Other studies involving the North American db/db mouse, in the assessment of growth factors on wound healing, include Greenhalgh *et al* (1990), Brown *et al* (1994) and Kirchner *et al* (2003).

7.4.2 Wound closure

Wound area was significantly reduced by the dextrin-rhEGF conjugate (Groups 3 and 4), when compared to either untreated or other Control Groups (Groups 1, 2 and 5). The most significant wound area reduction was observed at 11 days, with the greatest effect apparent in the high-dose (10 μg/mL), dextrin-rhEGF conjugate Group 4. This reduction in wound area was also observed on the termination of the Study (day 16), although, the degree of significance was less. The Control Groups (Groups 1 and 2) significantly under performed, when compared to the untreated, Control Group 5. Wound area was markedly greater, with both the succinoylated dextrin polymer and the rhEGF Controls.

The dosing schedule (100 μL, days 0 and 3) was adapted during the experiment to include an extra dose (25 μL, day 8), due to the limited observed progression in wound healing, in the dextrin-rhEGF conjugate Groups, during the initial stages of the Study. Previously reported studies involving rhEGF in *in vivo* models of wound healing (Brown *et al,* 1994; Ulubayram *et al*, 2001; Tanaka *et al*, 2005; Alemdaroglu *et al*, 2006), have involved the application of rhEGF on a minimum of a daily basis, via a number of delivery vehicles. The sustained-release data established in Chapters 3 and 4, highlighted the potential for reduced dosing of the dextrin-rhEGF conjugate. As high local concentrations of rhEGF must be prevented, if inhibition of wound healing is to be avoided (Lai *et al*, 1989; Breuing *et al*, 1997), this justified the application of the Study compounds, in a staggered manner. The effects of the dextrin-rhEGF conjugate, on wound area reduction, began to decline following the final, lower-dose on day 11. The instigation of further doses at this stage, or earlier, during the Study, may have increased the effects observed at the day 16 time-point. The Study duration could also have been increased to a point where wounds had fully healed (in the untreated Control Group 5). Previous studies involving the North American db/db mouse, have continued to between days 14 to 21, with an average of 19 days (Greenhalgh *et al*, 1990; Brown *et al*, 1994; Kirchner *et al*, 2003).

The sustained-release effect of dextrin-rhEGF appeared to be retained in the *in vivo* model. This is indeed a significant achievement, as this was the first experiment performed without the addition of a known quantity of exogenous α-amylase. As such, these findings provide further and significant support for the Polymer-masking UnMasking Protein Therapy (PUMPT) concept, for the first time *in vivo.* Although the α-amylase activity in mouse serum is approximately 10-times that of human serum, a combination of the *in vitro* data from Chapters 3 and 4 (at human physiological levels of α-amylase), and the *in vivo* findings reported herein, appear to suggest that the PUMPT concept would be a viable proposition in the human. rhEGF was not detected in any sera of the Study Groups, at day 16, so one must assume that even in the conjugated form, the rhEGF has been metabolised and excreted. This may have occurred at a local wound level, with proteolytic degradation of the rhEGF, or the conjugate may not have been absorbed systemically. Even, if absorbed into the lymphatic or systemic circulation, further

degradation may have occurred in these environments. Additional urine collection, throughout the course of the Study, would have revealed more pharmacokinetic information and potentially resolved some of the clearance issues.

The significant detrimental effect of the succinoylated dextrin and free rhEGF Controls (Groups 1 and 2, respectively) on retarding wound healing, may have been due to a series of factors. The effects approached significance at day 11, and by day 16, is pronounced. The dextrin polymer undergoes a series of purification steps, following succinoylation, by dialysis (Chapter 3), to remove excess reactants, but as has been shown, by fast protein liquid chromatography (FPLC) (Chapter 3), a quantity of dimethylaminopyridine (DMAP) remains. This is subsequently removed during the conjugation reaction and purification, by ultrafiltration, and hence is not present in the dextrin-rhEGF conjugate. However, unconjugated succinoylated dextrin does not undergo these purification procedures. Additionally, the pH of succinoylated dextrin is acidic, due to the incorporation the of the carboxylic groups. Therefore, a combination of potentially cytotoxic DMAP and the acidic pH, which are inherent in succinoylated dextrin, may explain the deleterious effects that have been observed with succinoylated dextrin, in the present Study (even at a low dose). Thus, the succinoylated dextrin, may not have acted as a true negative Control. Further purification of the succinoylated dextrin polymer, for example, by anion exchange chromatography, may result in a less toxic polymer Control.

In the Study by Brown *et al* (1994), rhEGF was applied to excisional wounds in North American db/db mice. The dose applied was 1 μg, in a 5% polyethylene glycol vehicle, applied daily, for 5 days. Wound healing was measured as "percentage wound closure", the inverse of percentage wound area reduction, as described in the present Study. rhEGF was consistently slower to heal wounds, but never to a level of significance, compared to the vehicle alone, over 21 days. In combination with 10 μg PDGF, the effect on wound closure was increased, but not to the levels of PDGF alone. It is this report that the choice of rhEGF concentrations employed in the present Study, were based upon. The suppression of wound healing in the free rhEGF Control Group (Group 2) may be a consequence of the down-regulation of EGF receptors (EGFR), on cells involved in the normal wound healing process. Indeed, this suppression of activity at high concentrations of rhEGF was identified in Chapter 4. *In vitro,* rhEGF had maximal activity at ng/mL concentration,

rather than the μg/mL concentrations, previously utilised *in vivo*. Indeed, the previously reported *in vivo* studies have all applied EGF at the μg/mL concentration (Franklin and Lynch, 1979; Buckley *et al*, 1985; Mustoe *et al*, 1991; Ulubayram *et al*, 2001; Tanaka *et al*, 2005; Alemdaroglu *et al*, 2006), of which the majority did not exhibit any suppression of wound healing. Even though the half-life of EGF is of the order of 1-2 hours, in animal tissues (Chan *et al*, 1991; Prats *et al*, 2002), any suppression caused by EGF in the early stages of wound healing, would cause a significant lasting effect on wound area reduction. Pruss and Herschman (1977) demonstrated that the interaction between EGF, and its receptor, had to be maintained for 10-12 hours, in order to obtain effective cellular responses, in terms of better organised granulation tissue, greater DNA and protein content, and a higher rate of cell proliferation. The conjugation of rhEGF to succinoylated dextrin, not only reduced any toxicity caused by either component, but enhanced wound healing, significantly more than the untreated Control Group, possibly through this controlled release effect. Based on these findings, a change to the dosing regimen may further enhance the beneficial effects observed. Further studies may also include other groups such as a 1 μg/mL rhEGF control, and continuation of the study to the point of wound closure.

7.4.3 Histology

Histological analysis of the wounds from each Study Group, confirmed the macroscopic findings, from the digital wound photography. Granulation tissue formation was significantly increased by the dextrin-rhEGF conjugate (10 μg/mL rhEGF equivalent, Group 4), compared to free rhEGF (Group 2) or untreated Controls (Group 5). Granulation tissue depth was reported by Nanney (1990), to be significantly increased in a porcine acute partial thickness wound models, proportional to the concentration of free rhEGF applied (10 or 30 μg/mL), although toxicity occurred at higher rhEGF doses (50 μg/mL). Interestingly, EGF is more commonly associated with increased rates of re-epithelialisation *in vivo*, rather than granulation tissue formation (Franklin and Lynch, 1979; Brown *et al*, 1989; Martin, 1997). Brown *et al* (1994) did not report any significant difference in granulation tissue formation, by rhEGF, in the genetically diabetic (db/db) mouse. However, the present Study demonstrated the controlled release of rhEGF, from the dextrin-rhEGF

conjugate, into the chronic wound environment, resulted in similar improved effects on granulation tissue formation, in a comparable manner to those observed in acute wounds.

A feature associated with the formation of granulation tissue, is the discrete increase in the number of angiogenic events, in response to growth factors, such as vascular endothelial growth factor (VEGF) (Roy *et al*, 2006, Bao *et al*, 2008). rhEGF (10 μg/mL) has been shown to increase the capillary area and number of blood vessels, in acute partial-thickness, porcine wounds (Roesel and Nanney, 1995). This mechanism of angiogenesis is dependent upon the expression of the epidermal growth factor receptor (EGFR), which is involved in multiple facets of the normal wound healing response, including inflammation, wound contraction, proliferation, migration and angiogenesis (Repertinger *et al*, 2004). In the present Study, angiogenesis was most marked at the wound centre, with diminishing activity towards the wound margin, in the untreated Control Group. Stimulation of angiogenesis, by the dextrin-rhEGF conjugate, was most pronounced at the wound margin, which may be due to the multiple actions of EGF, acting via the EGFR. The EGFR expression is reduced at the wound margin, in burn wounds, in the late post-burn period. Subsequently, increased activation may lead to the promotion of re-epithelialisation and granulation tissue formation (Wenczak *et al*, 1992). Again, the controlled release of bioactive rhEGF, from the dextrin-rhEGF conjugate, appears to modulate the temporal sequence of normal wound healing, whereas free rhEGF has a detrimental effect on wound healing, in the impaired dermal wound model.

The maturity of the wounds was judged by the relative distributions of inflammatory and proliferative cells, such as fibroblasts. In the normal wound healing response, the sequential transition from the inflammatory phase, to a proliferative phase, is pivotal to avoid the adoption of a chronic wound phenotype (Harding *et al*, 2002). If an overwhelming inflammatory reaction occurred, in response to the dextrin-rhEGF conjugate, or any of the conjugate components, then successful wound closure may not occur. In the present Study, wound maturity was significantly increased, in all Groups, at the wound margins, compared to the central wounds. Dextrin-rhEGF did not significantly affect wound maturity, but free rhEGF and free succinoylated dextrin, did induce an inflammatory response, at the wound centre. This effect was lost at the wound margin. As the wound re-epithelialises from the edge, the wound progresses from an inflammatory, to a proliferative wound.

Therefore, as the central wound area would be the final region to exhibit this progression, this may explain the delayed resolution of inflammation at the wound centre. Successful wound closure must occur, prior to the progression to a proliferative, or maturing, wound (Martin, 1997).

7.5 Conclusions

In summary, treatment with the dextrin-rhEGF conjugate was found to accelerate the closure of full-thickness, excisional wounds, in the diabetic (db/db) mouse, relative to wounds in receipt of no treatment, free succinoylated dextrin polymer alone, or rhEGF alone. This effect appeared to be associated with a combination of both enhanced wound contraction and accelerated re-epithelialisation. No significant differences ($p > 0.05$) were observed between the two dextrin-rhEGF conjugate treatment dosing regimes, in terms of wound closure, contraction or re-epithelialisation, although a non-significant trend, suggesting a dose-dependent increase in wound re-epithelialisation, was observed. The most significant effects were apparent in the "high-dose" (10 μg/mL rhEGF equivalent), dextrin-rhEGF conjugate Group, when compared to untreated Controls, which were markedly better, than the free rhEGF Group, at equivalent concentrations. These effects may be due to a combination of the sustained release of rhEGF, from the dextrin-rhEGF conjugate, in addition to the increased resistance of the dextrin-rhEGF conjugate to proteolytic degradation, or inactivation, in the impaired wound healing environment. In addition to this effect on wound closure, the dextrin-rhEGF conjugate was determined to significantly promote the initiation of wound healing processes, in the diabetic (db/db) mouse model.

Upon histological assessment, the dextrin-rhEGF conjugate was demonstrated to: (i) Display a tendency to promote the caudo-cranial contraction of the excisional wounds, (ii) increase granulation tissue deposition (in a potentially, dose-dependent manner), (iii) display a tendency to promote the cellular maturation of neo-dermal wound tissues, and (iv) increase wound angiogenesis (in a potentially, dose- dependent manner), relative to untreated Controls.

Further refinement of the dosing schedule may improve the efficacy of the dextrin-rhEGF conjugate, although in the present Study, the observations, thus far, have been the first to report an improvement in wound healing, using rhEGF, in this impaired wound healing model. The total dose of rhEGF applied, as a component of

the dextrin-rhEGF conjugate, was also much less than in previous studies, involving free rhEGF, which have usually been applied on a daily basis. It is evident that the dextrin-rhEGF conjugate allows the application of a much lower dose of rhEGF, but has the enhanced stability and release effects, required to preferentially modulate the wound healing responses. Further studies may investigate the pharmacokinetics of the dextrin-rhEGF conjugate, *in vivo*, but the baseline investigations reported in the present Study, identified no detectable systemic absorption of rhEGF, from the topical application of the dextrin-rhEGF conjugate.

Chapter Eight

General Discussion

Chapter Eight: General Discussion

Contents

8.1 General Discussion

This is the first Study to investigate the potential of polymer therapeutics in dermal wound healing. It has highlighted key areas, such as dextrin-recombinant human epidermal growth factor (dextrin-rhEGF) conjugate synthesis, characterisation and purification, in addition to the development of appropriate assays, in which to evaluate wound healing responses, including *in vitro*, *ex vivo* and *in vivo* models.

8.2 General comments: Dextrin-rhEGF as a bioresponsive nanomedicine to improve wound healing *in vitro*

The dextrin-rhEGF conjugates synthesised herein contained, on average, 16 weight percent (wt %) protein, which corresponded to approximately 2 rhEGF molecules per polymer chain. Heterogeneity of the product was unavoidable (evident by SDS-PAGE electrophoresis; Chapter 3), which may be attributable to the polydisperse nature of the dextrin fraction used for conjugation. A narrower molecular weight dextrin fraction could be used to improve conjugate homogeneity, if necessary, for clinical evaluation. However, this dextrin of average molecular weight of 42,000 g/mol, with approximately 19 mol % succinoylation was chosen based on previous studies (Duncan *et al*, 2008), that suggested this would maximise steric "masking" of rhEGF, whilst allowing a sufficiently slow rate of dextrin degradation, by α-amylase, to liberate rhEGF, at an optimal rate for sustained bioactivity. In addition, although α-amylase will degrade the glycosidic bonds within the succinoylated dextrin polymer, the degradation is slowed by the presence of carboxylic groups and amide bonds, within the polymer-protein conjugate (Hreczuk-Hirst *et al*, 2001a). Full degradation of the conjugate would require proteinase activity. It was confirmed that the conjugation of succinoylated dextrin to rhEGF, significantly increased its stability towards proteolysis, by the clinically most important protease in chronic wound fluid, neutrophil elastase (Trengove *et al*, 1999; Cullen *et al*, 2002) (Chapter 3).

As anticipated, succinoylated dextrin polymer conjugation also reduced the biological activity of rhEGF. However, consistent with the Polymer masking UnMasking Protein Therapy (PUMPT) concept, it was demonstrated that α-amylase, when added a concentrations known to be present in human serum and chronic

wound fluid, was able to "unmask"/release rhEGF. α-Amylase-triggered rhEGF liberation was confirmed by both FPLC and ELISA (Chapter 3). Polymer degradation would, at least initially, be expected to leave oligosaccharides and/or maltose, linked to the rhEGF surface. However, the fact that the liberated rhEGF was clearly identifiable by EGF immunoassay, and moreover, able to stimulate the clinically-relevant parameter of EGF-mediated cell proliferation, underlined the effectiveness of the dextrin-rhEGF conjugate.

HEp2 cells were chosen for the cell viability/proliferation assays, as this cell line has high levels of epidermal growth factor receptor (EGFR), and their relatively rapid doubling time, made it possible to explore the effect of dextrin-rhEGF conjugate, over the more clinically relevant time frame of 8 days. The importance of α-amylase, as a trigger for the dextrin-rhEGF conjugate activation was clear throughout all the cell viability/proliferation studies performed. Furthermore, it was apparent that the stimulation of HEp2 cell proliferation by the dextrin-rhEGF conjugate, was directly related to the units of α-amylase present (Chapter 4). In the extended HEp2 cell viability/proliferation assay, it was evident that the initial delayed release of rhEGF, from the dextrin-rhEGF conjugate, led to a lag phase of approximately 24 hours in cellular response, compared to that observed with free rhEGF. However, the sustained rhEGF release from the conjugate led to enhanced activity, far beyond that achieved with rhEGF alone. This is even more impressive given that the EGF ELISA assay, determined a total release of only approximately 60 % rhEGF, at 168 hours (Chapter 3).

The value of a slow, sustained introduction of bioactive rhEGF is underlined by the biphasic, concentration-dependence of rhEGF-induced proliferation (Chapter 4). Clearly, high local concentrations of rhEGF must be prevented if inhibition of wound healing is to be avoided (Lai *et al*, 1989; Breuing *et al*, 1997). More clinically relevant cells, HaCaT keratinocytes and fibroblasts, derived from both normal dermal and chronic wound origin, also demonstrated enhanced proliferation, in the presence of the dextrin-rhEGF conjugate, activated by physiological levels of α-amylase. Furthermore, it was identified that dextrin-rhEGF conjugates exposed to trypsin (as a model proteinase), prior to α-amylase exposure, retained the ability to promote cell proliferation. Experiments to investigate the cellular mechanism of action of the dextrin-rhEGF conjugate, in HEp2 cells, identified that the conjugate

exposed to α-amylase was able to induce EGFR and STAT3 phosphorylation (Chapter 5). This suggested a direct effect on the EGFR and a promotion on signal transduction. Such stimulatory effects on migration and wound repopulation would be key features of chronic wound repair *in vivo*.

8.3 General comments: Dextrin-rhEGF as a bioresponsive nanomedicine to improve wound healing *in vivo*

The dextrin-rhEGF conjugate, described herein, was synthesised with the aim of protecting the growth factor from the proteolytic chronic wound environment, whilst permitting the restoration of bioactivity, with time, when exposed to physiological concentrations of α-amylase, using the PUMPT concept (Duncan *et al*, 2008). Normal serum α-amylase concentrations occur between a range of 30-300 i.u./L (Raftery, 1998; Branca *et al*, 2001), whilst levels in chronic wound fluids occur in a similar range (Chapter 6). In this way, α-amylase levels in the chronic wound environment would be anticipated to generate novel therapeutics for improved wound repair. Traditional wound therapy involves the use of topical agents to clean, disinfect and stimulate healing (Menke *et al*, 2007). This can be a protracted, painful process, that is often associated with high levels of morbidity (Harding *et al*, 2002). In contrast to acute wounds, chronic wounds fail to show the controlled inflammatory, proliferative and remodelling phases of normal wound healing (Mustoe *et al*, 2006). Numerous factors can be responsible for this malfunction, including wound infection, tissue hypoxia, failed angiogenesis and the underlying uncoupling of the normal growth factor cascade. Many attempts have been made to find more effective therapies for chronic wounds, but there has been little success (Mekkes *et al*, 2003). Natural and synthetic polymers have been explored as biodegradable matrices or hydrogels for the controlled release of growth factors (Saltzman and Olbricht, 2002). However, although their topical application in conjugation with rhEGF, can increase the rate of re-epithelialisation, in acute wounds (Tanaka *et al*, 2005), little or no significant clinical improvement in chronic wound healing has ever been demonstrated (Falanga *et al*, 1992; Danilenko *et al*, 1995). Consequently, rhEGF remains an experimental protein and its fate seems to depend upon a reappraisal of delivery strategies (Prats *et al*, 2002).

With the implementation of two independent models of wound healing (Chapters 6 and 7), involving two different species of animal (a rat, *ex vivo* organotypic model of acute wound healing and a mouse, *in vivo* model of impaired dermal wound healing), a significant step-forward in the pre-clinical assessment of the dextrin-rhEGF conjugate, was achieved. The data obtained from the *in vitro* models of wound healing, involving the stimulation of cellular proliferation and migration of cells associated with the normal and pathological wound healing response, was reproduced in both animal models. Similar findings were obtained both *in vitro, ex vivo* and *in vivo*, including the concentration-dependent toxicity of high rhEGF concentration and the enhanced effect on wound healing by rhEGF, following release from the dextrin-rhEGF conjugate, by physiological levels of α-amylase.

The *ex vivo* model, by design, was similar to the *in vitro* model of cell migration. The experiments were performed over a similar time-scale, and the tissue culture medium used for the fibroblasts *in vitro* and the corneas *ex vivo,* was of the same composition. The exogenous α-amylase (93 i.u./L) utilised, was from the same source and prepared in an identical fashion. Although different batches of the dextrin-rhEGF were utilised in these experiments, similar results were observed, namely enhanced wound healing with the dextrin-rhEGF conjugate, "masking" and "unmasking" of the dextrin-rhEGF conjugate, in response to physiological levels of α-amylase, and the absence of wound healing, with individual component Controls.

Previous *in vivo* and clinical studies involving rhEGF have failed to demonstrate a significant clinical effect on wound area reduction, in impaired wound healing models (Falanga *et al*, 1992; Tsang *et al*, 2003; Choi *et al*, 2007). Suppression of the healing response, by free rhEGF, was reported by Choi *et al* (2008), in a similar fashion to the findings in the present Study. In acute wound models and clinical studies, rhEGF consistently reduces wound area compared to Controls (Brown *et al*, 1989; Mustoe *et al*, 1991; Tanaka *et al*, 2005; Kwon *et al*, 2006). However, it must be considered that these small sample number trials have not yet resulted in a USA/UK licensed product for use in humans.

Current products that are available in the wound healing field that contain rhEGF are at a high rhEGF concentration (ReGenD150; 150μg rhEGF per g of carrier matrix, resulting in mg quantities of rhEGF being applied to a large wound

area), to account for the protein degradation in chronic wounds (Krishna-Mohan, 2007). At high levels, the systemic uptake may be increased, potentially leading to peripheral side effects, due to rhEGF. EGF promotes tumour invasion in EGFR positive cancer cells (Zolfaghari and Djakiew, 1996; Kondapaka *et al*, 1997; Angelucci *et al*, 2006). Therefore, based upon the findings herein, the dextrin-rhEGF conjugate, containing rhEGF at a much lower concentration, would need less rhEGF for the manufacture of dextrin-rhEGF, and a less concentrated formulation will need to be applied. Indeed, stimulation of cells in these experiments occurred at pg/L concentrations, at levels that are similar to normal serum EGF levels (317 pg/mL ± 31 pg/mL; Savage *et al*, 1986). Thus, any systemic absorption, or release of rhEGF, from dextrin-rhEGF, would be at physiological levels. The most advanced clinical trial, involving rhEGF application to chronic wounds, has involved 135 participants in a multi-centre phase IV, post-marketing surveillance Study, which reported enhanced wound healing, with no significant side-effects, although some elements of the Study design and report may be questioned (Krishna-Mohan, 2007).

The reasons for the limited success of growth factor therapy has been attributed to (i) an inappropriate release profile in the clinical setting, (ii) the lack of stability of the protein in the delivery system or post-delivery, (iii) rapid protein degradation of rhEGF, by chronic wound proteinases or denaturation by reactive oxygen species (ROS) (James *et al*, 2003; Moseley *et al*, 2004), (iv) the lack of stability of the protein in the delivery vehicle used for application, and/or the toxicity of the polymeric carrier used (e.g. a polyethyleinimine-nitric oxide adduct; Bauer *et al*, 1998). It should be noted, however, that one approach, Regranex®, which is a topically-applied gel, containing recombinant human, platelet derived growth factor (rhPDGF), recently became the first recombinant growth factor to be approved by the US Food and Drug Administration (FDA), for the acceleration of wound healing and it is currently used in the treatment of diabetic foot ulcers. However, even in this case, Regranex® has been shown to be only effective in selected wounds (< 1.5 cm^2), in conjunction with good wound care, with no reduction in ulcer recurrence, when compared to good wound care alone (Steed, 2006). More recently, in March 2008, the FDA reported an ongoing safety review of Regranex®, concluding that people who have used three or more tubes of becaplermin gel, and who have or develop cancer, are more likely to die from the cancer than people who have cancer, and who

have not used becaplermin gel (FDA, 2008). However, despite these concerns, the product still remains licensed for use, at present.

The improvement in wound healing, reported in the present Study (Chapter 7), attributed to the dextrin-rhEGF conjugate, is more significant than other studies involving rhEGF and its application to chronic wounds *in vivo* (Choi *et al*, 2008). Regranex® has been reported to consistently improve the granulation tissue deposition, when applied *in vivo*, to wounds in genetically diabetic (db/db) mice, although wound closure is not significantly affected (Brown *et al*, 1994; LeGrand, 1998; Chan *et al*, 2006). The dextrin-rhEGF conjugate, not only enhanced granulation tissue deposition in the diabetic mouse model, but also significantly increased wound closure rates. The aforementioned concerns about the safety of Regranex®, may open the door for new wound healing products, such as the dextrin-rhEGF conjugate, given that dextrin has an established safety profile (Day, 2003), which may out-perform existing products. Further pre-clinical investigation may result in the production of the dextrin-rhEGF conjugate that could be scaled up to an industrial level (such as further purification, possibly via chromatographic techniques, to remove any residual free polymer). It has been previously argued that Regranex® is a cost-effective treatment for chronic wounds (Ghatnekar *et al*, 2001), but the observed effects are marginal (Persson *et al*, 2000). With lower component costs than Regranex®, dextrin-rhEGF may represent a more cost-effective option, although it must be considered that further developmental costs and industrial production, could significantly affect the final costings.

8.4 General comments: Polymer therapeutics to modulate cellular responses in impaired human wound healing

In conclusion, the present Study has demonstrated, for the first time, the potential of a bioresponsive, polymer therapeutic, as a nanomedicine for wound healing. For effective bioresponsive drug delivery, the system must have at least three components, a biosensor for detecting external signals; signal processing for determining when to respond; and an actuator for drug release. Many studies have shown that successful bioresponsive systems require additional functions, such as protecting the drug, until required, and releasing the drug in a timely, controlled manner (Park, 2008). The development of a bioresponsive polymer–drug conjugate,

designed specifically to promote wound healing, opens a new possibility of bioresponsive drug delivery, not only for treatment of acute and chronic dermal wounds, but also for drug targeting, based on specific stimuli found at a target site.

The positive effects observed with the dextrin-rhEGF conjugate during *in vitro, ex vivo* and *in vivo* Studies, would support the further evaluation of the conjugate towards clinical trials. First clinical studies would certainly involve the local, topical application of the dextrin-rhEGF conjugate to diabetic and/or venous leg ulcers. These pathologies are causative of the majority of non-healing, chronic wounds and as such, there is real clinical need for new treatment therapies. However, the dextrin-rhEGF conjugate also has potential for intravenous administration, as it would be expected to exhibit targeted delivery to wounds developing new blood vessels, by angiogenesis and thus, display localised vascular hyperpermeability, for example, via the enhanced permeability and retention (EPR) effect (Matsumara and Maeda, 1986). Given that recent studies have shown that polymer conjugates can be tailored to deliver an anticancer combination therapy (Vicent *et al*, 2005), the approach reported here has also has the versatility to deliver other established growth factors (and / or their combinations), integral to the enhancement of dermal wound healing. This Study also verifies the broader therapeutic potential of the PUMPT concept, especially using the combination of dextrin and α-amylase, as the enzyme is widely distributed in serum and extracellular fluids (Miyasaka and Rothman, 1982).

The present Study has formed the basis for further translational research and development of the dextrin-rhEGF conjugate, from the "bench to the bedside", hopefully to provide a more effective treatment strategy, for impaired dermal wound healing, than those currently available. Given the overwhelming evidence, described herein, to support the PUMPT concept, it could be further applied to other polymers and bioactive proteins, in the future treatment of a variety of medical disorders. The use of different growth factors, antimicrobial agents, or antioxidants, alone or in combination as a co-conjugate, may be applicable to areas of regenerative medicine involving different tissues, such as bone and cartilage, or more complex organs, including the kidney or brain.

Bibliography

Abdel-Latif D, Steward M, MacDonaold DL, Francis GA, Dinauer MC, Lacy P (2004) Rac2 is critical for neutrophil primary granule exocytosis. *Blood* **104:** 832-839

Abraham LC, Vorrasi J, Kaplan DL (2004) Impact of collagen structure on matrix trafficking by human fibroblasts. *Journal of Biomedical Materials Research Part A* **70:** 39-48

Abrams CK, Hamosh M, Dutta SK, Hubbard VS, Hamosh P (1987) Role of nonpancreatic lipolytic activity in exocrine pancreatic insufficiency. *Gastroenterology* **92:** 125-129

Abuchowski A, McCoy JR, Palczuk NC, van Es T, Davis FF (1977) Effect of covalent attachment of polyethylene glycol on immunogenicity and circulating life of bovine liver catalase. *Journal of Biological Chemistry* **252:** 3582-3586

Advanced Light Source (2008) http://www.infrared.als.lbl.gov/content/web-links/60-ir-band-positions. Accessed on 01/10/08

Ågren UM, Tammi RH, Tammi MI (1997) Reactive oxygen species contribute to epidermal hyaluronan catabolism in human skin organ culture. *Free Radical Biology and Medicine* **23:** 996-1001

Ahn ST, Mustoe TA (1990) Effects of ischemia on ulcer wound healing: A new model in the rabbit ear. *Annals of Plastic Surgery* **24:** 17-23

Ajani G, Sato N, Mack J, Maytin E (2007) Cellular responses to disruption of the permeability barrier in a 3-demensional organotypic model. *Experimental Cell Research* **313:** 3005-3015

Albelda SM, Muller WA, Buck CA, Newman PJ (1991) Molecular and cellular properties of PECAM-1 (endoCAM/CD31): A novel vascular cell-cell adhesion molecule. *Journal of Cell Biology* **114:** 1059-1068

Albrecht-Buehler G (1977) The phagokinetic tracks of 3T3 cells. *Cell* **11:** 359-404

Alemdaroglu C, Degim Z, Celebi N, Sengezer M, Alomeroglu M, Nacar A (2008) Investigation of epidermal growth factor containing liposome formulation effects on burn wound healing. *Journal of Biomedical Materials Research Part A* **85:** 271-283

Alemdaroglu C, Degim Z, Celebi N, Zor F, Ozturk S, Erdogan D (2006) An investigation on burn wound healing in rats with chitosan gel formulation containing epidermal growth factor. *Burns* **32:** 319-327

Al-Khateeb T, Stephens P, Shepherd JP, Thomas DW (1997) An investigation of preferential fibroblast wound repopulation using a novel *in vitro* wound model. *Journal of Periodontology* **68:** 1063-1069

Bode W, Maskos K (2003) Structural basis of the matrix metalloproteinases and their physiological inhibitors, the tissue inhibitors of metalloproteinases. *Biological Chemistry* **384:** 863-72

Bond JS, Duncan JAL, Sattar A, Boanas A, Mason T, O'Kane S, Ferguson MWJ (2008) Maturation of the human scar: An observational study. *Plastic and Reconstructive Surgery* **121:** 1650-1658

Boonstra J, Rijken P, Humbel B, Cremers F, Verkleij A, van Bergen en Henegouwen P (1995) The epidermal growth factor. *Cell Biology International* **19:** 413-430

Borradori L, Sonnenberg A (1996) Hemidesmosomes: Roles in adhesion, signaling and human diseases. *Current Opinion in Cell Biology* **8:** 647-656

Boukamp P, Petrussevska RT, Breitkreutz D, Hornung J, Markham A (1988) Normal keratinization in a spontaneously immortalized aneuploid human keratinocyte cell line. *Journal of Cell Biology* **106:** 761-771

Boulais N, Misery L (2008) The epidermis: A sensory tissue. *European Journal of Dermatology* **18:** 119-127

Boyden S (1962) The chemotactic effect of mixtures of antibody and antigen on polymorphonuclear leucocytes. *Journal of Experimental Medicine* **115:** 453-466

Brake AJ, Merryweather JP, Coit DG, Heberlein UA, Masiarz FR, Mullenbach GT, Urdea MS, Valenzuela P, Barr PJ (1984) α-Factor-directed synthesis and secretion of mature foreign proteins in *Saccharomyces cerevisiae*. *Proceedings of the National Academy of Sciences USA* **81:** 4642-4646

Branca P, Rodriguez M, Rogers JT, Ayo DJ, Moyers JP, Light RW (2001) Routine measurement of pleural fluid amylase in not indicated. *Archives of Internal Medicine* **161:** 228-232

Breuing K, Andree C, Helo G, Slama J, Liu PY, Ericksson E (1997) Growth factors in the repair of partial thickness porcine skin wounds. *Plastic and Reconstructive Surgery* **100:** 657-664

Breuss JM, Gallo J, DeLisser HM, Klimanskaya IV, Folkesson HG, Pittet JF, Nishimura SL, Aldape K, Landers DV, Carpenter W, Gillett N, Sheppard D, Matthay MA, Albelda SM, Kramer RH, Pytela R (1995) Expression of the β6 integrin subunit in development, neoplasia and tissue repair suggests a role in epithelial remodeling. *Journal of Cell Science* **108:** 2241-2251

Briggs SL (2005) The role of fibronectin in fibroblast migration during tissue repair. *Journal of Wound Care* **14:** 284-287

British National Formulary (2008) BMJ Group, London; and RPS Publishing, London

Broughton G, Janis JE, Attinger CE (2006a) The basic science of wound healing. *Plastic and Reconstructive Surgery* **117:** S12-S34

Broughton G, Janis JE, Attinger CE (2006b) Wound healing: An overview. *Plastic and Reconstructive Surgery* **117:** S1-S32

Brown GL, Nanney LB, Griffen J, Cramer AB, Yancey JM, Curtsinger LJ, Holtzin L, Schultz GS, Jurkiewicz MJ, Lynch JB (1989) Enhancement of wound healing by topical treatment with epidermal growth factor. *New England Journal of Medicine* **321:** 76-79

Brown J (2005) The role of the fibrin cuff in the development of venous leg ulcers. *Journal of Wound Care* 2005 **14:** 324-327

Brown RD, Jones GM, Laird RE, Hudson P, Long CS (2007) Cytokines regulate matrix metalloproteinases and migration in cardiac fibroblasts. *Biochemical and Biophysical Research Communications* **362:** 200-205

Brown RL, Breeden MP, Greenhalgh DG (1994) PDGF and TGF-α act synergistically to improve wound healing in the genetically diabetic mouse. *Journal of Surgical Research* **56:** 562-570

Bruneel D, Schacht E (1993a) Chemical Modification of Pullulan: 1. Periodate oxidation. *Polymer* **34:** 2628-2632

Bruneel D, Schacht E (1993b) Chemical Modification of Pullulan: 2. Chloroformate activation. *Polymer* **34:** 2633-2658

Bruneel D, Schacht E (1994) Chemical Modification of Pullulan: 3. Succinoylation. *Polymer* **35:** 2656-2658

Bucala R, Spiegel LA, Chesney J, Hogan M, Cerami A (1994) Circulating fibrocytes define a new leukocyte subpopulation that mediates tissue repair. *Molecular Medicine* **1:** 71-81

Bucalo B, Eaglstein WH, Falanga V (1993) Inhibition of cell proliferation by chronic wound fluid. *Wound Repair and Regeneration* **1:** 181-186

Buckley A, Davidson JM, Kamerath CD, Wolt TB, Woodward SC (1985) Sustained release of epidermal growth factor accelerates wound repair. *Proceedings of the National Academy of Sciences USA* **82:** 7340-7344

Bundred NJ, Chan K, Anderson NG (2001) Studies of epidermal growth factor receptor inhibition in breast cancer. *Endocrine-Related Cancer* **8:** 183-189

Burgeson RE, Christiano AM (1997) The dermo-epidermal junction. *Current Opinions in Cell Biology* **9:** 651-658

Burkart J (2004) Metabolic consequences of peritoneal dialysis. *Seminars in Dialysis* **6:** 498-504

Candiloros H, Muller S, Zeghari N, Donner M, Drouin P, Ziegler O (1995) Decreased erythrocyte membrane fluidity in poorly controlled IDDM. Influence of ketone bodies. *Diabetes Care* **18:** 549-551

Carmeliet P, Jain RK (2000) Angiogenesis in cancer and other diseases. *Nature* **407:** 249-257

Carpenter G, Cohen S (1990) Epidermal growth factor. *Journal of Biological Chemistry* **265:** 7709-7712

Carpenter G, King L, Cohen S (1978) Epidermal growth factor stimulates phosphorylation in membrane preparations *in vitro*. *Nature* **276:** 409-410

Carrino DA, Onnerfjord P, Sandy J, Cs-Szabo G, Scott PG, Sorrell JM, Heinegård D, Caplan AI (2003) Age-related changes in the proteoglycans of human skin. *Journal of Biological Chemistry* **278:** 17566-17572

Castro-Combs J, Noguera G, Cano M, Yew M, Gehlbach PL, Palmer J, Behrens A (2008) Corneal wound healing is modulated by topical application of amniotic fluid in an *ex vivo* organ culture model. *Experimental Eye Research* **87:** 56-63

Cavani A, Zambruno G, Marconi A, Manca V, Marchetti M, Giannetti A (1993) Distinctive integrin expression in the newly forming epidermis during wound healing in humans. *Journal of Investigative Dermatology* **101:** 600-604

Chaffee S, Mary A, Stiehm ER, Girault D, Fischer A, Hershfield MS (1992) IgG antibody response to polyethylene glycol-modified adenosine deaminase in patients with adenosine deaminase deficiency. *Journal of Clinical Investigation* **89:** 1643-1651

Chalfie M, Tu Y, Euskirchen G, Ward WW, Prasher DC (1994) Green fluorescent protein as a marker for gene expression. *Science* **263:** 802-805

Chan KC, Knox WF, Gee JM, Morris J, Nicholson RI, Potten CS, Bundred NJ (2002) Effect of epidermal growth factor receptor tyrosine kinase inhibition on epithelial proliferation in normal and premalignant breast. *Cancer Research* **62:** 122-128

Chan KY, Lindquist TD, Edenfield MJ, Nicolson MA, Banks AR (1991) Pharmacokinetic study of recombinant human epidermal growth factor in the anterior eye. *Investigative Ophthalmology and Visual Science* **32:** 3209-3215

Chan LS (1997) Human skin basement membrane in health and in autoimmune diseases. *Frontiers in Bioscience* **2:** 343-352

Chan RK, Liu PH, Pietramaggiori G, Ibrahim SI, Hechtman HB, Orgill DP (2006) Effect of recombinant platelet-derived growth factor (Regranex) on wound closure in genetically diabetic mice. *Journal of Burn Care Research* **27:** 202-205

Chen C, Schultz GS, Bloch M, Edwards PD, Tebes S, Mast BA (1999) Molecular and mechanistic validation of delayed healing rat wounds as a model for human chronic wounds. *Wound Repair and Regeneration* **7:** 486-494

Chen WY, Abatangelo G (1999) Function of hyaluronan in wound repair. *Wound Repair and Regeneration* **7:** 79-89

Chi CC, Wang SH, Kuo TT (2006) Localized cutaneous polyvinylpyrrolidone storage disease mimicking cheilitis granulomatosa. *Journal of Cutaneous Pathology* **33:** 454-457

Chiquet M, Renedo AS, Huber F, Fluck M (2003) How do fibroblasts translate mechanical signals into changes in extracellular matrix production. *Matrix Biology* **22:** 73-80

Chui HC, Hsiue GH, Lee YP, Huang LW (1999) Synthesis and characterization of pH-sensitive dextran hydrogels as a potential colon-specific drug delivery system. *Journal of Biomaterials Science* **10:** 591-608

Choi J, Leong K, Yoo H (2008) *In vivo* wound healing of diabetic ulcers using electrospun nanofibers immobilized with human epidermal growth factor (EGF). *Biomaterials* **29:** 587-596

Chong EJ, Phan TT, Lim IJ, Zhang YZ, Bay BH, Ramakrishna S, Lim CT (2007) Evaluation of electrospum PCL/gelatin nanofibrous scaffold for wound healing and layered dermal reconstruction. *Acta Biomaterialia* **3:** 321-330

Clark RAF (1993) Basics of cutaneous repair. *Journal of Dermatologic Surgery And Oncology* **19:** 693-706

Clark RAF, Lin F, Greiling D, An J, Couchman JR (2004) Fibroblast invasive migration into fibronectin/fibrin gels requires a previously uncharacterized dermatan sulfate-CD44 proteoglycan. *Journal of Investigative Dermatology* **122:** 266-277

Cohen S (1962) Isolation of a mouse submaxillary gland protein accelerating incisor eruption and eyelid opening in the new-born animal. *Journal of Biological Chemistry* **237:** 1555-1562

Coleman DL (1982) Diabetes-obesity syndromes in mice. *Diabetes* **31:** S1-S6

Constantine BE, Bolton LL (1986) A wound model for ischemic ulcers in the guinea pig. *Archives of Dermatological Research* **278:** 429-431

Cooper DM, Yu EZ, Hennessey P, Ko F, Robson MC (1994) Determination of endogenous cytokines in chronic wounds. *Annals of Surgery* **219:** 688-691

Costa SA, Reis RL (2004) Immobilisation of catalase on the surface of biodegradable starch-based polymers as a way to change its surface characteristics. *Journal of Materials Science* **15:** 335-342

Cromack DT, Porras-Reyes B, Purdy JA, Pierce GF, Mustoe TA (1993) Acceleration of tissue repair by transforming growth factor beta 1: Identification of *in vivo* mechanism of action with radiotherapy-induced specific healing deficits. *Surgery* **113:** 36-42

Crosson CE, Klyce SD, Beuerman RW (1986) Epithelial wound closure in the rabbit cornea: A biphasic process. *Investigative Ophthalmology and Visual Science* **27:** 464-473

Cullen B, Smith R, McCulloch E, Silcock D, Morrison L (2002) Mechanism of action of Promogran®, a protease modulating matrix, for the treatment of diabetic foot ulcers. *Wound Repair and Regeneration* **10:** 16-25

Curtsinger LJ, Pietsch JD, Brown GL, von Fraunhofer A, Ackerman D, Polk H, Jr, Schultz GS (1989) Reversal of adriamycin-impaired wound healing by transforming growth factor-beta. *Surgery Gynecology and Obstetrics* **168:** 517-522

Daniele S, Frati L, Fiore C, Santoni G (1979) The effect of the epidermal growth factor (EGF) on the corneal epithelium in humans. *Albrecht von Graefes Archiv fur Klinische und Experimentelle Ophthalmologie* **210**: 159-165

Danilenko DM, Ring BD, Tarpley JE, Morris B, Van GY, Morawiecki A, Callahan W, Goldenberg M, Hershenson S, Pierce GF (1995) Growth factors in porcine full- and partial-thickness burn repair. Differing targets and effects of keratinocyte growth factor, platelet-derived growth factor-BB, epidermal growth factor, and neu differentiation factor. *American Journal of Pathology* **147:** 1261-1277

Darby IA, Hewitson TD (2007) Fibroblast differentiation in wound healing and fibrosis. *International Review of Cytology* **257:** 143-179

Darnell JE (1997) STATs and gene regulation. *Science* **227:** 1630-1635

Davidson JM (1998) Animal models for wound repair. *Archives of Dermatological Research* **290:** S1-S11

Davies CE, Hill KE, Newcombe RG, Stephens P, Wilson MJ, Harding KG, Thomas DW (2007) A prospective study of the microbiology of chronic venous leg ulcers to re-evaluate the clinical predictive value of tissue biopsies and swabs. *Wound Repair and Regeneration* **15:** 17-22

Davies DS (1994) Kinetics of icodextrin. *Peritoneal Dialysis International* **14:** S45-S50

Davis SC, Cazzaniga AL, Ricotti C, Zalesky P, Hsu L, Creech J, Eaglestein WH, Mertz PM (2007) Topical oxygen emulsion. *Archives of Dermatology* **143:** 1252-1256

Davies SJ (2006) Exploring new evidence of the clinical benefits of icodextrin solutions. *Nephrology, Dialysis and Transplant* **21:** S47-S50

Dawra R, Sharif R, Phillips P, Dudeja V, Dhaulakhandi D, Saluja AK (2007) Development of a new mouse model of acute pancreatitis induced by administration of L-arginine. *American Journal of Physiology Gastrointestinal and Liver Physiology* **292:** 1009-1018

Day A (2003) Dextrin. In: *Handbook of Pharmacuetical Excipients.* Eds: Rowe RC, Shesky PJ, Welleb PJ. Pharmaceutical Press and American Pharmaceutical Association, Washington DC, pp 197-199

Desmouliere A, Chaponnier C, Gabiani G (2005) Tissue repair, contraction and the myofibroblast. *Wound Repair and Regeneration* **13:** 7-12

Desmouliere A, Gabbiani G (1996) The role of the myofibroblast in wound healing and fibrocontractive diseases, In: *The Molecular and Cellular Biology of Wound Repair.* Ed: Clark RAF. Plenum Press, New York, pp 391-423

Deuel TF, Huang JS (1984) Platelet-derived growth factor. Structure, function, and roles in normal and transformed cells. *Journal of Clinical Investigation* **74:** 669-676

Devakumar J, Mookambeswaran V (2007) A novel affinity-based controlled release system involving derivatives of dextran with enhanced osmotic activity. *Bioconjugate Chemistry* **18:** 477-483

Di Vita G, Patti R, D'Agostino P, Caruso G, Arcara M, Buscemi S, Bonventre S, Ferlazzo V, Arcoleo F, Cillari E (2006) Cytokines and growth factors in wound drainage fluid from patients undergoing incisional hernia repair. *Wound Repair and Regeneration* **14:** 259-264

Dibb NJ, Dilworth SM, Mol CD (2004) Switching on kinases oncogenic activation of BRAF and the PDGFR family. *Nature Reviews Cancer* **4:** 718-727

Dini V, Romanelli M, Piaggesi A, Stefani A, Mosca F (2006) Cutaneous tissue engineering and lower extremity wounds. *International Journal of Lower Extremity Wounds* **5:** 27-34

DiPietro LA (1995) Wound healing: The role of macrophages and other immune cells. *Shock* **4:** 233-240

Doljanski F (2004) The sculpturing role of fibroblast-like cells in morphogenesis. *Perspectives in Biology and Medicine* **47:** 339-356

Dormandy JA (1997) Pathophysiology of venous leg ulceration - An update. *Angiology* 1997 **48:** 71-75

Duncan R (2003) The dawning era of polymer therapeutics. *Nature Reviews Drug Discovery* **2:** 347-360

Duncan R (2005) N-(2-Hydroxypropyl)methacrylamide copolymer conjugates. In: *Polymeric Drug Delivery Systems*. Ed: Kwon GS. Marcel Dekker Inc., New York, pp 1-92

Duncan R (2006) Polymer conjugates as anticancer nanomedicines. *Nature Reviews Cancer* **6**: 688-701

Duncan R, Gilbert HRP, Carbajo RJ, Vicent MJ (2008) Polymer Masked-Unmasked Protein Therapy (PUMPT) 1. Bioresponsive dextrin-trypsin and -MSH conjugates designed for α-amylase activation. *Biomacromolecules* **9**: 1146-1154

Dunn P, Kuo T, Shih LY, Wang PN, Sun CF, Chang MJ (1998) Bone marrow failure and myelofibrosis in a case of PVP storage disease. *American Journal of Hematology* **57**: 68-71

Eckert RL (1989) Structure, function and differentiation of the keratinocyte. *Physiological Reviews* **69**: 1316-1346

Edmondson SR, Thumiger SP, Werther GA, Wraight CJ (2003) Epidermal homeostasis: The role of growth hormone and insulin-like growth factor systems. *Endocrinology Reviews* **24**: 737-764

Egles C, Shamis Y, Mauney JR, Volloch V, Kaplan DL, Garlick JA (2008) Denatured collagen modulates the phenotype of normal and wounded human skin equivalents. *Journal of Investigative Dermatology* **128**: 1830-1837

Elliott JH (1980) Epidermal growth factor: *In vivo* ocular studies. *Transactions of the American Ophthalmology Society* **78**: 629-656

Ellis DI, Goodacre R (2006) Metabolic fingerprinting in disease diagnosis: Biomedical applications of infrared and Raman spectroscopy. *The Analyst* **131**: 875-885

Ellis-Behnke RG, Liang YL, Tay DKC, Kau PWF, Schneider GE, Zhang S, Wu W, So K (2006) Nano hemostat solution: Immediate hemostasis at the nanoscale. *Nanomedicine: Nanotechnology, Biology and Medicine* **2**: 207-215

Engström W, Rees AR, Heath JK (1985) Proliferation of a human embryonal carcinoma-derived cell line in serum-free medium: Inter-relationship between growth factor requirements and membrane receptor expression. *Journal of Cell Science* **73**: 361-373

Escamez MJ, Garcia M, Larcher F, Meana A, Munoz E, Jorcano JL, Del Rio M (2004) An *in vivo* model of wound healing in genetically modified skin-humanized mice. *Journal of Investigative Dermatology* **123**: 1182-1191

European Science Foundation (2005) ESF: European Medical Research Councils (EMRC) Forward Look report, "Nanomedicine"

Even-Ram S, Yamada KM (2005) Cell migration in 3D matrix. *Current Opinion in Cell Biology* **17:** 524-532

Falanga V, Eaglstein WH, Bucalo B, Katz MH, Harris B, Carson P (1992) Topical use of human recombinant epidermal growth factor (h-EGF) in venous ulcers. *Journal of Dermatologic Surgery and Oncology* **18:** 604-606

Falanga V (1993) Growth factors and wound healing. *Dermatology Clinics* **11:** 667-675

Falanga V, Eaglestein WH (1993) The "trap" hypothesis of venous ulceration. *The Lancet* **341:** 1006-1008

Falasca M, Logan SK, Lehto VP, Baccante G, Lemmon MA, Schlessinger J (1998) Activation of phospholipase C gamma by PI 3-kinase-induced PH domain-mediated membrane targeting. *The EMBO Journal* **17:** 414-422

Falette N, Frappart L, Lefebvre MF, Saez S (1989) Increased epidermal growth factor receptor level in breast cancer cells treated with 1,25-dihydroxyvitamin D3. *Molecular and Cellular Endocrinology* **63:** 189-198

Farahani RM, Kloth LC (2008) The hypothesis of "biophysical matrix contraction": Wound contraction revisited. *International Wound Journal* **5:** 477-482

Fausto N (2000) Liver regeneration. *Journal of Hepatology* **32:** 19S-31S

Federal Drug Administration (2008) http://www.fda.gov/cder/drug/early_comm/becaplermin.htm. Accessed on 01/10/08

Ferguson E, Schmaljohann D, Duncan R (2006) Polymer-phospholipase conjugates as novel anti-cancer agents: Dextrin phospholipase A2. *Proceedings of the Controlled Release Society* **33:** 660

Ferguson KM, Berger MB, Mendrola JM, Cho H, Leahy DJ, Lemmon MA (2003) EGF activates its receptor by removing interactions that autoinhibit ectodomain dimerzation. *Molecular Cell* **11:** 507-517

Flueckiger F, Kodjikian L, Halberstadt M, Boehnke M, Garweg JG (2005) An *ex vivo*, whole-globe porcine model of corneoepithelial wound healing tested using immunomodulatory drugs. *Journal of Ocular Pharmacology and Therapeutics* **21:** 367-375

Fong J, Wood F (2006) Nanocrystalline silver dressings in wound management: A review. *International Journal of Nanomedicine* **1:** 441-449

Fowkes FG, Evans CJ, Lee AJ (2001) Prevalence and risk factors of chronic venous insufficiency. *Angiology* **52:** S5-15

Frampton JE, Plosker GL (2003) Icodextrin. A review of its use in peritoneal dialysis. *Drugs* **63:** 2079-2105

Franklin JD, Lynch JB (1979) Effects of topical applications of epidermal growth factor on wound healing. Experimental study on rabbit ears. *Plastic and Reconstructive Surgery* **64:** 766-770

Frati C, Scarpa C (1971) Treatment of experimental mouse burns with EGF (Epidermal Growth Factor) applied locally as a lotion. *Giornale Italiano di Dermatolotia Minerva Dermatologica* **46:** 73-76

Frew SE, Rezaie R, Sammut SM, Ray M, Daar AS, Singer PA (2007) India's health biotech sector at a crossroads. *Nature Biotechnology* **25:** 403-417

Fuchs E (2007) Scratching the surface of skin development. *Nature* **445:** 834-842

Gabbiani G (1992) The biology of the myofibroblast. *Kidney International* **41:** 530-533

Garcia M, Escamez MJ, Carretero M, Mirones I, Martinez-Santamaria L, Navarro M, Jorcano JL, Meana A, Del Rio M, Larcher F (2007) Modeling normal and pathological processes through skin tissue engineering. *Molecular Carcinogenesis* **46:** 741-745

Garlick JA, Taichamn LB (1994) Fate of human keratinocytes during reepithelialisation in an organotypic culture model. *Laboratory Investigation* **70:** 916-924

Gedda L, Olsson P, Ponten J, Carlsson J (1996) Development and *in vitro* studies of epidermal growth factor-dextran conjugates for boron neutron capture therapy. *Bioconjugate Chemistry* **7:** 584-591

Ghatnekar O, Persson U, Willis M, Odegaard K (2001) Cost effectiveness of Becaplermin in the treatment of diabetic foor ulcers in four European countries. *Pharmacoeconomics* **19:** 767-778

Ghohestani RF, Li K, Rouselle P, Uitto J (2001) Molecular organization of the cutaneous basement membrane zone. *Clinics in Dermatology* **19:** 551-562

Gildner CD, Lerner AL, Hocking DC (2004) Fibronectin matrix polymerization increases tensile strength of model tissue. *American Journal of Physiology Heart and Circulatory Physiology* **287:** H46-H53

Gill GN, Lazar CS (1981) Increased phosphotyrosine content and inhibition of proliferation in EGF-treated A431 cells. *Nature* **293:** 305-307

Gillitzer R, Goebeler M (2001) Chemokines in cuteneous wound healing. *Journal of Leukocyte Biology* **69:** 513-521

Godin B, Touitou E (2007) Transdermal skin delivery: Predictions for humans from *in vivo*, *ex vivo* and animal models. *Advanced Drug Delivery Reviews* **59:** 1152-1161

Goldman R (2004) Growth factors and chronic wound healing: Past, present and future. *Advances in Skin and Wound Care* **17:** 24-35

Goodson WH, Hunt TK (**1979a**) Deficient collagen formation by obese mice in a standard wound model. *American Journal of Surgery* **138:** 692-694

Goodson WH, Hunt TK (**1979b**) Wound healing and the diabetic patient. *Surgery, Gynecology and Obstetrics* **149:** 600-608

Gordon KJ, Blobe GC (2008) Role of transforming growth factor-β superfamily signalling pathways in human disease. *Biochemica et Biophysica Acta* **1782:** 197-228

Graves RA, Freeman T, Mandal TK (2007) *In vitro* dissolution methos for evaluation of buprenorphine *in situ* gel formation: A technical note. *American Association of Pharmaceutical Scientists PharmSciTech* **8:** E1-E4

Grazul-Bilska AT, Johnson ML, Bilski JJ, Redmer DA, Reynolds LP, Abdullah A, Abdullah KM (2003) Wound healing: The role of growth factors. *Drugs Today* **39:** 797-800

Greenhalgh DG, Sprugel KH, Murray MJ, Ross R (1990) PDGF and FGF stimulate wound healing in the genetically diabetic mouse. *American Journal of Pathology* **136:** 1235-1246

Greiling D, Clark RAF (1997) Fibronectin provides a conduit for fibroblast transmigration from collagenous stroma into fibrin clot provisional matrix. *Journal of Cell Science* **110:** 861-870

Grinnell F, Ho C, Tamariz E, Lee DJ, Skuta G (2003) Dendritic fibroblasts in three-dimensional collagen matrices. *Molecular Biology of the Cell* **14:** 384-395

Grinnell F, Ho CH (2002) Transforming growth factor-β stimulates fibroblast-collagen matrix contraction by different mechanisms in mechanically loaded and unloaded matrices. *Experimental Cell Research* **273:** 248-255

Grotendorst GR, Seppä HE, Kleinman HK, Martin GR (1981) Attachment of smooth muscle cells to collagen and their migration toward platelet-derived growth factor. *Proceedings of the National Academy of Sciences USA* **78:** 3669-3672.

Gruenberg J, Maxfield FR (1995) Membrane transport in the endocytic pathway. *Current Opinion in Cell Biology* **7:** 552-563

Guo J, Su H, Zeng Y, Liang Y, Wong W, Ellis-Behnke RG, So K, Wu W (2007) Reknitting the injured spinal cord by self-assembling peptide nanofiber scaffold. *Nanomedicine: Nanotechnology, Biology and Medicine* **3:** 311-321

Gurtner GC, Werner S, Barrandon Y, Longaker (2008) Wound repair and regeneration. *Nature* **453:** 314-321

Haapasalmi K, Zhang K, Tommesen M, Olerud J, Sheppard D, Salo T, Kramer R, Clark RAF, Uitto V, Larjava H (1996) Keratinocytes in human wounds express αvβ6 integrin. *Journal of Investigative Dermatology* **106:** 42-48

Hampton T (2007) Healing power found in nano knitting. *Journal of the American Medical Association* **297:** 31

Han D, Gouma P (2006) Electrospun bioscaffolds that mimic the topology of extracellular matrix. *Nanomedicine: Nanotechnology, Biology and Medicine* **2:** 37-44

Harding KG, Morris HL, Patel GK (2002) Science, medicine and the future: Healing chronic wounds. *British Medical Journal* **324:** 160-163

Hardingham TE, Fosang AJ (1992) Proteoglycans: many forms and many functions. *The FASEB Journal* **6:** 861-870

Harlin SL, Willard LA, Rush KJ, Ghisletta LC, Meyers WC (2008) Chronic wounds of the lower extremity: A preliminary performance and measurement set. *Plastic and Reconstructive Surgery* **121:** 142-155

Harper ME, Goddard L, Glynne-Jones E, Assender J, Dutkowski CM, Barrow D, Barrow D, Dewhurst OL, Wakeling AE, Nicholson RI (2002) Multiple responses to EGF receptor activation and their abrogation by a specific EGF receptor tyrosine kinase inhibitor. *The Prostate* **52:** 59-68

Harris JM, Chess RB (2003) Effect of PEGylation on pharmaceuticals. *Nature Reviews Drug Discovery* **2:** 214-221

Hashizume H, Baluk P, Morikawa S, McLean JW, Thurston G, Roberge S, Jain RK, McDonald DM (2000) Openings between defective endothelial cells explain tumor vessel leakiness. *American Journal Pathology* **156:** 1363-1380

Hee Na D, Seok Youn Y, Bok Lee I, Ji Park E, Jeon Park C, Choon Lee K (2006) Effect of molecular size of pegylated recombinant human epidermal growth factor on the biological activity and stability in rat wound tissue. *Pharmaceutical Development and Technology* **11:** 513-519

Heggers JP, Haydon S, Ko F, Hayward PG, Carp S, Robson MC (1992) Pseudomonas aeruginosa exotoxin A: its role in retardation of wound healing: the 1992 Lindberg award. *Journal of Burn Care and Rehabilitation* **13:** 512–8

Henson ES, Gibson SP (2006) Surviving cell death through epidermal growth factor (EGF) signal transduction pathways: Implications for cancer therapy. *Cellular Signalling* **18:** 2089-2097

Hernández-Sotomayor SM, Carpenter G (1992) Epidermal growth factor receptor: Elements of intracellular communication. *Journal of Membrane Biology* **128:** 81-89

Herouy Y, Nockowski P, Schopf E (1999) Lipodermatosclerosis and the significance of proteolytic remodelling in the pathogenesis of venous ulceration. *International Journal of Molecular Medicine* **3:** 511-515

Herrick SE, Sloan P, McGurk M, Freak L, McCollum CN, Ferguson MWJ (1992) Sequential changes in the histologic pattern and extra-cellular matrix deposition during the healing of chronic venous leg ulcers. *American Journal of Pathology* **141:** 1085-1095

Hershfield MS, Buckley RH, Greenberg ML, Melton AL, Schiff R, Hatem C, Kurtzberg J, Markert ML, Kobayashi RH, Kobayashi AL (1987) Treatment of adenosine deaminase deficiency with polyethylene glycol-modified adenosine deaminase. *New England Journal of Medicine* **316:** 589-596

Higley HR, Ksander GA, Gerhardt CO, Falanga V (1995) Extravasation of macromolecules and possible trapping of transforming growth factor-beta in venous ulceration. *British Journal of Dermatology* **132:** 79-85

Hinz B (2007) Formation and function of the myofibroblast during tissue repair. *Journal of Investigative Dermatology* **127:** 526-537

Hinz B, Phan SH, Thannickal VJ, Galli A, Bochaton-Piallat ML, Gabbiani G (2007) The myofibroblast: One function, multiple origins. *American Journal of Pathology* **170:** 1807-1816

Holmann DM, Kalaaji AN (2006) Cytokines in dermatology. *Journal of Drugs in Dermatology* **5:** 520-524

Hong JP, Kim YW, Jung HD, Jung KI (2006) The effect of various concentrations of human recombinant epidermal growth factor on split-thickness skin wounds. *International Wound Journal* **3:** 123-130

Hori K, Sotozono C, Hamuro J, Yamasaki K, Kimura Y, Ozeki M, Tabata Y, Kinishita S (2007) Controlled-release of epidermal growth factor from cationized gelatin hydrogel enhances corneal epithelial wound healing. *Journal of Controlled Release* **118:** 169-176

Hosie KB, Kerr DJ, Gilbert JA, Downes M, Lakin G, Pemberton G, Timms K, Young A, Stanley A (2003) A pilot study of adjuvant intraperitoneal 5-fluorouracil using 4% icodextrin as a novel carrier solution. *European Journal of Surgical Oncology* **29:** 254-260

Houben E, De Paepe K, Rogiers V (2007) A keratinocyte's course of life. *Skin Pharmacology and Physiology* **20:** 122-132

Hreczuk-Hirst D, Chicco D, German L, Duncan R (2001a) Dextrins as potential carriers for drug targeting: Tailored rates of dextrin degradation by introduction of pendant groups. *International Journal of Pharmaceutics* **230:** 57-66

Hreczuk-Hirst D, German L, Duncan R (2001b) Dextrins as carriers for drug targeting: Reproducible succinoylation as a means to introduce pendant groups. *Journal of Bioactive and Compatible Polymers* **16:** 353-365

Hubbard SR, Till JH (2000) Protein tyrosine kinase structure and function. *Annual Reviews Biochemistry* **69:** 373-398

Hubner G, Brauchle M, Smola H, Madlener M, Fassler R, Werner S (1996) Differential regulation of pro-inflammatory cytokines during wound healing in normal and glucocorticoid-treated mice. *Cytokine* **8:** 548-556

Hummel KP, Dickie MM, Coleman DL (1966) Diabetes, a new mutation in the mouse. *Science* **153:** 1127-1128

Hurtado M, Lozano JJ, Castellanos E, Lopez-Fernandez LA, Harshman K, Martinez-A C, Ortiz AR, Thomson TM, Paciucci (2007) Activation of the epidermal growth factor signalling pathway by tissue plasminogen activator in pancreas cancer cells. *Gut* **56:** 1266-1274

Huttenlocher A, Ginsberg MH, Horwitz AF (1996) Modulation of cell migration by integrin-mediated cytoskeletal linkages and ligand-binding affinity. *Journal of Cell Biology* **134:** 1551-1562

Huttenlocher A, Lakinshok M, Kinder M, Wu S, Truong T, Knudsen KA, Horowitz AF (1998) Integrin and cadherin synergy regulates contact inhibition of migration and motile activity. *Journal of Cell Biology* **141:** 515-526

Hyodo A, Reger SI, Negami S, Kambic H, Reyes E, Browne EZ (1995) Evaluation of a pressure sore model using monoplegic pigs. *Plastic and Reconstructive Surgery* **96:** 421-428

Ihle JN (1996) STATs: Signal transducers and activators of transciption. *Cell* **84:** 331-334

Imanishi J, Kamiyama K, Iguchi I, Kita M, Sotozono C, Kinoshita S (2000) Growth factors: Importance in wound healing and maintenance of transparency of the cornea. *Progress in Retinal and Eye Research* **19:** 113-129

Invitrogen (2008) *The Handbook – A Guide to Fluorescent Probes and Labelling Technologies,* Invitrogen, Paisley, UK

James TJ, Hughes MA, Cherry GW, Taylor RP (2000) Simple biochemical markers to assess chronic wounds. *Wound Repair and Regeneration* **8:** 264-269

James TJ, Hughes MA, Cherry GW, Taylor RP (2003) Evidence of oxidative stress in chronic venous ulcers. *Wound Repair and Regeneration* **11:** 172-176

Janacek S (1997) α-Amylase family: Molecular biology and evolution. *Progress in Biophysics and Molecular Biology* **67:** 67-97

Jones I, Currie L, Martin R (2002) A guide to biological skin substitutes. *British Journal of Plastic Surgery* **55:** 185-193

Jorissen RN, Walker F, Pouliot N, Garrett TPJ, Ward CW, Burgess AW (2003) Epidermal growth factor receptor: Mechanism of activation and signalling. *Experimental Cell Research* **284:** 31-53

Kandarakis AS, Page C, Kaufman HE (1984) The effect of epidermal growth factor on epithelial healing after penetrating keratoplasty in human eyes. *American Journal of Ophthalmology* **98:** 411-415

Kanitakis J (2002) Anatomy, histology and immunohistochemistry of normal human skin. *European Journal of Dermatology* **12:** 390-401

Kato Y, Onishi H, Machida Y (2004) N-succinyl-chitosan as a drug carrier: Water-insoluble and water-soluble conjugates. *Biomaterials* **25:** 907-915

Katz MH, Alvarez AF, Kirsner RS, Eaglstein WH, Falanga V (1991) Human wound fluid from acute wounds stimulates fibroblast and endothelial cell growth. *Journal of the American Academy of Dermatology* **25:** 1054-1058

Kawanabe T, Kawakami T, Yatomi Y, Shimida S, Soma Y (2007) Sphingosine 1-phospahte accelerates wound healing in diabetic mice. *Journal of Dermatological Science* **48:** 53-60

Keese M, Madgeburg RJ, Herzog T, Hasenberg T, Offterdinger M, Pepperkok R, Sturm JW, Bastiaens PIH (2005) Imaging epidermal growth factor receptor phosphorylation in human colorectal cancer cells and human tissues. *Journal of Biological Chemistry* **280:** 27826-27831

Kerr DJ, Young AM, Neoptolemos JP, Sherman M, Van-Geene P, Stanley A, Ferry D, Dobbie JW, Vincke B, Gilbert J, el Eini D, Dombros N, Fountzilas G (1996) Prolonged intraperitoneal infusion of 5-fluorouracil using a novel carrier solution. *British Journal of Cancer* **74:** 2032-2035

Kim J, Kuk E, Yu K, Kim J, Park S, Lee H, Kim S, Park Y, Park Y, Hwang C, Kim Y, Lee Y, Jeong D, Cho M (2007) Antimicrobial effects of silver nanoparticles. *Nanomedicine: Nanotechnology, Biology and Medicine* **3:** 95-101

Kim S, Kim S (2008) Antagonistic effect of EGF on FAK phosphorylation/dephosphorylation in a cell. *Cell Biochemistry and Function* **26:** 539-547

Kinstler O, Molineux G, Treuheit M, Ladd D, Gegg C (2002) Mono-N-terminal poly(ethylene glycol)-protein conjugates. *Advanced Drug Delivery Reviews* **54:** 477-485

Kira M, Sano S, Takagi S, Yoshikawa K, Takeda J, Itami S (2002) STAT3 deficiency in keratinocytes leads to compromised cell migration through hyperphosphorylation of p130. *Journal of Biological Chemistry* **277:** 12931-12936

Kirchner LM, Meerbaum SO, Gruber BS, Knoll AK, Bulgrin J, Taylor RAJ, Schmidt SP (2003) Effects of vascular endothelial growth factor on wound closure rates in the genetically diabetic mouse model. *Wound Repair and Regeneration* **11:** 127-131

Kiritsy CP, Lynch AB, Lynch SE (1993) Role of growth factors in cutaneous wound healing: A review. *Critical Reviews in Oral Biology and Medicine* 4: 729-760

Klenck C, Gebke K (2007) Practical management: Common medical problems in disabled athletes. *Clinical Journal of Sport Medicine* **17:** 55-60

Klingbeil CK, Cesar LB, Fiddes JC (1991) Basic fibroblast growth factor accelerates tissue repair in models of impaired wound healing. *Progress in Clinical and Biological Research* **365:** 443-458

Koivisto L, Jiang G, Hakkinen L, Chan B, Larjava H (2006) HaCaT keratinocyte migration is dependent on epidermal growth factor receptor signalling and glycogen synthase kinase-3α. *Experimental Cell Research* **312:** 2791-2805

Kondapaka SB, Fridman R, Reddy KB (1997) Epidermal growth factor and amphiregulin up-regulate matrix metalloproteinase-9 (MMP-9) in human breast cancer cells. *International Journal of Cancer* **70:** 722-726

Krishna-Mohan V (2007) Recombinant human epidermal growth factor (REGEN-D 150): Effect on healing of diabetic foot ulcers. *Diabetes Research and Clinical Practice* **78:** 405-411

Krupp MN, Connolly DT, Lane MD (1982) Synthesis, turnover, and down-regulation of epidermal growth factor receptors in human A431 epidermoid carcinoma cells and skin fibroblasts. *Journal of Biological Chemistry* **257:** 11489-11496

Kuo BS, Kusmik WF, Poole JC, Elsea SH, Chang J, Hwang KK (1992) Pharmacokinetic evaluation of two human epidermal growth factors (hEGF51 and hEGF53) in rats. *Drug Metabolism and Disposition* **20:** 23-30

Kuwabara T, Perkins DG, Cogan DG (1976) Sliding of the epithelium in experimental corneal wounds. *Investigative Ophthalmology* **15:** 4-14

Kwon S, Carson JH (1998) Fluorescence quenching and dequenching analysis of RNA interactions *in vitro* and *in vivo*. *Analytical Biochemistry* **264:** 133-140

Kwon Y, Kim H, Roh D, Yoon S, Baek R, Lim J, Kweon H, Lee K, Park Y, Lee J (2006) Topical application of epidermal growth factor accelerates wound healing by myofibroblast proliferation and collagen synthesis in rat. *Journal of Veterinary Science* **7:** 105-109

Laemmli UK (1970) Cleavage of structural proteins during the assembly of the head of bacteriophage T4. *Nature* **227:** 680-685

Lai WH, Cameron PH, Wada I, Doherty J, Kay DG, Posner BI, Bergeron JJM (1989) Ligand-mediated internalization, recycling and downregulation of the epidermal growth factor receptor *in vivo*. *Journal of Cell Biology* **109:** 2741-2749

Larsen M, Artym VV, Green JA, Yamada KM (2006) The matrix reorganized: Extracellular matrix remodeling and integrin signaling. *Current Opinion in Cell Biology* **18:** 463-471

Lattanzio FA (1990) The effects of pH and temperature on fluorescent calcium indicators as determined with Chelex-100 and EDTA buffer systems. *Biochemical and Biophysical Research Communications* **171:** 102-108

Lauer-Fields JL, Juska D, Fields GB (2002) Matrix metalloproteinases and collagen catabolism. *Bioploymers* **66:** 19-32

Laurent TC, Fraser JR (1992) Hyaluronan. *The FASEB Journal* **6:** 2397-2404

Lawal OS (2004) Succinyl and acetyl starch derivatives of a hybrid maize: Physicochemical characteristics and retrogradation properties monitored by differential scanning calorimetry. *Carbohydrate Research* **339:** 2673-2682

Lee H, Jang I, Ryu S, Park T (2003) N-terminal site-specific mono-PEGylation of epidermal growth factor. *Pharmaceutical Research* **20:** 818-825

Lee PHA, Trowbridge JM, Taylor KR, Morhenn VB, Gallo RL (2004) Dermatan sulfate proteoglycan and glycosaminoglycan synthesis is induced in fibroblasts by transfer to a three-dimensional extracellular matrix. *Journal of Biological Chemistry* **279:** 48640-48646

LeGrand EK (1998) Preclinical promise of becaplermin (rhPDGF-BB) in wound healing. *American Journal of Surgery* **176:** S48-S54

Leung PC (2007) Diabetic foot ulcers - A comprehensive review. *Surgeon* **5:** 219-31

Levenson SM, Demetriou AA (1992) Metabolic factors in wound healing; biochemical and clinical aspects. In: *Wound Healing: Biochemical and Clinical Aspects*. Eds: Cohen IK, Diegelmann RF, Lindblad WJ. WB Saunders, Philadelphia, pp 248-273

Levkowitz G, Waterman H, Zamir E, Kam Z, Oved S, Langdon WY, Beguinot L, Geiger B, Yarden Y (1998) c-Cbl/Sli-1 regulates endocytic sorting and ubiquitation of the epidermal growth factor receptor. *Genes and Development* **12:** 3663-3674

Li J, Chen J, Kirsner R (2007) Pathophysiology of acute wound healing. *Clinics in Dermatology* **25:** 9-18

Lichtman JW, Conchello J (2005) Fluorescence microscopy. *Nature Methods* **2:** 910-919

Liu G, Swihart MT, Neelamegham S (2005) Sensitivity, principle component and flux analysis applied to signal transduction: The case of epidermal growth factor mediated signalling. *Bioinformatics* **21:** 1194-1202

Lopez JG, Chew SJ, Thompson HW, Malter JS, Insler MS, Beuerman RW (1992) EGF cell surface receptor quantitation on ocular cells by an immunocytochemical flow cytometry technique. *Investigative Ophthalmology and Visual Science* **33:** 2053-2062

Lott JA, Lu CJ (1991) Lipase isoforms and amylase isoenzymes: Assays and application in the diagnosis of acute pancreatitis. *Clinical Chemistry* **37:** 361–368

Lowry OH, Rosebrough NJ, Farr AL, Randall RJ (1951) Protein measurement with the Folin phenol reagent. *Journal of Biological Chemistry* **193:** 265-275

Lu H, Chai J, Li M, Huang B, He C, Bi R (2001) Crystal structure of human epidermal growth factor and its dimerisation. *Journal of Biological Chemistry* **276:** 34913-34917

Lygoe KA, Wall I, Stephens P, Lewis MP (2007) The role of vitronectin and fibronectin receptors in oral mucosal and dermal myofibroblast differentiation. *Biology of the Cell* **99:** 601-614

Lynch SE, Colvin RB, Antoniades HN (1989) Growth factors in wound healing. Single and synergistic effects on partial thickness porcine skin wounds. *Journal of Clinical Investigation* **84:** 640-646

Madison KC (2003) Barrier function of the skin: "La Raison d'Etre" of the epidermis. *Journal of Investigative Dermatology* **121:** 231-241

Madri JA, Sankar S, Romanic AM (1996) Angiogenesis. In: *The Molecular and Cellular Biology of Wound Repair.* Ed: Clark RAF. Plenum Press, New York, pp 355-371

Maeda H, Matsumura Y (1989) Tumoritropic and lymphotropic principles of macromolecular drugs. *Critical Reviews in Therapeutic Drug Carrier Systems* **6:** 193-210

Mani R (1999) Science of measurements in wound healing. *Wound Repair and Regeneration* **7:** 330-334

Margulis A, Zhang W, Garlick JA (2005) *In vitro* fabrication of engineered human skin. *Methods in Molecular Biology* **289:** 61-70

Marques MM, Martinez N, Rodriguez-Garcia I, Alonso A (1999) EGFR family-mediated signal transduction in the human keratinocyte cell line HaCaT. *Experimental Cell Research* **252:** 432-438

Martin P, Hopkinson-Woolley J, McClusky J (1992) Growth factors and cutaneous wound repair. *Progress in Growth Factor Research* **4:** 25-44

Martin P (1997) Wound healing – Aiming for perfect skin regeneration. *Science* **276:** 75-81

Martin P, Leibovich SJ (2005) Inflammatory cells during wound healing: The good, the bad and the ugly. *Trends in Cellular Biology* **15:** 599-607.

Masunaga T (2006) Epidermal basement membrane: Its molecular organization and blistering disorders. *Connective Tissue Research* **47:** 55-66

Matsuda M, Ubels JL, Edelhauser HF (1985) A larger corneal epithelial wound closes at a faster rate. *Investigative Ophthalmology and Visual Science* **26:** 897-900

Matsumura Y, Maeda H (1986) A new concept for macromolecular therapies in cancer chemotherapy: Mechanism of tumouritropic accumulation of proteins and the antitumour agent SMANCS. *Cancer Research* **6:** 6387-6392

Mauer SM, Lane P, Hattori M, Fioretto P, Steffes MW (1992) Renal structure and finction in insulin-dependent diabetes mellitus and type 1 membranoproliferative glomerulonephritis in humans. *Journal of the American Association of Nephrologists* **2:** S181-S184

McClain SA, Simon M, Jones E, Nandi A, Gailit JO, Tonnesen MG, Newman D, Clark RAF (1996) Mesenchymal cell activation is the rate-limiting step of granulation tissue induction. *American Journal of Pathology* **149:** 1257-1270

McDonald DM, Foss AJ (2000) Endothelial cells of tumor vessels: Abnormal but not absent. *Cancer and Metastasis Reviews* **19:** 109-120

McFarlane RM, de Young G, Henry RA (1965) The design of a pedicle flap in the rat to study necrosis and its prevention. *Plastic and Reconstructive Surgery* **35:** 177-182

McGrath JA, Eady RAJ (1997) Heparan sulphate proteoglycan and wound healing in skin. *Journal of Pathology* **183:** 251-252

McNeill H, Jensen PJ (1990) A high-affinity receptor for urokinase plasminogen activator on human keratinocytes: Characterization and potential modulation during migration. *Cell Regulation* **1:** 843-852

Mekkes JR, Loots MAM, Van der Waal AC, Bos JD (2003) Causes, investigation and treatment of leg ulceration. *British Journal of Dermatology* **148:** 388-401

Mendez MV, Stanley A, Park HY, Shon K, Phillips T, Menzoian JO (1998) Fibroblasts cultured from venous ulcers display cellular characteristics of senescence. *Journal of Vascular Surgery* **28:** 876-883

Mendez MV, Raffetto JD, Phillips T, Menzoian JO, Park HY (1999) The proliferative capacity of neonatal skin fibroblasts is reduced after exposure to venous ulcer wound fluid: a potential mechanism for senescence in venous ulcers. *Journal of Vascular Surgery* **30:** 734-743

Menke NB, Ward KR, Witten TM, Bonchev DG, Diegelmann RF (2007) Impaired wound healing. *Clinics in Dermatology* **25:** 19-25

Meran S, Thomas DW, Stephens P, Martin J, Bowen T, Phillips A, Steadman R (2007) Involvement of hyaluronan in regulation of the fibroblast phenotype. *Journal of Biological Chemistry* **282:** 25687-25697

Meshel AS, Wei Q, Adelstein RS, Sheetz MP (2005) Basic mechanism of three-dimensional collagen fibre transport by fibroblasts. *Nature Cell Biology* **7:** 157-164

Michaels J, Churgin SS, Blechman KM, Greives MR, Aarabi S, Galiano RD, Gurtner GC (2007) db/db mice exhibit severe wound-healing impairments compared with other murine diabetic strains in a silicone-splinted excisional wound model. *Wound Repair and Regeneration* **15:** 665-670

Mitchison TJ, Cramer LP (1996) Actin-based cell motility and cell locomotion. *Cell* **84:** 371-379

Miyasaka K, Rothman SS (1982) Redistribution of amylase activity accompanying its secretion by the pancreas. *Proceedings of the National Academy of Sciences USA* **79:** 5438-5442

Miyasaki K (1975) Experimental polymer storage disease in rabbits. An approach to the histogenesis of sphingolipidoses. *Virchows Archive A: Pathological Anatomy and Histology* **365:** 351-365

Mlcochova P, Bystricky S, Steiner B, Machova E, Koos M, Velebny V, Krcmar M (2006) Synthesis and characterization of new biodegradable hyaluronan alkyl derivatives. *Biopolymers* **82:** 74-79

Moffitt EA (1975) Blood substitutes. *Canadian Anesthetic Society Journal* **22:** 12-19

Mohan RR, Sharma A, Netto MV, Sinha S, Wilson SE (2005) Gene therapy in the cornea. *Progress in Retinal and Eye Research* **24:** 537-559

Mola E, Acevedo B, Silva R, Tormo B, Montero R, Herrera L (2003) Development of Cuban biotechnology. *Journal of Commercial Biotechnology* **9:** 147-152

Moore A, Sabachewsky L, Toolan HW (1955) Culture characteristics of four permanent lines of human cancer cells. *Cancer Research* **15:** 598-602

Moore A (1958) Tumorigenic activity of cultures. *Annals of the New York Academy of Sciences* **76:** 497-505

Moseley R, Leaver M, Walker M, Waddington RJ, Parsons D, Chen WYJ, Embery G (2002) Comparison of the antioxidant properties of HYAFF®-11p75, AQUACEL® and hyaluronan towards reactive oxygen species *in vitro*. *Biomaterials* **23:** 2255-2264

Moseley R, Stewart JE, Stephens P, Waddington RJ, Thomas DW (2004) Extracellular matrix metabolites as potential biomarkers of disease activity in wound fluid: Lessons learned from other inflammatory diseases? *British Journal of Dermatology* **150:** 401-413

Mosmann T (1983) Rapid colorimetric assay for cellular growth and survival: application to proliferation and cytotoxicity assays. *Journal of Immunological Methods* **65:** 55-63

Moustafa M, Bullock AJ, Creagh FM, Heller S, Jeffcoate W, Game F, Amery C, Tesfaye S, Ince Z, Haddow DB, MacNeil S (2007) Randomized, controlled, single-blinded study on the use of autologous keratinocytes on a transfer dressing to treat nonhealing diabetic ulcers. *Regenerative Medicine* **2:** 887-902

Mumcuoglu KY (2001) Clinical applications for maggots in wound care. *American Journal of Clinical Dermatology* **2:** 219-227

Mustoe TA, Pierce GF, Morishima C, Deuel TF (1991) Growth factor-induced acceleration of tissue repair through direct and inductive activities in a rabbit dermal ulcer model. *Journal of Clinical Investigation* **87:** 694-703

Mustoe TA, Purdy J, Gramates P, Deuel TF, Thomason A, Pierce GF (1989) Reversal of impaired wound healing in irradiated rats by platelet-derived growth factor-BB. *American Journal of Surgery* **158:** 345-350

Mustoe TA, O'Shaughnessy K, Kloeters O (2006) Chronic wound pathogenesis and current treatment strategies: A unifying hypothesis. *Plastic and Reconstructive Surgery* **117:** 35S-41S

Nagase H, Visse R, Murphy G (2006) Structure and function of metalloproteinases and TIMPs. *Cardiovascular Research* **69:** 562-573

Nagy JA, Benjamin L, Zeng H, Dvorak AM, Dvorak HF (2008) Vascular permeability, vascular hyperpermeability and angiogenesis. *Angiogenesis* **11:** 109-119

Nakamura T (1991) Structure and function of hepatocyte growth factor. *Progress in Growth Factor Research* **3:** 67-85

Nanney LB (1990) Epidermal and dermal effects of epidermal growth factor during wound repair. *Journal of Investigative Dermatology* **94:** 624-629

Nanney LB, King LE (1996) Epidermal growth factor and transforming growth factor-α. In: *The Molecular and Cellular Biology of Wound Repair.* Ed: Clark RAF. Plenum Press, New York, pp 171-195

Nanney LB, Woodrell CD, Greives MR, Cardwell NL, Pollins AC, Bancroft TA, Chesser A, Michalak M, Rahman M, Siebert JW, Gold LI (2008) Calreticulin enhances porcine wound repair by diverse biological effects. *American Journal of Pathology* **173:** 610-630

Nelson RD, Quie PG, Simmons RL (1975) Chemotaxis under agarose: A new and simple method for measuring chemotaxis and spontaneous migration of human polymorphonuclear leucocytes and monocytes. *Journal of Immunology* **115:** 1650-1656

Nickoloff BJ, Mitra RS, Riser BL, Dixit VM, Varani J (1988) Modulation of keratinocyte motility. Correlation with production of extracellular matrix molecules in response to growth promoting and antiproliferative factors. *American Journal of Pathology* **132:** 543-551

Nishimura Y, Yoshioka K, Bereczky B, Itoh K (2008) Evidence for efficient phosphorylation of EGFR and rapid endocytosis of phosphorylated EGFR via the early/late endocytic pathway in a gefitinib-sensitive non-small cell lung cancer cell line. *Molecular Cancer* **7:** 42

O'Connor NE, Mulliken JB, Banks-Schlegel S, Kehinde O, Green H (1981) Grafting of burns with cultured epithelium prepared from autologous epidermal cells. *The Lancet* **317:** 75-78

Obersyzyn TM (2007) Inflammation and wound healing. *Frontiers in Bioscience* **12:** 2993-2999

Olayioye MA, Neve RM, Lane HA, Hynes NE (2000) The ErbB signaling network: Receptor heterodimerization in development and cancer. *The EMBO Journal* **19:** 3159–3167

Ortega MR, Ganz T, Milner SM (2000) Human beta defensin is absent in burn blister fluid. *Burns* **26:** 724-6

Oupicky D, Konak C, Ulbrich K, Wolfert MA, Seymour LW (2000) DNA delivery systems based on complexes of DNA with synthetic polycations and their copolymers. *Journal of Controlled Release* **65:** 149-71

Palmer DA, Evans M, Miller JN (1994) Thiophilic gels: An alternative to protein A and G for use in flow injection immunoassays. *Analytical Proceedings Including Analytical Communications* **31:** 123-125

Pandey A, Nigam P, Soccol CR, Soccol VT, Singh D, Mohan R (2000) Advances in microbial amylases. *Biotechnology and Applied Biochemistry* **31:** 135-152

Park K (2008) Bioresponsive drug delivery for regenerative medicine. *Journal of Controlled Release* **130:** 201

Park OK, Schaefer TS, Nathans D (1996) *In vitro* activation of STAT3 by epidermal growth factor receptor kinase. *Proceedings of the National Academy of Sciences USA* **93:** 13704-13708

Pasonen-Seppänen S, Suhonen TM, Kirjavainen M, Miettinen M, Urtti A, Tammi M, Tammi R (2001) Formation of permeability barrier in epidermal organotypic culture for studies on drug transport. *Journal of Investigative Dermatology* **117:** 1322-1324

Pastor JC, Colange M (1992) Epidermal growth factor and corneal wound healing. A mulitcenter study. *Cornea* **11:** 311-314

Pasut G, Sergi M, Veronese FM (2008) Anti-cancer PEG-enzymes: 30 years old, but still a current approach. *Advanced Drug Delivery Reviews* **60:** 69-78

Patel GK, Wilson CH, Harding KG, Finlay AY, Bowden PE (2006) Numerous keratinocyte subtypes involved in wound re-epithelialisation. *Journal of Investigative Dermatology* **126:** 497-502

Pearse DB, Sylvester JT (1992) Spontaneous injury in isolated sheep lungs: Role of resident polymorphonuclear leukocytes. *Journal of Applied Physiology* **72:** 2475-2481

Peers E, Gokal R (1998) Icodextrin provides long dwell peritoneal dialysis and maintenance of intraperitoneal volume. *Artificial Organs* **22:** 8-12

Persson U, Willis M, Odegaard K, Apelqvist J (2000) The cost-effectiveness of treating diabetic lower extremity ulcers with becaplermin (Regranex®): A core model with an application using Swedish cost data. *Value in Health* **3:** S39-S46

Pfeilschifter J, Eberhardt W, Huwiler A (2001) Nitric oxide and mechanisms of redox signalling: Matrix and matrix-metabolizing enzymes as prime nitric oxide targets. *European Journal of Pharmacology* **429:** 279-286

Pfister RR (1975) The healing of corneal epithelial abrasions in the rabbit: A scanning electron microscope study. *Investigative Ophthalmology* **14:** 648-661

Pham C, Greenwood J, Cleland H, Woodruff P, Maddern G (2007) Bioengineered skin substitutes for the management of burns: A systematic review. *Burns* **33:** 946-957

Philpott MP, Green MR, Kealey T (1990) Human hair growth *in vitro*. *Journal of Cell Science* **97:** 463-471

Pierce Chemical Protein Assay Technical Handbook (2005) http://www.piercenet.com/files/1601325ProteinAssay.pdf. Accessed 01/10/08

Pierce GF, Mustoe TA, Senior RM, Reed J, Griffin GL, Thomason A, Deuel TF (1988) *In vivo* incisional wound healing augmented by platelet-derived growth factor and recombinant c-sis gene homodimeric proteins. *Journal of Experimental Medicine* **167:** 974-987

Pierce GF, Mustoe TA, Lingelbach J, Masakowski VR, Griffin GL, Senior RM, Deuel TF (1989) Platelet-derived growth factor and transforming growth factor-β enhance tissue repair activities by unique mechanisms. *Journal of Cell Biology* **109:** 429-440

Pittelkow MR (1992) Growth factors in cutaneous biology and disease *Advances in Dermatology.* **7:** 55-81

Plummer DT (1978) *An Introduction to Practical Biochemistry*, Second Edition. McGraw-Hill Book Company Limited, London.

Pollock JS, Webb W, Callaway D, Sathyanarayana, O'Brien W, Howdieshell TR (2001) Nitric oxide synthase isoform expression in a porcine model of granulation tissue formation. *Surgery* **129:** 341-350

Ponec M (2002) Skin constructs for replacement of skin tissues for *in vitro* testing. *Advanced Drug Delivery Reviews* **54:** S19-S30

Prats PA, Duconge J, Valenzuela C, Berlanga J, Edrosa CR, Fernandez-Sanchez E (2002) Disposition and receptor-site binding of ^{125}I-EGF after topical administration to skin wounds. *Biopharmaceutics and Drug Disposition* **23:** 67-76

Price P, Harding KG (2004) Cardiff wound impact schedule: The development of a condition-specific questionnaire to assess health-related quality of life in patients with chronic wounds of the lower limb. *International Wound Journal* **1:** 10-17

Price RD, Berry MG, Navsaria HA (2007) Hyaluronic acid: The scientific and clinical evidence. *Journal of Plastic, Reconstructive and Aesthetic Surgery* **60:** 1110-1119

Prockop DJ, Kivirikkö KI (1995) Collagens: Molecular biology, diseases and potential for therapy. *Annual Review of Biochemistry* **64:** 403-434

Providence KM, Kutz SM, Staiano-Coico L, Higgins PJ (2000) PAI-1 gene expression is regionally induced in wounded epithelial cell monolayers and required for injury repair. *Journal of Cell Physiology* **182:** 269-280

Pruss RM, Herschman HR (1977) Variants of 3T3 cells lacking mitogenic response to epidermal growth factor. *Proceedings of the National Academy of Sciences USA* **74:** 3918-3921

Quan D (2008) Diabetic neuropathy. http://www.emedicine.com/neuro/topic88.htm. Accessed 01/10/2008

Quan TE, Cowper S, Wu SP, Bockenstedt LK, Bucala R (2004) Circulating fibrocytes: Collagen-secreting cells of the peripheral blood. *International Journal of Biochemistry and Cell Biology* **36:** 598-606

Quirinia A, Jensen FT, Viidik A (1992) Ischemia in wound healing I: Design of a flap model–changes in blood flow. *Scandinavian Journal of Plastic and Reconstrucive Surgery and Hand Surgery* **26:** 21–28

Raftery AT (1998) *Churchill's Pocketbook of Surgery.* Churchill Livingstone, Edinburgh, pp 258-260

Rajendran S, Rigby AJ, Anand SC (2007) Venous leg ulcer treatment and practice - part 1: The causes and diagnosis of venous leg ulcers. *Journal of Wound Care* **16:** 24-26

Raman R, Sasisekharan V, Sasisekharan R (2005) Structural insights into biological roles of protein-glycosaminoglycan interactions. *Chemistry and Biology* **12:** 267-277

Ramasubbu N, Paloth V, Luo Y, Brayer GD, Levine MJ (1996) Structure of human salivary alpha-amylase at 1.6 A resolution: implications for its role in the oral cavity. *Acta Crystallographica Section D: Biological Crystallography* **52:** 435-446

Ramirez HL, Valdivia A, Cao R, Torres-Labandeira JJ, Fragoso A, Villalonga R (2006) Cyclodextrin-grafted polysaccharides as supramolecular carrier systems for naproxen. *Bioorganic and Medicinal Chemistry Letters* **16:** 1499-1501

Raspaglio G, Ferrandina G, Ferlini C, Scambia G, Ranelletti FO (2003) Epidermal growth factor-responsive laryngeal squamous cancer cell line HEp2 is more sensitive than unresponsive co-k3 one to quercetin and tamoxifen apoptotic effects. *Oncology Research* **14:** 83-91

Reddy KR, Modi MW, Pedder S (2002) Use of peginterferon alfa-2a (40 KD) (Pegasys®) for the treatment of hepatitis C. *Advanced Drug Delivery Reviews* **54:** 571-586

Reddy LH (2005) Drug delivery to tumours: recent strategies. *Journal of Pharmacy and Pharmacology* **57:** 1231-1242

Reiber GE, Lipsky BA, Gibbons GW (1998) The burden of foot ulcers. *American Journal of Surgery* **176:** 5S-10S

Reid B, Song B, McCaig CD, Zhao M (2005) Wound healing in the rat cornea: the role of electric currents. *The FASEB Journal* **19:** 379-386

Repertinger SK, Campagnaro E, Fuhrman J, El-Abaseri T, Yuspa SH, Hansen LA (2004) EGFR enhances early healing after cutaneous incisional wounding. *Journal of Investigative Dermatology* **123:** 982-989

Rerup CC (1970) Drugs producing diabetes through damage of the insulin secreting cells. *Pharmacology Reviews* **22:** 485-518

Revis DR, Caffee HH (2008) Pressure ulcers, non-surgical treatment and principles. http://www.emedicine.com/plastic/topic424.htm. Accessed 01/10/08

Rheinwald JG, Green H (1975) Serial cultivation of strains of human epidermal keratinocytes: The formation of keratinizing colonies from single cells. *Cell* **6:** 331-343

Rheinwald JG, Green H (1977) Epidermal growth factor and the multiplication of cultured human epidermal keratinocytes. *Nature* **265:** 421-424

Rho KS, Jeong L, Lee G, Seo B, Park YJ, Hong S, Roh S, Cho JJ, Park WH, Min B (2006) Electrospinning of collagen nanofibers: Effects on the behaviour of normal human keratinocytes and early-stage wound healing. *Biomaterials* **27:** 1452-1461

Richardson SCW, Wallom K, Ferguson EL, Deacon SPE, Davies MW, Powell AJ, Piper RC, Duncan R (2008) The use of fluorescence microscopy to define polymer localization to the late endocytic compartments in cells that are targets for drug delivery. *Journal of Controlled Release* **127:** 1-11

Rizk M, Witte MB, Barbul A (2004) Nitric oxide and wound healing. *Wound Journal of Surgery* **28:** 301-306

Roberts MJ, Bentley MD, Harris JM (2002) Chemistry for peptide and protein PEGylation. *Advanced Drug Delivery Reviews* **54:** 459-476

Roberts PJP, Whelan WJ (1960) The mechanism of carboydrase action. *Biochemistry Journal* **76:** 246-253

Robson MC, Phillips LG, Thomason A, Robson LE, Pierce GF (1992a) Platelet-derived growth factor BB for the treatment of chronic pressure ulcers. *The Lancet* **339:** 23-25

Robson MC, Phillips LG, Thomason A, Altrock BW, Pence PC, Heggers JP, Johnston AF, McHugh TP, Anthony MS, Robson LE (1992b) Recombinant human platelet-derived growth factor-BB for the treatment of chronic pressure ulcers. *Annals of Plastic Surgery* **29:** 193-201

Roda A, Pasini P, Mirasoli M, Michelini E, Guardigli M (2004) Biotechnological applications of bioluminescence and chemiluminescence. *Trends in Biotechnology* **22:** 295-303

Roesel JF, Nanney LB (1995) Assessment of differential cytokine effects on angiogenesis using an *in vivo* model of cutaneous wound repair. *Journal of Surgical Research* **58:** 449-459

Rongen HAH, Hoetelmans RMW, Bult A, Van Bennekom WP (1994) Chemiluminescence and immunoassays. *Journal of Pharmaceutical and Biomedical Analysis* **12:** 433-462

Roy H, Bhardwaj S, Yla-Herttuala S (2006) Biology of vascular endothelial growth factors. *FEBS Letters* **580:** 2879-2887

Rudolph R, Suzuki M, Luce JK (1979) Experimental skin necrosis produced by adriamycin. *Cancer Treatment Reports* **63:** 529–537

Rupprich C, Becker M, Buttner W, Boeden HF, Schroder KL, Hansicke A, Konnecke A (1990) Biospecific adsorbents on the basis of chloroformate-activated bead cellulose. *Biomaterials, Artificial Cells, and Artificial Organs* **18:** 665-670

Ryan TA (2000) Diseases of the skin. In: *Concise Oxford Textbook of Medicine*. Eds: Leddingham JGG, Worrall DA. Oxford University Press, Oxford, pp 1102

Saarialho-Kere U, Pentland AP, Birkedal-Hansen H, Parks WC, Welgus HG (1994) Distinct populations of basal keratinocytes express stromeolysin-1 and stromeolysin-2 in chronic wounds. *Journal of Clinical Investigation* **94:** 79-88

Saarialho-Kere U, Kerkela E, Jahkola T, Suomela S, Keski-Oja J, Lohi J (2002) Epilysin (MMP-28) expression is associated with cell proliferation during epithelial repair. *Journal of Investigative Dermatology* **119:** 14-21

Sadowski HB, Shuai K, Darnell JE, Gilman MZ (1993) A common nuclear signal transduction pathway activated by growth factor and cytokine receptors. *Science* **261:** 1739-1744

Sako Y, Ichinose J, Morimatsu M, Ohta K, Uyemura T (2003) Optical bioimaging: From living tissue to a single molecule: Single-molecule visualisation of cell signalling processes of epidermal growth factor receptor. *Journal of Pharmacological Science* **93:** 253-258

Salcido R, Popescu A, Ahn C (2006) Animal models in pressure ulcer research. *Journal of Spinal Cord Medicine* **30:** 107-116

Salo T, Makela M, Kylmaniemi M, Autio-Harmainen H, Larjava H (1994) Expression of matrix metalloproteinase-2 and -9 during early human wound healing. *Laboratory Investigation* **70:** 176-182

Salomon DS, Brandt R, Ciardiello F, Normanno N (1995) Epidermal growth factor-related peptides and their receptors in human malignancies. *Critical Reviews in Oncology and Haematology* **19:** 183-232

Saltzman WM, Olbricht WL (2002) Building drug delivery into tissue engineering. *Nature Reviews Drug Discovery* **1**: 177-186

Sano S, Itami S, Takeda K, Tarutani M, Yamaguchi Y, Miura H, Yoshikawa K, Akira S, Takeda J (1999) Keratinocyte-specific ablation of STAT3 exhibits impaired skin remodeling, but does not affect skin morphogenesis. *The EMBO Journal* **18:** 4657-4668

Sano S, Chan KS, DiGiovanni J (2008) Impact of STAT3 activation upon sin biology: A dichotomy of its role between homeostasis and diseases. *Journal of Dermatological Science* **50:** 1-14

Sarkar P, Ballantyne S (2000) Management of leg ulcers. *Post Graduate Medical Journal* **76:** 674-682

Sasaki M, Kashima M, Ito T, Watanabe A, Izumiyama N, Sano M, Kagaya M, Shioya T, Miura M (2000) Differential regulation of metalloproteinase production, proliferation and chemotaxis of human lung fibroblasts by PDGF, interleukin-1β and TNF-α. *Mediators of Inflammation* **9:** 155-160

Sato H (2002) Enzymatic procedure for site-specific PEGylation of proteins. *Advanced Drug Delivery Reviews* **54:** 487-504

Savage AP, Chatterjee VK, Gregory H, Bloom SR (1986) Epidermal growth factor in blood. *Regulatory Peptides* **30:** 199-206

Schacht E, Vandoorne F, Vermeersch J, Duncan R (1987) Polysaccharides as drug carriers - Activation procedures and biodegradation studies. *American Chemical Society Symposium Series* **348:** 188-200

Schindler C, Levy DE, Decker T (2007) JAK-STAT signaling: From interferons to cytokines. *Journal of Biological Chemistry* **282:** 20059-20063

Schlessinger J (2000) Cell signalling by receptor tyrosine kinases. *Cell* **103:** 211-225

Schmidt AM, Yan SD, Brett J, Mora R, Nowygrod R, Stern D (1993) Regulation of human mononuclear phagocyte migration by cell surface-binding protein for advanced glycation end products. *Journal of Clinical Investigation* **91:** 2155-2168

Schneider A, Garlick JA, Egles C (2008) Self-assembling peptide nanofiber scaffolds accelerate wound healing. *PLoS ONE* **3:** e1410

Scott HJ, Coleridge Smith PD, Scurr JH (1991) Histological study of white blood cells and their association with lipodermatosclerosis and venous ulceration. *British Journal of Surgery* **78:** 210-211

Sempowski, DG, Borello MA, Phipps RP, Barth RK, Phipps RP (1995) Fibroblast heterogeneity in the healing wound. *Wound Repair and Regeneration* **3:** 120-131

Sen CK, Khanna S, Gordillo G, Bagchi D, Bagchi M, Roy S (2002) Oxygen, oxidants, and antioxidants in wound healing: An emerging paradigm. *Annals of the New York Academy of Sciences* **957:** 239-249

Senter LH, Legrand EK, Laemmerhirt KE, Kiorpes TC (1995) Assessment of full-thickness wounds in the genetically diabetic mouse for suitability as a wound healing model. *Wound Repair and Regeneration* **3:** 351-358

Seppa H, Grotendorst G, Seppa S, Schiffman E, Martin G (1982) Platelet-derived growth factor is chemotactic for fibroblasts. *Journal of Cell Biology* **92:** 584-588

Seymour LW, Ferry DR, Anderson D, Hesslewood S, Julyan PJ, Poyner R, Doran J, Young AM, Burtles S, Kerr DJ (2002) Hepatic drug targeting: Phase I evaluation of polymer-bound doxorubicin. *Journal of Clinical Oncology* **20:** 1668-1676

Shaunak S, Thomas S, Gianasi E, Godwin A, Jones E, Teo I, Mireskandari K, Luthert P, Duncan R, Patterson S, Khaw P, Brocchini S (2004) Polyvalent dendrimer glucosamine conjugates prevent scar tissue formation. *Nature Biotechnology* **22:** 977-984

Shelton DN, Chang E, Whittier PS, Choi D, Funk WD (1999) Microarray analysis of replicative senescence *Current Biology* **9:** 939-945

Shimizu H (1998) New insights into the immunoultrastructural organization of cutaneous basement membrane zone molecules. *Experimental Dermatology* **7:** 303-313

Shin D, Minn KW (2004) The effect of the myofibroblast on contracture of hypertrophic scar. *Plastic and Reconstructive Surgery* **113:** 633-640

Shingel KI (2004) Current knowledge on biosynthesis, biological activity, and chemical modification of the exopolysaccharide, pullulan. *Carbohydrate Research* **339:** 447-460

Shiraha H, Gupta K, Drabik K, Wells A (2000) Aging fibroblasts present reduced epidermal growth factor (EGF) responsiveness due to preferential loss of EGF receptors. *Journal of Biological Chemistry* **275:** 19343-19351

Shutt DC, Daniels KJ, Carolan EJ, Hill AC, Soll DR (2000) Changes in the motility, morphology, and F-actin architecture of human dendritic cells in an *in vitro* model of dendritic cell development. *Cell Motility and the Cytoskeleton* **46:** 200-221

Sibbald RG, Contreras-Ruiz J, Coutts P, Fierheller M, Rothman A, Woo K (2007) Bacteriology, inflammation and healing: A study of nanocrystalline silver dressings in chronic venous leg ulcers. *Advances in Skin and Wound Care* **20:** 549-558

Siegbahn A, Hammacher A, Westermark B, Heldin C (1990) Differential effects of the various isoforms of platelet-derived growth factor on chemotaxis of fibroblasts, monocytes and granulocytes. *Journal of Clinical Investigation* **85:** 916-920

Silva J, Beckerdorf A, Bieberich E (2003) Osteoblast-derived oxysterol is a migration-inducing factor for human breast cancer cells. *Journal of Biological Chemistry* **278:** 25376-25385

Silver FH, Siperko LM, Seehra GP (2003) Mechanobiology of force transduction in dermal tissue. *Skin Research and Technology* **9:** 3-23

Singer AJ, Clark RAF (1999) Mechanisms of disease: Cutaneous wound healing. *The New England Journal of Medicine* **341:** 738-746

Singer JW, Baker B, De Vries P, Kumar A, Shaffer S, Vawter E, Bolton M, Garzone P (2003) Poly-(L)-glutamic acid-paclitaxel (CT-2103) [XYOTAX], a biodegradable polymeric drug conjugate: Characterization, preclinical pharmacology, and preliminary clinical data. *Advances in Experimental Medicine and Biology* **519:** 81-99

Sivamani R, Garcia MS, Isseroff RR (2007) Wound re-epithelialization: Modulating kerationcyte migration in wound healing. *Frontiers in Bioscience* **12:** 2849-2868

Skin Care Forum (www.scf-online.com) (2001a) Schematic diagram of the human skin **27:** 1

Skin Care Forum (www.scf-online.com) (2001b) The life cycle of a horny cell **35:** 1

Skrabut EM, Hebda P, Samuels JA, Richards SM, Edmunds T, Cunneen MF, Vaccaro CA, McPherson JM. (1996) Removal of necrotic tissue with an ananain-based enzyme debriding preparation. *Wound Repair and Regeneration* **4:** 433-443

Smiell JM, Wieman TJ, Steed DL, Perry BH, Sampson AR, Schwab BH (1999) Efficacy and safety of becaplermin (recombinant human platelet-derived growth factor-BB) in patients with nonhealing, lower extremity diabetic ulcers: A combined analysis of four randomized studies. *Wound Repair and Regeneration* **7:** 335-346

Smith PK, Krohn RI, Hermanson GT, Mallia AK, Gartner FH, Provenzano MD, Fujimoto EK, Goeke NM, Olson BJ, Klenk DC (1985) Measurement of protein using bicinchoninic acid. *Analytical Biochemistry* **150:** 76-85

Song JI, Grandis JR (2000) STAT signalling in head and neck cancer. *Oncogene* **19:** 2489-2495

Sorrell JM, Caplan AI (2004) Fibroblast heterogeneity: More than skin deep. *Journal of Cell Science* **117:** 667-675

Sorrell JM, Baber MA, Caplan AI (2007) Human dermal fibroblast subpopulations; differential interactions with vascular endothelial cells in coculture: Nonsoluble factors in the extracellular matrix influence interactions. *Wound Repair and Regeneration* **16:** 300-309

Sottile J, Hocking DC (2002) Fibronectin polymerization regulates the composition and stability of extracellular matrix fibrils and cell-matrix adhesions. *Molecular Biology of the Cell* **13:** 3546-3559

Spessoto P, Giacomello E, Perri R (2002) Improving fluorescence-based assays for the *in vitro* analysis of cell adhesion and migration. *Molecular Biotechnology* **20:** 285-304

Stacey MC, Burnand KG, Bhogal BS, Black MM (2000) Pericapillary fibrin deposits and skin hypoxia precede the changes of lipodermatosclerosis in limbs at increased risk of developing a venous ulcer. *Cardiovascular Surgery* **8:** 372-380

Stallmeyer B, Kampfer H, Kolb N, Pfeilschifter J, Frank S (1999) The function of nitric oxide in wound repair: Inhibition of inducible nitric oxide-synthase severely impairs wound reepithelialisation. *Journal of Investigative Dermatology* **113:** 1090-1098

Steed DL (2006) Clinical evaluation of recombinant human platelet-derived growth factor for the treatment of lower extremity ulcers. *Plastic and Reconstructive Surgery* **117:** 143S-149S

Stephens P, Davies KJ, Al-Khateeb T, Shepherd JP, Thomas DW (1996) A comparison of the ability of intra oral and extra oral fibroblasts to stimulate extracellular matrix reorganization in a model of wound contraction. *Journal of Dental Research* **75:** 1358-1364

Stephens P, Davies KJ, Occleston NE, Pleass RD, Kon C, Daniels J, Khaw PT, Thomas DW (2001) Skin and oral fibroblasts exhibit phenotypic differences in extracellular matrix reorganisation and matrix metalloproteinase activity. *British Journal of Dermatology* **144:** 229-237

Stephens P, Cook H, Hilton J, Jones CJ, Haughton MF, Wylie FS, Skinner JW, Harding KG, Kipling D, Thomas DW (2003) An analysis of replicative senescence in dermal fibroblasts derived from chronic leg wounds predicts that telomerase therapy wound fail to reverse their disease-specific cellular and proteolytic phenotype. *Experimental Cell Research* **283:** 22-35

Stephens P, Grenard P, Aeschlimann P, Langley M, Blain E, Errington R, Kipling D, Thomas D, Aeschlimann D (2004) Crosslinking and G-protein functions of transglutaminase 2 contribute differentially to fibroblast wound healing responses. *Journal of Cell Science* **117:** 3389-3403

Stillman R (2008) Diabetic Ulcers. http://www.emedicine.com/med/topic551.htm. Accessed 01/10/2008

Sugahara K, Mikami T, Uyama T, Mizuguchi S, Nomura K, Kitagawa H (2003) Recent advances in the structural biology of chondroitin sulfate and dermatan sulfate. *Current Opinion in Structural Biology* **13:** 612-620

Sugimoto K, Murakawa Y, Sima AA (2000) Diabetic neuropathy - A continuing enigma. *Diabetes/Metabolism Research and Reviews* **16:** 408-433

Sunderkotter C, Steinbrink K, Goebeler M, Bhardwaj R, Sorg C (1994) Macrophages and angiogenesis. *Journal of Leukocyte Biology* **55:** 410-422

Sutherland J, Denyer M, Britland S (2005) Motogenic substrata and chemokinetic growth factors for human skin cells. *Journal of Anatomy* **207:** 67-78

Takagi C, King GL, Clermont AC, Cummins DR, Takagi H, Bursell SE (1995) Reversal of abnormal retinal hemodynamics in diabetic rats by acarbose, an alpha-glucosidase inhibitor. *Current Eye Research* **14:** 741-749

Takahashi N, Camacho P, Lechleiter J, Herman B (1999) Measurement of intracellular calcium. *Physiology Reviews* **79:** 1089-1125

Tammi R, Pasonen-Seppanen S, Kolehmainen, Tammi M (2005) Hyaluronan synthase induction and hyaluronan accumulation in mouse epidermis following skin injury. *Journal of Investigative Dermatology* **124:** 898-905

Tanaka A, Nagate T, Matsuda H (2005) Acceleration of wound healing by gelatin film dressings with epidermal growth factor. *Journal of Veterinary Medical Science* **67:** 909-913

Tarnuzzer RW, Macauley SP, Mast BA, Gibson JS, Stacey MC, Trengrove N, Moldawer LL, Burslem F, Schultz GS (1997) Epidermal growth factor in wound healing: A model for the molecular pathogenesis of chronic wounds. In: *Growth Factors and Wound Healing: Basic Science and Potential Clinical Applications*; Eds: Ziegler TR, Pierce GF, Herndon DN. Springer-Verlag, New York, pp 206–228

Taylor KR, Gallo RL (2006) Glycosaminoglycans and their proteoglycans: host-associated molecular patterns for initiation and modulation of inflammation. *The FASEB Journal* **20:** 9-22

Telgenhoff D, Shroot B (2005) Cellular senescence mechanisms in chronic wound healing. *Cell Death and Differentiation* **12:** 695-698

Tenenhaus M, Bhavsar D, Rennekampff H (2007) Treatment of deep partial thickness and intermediate depth facial burn wounds with water-jet debridement and a biosynthetic dressing. *Injury* **38:** S38-S44

Tennant JR (1964) Evaluation of the Trypan Blue technique for determination of cell viability. *Transplantation* **2:** 685-694

Thomas TP, Shukla R, Kotlyar A, Liang B, Ye J, Norris TB, Baker JR (2008) Dendrimer-epidermal growth factor conjugate displays superagonist activity. *Biomacromolecules* **9:** 603-609

Thorn P, Parker I (2005) Two phases of zymogen granule lifetime in mouse pancreas: Ghost granules linger after exocytosis of contents. *Journal of Physiology* **563:** 433-442

Tian X, Fei J, Pi Z, Yang C, Luo D (2005) Synthesis and characterisation of amoxicillin nanostructures. *Nanomedicine: Nanotechnology, Biology and Medicine* **1:** 323-325

Tonnesen MG, Feng X, Clark RAF (2000) Angiogenesis in wound healing. *Journal of Investigative Dermatology Symposium Proceedings* **5:** 40-46

Toolan H (1954) Transplantable human neoplasms maintained in cortisone-treated laboratory animals: H.S. No. 1; H.Ep. No. 1; H.Ep. No. 2; H.Ep. No. 3; and H.Emb.Rh. No. 1. *Cancer Research* **14:** 660-666

Torchilin VP, Voronkov JI, Mazoev AV (1982) The use of immobilised streptokinase (Streptodekaza) for the therapy of thromboses. *Therapeutic Archives Russia* **54:** 21-25

Toyoda M, Takayama H, Horiguchi N, Otsuka T, Fukusato T, Merlino G, Takagi H, Mori M (2001) Overexpression of hepatocyte growth factor promotes vascularisation and granulation tissue formation *in vivo*. *FEBS Letters* **509:** 95-100

Tredget EB, Dmeare J, Chandran G, Tredget E, Yang L, Ghahary A (2005) Transforming growth factor-β and its effect on reepithelialisation of partial thickness ear wounds in transgenic mice. *Wound Repair and Regeneration* **13:** 61-67

Trengove NJ, Langton SR, Stacey MC (1996) Biochemical analysis of wound fluid from nonhealing and healing chronic leg ulcers. *Wound Repair and Regeneration* **4:** 234-239

Trengove NJ, Stacey MC, MacAuley S, Bennett N, Gibson J, Burslem F, Murphy G, Schultz G (1999) Analysis of the acute and chronic wound environments: The role of proteases and their inhibitors. *Wound Repair and Regeneration* **7:** 442-452

Trengove NJ, Bielefeldt-Ohmann H, Stacey MC (2000) Mitogenic activity and cytokine levels in non-healing and healing chronic leg ulcers. *Wound Repair and Regeneration* **8:** 13-25

Tsang MW, Wong WKR, Hung CS, Lai K, Tang W, Cheung EYN, Kam G, Leung L, Chan CW, Chu CM, Lam EKH (2003) Human epidermal growth factor enhances healing of diabetic foot ulcers. *Diabetes Care* **26:** 1856-1861

Tsuboi R, Shi CM, Rifkin DB, Ogawa H (1992) A wound healing model using healing-impaired diabetic mice. *Journal of Dermatology* **19:** 673–675

Tung JW, Parks DR, Moore WA, Herzenberg LA, Herzenberg LA (2004) New approaches to fluorescence compensation and visualisation of FACS data. *Clinical Immunology* **110:** 277-283

Tyrone JW, Mustoe TA (1999) In: *Plastic Surgery Secrets.* Ed: Weinzweig J. Hanley & Belfus, Philadelphia, pp 2-5

Ubels JL, Edelhauser HF, Foley KM, Liao JC, Gressel P (1985) The efficacy of retinoic acid ointment for treatment of xerophthalmia and corneal epithelial wounds. *Current Eye Research* **4:** 1049-1057

Ulubayram K, Cakar AN, Korkusuz P, Ertan C, Hasirci N (2001) EGF containing gelatin-based wound dressings. *Biomaterials* **22:** 1345-1356

Underwood JCE (1994) *General and Systematic Pathology.* Churchill Livingstone, Edinburgh, pp 177-200

Valencia IC, Falabella A, Kirsner RS, Eaglstein WH (2001) Chronic venous insufficiency and venous leg ulceration. *Journal of the American Academy of Dermatology* **44:** 401-421

Van der Rest M, Garrone R (1991) Collagen family of proteins. *The FASEB Journal* **5:** 2814-2823

Vasey PA, Kaye SB, Morrison R, Twelves C, Wilson P, Duncan R, Thomson AH, Murray LS, Hilditch TE, Murray T, Burtles S, Fraier D, Frigerio E, Cassidy J (1999) Phase I clinical and pharmacokinetic study of PK1 [N-(2-hydroxypropyl)methacrylamide copolymer doxorubicin]: First member of a new class of chemotherapeutic agents-drug-polymer conjugates. Cancer Research Campaign Phase I/II Committee. *Clinical Cancer Research* **5:** 83-94

Vercauteren R, Bruneel D, Schacht E, Duncan R (1990) Effect of the chemical modification of dextran on the degradation by dextranase. *Journal of Bioactive and Compatible Polymers* **5:** 346-357

Vercauteren R, Schacht E, Duncan R (1992) Effect of the chemical modification of dextran on the degradation by rat liver lysosomal enzymes. *Journal of Bioactive and Compatible Polymers* **5:** 4-15

Veronese FM, Morpurgo M (1999) Bioconjugation in pharmaceutical chemistry. *Il Farmaco* **54:** 497-516

Veronese FM, Harris JM (2002) Introduction and overview of peptide and protein pegylation. *Advanced Drug Delivery Reviews* **54:** 453-456

Veronese FM, Pasut G (2005) PEGylation, successful approach to drug delivery. *Drug Discovery Today* **10:** 1451-1458

Vicent MJ, Greco F, Nicholson RI, Paul A, Griffiths PC, Duncan R (2005) Polymer therapeutics designed for a combination therapy of hormone-dependent cancer. *Angewandte Chemie International Edition* **44:** 4061-4066

Visse R, Nagase H (2003) Matrix metalloproteinases and tissue inhibitors of metalloproteinases. *Circulation Research* **92**: 827-839

Vlachou E, Chipp E, Shale E, Wilson YT, Papini R, Moiemen NS (2007) The safety of nanocrystalline silver dressings on burns: A study of systemic silver absorption. *Burns* **33:** 979-985

Vogt PM, Lehnhardt M, Wagner D, Jansen V, Krieg M, Steinau HU (1998) Determination of endogenous growth factors in human wound fluid: Temporal presence and profiles of secretion. *Plastic and Reconstructive Surgery* **102:** 117-123

Waddington RJ, Moseley R, Embery G (2000) Reactive oxygen species: A potential role in the pathogenesis of periodontal diseases. *Oral Diseases* **6:** 138-151

Wall IB, Moseley R, Baird DM, Kipling D, Giles P, Laffafian I, Price PE, Thomas DW, Stephens P (2008) Fibroblast dysfuction is a key factor in the non-healing of chronic venous leg ulcers. *Journal of Investigative Dermatology* **128:** 2526-2540

Wang XJ, Liao HJ, Chattopadhyay A, Carpenter G (2001) EGF-dependent translocation of green fluorescent protein-tagged PLC-gamma1 to the plasma membrane and endosomes. *Experimental Cell Research* **267:** 28–36

Watson P, Jones AT, Stephens DJ (2005) Intracellular trafficking pathways and drug delivery: Fluorescence imaging of living and fixed cells. *Advanced Drug Delivery Reviews* **57:** 43-61

Webster TJ (2005) Nanomaterials for tissue engineering nanomedicine. *Nanomedicine: Nanotechnology, Biology and Medicine* **1:** 251

Weinstein GD, McCullough JL, Ross P (1984) Cell proliferation in normal epidermis. *Journal of Investigative Dermatology* **82:** 623-628

Wenczak BA, Lynch JB, Nanney LB (1992) Epidermal growth factor receptor distribution in burn wounds. *Journal of Clinical Investigation* **90:** 2392-2401

Werle M, Bernkop-Schnurch A (2006) Strategies to improve plasma half-life time of peptide and protein drugs. *Amino Acids* **30:** 351-367

Werner S, Smola H, Liao X, Longaker MT, Krieg T, Hofschneider PH, Williams LT (1994) The function of KGF in morphogenesis of epithelium and reepithelialisation of wounds. *Science* **266:** 819-822

Werner S, Grose R (2003) Regulation of wound healing by growth factors and cytokines. *Physiology Reviews* **83:** 835-870

Werner S, Krieg T, Smola H (2007) Keratinocyte-fibroblast interactions in wound healing. *Journal of Investigative Dermatology* **127**: 998-1008

West MD, Pereira-Smith OM, Smith JR (1989) Replicative senescence of human skin fibroblasts correlates with a loss of regulation and overexpression of collagenase activity *Experimental Cell Research* **184**: 138-147

Wetzler C, Kampfer H, Stallmeyer B, Pfeilschifter J, Frank S (2000) Large and sustained induction of chemokines during impaired wound healing in the genetically diabetic mouse: prolonged persistence of neutrophils and macrophages during the late phase of repair. *Journal of Investigative Dermatology* **115**: 245-253

Whitcomb DC, Lowe ME (2007) Human pancreatic digestive enzymes. *Digestive Diseases and Sciences* **52**: 1-17

Wieman TJ, Smiell JM, Su Y (1998) Efficacy and safety of a topical gel formulation of recombinant human platelet-derived growth factor-BB (becaplermin) in patients with chronic neuropathic diabetic ulcers. A phase III randomized placebo-controlled double-blind study. *Diabetes Care* **21**: 822-827

Wiepz GJ, Edwin F, Patel T, Bertics PJ (2006) Methods for determining the proliferation of cells in response to EGFR ligands. *Methods in Molecular Biology* **327**: 179-187

Wilhelmi BJ, Neumeister M (2008) Pressure ulcers, surgical treatment and principles http://www.emedicine.com/plastic/topic462.htm. Accessed 01/10/2008

Winn R, Maunder R, Chi E, Harlan J (1987) Neutrophil depletion does not prevent lung edema after endotoxin infusion in goats. *Journal of Applied Physiology* **62**: 116-121

Wlascheck M, Peus D, Achterberg V, Meyer-Ingold W, Scharfetterr-Kochanek K (1997) Protease inhibitors protect growth factor activity in chronic wounds. *British Journal of Dermatology* **137**: 646-663

Wlascheck M, Scharfetterr-Kochanek K (2005) Oxidative stress in chronic venous leg ulcers. *Wound Repair and Regeneration* **13**: 452-461

Wong KKY, Tain J, Ho C, Lok C, Che C, Che J, Tam PKH (2006) Topical delivery of silver nanoparticles reduces systemic inflammation of burn and promotes wound healing. *Nanomedicine: Nanotechnology, Biology and Medicine* **2**: 306

Woo K, Ayello EA, Sibbald RG (2007) The edge effect: Current therapeutic options to advance the wound edge. *Advances in Skin and Wound Care* **20**: 99-117

Woolfson AMJ, Ricketts CR, Hardy SM, Saour JN, Pollard BJ, Allision SP (1976) Prolonged nasogastric tube feeding in critically ill and surgical patients. *Postgraduate Medical Journal* **52**: 678-682

Yager DR, Chen SM, Ward SI, Olutoye OO, Diegelmann RF, Cohen IK (1997) Ability of chronic wound fluids to degrade peptide growth factors is associated with increased levels of elastase activity and dimished levels of proteinase inhibitors. *Wound Repair and Regeneration* **5:** 23-32

Yager DR, Kulina RA, Gilman LA (2007) Wound fluids: A window into the wound environment. *International Journal of Lower Extremity Wounds* **6:** 262-272

Yanagishita M (1993) Function of proteoglycans in the extracellular matrix. *Acta Pathologica Japonica* **43:** 283-293

Yang C-C, Lin S-D, Yu H-S (1997) Effect of growth factors on dermal fibroblast contraction in normal skin and hypertrophic scar. *Journal of Dermatological Science* **14:** 162-169

Yarden Y, Ullrich A (1988) Growth factor receptor tyrosine kinases. *Annual Reviews of Biochemistry* **57:** 443-478

Zeng F, Lee H, Allen C (2006) Epidermal growth factor-conjugated poly(ethylene glycol)-block-poly(δ-valerolactone) copolymer micelles for targeted delivery of chemotherapeutics. *Bioconjugate Chemistry* **17:** 399-409

Zhao B, Cooper LJ, Brahma A, MacNeil S, Rimmer S, Fullwood NJ (2006) Development of a three-dimensional organ culture model for corneal wound healing and corneal transplantation. *Investigative Ophthalmology and Visual Science* **47:** 2840-2846

Zhao M, Song B, Pu J, Forrester JV, McCaig CD (2003) Direct visualisation of a stratified epithelium reveals that wounds heal by unified sliding of cell sheets. *The FASEB Journal* **17:** 397-406

Zhong Z, Wen Z, Darnell JE (1994) STAT3: A STAT family member activated by tyrosine phosphorylation in response to epidermal growth factor and interleukin-6. *Science* **264:** 95-98

Zhou M, Felder S, Rubinstein M, Hurwitz DR, Ullrich A, Lax I, Schlessinger J (1993) Real time measurements of kinetics of EGF binding to soluble EGF receptor monomers and dimers support the dimerization model for receptor activation. *Biochemistry* **32:** 8193-8198

Zhou Y, Yang D, Chen X, Xu X, Xu Q, Lu F, Nie J (2008) Electrospun water-soluble carboxyethyl chitosan/poly(vinyl alcohol) nanofibrous membrane as potential dressing for skin regeneration. *Biomacromolecules* **9:** 349-354

Zolfaghari A, Djakiew D (1996) Inhibition of chemomigration of a human prostatic carcinoma cell line by inhibition of epidermal growth factor receptor function. *Prostate* **28:** 232-238

Appendix

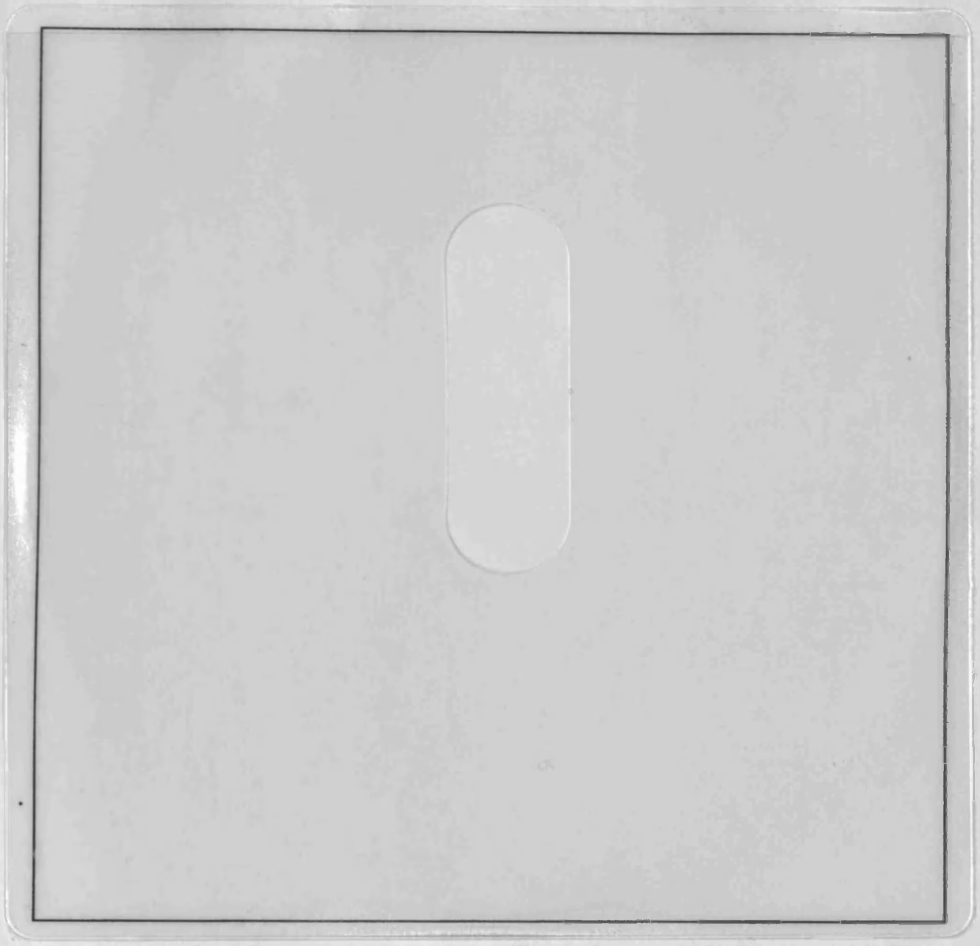

This appendix DVD contains:

Disc 1:

1. *In vitro* scratch wound assay QuickTime™ movie files (.mov) of HaCaT keratinocytes, normal dermal fibroblasts and chronic wound fibroblasts (typical representative files).

Disc 2:

2. An electronic copy of this Thesis (.doc).

3. Electronic copies of publications arising from this Thesis (.pdf).

4. *In vivo* digital wound photography and wound histology images (all are PowerPoint® presentation files, .ppt).

follows:

- Firstly, dextrin-rhEGF conjugates will be synthesised, and characterised. To assess the ability of the dextrin-rhEGF conjugate to release rhEGF, in response to α-amylase, degradation studies will be performed under simulated physiological conditions, to confirm the stability of the dextrin-rhEGF conjugate in response to proteolysis (Chapter 3).
- *In vitro* studies will be used to determine the bioactivity of the dextrin-rhEGF conjugate, in both "masked" and "unmasked" conditions, using models of wound healing involving cell lines derived from normal human skin (keratinocytes and fibroblasts) and chronic wounds (fibroblasts). Cellular proliferation and migration in response to unmodified rhEGF and conjugated rhEGF will also be investigated (Chapter 4).
- After confirmation of rhEGF release from the polymer, *in vitro* assays of bioactivity will be performed to ensure that the modified rhEGF retains the ability to bind to the specific cell-surface receptor, and activate intracellular signalling pathways. (Chapter 5).
- Having established the bioactivity *in vitro*, an *ex vivo* model of acute wound healing will be developed, using rat corneas. Other *ex vivo* studies include the collection and analysis of human wound fluid from acute and chronic dermal wounds, to confirm the presence and activity of α-amylase (pivotal for dextrin-rhEGF degradation and activation) and a characteristic wound proteinase (neutrophil elastase) (Chapter 6).
- Having established the activity of the dextrin-rhEGF conjugate, both *in vitro* and *ex vivo*, an *in vivo* animal (mouse) model of impaired wound healing will be utilised for the final stage of pre-clinical assessment (Chapter 7).

Based upon this synthetic and pre-clinical assessment study of dextrin-rhEGF as a bioresponsive nanomedicine for dermal wound healing, future aims would be to expand the types of polymer and mediators of wound healing (other growth factors, antibiotics, anti-inflammatory agents), used in the construction of healing-promoting polymer therapeutics, leading to novel treatments to alleviate the increasing burden of chronic wounds.

Chapter Two

General Materials And Methods

3.2.6.1 Degradation assays of dextrin, succinoylated dextrin and the dextrin-rhEGF conjugate, by GPC

Samples of dextrin, succinoylated dextrin and the dextrin-rhEGF conjugate (1 mg/mL) were added to physiologically relevant α-amylase concentrations (93 i.u./L), in PBS. These were incubated at 37 °C, 100 μL samples (x 3) removed and snap-frozen in liquid nitrogen, at time points between 0 and 168 h. These samples were analysed in triplicate, using GPC (Section 2.6.2.1).

3.2.6.2 Degradation assays of the dextrin-rhEGF conjugate, by FPLC

The dextrin-rhEGF conjugate (1 mg/mL in PBS) was incubated at 4 °C and at 37 °C, in α-amylase-free conditions, for 168 h. α-Amylase (93 i.u./L) was added to samples of the dextrin-rhEGF conjugate (1 mg/mL in PBS) and incubated at 37 °C. The dextrin-rhEGF conjugate was also lyophilised and stored at -20 °C for 168 h. Samples (100 μL) were snap-frozen in liquid nitrogen, at time points between 0 and 168 h. The samples were thawed and analysed using FPLC (Section 2.6.1). Chromatogram peak areas, corresponding to the dextrin-rhEGF conjugate and free rhEGF, were recorded. The ratios of free rhEGF : dextrin-rhEGF were subsequently calculated.

3.2.6.3 Determination of rhEGF concentration by ELISA

For quantification of free rhEGF, liberated from the dextrin-rhEGF conjugate, in the presence and absence of physiological α-amylase levels, an ELISA was employed. This colorimetric assay had a range of detection of 0.7–250 pg/mL. As such, samples of the dextrin-rhEGF conjugate were diluted to 250 pg/mL rhEGF equivalent in dilution buffer (RD5E, in ELISA kit), in the presence, or absence of physiological α-amylase concentrations (93 i.u./L). Samples (200 μL, x 3) were taken at time points between 0 and 168 h and snap-frozen in liquid nitrogen. The ELISA was performed, as described in Section 2.6.2.5.

3.2.7 Stability of rhEGF and the dextrin-rhEGF conjugate, in response to proteinases

The dextrin-rhEGF conjugate (1 mg/mL) and rhEGF (1 mg/mL) were dissolved separately in PBS (1 mL). To assess stability to proteolytic degradation,

human neutrophil elastase (100 μg/mL) or trypsin-EDTA (0.025 %) was added to these samples and incubated at 37°C. Aliquots (200 μL) were taken at time points between 0 and 24 h, and snap-frozen in liquid nitrogen. On completion of the experiment, all samples were thawed and analysed by FPLC, as described in Section 2.6.1. Degradation of rhEGF and the dextrin-rhEGF conjugate were assessed by the changes in the area of the characteristic chromatogram peaks.

3.2.8 Statistical analysis

Statistical analyses were undertaken using GraphPad Prism® version 4.00 (GraphPad Software, San Diego, USA). Data were compared using a Student's t-test and a one-way ANOVA, with a Bonferroni post-test. Results are expressed as a mean and standard deviation (S.D.), or standard error of the mean (S.E.M.). Statistical significance was considered at a probability of $p < 0.05$.

3.3 Results

3.3.1 Synthesis and characterisation of the dextrin-rhEGF conjugate

When dextrin (51,000 g/mol) was succinoylated, the degree of modification was confirmed by titration to be between 19 - 21 mol %. Typically, the reaction conversion efficiency for succinoylation was approximately 30 - 40 % of the theoretical maximum.

Characterisation of dextrin by FTIR (Figure 3.6) showed characteristic peaks at 3,640 (OH), and 1,450 cm^{-1} ($O\text{-}CH_2$). On succinoylation, the ester peak at 1,720 cm^{-1} was observed to increase in signal strength, in relation to the degree of modification. GPC, using pullulan standards, suggested an apparent molecular weight increase from 57,000 ± 500 g/mol (mean ± S.D., n = 3) to 84,000 ± 1,500 g/mol (mean ± S.D., n = 3), following succinoylation, with little change in polydispersity (dextrin = 1.73, succinoylated dextrin = 1.75) (Figure 3.7).

The ninhydrin assay estimated the mean numbers of primary amines as 1.2 ± 0.1 (mean ± S.D., n = 3), per molecule of rhEGF for conjugation. When the succinoylated dextrin intermediate was conjugated to rhEGF, using EDC and sulfo-NHS, SDS-PAGE confirmed the presence of a high molecular weight conjugate with

Chapter Five

Mechanistic Studies With The Dextrin-rhEGF Conjugate

Chapter Five: Mechanistic Studies With The Dextrin-rhEGF Conjugate

Contents

the dextrin-rhEGF conjugate, rather than free rhEGF. It must be considered, however, that the ELISA employed herein, will detect the presence of EGF, but not the activity of EGF. The absence of detectable EGF within chronic wound fluid is similar to the findings of Wlascheck *et al* (1997), who described the degradation of growth factors in response to chronic wound fluid. The levels of EGF in acute wound fluids (34 ± 22 pg/mL) were lower than human plasma levels (317 ± 31 pg/mL) (Savage *et al*, 1986), which may suggest an instability of rhEGF in acute wound fluids, in response to other wound proteinases, other than neutrophil elastase, which was undetected in acute wound fluids. It may also be due to the short plasma half-life of EGF (Kuo *et al*, 1992).

6.5 Conclusions

The efficacy of the dextrin-rhEGF conjugate, in an *ex vivo* model of acute wound healing, was established in this Chapter. Dextrin-rhEGF conjugate activity was dependent upon activation by α-amylase, at a physiological concentration (the PUMPT hypothesis), as in the inactive "masked" state; there was no significant rhEGF bioactivity, compared to rhEGF-free controls. The *ex vivo* model of corneal wound healing, has been shown to be reproducible, and that it is a reliable model for further analysis of polymer-protein conjugates. In addition, wound fluid analysis has confirmed the presence of α-amylase, equivalent to serum concentrations, in both acute and chronic wound fluids, relevant to dermal repair situations. This has, therefore, justified the use of physiological concentrations of α-amylase, in the characterisation and evaluation of the dextrin-rhEGF conjugate. Previous studies on the degradation of succinoylated dextrin and its conjugates, involved the use of non-human, α-amylase, at much higher concentrations (Hreczuk-Hirst *et al*, 2001a). This Study has confirmed these previous findings, but in a more clinically relevant setting.

The next line of investigation involved the establishment of an *in vivo* model of impaired dermal wound healing, and the evaluation of both rhEGF and the dextrin-rhEGF conjugate, in the promotion of wound repair, in this context.

Chapter Seven

Dextrin-rhEGF Conjugate Evaluation in an In Vivo Model of Impaired Wound Healing

Almond A (2007) Hyaluronan. *Cellular and Molecular Life Sciences* **64:** 1591-1596

Alpers DH (1994) Digestion and absorption of carbohydrates and proteins. In: *Physiology of the Gastrointestinal Tract.* Ed: Johnson LR. Raven Press, New York, pp 1723-1749

Alroy I, Yarden Y (1997) The ErbB signaling network in embryogenesis and oncogenesis: Signal diversification through combinatorial ligand–receptor interactions. *FEBS Letters* **410:** 83-86

Alsop MR (1994) History, chemical and pharmaceutical development of icodextrin. *Peritoneal Dialysis International* **14:** S5

Ando Y, Jensen PJ (1993) Epidermal growth factor and insulin-like growth factor I enhance keratinocyte migration. *Journal of Investigative Dermatology* **100:** 633-639

Andrews RK, Lopez JA, Berndt MC (1997) Molecular mechanisms of platelet adhesion and activation. *International Journal of Biochemistry and Cell Biology* **29:** 91-105

Andriani F, Margulis A, Lin N, Griffey S, Garlick JA (2003) Analysis of microenvironmental factors contributing to basement membrane assembly and normalized epidermal phenotype. *Journal of Investigative Dermatology* **120:** 923-931

Angelucci A, Gravina GL, Rucci N, Millimaggi D, Festuccia C, Muzi P, Teti A, Vicentini C, Bologna M (2006) Suppression of EGF-r signalling reduces the incidence of prostate cancer metastasis in nude mice. *Endocrine-Related Cancer* **13:** 197-210

auf dem Keller U, Krampert M, Kümin A, Braun S, Werner S (2004) Keratinocyte growth factor: Effects on keratinocytes and mechanisms of action. *European Journal of Cell Biology* **83:** 607-612

Bahnson A, Charalambos A, Koebler D, Qian L, Shun T, Shields D, Yu H, Wang H, Goff J, Cheng T, Houck R, Cowsert L (2005) Automated measurement of cell motility and proliferation. *BioMed Central Cell Biology* **6:** 19

Baker EA, El-Gaddal S, Aitken DG, Leaper DJ (2003) Growth factor profiles in intraperitoneal drainage fluid following colorectal surgery: Relationship to wound healing and surgery. *Wound Repair and Regeneration* **11:** 261-267

Balasubramani M, Kumar TR, Babu M (2001) Skin substitutes: A review. *Burns* **27:** 534-544

Bandyopadhyay B, Fan J, Guan S, Li Y, Chen M, Woodley DT, Li W (2006) A "traffic control" role for $TGF\beta_3$: Orchestrating dermal and epidermal cell motility during wound healing. *Journal of Cell Biology* **172:** 1093-1105

Bao P, Kodra A, Tomic-Canic M, Golinko MS, Erlich HP, Brem H (2008) The role of vascular endothelial growth factor in wound healing. *Journal of Surgical Research* In press: DOI: 10.1016/j.jss.2008.04.023

Baranoski S (2006) Raising awareness of pressure ulcer prevention and treatment. *Advances in Skin and Wound Care* **19:** 398-405

Barczak CA, Barnett RI, Childs EJ, Bosley LM (1997) Fourth national pressure ulcer prevalence survey. *Advances in Wound Care* **10:** 18-26

Barnes DW (1982) Epidermal growth factor inhibits growth of A431 human epidermoid carcinoma in serum-free culture. *Journal of Cell Biology* **93:** 1-4

Barrandon Y, Green H (1987) Cell migration is essential for sustained growth of keratinocyte colonies: the roles of transforming growth factor-α and epidermal growth factor. *Cell* **50:** 1131-1137

Bauer JA, Rao W, Smith DJ (1998) Evaluation of linear polyethyleneimine/nitric oxide adduct on wound repair: Therapy versus toxicity. *Wound Repair and Regeneration* **6:** 569-577.

Bazley LA, Gullick WJ (2005) The epidermal growth factor receptor family. *Endocrine-Related Cancer* **12:** S17-S27

Ben-Levy R, Peles E, Goldman-Michael R, Yarden Y (1992) An oncogenic point mutation confers high affinity ligand binding to the neu receptor. Implications for the generation of site heterogeneity. *Journal of Biological Chemistry* **267:** 17304-17313

Bhattacharyya M, Bradley H (2008) A case report of the use of nanocrystalline silver dressing in the management of acute surgical site wound infection with MRSA to prevent cutaneous necrosis following revision surgery. *International Journal of Lower Extremity Wounds* **7:** 45-48

Bircher AJ, Harr T, Hohenstein L, Tsakiris DA (2006) Hypersensitivity reactions to anticoagulant drugs: Diagnosis and management options. *Allergy* **61:** 1432-1440

Bisaccia E, Lugo A, Torres O, Johnson B, Scarborough D (2007) Persistent inflammatory reaction to hyaluronic acid gel: A case report. *Cutis* **79:** 388-389

Black FL, Melnick JL, Reissig M (1956) Propagation of measles virus in a strain of human eopidermoid cancer cells (Hep-2). *Proceedings of the Society of Experimental Biology and Medicine* **93:** 107-108

Blakytny R, Jude E (2006) The molecular biology of chronic wounds and delayed healing in diabetes. *Diabetes Medicine* **23:** 594-608

Bode W, Fernadez-Catalan C, Grams F, Gomis-Ruth F, Nagase H, Tschesche H, Maskos K (1999) Insights into MMP-TIMP interactions. *Annals of the New York Academy of Sciences* **878:** 73-91